SURFACE SOIL STRUCTURE, THE SOIL WATER BALANCE AND THE EFFECTS OF TILLAGE

A thesis
submitted in partial fulfilment
of the requirements for the degree

of

Doctor of Philosophy

In the
University of Canterbury

by
Hamish Peter Cresswell

Lincoln University
1990

Abstract of a thesis presented for the degree of
Doctor of Philosophy

SURFACE SOIL STRUCTURE, THE SOIL WATER BALANCE AND THE EFFECTS OF TILLAGE

by Hamish Peter Cresswell

This study considers the effects of multiple-pass tillage on the surface soil structure of a Templeton silt-loam soil in Canterbury, New Zealand. The effects of pre-tillage soil water content (PTSW) and type of tillage operation are assessed for the freshly-tilled soil. A numerical simulation model (CONSERVB, van Bavel and Hillel, 1976) is evaluated as a method to assist in the identification of the soil properties which are most significant in determining evaporative loss of soil water.

PTSW and intensity of tillage operations interact to determine the aggregate size distribution resulting from multiple-pass tillage. Intensive tillage of a dry soil produces a high proportion of small wind-erodible soil aggregates and particles. The avoidance of intensive tillage reduces the likelihood of a PTSW effect occurring. Aggregates produced from tilling this soil at a water content near the lower plastic limit (LPL) are less mechanically stable (when dry) than those produced from tilling dry soil. Aggregate stability must be considered when assessing the most appropriate PTSW for the desired tillage objectives. Tillage-induced random roughness was quantified using a geostatistical method. Intensive tillage reduces aggregate size resulting in a smoother soil surface with a lower surface area.

Intensive tillage decreases the macro-pore volume mainly through a decrease in the volume of aeration pores (pores >300μm diameter). PTSW does not have significant effects on macro-porosity or available water holding capacity. Near-saturation hydraulic conductivity is significantly reduced by intensive tillage as a result of decreased macro-pore volume. The Jackson (1972) model was evaluated by sensitivity analysis and found unsuitable for assessing the effects of tillage on unsaturated

hydraulic conductivity. The output from the Jackson model showed extreme sensitivity to the 0 to -1.0 kPa matric potential section of the water characteristic input. Tillage-induced changes in soil porosity are reflected by changes in soil volumetric heat capacity and thermal conductivity. Tillage-induced soil structure changes affected shortwave albedo but to a smaller extent than previous studies indicated. The shortwave albedo on the tilled soil was low, due to the high organic matter content and rough surfaces.

Predictions of evaporation, soil water content and soil temperature from the numerical simulation model CONSERVB were compared with field measurements from the tilled Templeton silt-loam soil. The CONSERVB model accurately simulated bare soil evaporation when the unsaturated hydraulic conductivity input function was determined by calibration. Simulated soil water and temperature profiles were generally good although water content near the soil surface was sometimes under-estimated and surface soil temperature was over-estimated in warm conditions. The CONSERVB model could be used in future to help in predicting benefits and risks from tillage operations. Identifying the tillage-sensitive soil properties which have the greatest influence on evaporative soil water loss is a research priority.

ACKNOWLEDGEMENTS

This research was made possible by funding from the University Grants Committee and the National Water and Soil Conservation Authority (both organisations now discontinued). Additional financial support, for which I am extremely grateful, was provided by my parents.

I should like to express my thanks to my supervisors, Dave Painter and Keith Cameron, for their guidance and support throughout this project. They have given their time, energy and enthusiasm in assisting me in many areas of this work. Their assistance has been much appreciated.

A large proportion of the time spent on this project has been in the design, construction and calibration of experimental apparatus and in field site preparation and sample collection. I should like to offer my special thanks to Dave Lees for the help which he has given in this phase of the work. Thanks also to the staff of the Field Service Centre, Lincoln University; to Rick Diehl; to the staff of the Agricultural Engineering Institute, especially Ian Woodhead and Peter Carran; to Lindsay Dickson; and to the staff and post-graduate students of the Department of Natural Resources Engineering and of the Department of Soil Science, Lincoln University.

Graeme Buchan and Tim Davies have given of their time to review parts of the thesis manuscript. Their input has been much appreciated. A special thanks to Jeff Warburton for time spent reviewing parts of the manuscript and for assistance with production of graphs and diagrams. Thanks to Helen Richards who typed the references, and to the staff of the Library and the Centre for Computing and Biometrics, Lincoln University.

Personal thanks go to: Roger McLenaghen, Jeff Reid, Chris Phillips, Bill Young, Gavin Kenny, Jagath Ekanayaka, Benno Zarn, Ross Dickson, and to the firefighters from the Lincoln Volunteer Fire Brigade. My final thanks are reserved for my family, especially my parents. My parents have given their love and support throughout my eight years at University. This support has contributed greatly to the successful completion of this study.

TABLE OF CONTENTS

7 EXPERIMENTAL VERIFICATION OF THE CONSERVB MODEL

LIST OF FIGURES

LIST OF TABLES

NOTATION

Symbol	Description	Units
AWHC	Available water holding capacity	%
A_ρ	Area of exposure of pores of mean size ρ	m^2
A_σ	Area of exposure of pores of mean size σ	m^2
A_s	Surface area	$m^2\ m^{-2}$
C	Volumetric heat capacity of soil	$kJ\ m^{-3}\ K^{-1}$
C_p	Specific heat of air at constant pressure	$J\ kg^{-1}\ {}^oC^{-1}$
E	Evaporative flux	$kg\ m^{-2}\ s^{-1}$
E_o	Evaporation from open water	$mm\ d^{-1}$
E_{so}	Sub-surface evaporation	$mm\ d^{-1}$
ET	Evapotranspiration	$mm\ d^{-1}$
F_{ij}	View factor	-
H	Sensible heat flux	$W\ m^{-2}$
H_a	Humidity of the air	$kg\ m^{-3}$
H_o	Saturation humidity	$kg\ m^{-3}$
H_s	Absolute humidity of air at the soil surface	$kg\ m^{-3}$
J	Steady state flow rate	$m\ s^{-1}$
K	Hydraulic conductivity	$m\ s^{-1}$
K_i	Hydraulic conductivity at the ith increment	$cm\ hr^{-1}$
K_s	Saturated hydraulic conductivity	$m\ s^{-1}$
K_T	Hydraulic conductivity at temperature, T	$m\ s^{-1}$
LD	Surface roughness index	-
LPL	Lower plastic limit	%, w/w
LS	Surface roughness index	-
L_v	Latent heat of vaporization	$J\ m^{-3}$
* M	Miscellaneous energy term	$W\ m^{-2}$
	Experimental constant	-
MO	Monin-Obukhov length	m
N	Constant in mass transport equations (Chapter 2)	-
P_1	Stability correction	-
P_2	Stability correction	-
* m	Molecular weight of water	$kg\ mol^{-1}$

Q	Volume flow of water through a section of defined length per unit time	$cm^3\ s^{-1}$
R	Upper pore size limit	mm
	Universal gas constant	$J\ kg^{-1}K^{-1}mol^{-1}$
RH	Relative humidity	%
R_g	Global radiation	$W\ m^{-2}$
Ri	Richardson number	-
R_l	Longwave radiation	$W\ m^{-2}$
R_s	Solar radiation	$W\ m^{-2}$
R_n	Net radiation	$W\ m^{-2}$
R_{no}	Net radiation over water	$W\ m^{-2}$
S	Soil heat flux	$W\ m^{-2}$
S_i	Isothermal soil heat flux	$W\ m^{-2}$
S_t	Thermal soil heat flux	$W\ m^{-2}$
SR	Surface roughness index	-
St	Stability correction factor	-
T	Temperature	^oC
T_a	Air temperature	^oC
T_d	Dew point temperature	^oC
T_s	Surface temperature	^oC
T_1	Temperature at centre of surface soil layer	^oC
X	Distance	mm
Z_h	Mean absolute elevation	mm
Z_i	Deviations of Z about zero	-
a	Albedo	-
a_d	Albedo of a dry soil	%
a_w	Albedo of a wet soil	%
c	Specific heat capacity of soil	$kJ\ kg^{-1}\ K^{-1}$
d	Diameter	mm
e	Vapour pressure	kPa
e_a	Actual vapour pressure	kPa
e_o	Vapour pressure at surface	kPa
e_s	Saturation water vapour pressure in air	kPa
g	Acceleration due to gravity	$m\ s^{-2}$

h	Hydraulic head	m
h_{ij}	Height reading in ith row and jth column	mm
h_{ij}'	Corrected height reading	mm
$\overline{h_{.j}}$	Mean reading in jth column	mm
$\overline{h_{i.}}$	Mean reading in ith row	mm
$\overline{h_{..}}$	Overall mean	mm
i	Summation indices	-
j	Summation indices	-
k	Von Karman's constant	-
l	Distance above infiltrometer base	mm
n	Index of refraction of water	-
	Number of observations	-
	Number of pore classes	-
p	Pressure	kPa
	Experimental constant (pore interaction term)	-
q	Volume of water flowing through unit cross-sectional area per unit time	$cm^3\ s^{-1}\ m^{-2}$
r_a	Effective resistance to heat and vapour transfer in neutral conditions	$s\ m^{-1}$
r_c	Corrected aerodynamic resistance	$s\ m^{-1}$
r	radius	m
r_i	Radius of disk i	m
r_k	Radius of disk k	m
t	Time	s
x_a	Ratio between space average of the temperature gradient in the air relative to the water phase (shape factor for gas-filled pores)	-
x_s	Ratio between space average of the temperature gradient in the solid relative to the water phase (solid particle shape factor)	-
z	Height	m
	Length	m
	Distance	m
z_o	Aerodynamic roughness parameter	m

	e	Emittance	-
	e_T	Total porosity	$m^3\ m^{-3}$
	γ	Psychrometric constant	$mb\ {}^oC^{-1}$
		Surface tension of water	$J\ m^{-2}$
	γ_h	Semi-variance	-
	η	Viscosity	$g\ m^{-1}\ s^{-1}$
	η_T	Viscosity at temperature T	$g\ m^{-1}\ s^{-1}$
	σ	Stephan-Boltzman constant	$W\ m^{-2}\ K^{-4}$
	σ^2	Variance	-
*	ψ_g	Gravitational potential	kPa
	ψ_m	Matric potential	kPa
	ψ_o	Osmotic potential	kPa
	ψ_t	Total potential	kPa
	ρ_w	Density of water	$g\ cm^{-3}$
	ρ_a	Density of air	$g\ cm^{-3}$
	ρ_b	Bulk density	$Mg\ m^{-3}$
	ρ_p	Particle density	$Mg\ m^{-3}$
	f_a	Volume fraction of air	-
	f_s	Volume fraction of soil solids	-
	f_w	Volume fraction of water	-
	Δ	Change in	-
	Θ	Water content	$g\ g^{-1}$
	Θ_v	Volumetric water content	$m^3\ m^{-3}$
	λ	Thermal conductivity	$W\ m^{-1}\ K^{-1}$
	λ_a	Specific thermal conductivity of air	$W\ m^{-1}\ K^{-1}$
	λ_s	Specific thermal conductivity of soil solids	$W\ m^{-1}\ K^{-1}$
	λ_w	Specific thermal conductivity of water	$W\ m^{-1}\ K^{-1}$
	λ_1	Thermal conductivity of surface layer	$W\ m^{-1}\ K^{-1}$
	Π	3.1416	-
*	ψ_p	Pressure potential	m

CHAPTER 1

General Introduction

1.1 Overview

Much of the current level of agricultural production, world-wide, is being achieved at the expense of non-renewable soil resources. Technological improvements have obscured past and current soil productivity losses. A priority is for the development of technology which allows at least sustainable agricultural productivity while at the same time helping to regenerate, rather than deplete, our soils. The possibility of maintaining the same high crop yields while minimising and economising tillage operations might be a more desirable approach as compared with the introduction of new, more elaborate tillage methods in an effort to obtain greater yields.

The management of soil structure influences crop growth and yield as well as erosion by wind and water. In order to manage soil structure the precise effects of tillage on soil structure must be defined and then optimised. The study of soil structure management involves the definition of an optimal soil physical state for any given purpose and the determination of the best means to achieve such an optimal state. For the proper evaluation of different tillage systems we need to be able to measure and to predict their likely effect on soil properties and processes, and in turn on plant growth and yield.

The present study considers the effects of multiple-pass tillage and soil conditions at the time of tillage on surface soil structure. Tillage-induced changes in some of the soil properties that are important in the context of soil conservation or that affect the soil water and energy balances are quantified. Emphasis is placed on the soil physical properties which are important in determining susceptibility of a soil to wind erosion.

Soil water relations in the field involve complex interacting processes, some of which incorporate soil properties affected by tillage. Simulation modelling could provide

an approach which will allow the integration of these various properties and processes in the determination of the soil water balance. The computer modelling approach is a method which might allow the isolation of tillage-affected variables and hence the determination of the soil properties which have the most significant effects on the soil water balance. In this study the numerical simulation model CONSERVB (van Bavel and Hillel, 1976) is evaluated for use in tillage research.

1.2 Project objectives

The aims of this research are:

1. To investigate the effects that soil water content at time of multiple-pass tillage, and type of tillage operation, have on the surface structural properties of a freshly-tilled, medium-textured, wind-erosion-susceptible soil.

2. To investigate the effects that soil water content at time of multiple-pass tillage, and type of tillage operation, have on soil hydraulic characteristics.

3. To investigate the influence that surface soil structure and surface soil water content have on shortwave albedo of a bare, tilled, soil.

4. To measure the evaporation, changes in soil water content and changes in soil temperature of a bare, tilled soil together with the relevant meteorological parameters and to use the data to evaluate the numerical simulation model CONSERVB (van Bavel and Hillel, 1976).

5. To evaluate the CONSERVB model for use as a research tool to help in the identification of the tillage-affected soil properties which significantly affect the soil water balance.

1.3 Thesis organisation

This thesis is organised into eight chapters. Chapter 2 is a review of literature which describes previous research relevant to the topic of study and shows where further research is required, thereby providing the context for this study. In Chapter 3 the experimental site, methods and apparatus are detailed. Chapter 4 describes the effects of multiple-pass tillage and pre-tillage soil water content on properties of surface soil structure including aggregate size distribution, aggregate stability, soil surface roughness and bulk density.

The effects of tillage operations on total porosity, the soil water characteristic, functional pore size classes, near-saturation hydraulic conductivity, soil thermal properties and shortwave albedo are all described in Chapter 5. The chapter also includes an evaluation, by sensitivity analysis, of the Jackson (1972) method of unsaturated hydraulic conductivity calculation. In Chapter 6 a detailed description of the numerical simulation model CONSERVB (van Bavel and Hillel, 1976) is given. The results of previous verification studies on the CONSERVB model are described and a preliminary assessment of the model is made. The simulation of the soil water and energy balances by the CONSERVB model is compared with field measurements in an investigation described in Chapter 7. Finally, in Chapter 8, the results from the study are summarised and discussed, areas for further research are suggested, and the major conclusions are listed.

CHAPTER 2

Literature Review

2.1 Introduction

2.1.1 Wind erosion

Many agricultural areas throughout the world are susceptible to wind erosion (FAO, 1960; Skidmore, 1976). Wind erosion is the dominant problem on about 30 million hectares of land in the United States (USDA, 1965). About two million hectares are moderately to severely damaged each year. Bennett (1939) estimated that a single dust storm occurring on May 12th 1934 carried 272 million tonnes of topsoil from the Great Plains area of the United States of America. Hagen and Woodruff (1973) estimated that the eroding lands of the Great Plains area contributed 220 and 70 million tonnes of dust per year into the atmosphere in the 1950's and 1960's respectively.

Wind erosion of arable and pastoral land is considered to be a significant potential limitation to agricultural production in New Zealand. In New Zealand there are 1.6 million hectares of arable land with slight or moderate wind erosion severity. In total an estimated 3.4 million hectares, or 12%, of New Zealand's land area is affected by wind erosion (Eyles, 1983). Local erosion events in Waipara (North Canterbury) during March 1973 were reported to have removed up to 50 mm of topsoil from parts of some paddocks. Lucerne plants had their leaves sand-blasted away and were left lying on the ground with the upper parts of their roots exposed. On November 26th 1975, during an erosion event in Canterbury, Painter (1976) measured a peak rate of erosion equivalent to 40 kg ha^{-1} min^{-1} with a total daily loss of approximately 5 t ha^{-1}. Results from the collecting masts used by Painter showed that soil was moving about the countryside

even when no obvious events were occurring. 'Mild' wind erosion occurs so slowly that its dangers can escape notice. Soil removal can outstrip the soil forming processes but remain undetected for generations.

Serious wind erosion events occurred in Canterbury on the 4th and 15th of October 1988 when gusts from the north-westerly foehn wind reached 93 km hr^{-1} (McGuigan, 1989). These high winds followed a cold spring during which frost action was severe, causing considerable aggregate breakdown. At the time of the erosion damage soil water contents were low, with rainfall for the preceding eight months being only 59% of the average for the period. Where serious erosion occurred, vegetative cover was often sparse with late sown crops at pre-emergence or early seedling stages of growth. In most cases the damaged soils had either been heavy rolled or intensively cultivated to produce a fine seedbed. The measured soil loss from these events, together with other recent local events, are summarised in Table 2.1. These measured losses do not account for dust losses and hence are conservative.

Table 2.1 Soil loss from recent Canterbury wind erosion events (after McGuigan, 1989).

DATE	LOCATION	SOIL TYPE	SOIL LOSS t ha^{-1}
AUGUST 1975	DARFIELD	CHERTSEY zl*	61
NOVEMBER 1975	RAKAIA	PAPARUA zl	20
APRIL 1981	WAIPARA	GLASNEVIN STONY zl	71
NOVEMBER 1984	CUST	WAIMAIRI PEAT	107
OCTOBER 1988	OXFORD	TEMPLETON zl	125

* zl indicates silt-loam soil texture.

2.1.2 The effects of wind erosion on agricultural productivity

Wind acts on many soils by removing the fine porous fractions and leaving the coarser, denser ones behind (Chepil, 1957). Silt and clay fractions are removed first, leaving the coarser sand and gravel. The largest soil particles return to the surface first. The fine sand then settles out, well sorted into a range of sizes. This sorting can also take place across humps and hollows within a paddock. When a crop is at maturity, or is water stressed, marked variations in growth result from wind-produced soil variability.

Sometimes wind erosion completely removes a layer of the surface soil (Chepil, 1957). Such non-selective removal by wind is associated with loess soils that were sorted and deposited from the atmosphere during past geological eras (Lyles, 1975; Skidmore, 1976). Wind erosion physically removes the most fertile portion of the soil, including lime, fertilizer, seed, and organic matter (Daniel and Langham, 1936) and, therefore, lowers productivity. The cultivated surface soil layer is disrupted and sometimes even young plants are removed. Blowing soil reduces seedling survival and growth, lowers the marketability of vegetative crops like asparagus, green beans and lettuce (Lyles, 1975) and increases the susceptibility to, and the transmission of, some diseases (Claflin et al., 1973). Dust obscures visibility and pollutes the air, causes traffic hazards, fouls machinery and threatens animal and human health (Skidmore, 1976).

The full economic costs of wind erosion are difficult to determine. Lyles (1975) described a procedure to determine the effects of wind erosion on crop production, by relating topsoil thickness or topsoil removed (excluding the effect of fertilizer) and then computing the potential average annual soil loss using the wind erosion equation (Woodruff and Siddoway, 1965). By converting annual soil loss into depth of soil removed, the corresponding loss in crop yield could be estimated. The procedure is limited by assumptions about factors in the wind erosion equation, the accuracy of the equation itself and by the requirement for yield-soil thickness data for the areas to which the approach is applied.

Shearer (1982) calculated the weight of soil nutrients lost with 100 tonnes of eroded soil (Table 2.2). The calculations are based on a soil representative of the

Hakataramea Valley which is a South Island area damaged severely by wind erosion. At current prices the equivalent amount of fertiliser required for short term nutrient restoration would cost in excess of \$1100 ha^{-1}. While the fertility losses might be overcome in the short-term by applying amendments, the poor soil structure, reduced water-holding capacity and reduced rooting depth are not easily repaired. On the shallow, drought-prone soils which are susceptible to wind erosion in Canterbury, depth of fine-textured soil material above the underlying gravels is often an important determinant of crop yield. Webb and Purves (1983) showed that on Wakanui, Templeton and Eyre soils a 1 cm increase in depth of topsoil corresponded to a 36 kg ha^{-1} increase in yield of oats and a 31 kg ha^{-1} increase in wheat yield. Follet and Stewart (1985) have reviewed wind erosion effects on crop productivity.

Table 2.2 Estimated nutrient loss in 100 tonnes of wind eroded soil from the Hakataramea Valley (after Shearer, 1982).

NUTRIENT	APPROX. WEIGHT PER 100 TONNES TOP SOIL kg	APPROX. EQUIV. FERTILISER WEIGHT t
TOTAL PHOS. TOTAL SULPHUR TOTAL MAGNESIUM	85 55 640	1.3 REVERTED SUPER PHOSPHATE
NITROGEN	355	0.8 UREA
TOTAL CALCIUM	1060	3.0 LIME
TOTAL POTASSIUM	1015	2.0 POTASSIUM CHLORIDE

2.2 The mechanics of wind erosion

2.2.1 The surface wind

The wind structure near the ground directly influences the movement of soil by wind, as well as the turbulent exchange of heat and water vapour between the soil and the atmosphere. The natural wind near the soil surface is a turbulent air flow with irregular fluctuations in motion (Wilson and Cooke, 1980). Mechanical turbulence is generated by the friction effects of the surface and thermal turbulence is the result of buoyancy effects (Monteith, 1973). A smooth surface is generally more erodible by wind than is a rough one, because it is less effective in reducing the wind velocity near the ground. A smooth surface reduces turbulence, but the effect that this turbulence has in reducing wind erodibility usually does not compensate entirely for the increased surface velocity (Chepil and Milne, 1941).

2.2.2 Soil particle movement

2.2.2.1 Modes of transport

Soil transport by wind occurs in three distinct modes: suspension, saltation and surface creep. The smaller particles move in suspension in the form of dust clouds, sometimes rising very high above the earth. Saltation is the process where soil particles jump into the air almost vertically, rise to a height of 15-30 cm, and return to the soil surface at an angle of between 6 and 12 degrees to the horizontal (Chepil, 1945) either to rebound or be embedded. Larger particles move by sliding and rolling in the process of surface creep. The size ranges of particles transported by the processes of suspension, saltation and surface creep are 0.002 to 0.1 mm, 0.1 to 0.5 mm and 0.5 to 1.0 mm respectively (Chepil, 1957). Suspension can account for between 3 and 40% of total transport, whereas saltation and surface creep can account for between 50 and 75% and between 5 and 25% respectively (Chepil, 1945).

Saltation is the major source of aggregate breakdown during wind erosion. The process also initiates and sustains suspension, drives surface creep transport, and influences the aggregate size distribution at the soil surface. The transfer of the particles and their degrading action increase downstream with distance from the origin of erosion (Chepil and Woodruff, 1963).

2.2.2.2 Wind velocity threshold

Different size materials have different velocity thresholds for movement in wind. Progressively faster air flow is required to move increasingly large particles. There is no single value of windspeed which is an appropriate threshold value for different field soils with different particle size distributions. In a mixture of particle sizes the threshold is determined by the dominant particle size range (Painter, 1976). In practice there are a wide range of threshold velocities for any soil (WMO, 1983). Recently cultivated, non-eroded soil contains a wide size range of particles. Very fine dust protects other erodible fractions, but is carried away in suspension faster than the larger, erodible particles. The latter are then affected, and their movement in saltation breaks down other, previously non-erodible clods, into susceptible material. With each wind storm (until all of the erodible material has been removed) the susceptibility of the soil increases and the threshold velocity decreases.

2.2.2.3 Particle geometry

Both size and density determine the weight of individual particles and therefore their erodibility (Chepil and Woodruff, 1963). At particle diameters larger than 0.1 mm lighter material is more erodible than heavy material. The most erodible particles of 2.65 $Mg\,m^{-3}$ density are about 0.1 mm in diameter. Sizes greater and smaller than 0.1 mm diameter are less erodible by wind (Chepil and Woodruff, 1963). Soil clods or aggregates that are just large enough not to be moved by wind are most effective in protecting the erodible soil particles (Chepil, 1958). Relatively few particles larger than about 0.84 mm in diameter are moved by commonly erosive winds (Chepil and Woodruff, 1963). The 0.84 mm square sieve opening has been used to separate the so-called 'erodible' from the 'non-erodible' soil fractions (Chepil and Bisal, 1943; Chepil, 1952).

2.3 Surface soil structure

2.3.1 Soil aggregation

Soil aggregates, composed of primary particles and binding agents are the basic units of soil structure. The soil pore size distribution is determined by the size, shape, arrangement and stability of soil aggregates. Thus, soil aggregation influences a wide range of soil properties (e.g. drainage and aeration) and, therefore, ultimately affects crop production as well as the risk of soil erosion.

2.3.1.1 Aggregate formation

The formation of aggregates is due mainly to physical forces such as wetting and drying, freezing and thawing, and the compressive and drying action of roots. Once the primary particles have been brought into close proximity to each other they are bound together, and thus stabilised, primarily by organic materials. These include the products of decomposition of plant, animal and microbial remains; the micro-organisms themselves; and the products of microbial synthesis (Lynch and Bragg, 1985).

2.3.1.2 Aggregate stability

Wind erodibility of a soil depends on the mechanical stability of the dry aggregates, as well as on their size, shape and density. Mechanical stability describes the resistance of a dry soil to breakdown by mechanical agents such as tillage, wind force, raindrop impact, and abrasion from windborne materials. Soils with a weak structure and ample initial supplies of erodible material can be rapidly abraded, thereby producing more erodible particles and aggregates and resulting in greater soil loss. Soil mechanical stability assumes greatest importance where large areas of bare soil occur (Chepil and Woodruff, 1963).

It is important to differentiate between the primary or water-stable aggregates and secondary aggregates or clods. Water-stable aggregates are often the product of breakdown from secondary aggregates. The two structural units have different degrees of mechanical stability and resistance to abrasion. Water-stable aggregates seldom exceed 1 mm diameter in cultivated soils and are held together by cementing agents which are insoluble in water. Secondary aggregates or clods generally exhibit less mechanical stability than water-stable aggregates. They are held together when dry primarily by water-dispersible cementing agents.

Aggregate stability can be assessed by wet-sieving techniques. Aggregates are submerged in water and the size distribution of the intact aggregates is measured following a period of sieve motion (Kemper and Rosenau, 1986). In the study of wind erosion, dry aggregate stability is of importance. Dry aggregate stability can be measured by repeated rotary sieving of dry aggregates (Chepil, 1962). The assessment of soil aggregate stability by wet-sieving gives an indication of the likely stability of the soil after a number of field wetting and drying events and as such gives a 'medium-term' indication of soil structural stability. Repeated dry-sieving differs in that it gives an indication of the structural stability at the time of sampling. While wet-sieving is a more appropriate technique for the assessment of soil structure in long-term soil management studies or in studies of water erosion, dry-sieving is a more appropriate assessment in the study of wind erosion.

2.3.1.3 The role of soil organic matter

Aggregate stability changes in response to soil organic matter levels and cropping sequences. The aggregate stability of a large number of agriculturally productive soils in England was measured, using wet-sieving techniques, by Chaney and Swift (1984). They concluded that soil organic matter was the major factor involved in aggregate stabilisation. Where a soil is cultivated frequently, previously inaccessible organic matter is exposed to micro-organisms, oxidation is stimulated and loss of organic matter is the result (Adu and Oades, 1978). The decline in organic matter is usually accompanied by a decrease in the number of water-stable aggregates (Tisdall and Oades, 1982). The stability of larger soil aggregates depends on the density of the roots and fungal hyphae which increases under pasture and decreases with arable cropping (Tisdall and Oades, 1982). The addition of straw, green manures and

farmyard manures lessens the rate of decrease of soil structural stability under arable farming, compared with no return of crop residues. However, the most effective way of building up organic matter levels is to leave an area in pasture (Morgan, 1986).

2.3.1.4 Soil aggregate breakdown

Some of the same processes which are instrumental in the formation of aggregates can contribute to their eventual breakdown. The processes of wetting and drying, as well as freezing and thawing in soil, can result in the production of a fine tilth suitable for planting a crop (Batey, 1988). However, if these processes lead to excessive breakdown of clods then the erosion risk can be increased. Rapid soil drying could cause non-uniform shrinkage producing cracks. On re-wetting, unequal swelling might occur producing further fragmentation. Repetition of this drying-wetting cycle causes a high degree of disintegration of cohesive soil clods. In soils with significant clay content alternate freezing and thawing can also cause fragmentation due to the expansion of water upon freezing.

Soil splash by falling raindrops is another process contributing to the breakdown in surface soil structure, which can, in turn, induce wind erosion. Raindrop impact can cause dispersion of surface soil material. On drying, the dispersed soil forms a surface crust which is more compact and mechanically stable than the soil below. Surface crusting, although a generally undesirable structural feature, can increase the wind velocity required to initiate particle movement.

2.3.2 Tillage-induced surface soil structure and crop production

Any significant change in soil structure due to tillage affects soil water, soil aeration, soil heat and soil mechanical resistance properties, as well as soil chemical and biological properties, in both the short and in the long-term.

2.3.2.1 Soil water

a) Infiltration and evaporation of water

The number and geometrical properties of water-conducting soil pores determine the effect of tillage on infiltration. Large, continuous, vertical soil pores, which open to the soil surface, enhance infiltration. The blocking of water conducting pores, as could occur with compaction or where there are unstable surface clods, decreases the amount of stored water and increases the risks of runoff and water-induced soil erosion (Unger and McCalla, 1980). Changes in soil water infiltration rate in response to tillage were considered by Ehlers (1975), Edwards (1982), Tisdall and Adem (1986) and others.

Evaporation can be reduced by a coarse soil structure on top of the tilled layer (Hillel and Hadas, 1972). A thick mulch layer has also been shown to be effective (Bond and Willis, 1969). Hillel and Hadas (1972) observed that field studies of the possible effects of tillage practices on water loss by evaporation were giving conflicting results. Ojeniyi and Dexter (1984) reported that low soil water content in a tilled soil, on a seasonal basis, could be attributed to the presence of 4-8 mm and 8-16 mm diameter voids and increased mean aggregate size and macro-porosity in the top layer of tilled soil. This could be due to reduced penetration of turbulent air currents into inter-aggregate cavities where voids are less than 4 mm diameter (Hillel and Hadas, 1972). In tilled soil with a coarse structure, daylight evaporative water loss was reduced compared to finer structured soil. However, during the night this trend was apparently reversed (Ojeniyi and Dexter, 1984). Soil surface roughness affects soil thermal properties and the energy balance (Allmaras et al., 1972; 1977; Cruse et al., 1980), solar radiation reflection (Bowers and Hanks, 1965; Allmaras et al., 1972; Cruse et al., 1980) and, therefore, evaporation (Allmaras et al., 1977; Linden, 1982).

The identification of the most important structural features determining water loss from a tilled soil would enable modification of tillage methods to conserve water for the survival of the seedling. It was noted by Wingate-Hill (1978) that relationships between soil structure and water supply had not progressed to the stage where it was possible to define, in any quantitative manner, tillage requirements for cereal crop production.

b) Water storage capacity

The amount of plant-available water (i.e. the volumetric water content between field capacity (soil matric potential of -33 kPa) and wilting point (-1500 kPa)) can be strongly affected by tillage and traffic (Boone, 1988). Severe deformation of wet soil (Boone et al., 1984), or extreme crumbling (Kuipers, 1961), could cause large increases in the water content at field capacity, possibly leading to reduced plant growth due to lack of aeration. A large water storage capacity, or total porosity, is desirable because it helps prevent temporary saturation after heavy rain thereby reducing surface aggregate slaking, runoff and water erosion.

c) Soil water movement

In order for water to be supplied to plant roots the soil must be readily able to transmit water to the root surfaces in response to potential gradients. Minimum hydraulic conductivity of the bulk soil must be around 10^{-4} to 10^{-5} mm day^{-1} if water supply is not to restrict plant development (Taylor and Klepper, 1975; Reicosky and Ritchie, 1976). The number, continuity and size of the largest soil pores or cracks, determines the saturated hydraulic conductivity (K_S) of the soil. Compaction will therefore decrease K_S. Pore discontinuities, caused by soil deformation when wet, can reduce K_S. Rapid water transport might enhance drainage to greater depths. Investigations into changes in soil hydraulic properties in response to tillage include those of Ehlers (1976); Douglas et al. (1980); Klute (1982) and Mielke et al. (1986).

2.3.2.2 Soil aeration

Slaking or puddling of a soil surface reduces gas diffusion. Rathore et al. (1982) reported a 50% reduction in the rate of oxygen diffusion in a soil within 24 hours of the formation of a wet soil crust. Surface sealing, in terms of gas diffusion, only occurs when all pores at the soil surface are water-filled. Oxygen diffuses through water at a rate approximately 10000 times slower than through air. Continuous air-filled pores are required in the soil down to the optimum depth of rooting of the plants (Boone, 1988). Typically, for normal plant development, at least 10% of the soil volume at field capacity is required to be gas-filled pores where at least 10% of the gas in these pores is oxygen (Dexter, 1988). In a soil with large, continuous pores, water infiltrates quickly and hence

the surface is sealed for a shorter period. Soil surface roughness affects soil air exchange (Allmaras et al., 1977).

2.3.2.3 Soil temperature

Surface radiation reflection, absorption and emission characteristics and aerodynamic roughness are all tillage-related factors affecting heat flux into and out of the soil. The processes involved in the interaction between micro-climate and the soil are complex, dynamic and not well documented for tillage effects (Cruse et al., 1982). Modification of the soil surface structure might allow earlier sowing by extending the period during which the seedbed is above a critical minimum temperature. Examples where tillage effects on soil temperature and heat balance have been measured include Allmaras et al. (1977); Cruse et al. (1982), and Gupta et al. (1984).

2.3.2.4 Soil mechanical impedance

a) Plant establishment

Tillage-induced soil structure directly influences the surface penetration of growing plant shoots and their subsequent success in establishment. Changes in soil mechanical impedance were discussed by Cassel (1982) and Cassel and Nelson (1985). Rainfall intensity and other climatic conditions interact with soil properties in determining the extent to which the soil surface is slaked and the mechanical strength of the surface crust at time of emergence (Rawitz et al., 1985). The uptake of water and oxygen by the establishing plant is determined by the properties of the soil in contact with, and in the immediate vicinity of, the emerging seed (Hadas and Russo, 1974a,b).

b) Root growth

Roots growing through the soil take the path of least mechanical resistance, often growing through continuous cracks, large pores and along planes of weakness. Stratification of soil structure by the creation of a seedbed or of a ploughpan (Ehlers et al., 1980), or abrupt changes in soil texture with depth, modifies this root-mass distribution. In a dense soil, the artificial modification of the number, dimension and

distribution of large pores and cracks could greatly change the rooting pattern and the root density (Boone, 1976).

2.3.2.5 Soil nutrient factors

The availability of nutrients with depth is affected by the degree of soil inversion by tillage. Generally, when a soil is inverted deeper than the arable layer, less fertile soil is brought to the surface. In addition to slower early plant growth due to a lower nutrient concentration, a lower surface organic matter content could increase the risk of surface slaking or wind erosion. Changes to the soil water balance or to the plant root distribution which might occur as a result of tillage will have indirect effects on the plant availability of nutrients.

2.3.2.6 The ideal seedbed from an agronomic perspective

Authors disagree on which range of aggregate size provides the ideal seedbed (Adem et al., 1984), but most suggest low amounts of particles less than 0.5 mm diameter and clods larger than 20 mm diameter. Desirable aggregate sizes quoted vary from 1 to 5 mm, 2 to 3 mm, 1 to 10 mm diameter, 50% aggregates 3 to 6 mm diameter and the rest smaller, and 75% aggregates 1 to 12 mm diameter (Russell, 1973; Taylor, 1974). It is important that there is always less than 15% of fine material (<250 μm) which can block the larger pores (Dexter, 1988). The seedbed should provide adequate soil-seed contact for water supply to enable swelling and germination, and also adequate aeration. A broad requirement is for 10% of the soil volume to be in pores larger than 30 μm for aeration, and a maximum volume of pores between 30 and 0.2 μm for water storage (Dexter, 1988). The optimum environment for germination and early growth is needed only in the vicinity of the seeds. The seedbed might require larger aggregates nearer to the surface for the prevention of water and wind erosion. Uniform depth of seeding is required for uniform crop development (Boone, 1988). The definition of the soil condition needed for agronomic objectives and the development of soil dynamics for prescribing the soil manipulation which will produce the desired soil condition, is an important priority in agricultural research (Schafer and Johnson, 1982).

2.3.3 Tillage and soil structure

Tillage is used to prepare seedbeds, incorporate amendments, control weeds and pests, enhance infiltration, conserve water and control erosion. Excessive and improper tillage often causes excessive soil loosening and pulverisation increasing the risks of erosion by wind (Woodruff and Chepil, 1956).

2.3.3.1 Soil-implement relations

Tillage tools are designed to apply an upward force to cut and loosen compacted soil, sometimes to invert and mix it, and to smooth and shape the surface. Cooper (1971) described the mechanical reactions of the soil to tillage as follows: (a) parting of the soil particles due to insertion of the tillage tool; (b) compressing the soil due to the force applied to the soil and its resistance to motion; (c) shearing the soil due to indirect tension forces resulting from compressive forces; (d) bending, twisting, or transporting the soil dependent on the shape of the tool and the material; (e) accelerating due to, or transporting dependent on, the shape of the tool and the material.

The reaction of the soil to tillage operations is dependent on soil physical properties and conditions such as soil water content, aggregate and bulk strength, plant residue content, and soil texture. There is a need for improved prediction of post-tillage soil structural state, and consequent soil mechanical, hydraulic and thermal properties (Hadas et al., 1988). Soil water content is significant in influencing soil strength. The mechanical forces of tillage easily compact a wet soil which will flow in a manner consistent with a plastic material. The strength of an excessively dry soil is such that fracture can only be induced by applying large forces to break large clods from the soil mass (Gill, 1967). In very dry, brittle, clod-forming soil, the fragmentation process with moldboard ploughing is through brittle fracturing of the moving clods and by abrasive action between the clods themselves and between clods and the share surface. Fragmentation is not achieved, in such soils, by the cutting and shearing of the sliced soil, as is commonly accepted for moist, ductile soils (Wolf and Hadas, 1987).

Soil consistence state is, therefore, one of the most important criteria determining ease of seedbed preparation. As soil water content increases from the friable to the

plastic range, resistance to compaction and smearing decreases and implement draught increases (Archer, 1975). As soil water content decreases from the friable range to the hard range, cultivations tend to re-arrange aggregates but do not produce a satisfactory tilth unless very high forces are applied (MAFF, 1982). Utomo and Dexter (1981) and others found that soil was most friable when the water content of the soil was at about the lower plastic limit.

A stochastic procedure for predicting tillage-induced soil porosity was proposed by Dexter (1976). This prediction of soil voids accounts for implement characteristics, management practice, soil water content at time of tillage, consecutive implement passes, depth of operation, and compaction or rearrangement of soil units. Applicability has not been tested adequately because many measurements are needed to provide a new calibration for each crop management site and parameter involved (Hadas et al., 1988).

2.3.3.2 Primary and secondary tillage

A standard or conventional tillage system involving moldboard ploughing (primary tillage), secondary tillage with one or more passes using spring-tined cultivators and rigid-tined harrows followed by planting, has been used extensively on a wide range of Canterbury soils (Stringer pers. com., 1986). Seedbed consolidation by rolling is sometimes included in the tillage system. The moldboard plough has been suggested as the most suitable primary tillage implement for effective, cost efficient weed control (Patterson, 1982; Traulsen, 1982). An increase in weed growth on replacement of the moldboard plough by a tined implement has been reported (McClean, 1980; Traulsen, 1982). Ploughing buries weed seeds to a depth from which emergence is unlikely.

A single pass of a tillage implement is usually insufficient to form a good seedbed from settled soil. Multiple implement passes are therefore used to create the desired soil condition. Secondary cultivation forms the seedbed, resulting in decreased surface roughness and aggregate size due to fragmentation, and removes weeds. Ojeniyi and Dexter (1979b) reported that the first pass of an implement produces most of the soil break-up although further break-up is caused by the second pass. The third and subsequent implement passes do not cause much further change in soil structure and appear mainly to stir up what is already there. Aggregates tend to be sorted, with the

smaller ones tending to sink to the bottom of the tilled layer and the larger ones tending to rise to the surface (Ojeniyi and Dexter, 1979b). This sorting process is beneficial with a zone of fine structure where the seed will be sown and roots will proliferate, and a zone of coarse structure at the surface which will reduce erosion by wind and water and which will impede the formation of surface crusts (Ojeniyi and Dexter, 1979b). This process is well known and practised but there is still little quantitative information available on the effects of multiple implement passes on soil macro-structure (Ojeniyi and Dexter, 1979b; Hadas and Wolf, 1983). Although some workers have reported the effect of tillage on surface roughness (e.g. Allmaras et al., 1966; Currence and Lovely, 1970) many researchers ignore this important aspect when evaluating tillage management. Further research is required in this area to evaluate the effects of tillage-induced soil roughness on the soil water and soil thermal regimes as well as on soil erosion.

Chisel ploughs are gaining acceptance as primary tillage implements, especially on stony soils. In a comparison of moldboard ploughing with chisel ploughing, Kouwenhoven (1986) observed only slight differences in seedbed quality on light, medium and heavy-textured soils. Chisel ploughing produced greater surface roughness and a higher degree of crumbling although surface trash caused some difficulty with subsequent seedbed preparation and sowing. Shallow chiselling improves water intake, soil water storage, and reduces erosion (Oschwald, 1973; Wischmeier, 1973) as compared to moldboard ploughing.

2.3.3.3 Tillage and soil water content.

Tillage at different soil water contents produces seedbeds with different aggregate size distributions (Lyles and Woodruff, 1962; Hoyle et al., 1972; Ojeniyi and Dexter, 1979a,b; Adem et al., 1984; Tisdall and Adem, 1986). Lyles and Woodruff (1962) reported that for a silty-clay-loam soil more erodible particles (<0.84 mm diameter) and fewer large clods were created by primary tillage at intermediate soil water contents (15-23%, no lower plastic limit reported). Wet-sieving analysis however, showed no measurable effect of soil water content at time of primary tillage on the proportion of water-stable aggregates less than 0.84 mm in diamter. The differences in aggregate size distribution which occurred due to soil water content at primary tillage were quickly obliterated by weathering, especially with high rainfall, and by secondary tillage

operations during which no soil water content treatments were imposed. Lyles and Woodruff (1962) found that tillage differences on aggregate size and stability due to type of implement were greater than, and persisted longer, than did differences due to soil water content at time of tillage. Clods formed at low soil water content had three to four times more resistance to crushing than those formed at high water contents (> 16% w/w).

Hoyle et al. (1972) reported that when a wet soil is tilled with a rotary cultivator, aggregates larger than 12 mm in diameter were broken down and aggregates less than 0.5 mm in diameter were bound together into aggregates no larger than 12 mm in diameter. Bhushan and Ghildyal (1972) examined the mean weight diameters of aggregates produced by moldboard ploughing a lateritic sandy-loam soil. Tillage was done at water contents corresponding to 0.60, 0.77 and 0.99 times the lower plastic limit. They found that a more cloddy seedbed was more often produced by tillage at 0.60 and 0.99 times the lower plastic limit than at 0.77 times the lower plastic limit although there were differences between ploughs with different moldboard design. With some ploughs, the cloddiness appeared to be still decreasing at water contents of 0.99 of the lower plastic limit.

Ojeniyi and Dexter (1979a) showed large effects of tillage management and cropping history on the structure of a loam soil (hard-setting phase of a red-brown earth). The effect of water content on the aggregate size distributions produced from tilling to a depth of 8 to 10 cm with a tined implement, as observed by Ojeniyi and Dexter (1979a), is shown in Table 2.3. They found that a chisel plough produced a maximum number of small aggregates and a minimum number of large voids at a moisture content of approximately 90% of the lower plastic limit. Ojeniyi and Dexter (1979b) showed that consecutive passes with tillage implements reduced the aggregate size, with a second implement pass having more effect on soil structure when soil water content was at 1.3 times the lower plastic limit, than when it was at 0.65 times the lower plastic limit. Ojeniyi and Dexter (1979a,b) quantified the structure of a tilled soil by using samples impregnated with paraffin wax (Dexter, 1976) which were cut into sections before aggregate and void size distributions were calculated (Dexter and Hewitt, 1978). Johnson et al. (1979) observed that ploughing a wet silt-loam to silty-clay-loam soil increased soil surface roughness and that clods resulting from ploughing wet soil showed lower wet-stability than clods formed from ploughing nearer the lower plastic

limit. They also reported a decrease in pore space in soils ploughed at water contents above the lower plastic limit, as would be expected if compaction was occurring.

Table 2.3 Aggregate size distributions following tillage of a loam soil at different water contents with a tined implement (after Ojeniyi and Dexter, 1979a).

AGGREGATE SIZE (mm)	PROPORTION OF AGGREGATES LARGER THAN SIZE INDICATED AFTER TILLAGE AT GIVEN WATER CONTENT					
	WATER CONTENT AS PROPORTION OF PLASTIC LIMIT					
	0.55	0.65	0.81	0.87	0.94	1.3
1	0.97	0.98	0.92	0.91	0.96	0.89
2	0.88	0.82	0.75	0.67	0.90	0.75
4	0.78	0.63	0.57	0.46	0.66	0.58
8	0.61	0.44	0.42	0.30	0.45	0.41
16	0.39	0.22	0.22	0.13	0.21	0.21
32	0.15	0.06	0.06	0.03	0.04	0.07
64	0.02	0.01	0.01	0.00	0.00	0.01

Adem et al. (1984) described a system in which the secondary tillage operations are undertaken when the soil is wet and friable using a specialised tined implement, so allowing the seed to be sown into wet soil after a small number of implement passes. They reported that on a fine sandy-loam soil there was a relationship between water content at tillage and the percentage of aggregates less than 0.5 mm diameter and 10-20 mm diameter, but little or no relationship with intermediate size fractions. As the water content of the soil increased from 13% (w/w) to 22% (w/w) (lower plastic limit was 19.7% w/w), the percentage of aggregates less than 0.5 mm diameter decreased by 44% and the percentage of aggregates 10-20 mm diameter increased by 34%. Therefore, as the water content increased, tillage either (a) bound up more aggregates less than 0.5 mm diameter into larger aggregates, or (b) broke up fewer aggregates 10-20 mm diameter into finer aggregates.

In most of the investigations on soil structural changes due to tillage and on the effects of soil water content at tillage, soil structure has been described using aggregate size distributions from dry-sieving. Sieving, although especially useful in wind erosion

studies, gives no information about the soil pore size distribution. Data on the relationships between water content, matric potential and hydraulic conductivity in freshly-tilled soil are practically non-existent (Linden, 1982).

2.3.3.4 Conservation tillage

Conventional tillage might not be suitable for soils with a high clay content, or for soils with poor structural condition. Conventional tillage of heavy soils could result in a compacted zone of soil being developed below the depth of ploughing. This plough pan can restrict the growth of plant roots and limit the movement of water and air through the soil (Batey, 1988). Very dry soils with high sand contents might also be poorly suited to conventional cultivation. In this circumstance, tillage might pulverise the surface soil, producing on drying, a fine tilth readily susceptible to erosion by wind.

To overcome these adverse affects, tillage operations can be restricted by reducing their number or by carrying out as many operations as possible in one pass (minimum-tillage), by tilling only the rows where the plants grow and leaving the remaining area untilled (strip-zone tillage), by leaving a large percentage of residual plant material on or near the surface as a protective mulch (mulch-tillage), or by not tilling and drilling the seed directly into the stubble of the previous crop thereby relying on herbicides for weed control (no-tillage). Collectively these tillage systems are termed conservation tillage systems. A conservation tillage system is one in which either crop residues are retained on or near the surface, or soil roughness is maintained, or both, to control soil erosion and to achieve good soil-water relations (Allmaras et al., 1985). Conservation tillage was considered by the USDA in 1980 as 'the most economical and effective means of soil erosion control' (Allmaras and Dowdy, 1985).

The success of different conservation tillage systems is highly soil-specific and also dependent on how well weeds, pests and diseases have been controlled. The results from conservation tillage systems have been variable (Davies and Cannell, 1975; Cannell et al., 1980; Unger and McCalla, 1980; Chaney et al., 1985) and this has probably contributed to a reluctance to include such techniques in New Zealand arable farming systems. Economic analysis of conservation tillage systems indicate that there are significant short-term economic penalties and risks associated with conservation tillage systems (Jolly et al., 1983; Ladewig and Garibay, 1983; Napier et al., 1984).

Farmers are reluctant to adopt conservation tillage systems because of uncertain and complex technology inputs and increased risk. Unless yield gains are substantial, there is insufficient incentive to assume the risk.

2.4 Surface soil water

2.4.1 The effect of soil water content on soil erodibility to wind

Soil with a moist upper layer has increased resistance to soil loss by wind erosion (Chepil and Woodruff, 1963). Soil erodibility by wind is a function of the cohesive force of the water films surrounding the discrete soil particles. This very effective cohesive force between erodible particles increases directly with water content. One of the main problems of studying the influence of soil water on erosion processes is to determine the greatest possible water content below which wind erosion is possible, often termed the 'critical water content'. Another important question is the determination of the length of the time interval during which the soil's moisture properties, which protect it from wind action, are preserved. Little attention has been given to this question and there are few studies (Businger, 1975) in which attempts been made to determine the critical soil water content.

Wind erosion is likely to be significant only if the soil surface is 'very dry' according to qualitative judgement (WMO, 1983). Table 2.4 illustrates the effect of different equivalent water contents on movement of soil at three levels of wind velocity at 15 cm above the surface (equivalent water is defined as the ratio of soil water content to soil water content at -1500 kPa matric potential). A large increase in windspeed is required to move discrete soil particles when their water content is increased even slightly above the -1500 kPa percentage.

Table 2.4 Effect of equivalent water content on rate of soil erosion (silt-loam soil) in g m^{-1} (width) s^{-1} (adapted from Chepil and Woodruff, 1963).

EQUIVALENT WATER*	WIND VELOCITY (km hr^{-1}) at 15 cm		
	32	42	51
0.01	31.5	60.5	82.0
0.25	29.5	63.0	78.0
0.29	23.5	59.0	71.0
0.34	23.0	54.0	64.0
0.71	6.8	29.0	39.0
1.03	0.2	4.9	4.0

* Equivalent water is the ratio of actual soil moisture content to the moisture content at -1500 kPa matric potential.

2.4.2 The surface energy balance

Solar radiation received at the earth's surface is the major component of the surface energy balance. Solar radiation (R_S) reaches the outer surface of the atmosphere at a nearly constant flux of about 1350-1400 W m^{-2}. Nearly all of this radiation is of wavelength range 0.3-3.0 μm and about half of this is of 0.4-0.7 μm (visible) wavelength (Monteith, 1973). The earth also emits radiation but of lower intensity and greater wavelength (3-50 μm) than solar radiation. The radiation from the sun and the earth are referred to as shortwave and longwave radiation respectively. The atmosphere reflects, absorbs and scatters the incoming R_S and hence about 50% of the original flux density reaches the ground. A part of the previously reflected and scattered radiation also reaches the ground. The total of these two sources (termed direct and diffuse radiation) is referred to as global radiation. Of the shortwave radiation incident on a surface, a proportion is reflected back into the atmosphere (shortwave albedo). In addition to these shortwave radiation fluxes, there is also a longwave radiation (heat) exchange. The earth emits radiation and at the same time the atmosphere absorbs and emits longwave radiation, a part of which reaches the surface. The difference between these outgoing and incoming radiation fluxes is the net

longwave radiation. Net longwave radiation is a small part of the total radiation balance during the day, but at night, in the absence of direct R_s, the heat exchange between the land surface and the atmosphere dominates the radiation balance. The difference between the outgoing and the incoming radiation (including both short and longwave components) is termed net radiation (R_n); it expresses the rate of radiant energy absorption by a land surface.

The partitioning of the absorbed radiant energy is described by the energy balance equation:

$$R_n = L_vE + H + S + M \qquad \ldots (2.1)$$

where L_vE is the proportion of energy absorbed as latent heat in the processes of evaporation and transpiration (a product of the rate of water evaporation, E, and the latent heat of vaporization, L_v). H is the flux of sensible heat between surface and air; S is the flux of heat into or out of the soil, water and vegetation; and M is a miscellaneous energy term accounting for processes such as photosynthesis and respiration. The major portion of the total daily net radiation goes into latent and sensible heat. The proportionate allocation of these terms depends on the availability of water for evaporation. In most agriculturally productive areas the latent heat term dominates the sensible heat term.

2.4.3 Shortwave albedo

When radiant energy is incident on a soil surface it is distributed through the processes of reflection and absorption. Shortwave albedo, or reflectance, is defined as the proportion of the solar radiation incident on a surface which is reflected away from that surface. The various thermally-dependent soil processes such as evaporation, are influenced by shortwave albedo. An understanding of the relationships between shortwave albedo, surface soil colour, surface soil moisture and soil aggregate size distribution is therefore essential for the accurate prediction of evaporation and surface soil moisture content. A review of the reflectance properties of soils was given by Baumgardner et al. (1985).

2.4.3.1 Factors affecting shortwave albedo

a) Solar radiation angle of incidence and wavelength

The shortwave albedo of most surfaces varies both with the wavelength and angle of incidence of the light rays. Coulson and Reynolds (1971) reported that the reflectance from soils generally increases with increasing wavelength throughout the 0.320-0.795 μm region. Shortwave albedo over snow-free surfaces is a function of the angle of incidence of the solar radiation, with the highest values often occurring near sunrise and sunset. The reflectance of most surfaces appears to reach a maximum at sun elevations of 10-20^{o}. While this would explain the decrease of reflectance with increasing sun elevation, a second contributing effect is the rapid shift in ratio of direct to diffuse light which occurs at low sun elevations. The decrease of reflectance with increasing sun elevation, which sometimes occurs from surfaces of a complex nature, probably occurs because part of the incident radiation is trapped within soil crevices (Coulson and Reynolds, 1971).

b) Soil organic matter, soil water content, and soil water potential

A colour effect on soil temperatures is often observed. The elevated daytime temperatures of dark-coloured soils are attributed to their greater absorption (and hence less reflectance) of solar radiant energy. Since organic matter is one of the primary soil colouring constituents, its absence or presence will influence reflectance. Baumgardner et al. (1985) reported that organic matter content plays a dominant role in bestowing spectral properties upon soils when the organic matter content exceeds 2.0%. As the organic matter content drops below 2.0% it becomes less effective in masking the effects of other soil constituents on reflectance.

The relation between reflectance and soil water content has been studied for a variety of soils by a number of different researchers (e.g. Bowers and Hanks 1965; Dolgov and Vinogradova, 1973; Graser and van Bavel, 1982; and Idso et al., 1975). Angstrom (1925) (as cited by Graser and van Bavel, 1982) suggested that radiation is absorbed while being transmitted through the soil water films before and after reflection from the soil particles. In addition, he proposed that radiation is trapped in the soil water

films by total internal reflection. Angstrom quantified this mechanism with the following relationship:

$$a_w = \frac{a_d}{\left[n^2 \times (100 - a_d) + a_d\right]} \times 100 \qquad \ldots (2.2)$$

where a_w and a_d are the albedo of wet and dry soil (%) and n is the index of refraction of water, usually taken as 1.33 at 589 nm (Graser and van Bavel, 1982).

The mechanism of total internal reflection proposed by Angstrom (1925) (as cited by Graser and van Bavel, 1982) does not refer to a specific water film thickness, but instead only to wet and dry soils. This concept is consistent with the abrupt change in albedo found, although no criterion to distinguish effectively wet soils from effectively dry soils has been found.

2.4.3.2 A predictive model for shortwave albedo

Cruse et al. (1980) described a model for simulating the multiple reflection process of solar radiation absorption into soil. The generation of a model surface (Linden, 1979) was based on soil surface random roughness. The amount of radiation absorbed through a double reflection process was determined. The amount of incoming solar radiation striking the model surface, which was absorbed initially, was based on the value of the soil reflection coefficient for a smooth soil at the existing water content. The portion of the incoming solar radiation which was not absorbed was reflected in a semicircular pattern of uniform intensity. That portion of reflected radiation which fell below the peak of adjacent elements underwent a second absorption-reflection process. Radiation reflected from the second surface element was assumed lost to the atmosphere.

Field research is required to quantify the magnitude of the changes in soil reflectance which might result from tillage operations. Research is also required to show the net effects on the soil water and soil thermal regimes which might result from tillage-induced changes in soil reflectance.

2.4.4 Soil heat flux

Soil temperature is affected by the energy exchange processes which take place through the soil surface. The effect of these processes on the soil profile is dependent on the various transport processes, which themselves are affected by soil properties. Heat flow through the soil is important in the energy balance and hence affects evaporation. Steady state heat conduction through a homogeneous solid body is proportional to the temperature gradient and is described by Fourier's law (Marshall and Holmes, 1988):

$$S = - \lambda \frac{dT}{dz} \qquad \ldots (2.3)$$

where T is temperature (K), λ is thermal conductivity, z is distance in the vertical direction, and S is the amount of heat conducted across a unit cross-sectional area in unit time (flux density of heat). When S is in units of J m^{-2} s^{-1} the temperature gradient, dT/dz, is expressed as K m^{-1} and therefore thermal conductivity, λ, has units of J m^{-1} $s^{-1}K^{-1}$ or W m^{-1} K^{-1}. In the field, soil temperature and the temperature gradients are generally not steady. The continuity equation is, therefore, used in combination with the Fourier equation to describe the non-steady temperature regime. The continuity equation is obtained by equating the differences between the amount of heat entering and leaving a volume of soil in unit time, with the change in heat content of that soil in unit time (i.e. the law of energy conservation). Combining Equation 2.3 and the continuity equation (Marshall and Holmes, 1988) yields:

$$\frac{\partial T}{\partial t} = \left[\frac{\lambda}{\rho_b c}\right] \frac{\partial^2 T}{\partial z^2} \qquad \ldots (2.4)$$

where c is the specific heat capacity of the soil, ρ_b is bulk density, and t is time. The equation describes the conduction of heat through a body with conductivity, λ, and volumetric heat capacity, C (= ρ_b x c). In order to solve these equations, the soil thermal properties C and λ need to be evaluated.

2.4.4.1 Volumetric heat capacity

The volumetric heat capacity of a soil (C) is the change in heat content of a unit bulk volume of soil per unit change in temperature (J m^{-3} K^{-1}). The volumetric heat capacity of a soil depends on the relative volume fractions of the soil constituents i.e. water, air, mineral solids and organic solids. The value of C is given by the addition of the heat capacities of the various constituents, weighted according to their volume fractions (de Vries, 1963).

2.4.4.2 Thermal conductivity

Thermal conductivity (λ) is the amount of heat transferred per unit area in unit time under a unit temperature gradient (W m^{-1} K^{-1}). The thermal conductivities of the various soil constituents vary markedly and hence the average thermal conductivity of a soil volume depends on its mineral composition, organic matter content, and volume fractions of water and air. Air is a poor conductor and in soil it reduces the effectiveness of the solid and liquid phases in conducting heat. The solid phase has the highest conductivity and hence a reduction in bulk density, which could occur from tillage, will result in a decrease in conductivity (Figure 2.1). Water content has a large effect on average conductivity of a soil. As water replaces air in a soil, it provides bridges between particles that greatly increase the conductivity (Figure 2.1). Tillage and soil water content then, have large effects on the flow of heat into the soil and hence on the entire thermal regime. De Vries (1963) suggested a method to calculate thermal conductivity. The overall thermal conductivity of a soil is a function of the specific conductivities and volume fractions of the soil constituents, but is also dependent on the size and shape of the soil particles and on their packing arrangement. The de Vries approach was expressed for an unsaturated soil by van Bavel and Hillel (1976) as:

$$\lambda = \frac{f_w\lambda_w + x_s f_s \lambda_s + x_a f_a \lambda_a}{f_w + x_s f_s + x_a f} \qquad \ldots \quad (2.5)$$

where λ_w, λ_a and λ_s are the specific thermal conductivities of water, air and the mean value for soil solids respectively. The factor x_s is a shape factor, which represents the ratio between the space average of the temperature gradient in the solid relative to the liquid phase. The value of x_s depends on the array of particle shapes, as well as on

mineral composition and organic matter content. The x_a factor is the corresponding ratio for the thermal gradient in the air and water phases. Volume fractions of water, soil solids and air are designated f_w, f_s and f_a respectively.

Figure 2.1 Effect of water content and bulk density on the thermal conductivity of a loam soil (after Marshall and Holmes, 1988).

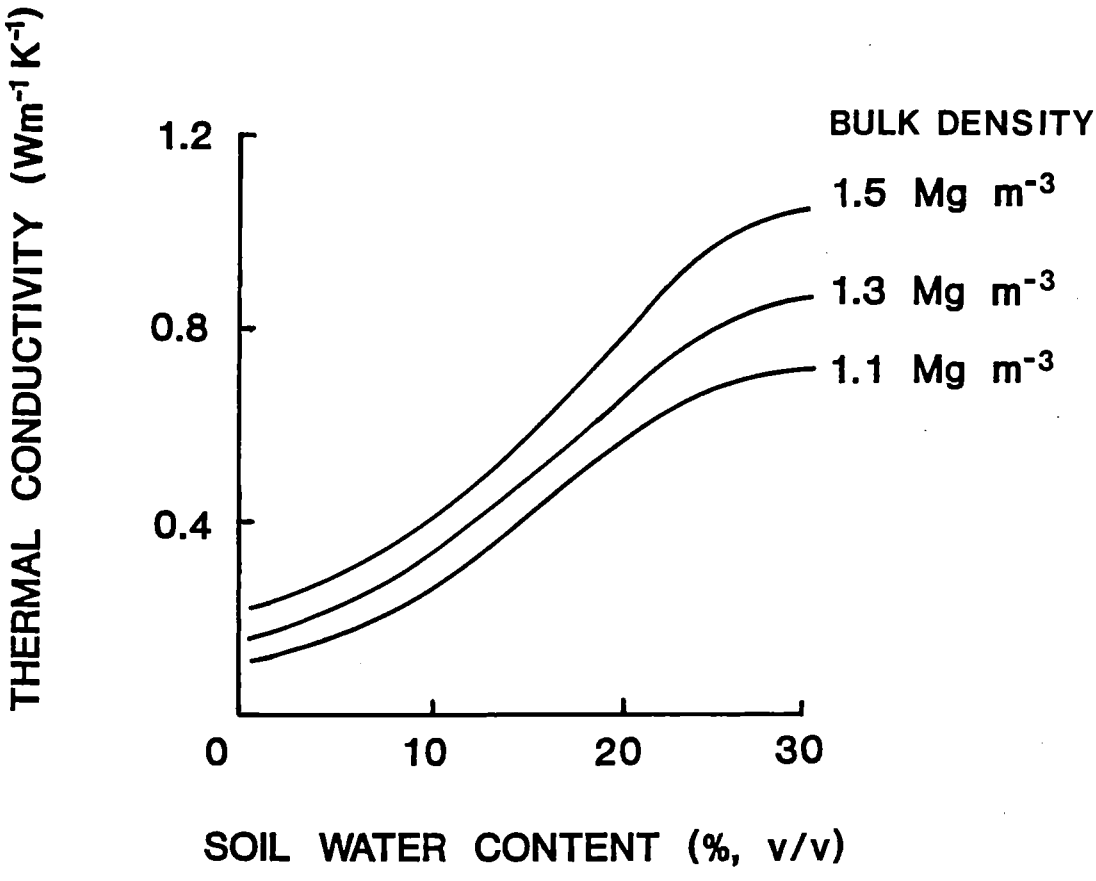

De Vries and Philip (1986) reported that the de Vries model can predict soil thermal conductivity with an accuracy of 5 to 10% depending on the soil water content. In using the de Vries model the thermal conductivity of the saturated soil should preferably be measured to check on the shape factors of the solid particles. In general, the defining of the shape factors is the most difficult problem in using the de Vries

model. However, the results from the de Vries model are not very sensitive to the values assigned to the shape factors (G.D. Buchan, pers. com., 1989).

A significant amount of heat can be moved by the bulk flow of liquid water in the soil (Kimball and Jackson, 1979). As the soil dries, water content gradients can become large and diffusion of water vapour can become significant; soil heat is moved with this water vapour. The influence of latent heat transfer by water vapour in the air-filled pores is proportional to the temperature gradient in these pores. It can be accounted for by adding an apparent conductivity due to evaporation, transport and condensation of water vapour to the thermal conductivity of air (van Bavel and Hillel, 1976; Hillel, 1977). This value is strongly temperature-dependent, rising with increasing temperature.

2.4.5 Soil water evaporation

2.4.5.1 Introduction

Soil evaporation commonly occurs under unsteady conditions and results in a net loss of water from the soil. Three physical conditions are necessary in order that water evaporation can occur: (i) there must be a continual supply of energy to the soil evaporating sites, (ii) there must be a vapour pressure gradient away from the surface, (iii) the water must be able to move through the soil to the evaporating surfaces. It was reported by Idso et al. (1974) that three stages of soil drying can occur in naturally varying field conditions. An initial constant-rate stage occurs early in the process while the soil is wet and conductive enough to supply water to the site of evaporation at a rate equal to the evaporative demand. During this stage, the evaporation rate is limited by external meteorological conditions (i.e. radiation, wind, air humidity etc.) rather than by the properties of the soil profile. The evaporation rate during this stage could also be influenced by processes dependent on soil surface conditions (e.g. shortwave albedo, windspeed and turbulence). In a dry climate, this stage of evaporation is generally brief and might last only a few hours or at most a few days.

An intermediate falling-rate stage occurs during which the evaporation rate falls progressively below the potential rate. At this stage the evaporation rate is limited by the rate at which the gradually drying soil profile can deliver water toward the

evaporation zone. This soil profile-controlled stage might persist for a much longer period than the first stage. During second stage drying, soil evaporation decreases approximately as the square root of the time elapsed (Ritchie, 1972; Gardner, 1974).

A residual slow-rate stage is established eventually and could persist at a nearly steady rate for many days. This stage comes about after the surface zone becomes so desiccated that further liquid water conduction through it effectively ceases. This stage 3 drying appears to be initiated at a surface water content that corresponds to a retention of two molecular layers of water about the soil particles at that level (Idso et al., 1974). Water transmission through the desiccated layer therefore occurs primarily by the slow process of vapour diffusion. This vapour diffusion stage can be important where the surface layer is such that it becomes quickly desiccated (e.g. a loose assemblage of clods).

During seasons of low evaporative demand oscillation between stages 2 and 3 might continue for several days. Hence in the field, evaporation is not constant, but intermittent as it fluctuates diurnally and varies from day to day. It can become difficult or impossible to distinguish between the stages described above. The resulting course of evaporation might not be described accurately by a simplistic theory based on the assumption of constant evaporativity. To account for the effect of varying meteorological conditions on evaporation dynamics, it is useful to construct a simulation model capable of monitoring the process continually through repeated cycles of increasing and decreasing evaporativity. Such a modelling approach might help to clarify the influence that diurnal variation in evaporativity has on the overall quantity of evaporation and water distribution in space and time.

2.4.5.2 Climatic influences on evaporation

a) Net radiation and sensible heat advection

Net radiation (R_n) is the major source of energy for evaporation. In humid regions, net radiation generally sets the upper limit on the amount of energy partitioned into L_vE. The availability of water determines the partitioning of energy among the sensible, latent and soil heat fluxes. In a wet soil almost all energy supplied is

consumed as latent heat. With a dry surface, latent heat is much reduced and sensible heat dominates the partitioning (Fritschen and van Bavel, 1962).

The advection of heat, which is the transport of energy horizontally, solely by the wind, normally occurs in the natural environment. In such conditions, latent heat flux exceeds the sum of net radiation and soil heat flux. Sensible heat advection can be a major source of energy for evaporation. Sensible heat advection, on a regional scale, has been shown to be a major component of the energy balance in regions of USA (Rosenberg, 1969a,b, 1972). Local scale advection occurs when the wind blows across a surface that is discontinuous in temperature, humidity, or roughness, as from a dry field to an adjacent irrigated field.

b) The wind

The wind has a large influence on the evaporative process. Strong winds increase turbulence which reduces the aerodynamic boundary layer resistance. The wind moves vapour-laden air away from the evaporation sites, thereby maintaining a vapour pressure gradient away from the soil surface. The wind transports sensible heat in the advection process. Wind-breaks can result in reduced evaporation from wet surfaces by reducing windspeed (Skidmore and Hagen, 1970).

c) Humidity

Evaporation is influenced by the water vapour content of the nearby air. If the air is saturated, evaporation will not occur. Evaporation increases in response to an increasing difference between vapour pressure at the evaporating surface and vapour pressure of the air.

d) Temperature

The evaporation process is influenced by the temperature of the air and/or that of the evaporating surface. In general, the higher the temperature, whether of the air or the evaporating surface, the higher the evaporation. The amount of water vapour that air can hold increases exponentially with temperature. If soil surface temperature increases, then the vapour pressure at the evaporating surface increases, as does the

vapour pressure deficit between the surface and the air. Thus, evaporation demand is increased. The water supply must be sufficient to nearly saturate the air at the evaporating surface for this vapour pressure deficit increase to occur.

2.4.5.3 Soil water flux

a) Soil water theory

The storage and movement of water and air in the soil is dependent on the system of pores between soil particles and aggregates. The dry bulk density of a soil (ρ_b) is defined as the mass of oven dried soil per unit volume of soil, and has units of g cm^{-3} or Mg m^{-3}. Soil particle density (ρ_p) is the mass of solid particles per volume of solid particles and has the same units as bulk density. The total pore volume per unit volume of soil, total porosity (e_T) is defined thus:

$$e_T = 1 - \frac{\rho_b}{\rho_p} \qquad \ldots (2.6)$$

The porosity consists of an air-filled and a water-filled portion. Soil water content can be defined on a mass (g g^{-1}) or on a volume basis (g cm^{-3}, m^3m^{-3}). Methods for determining soil water content were reviewed by Schmugge et al. (1980), Gardner (1986) and Stafford (1988).

Water is retained in the soil matrix by molecular adsorption on the surface of particles and by capillarity in soil pores. Differences in potential energy of soil water between two positions causes water to flow in soil. The total potential of soil water (ψ_t) is the sum of the gravitational potential (ψ_g), matric (or pressure) potential (ψ_m), and osmotic potential (ψ_o). Hydraulic potential is defined as the sum of the pressure and gravitational components only. Gravitational potential of soil water is determined by its elevation relative to some reference level (usually the soil surface). Matric potential arises from the interaction of soil water with the solid soil matrix. Osmotic potential arises from the presence of solutes in soil water. For water moving as a liquid through soil, the force is equal to the gradient of the hydraulic potential. Soil water potential per unit volume is expressed in units of kPa.

The relation between soil water content and soil water potential is termed the water characteristic or water retention curve. The amount of water held by a soil at any potential is influenced by soil texture, structure, organic matter content and by the nature of the clay minerals. As water potential gradually decreases, water is drawn out of the soil with large pores emptying first, followed by progressively smaller pores, until at low water potentials only the very narrow pores are able to retain water. A decreasing water potential corresponds to a decreasing thickness of hydration envelopes covering the soil particle surfaces. Decreasing water potential is thus associated with decreasing soil water content. In a non-shrinking soil, the soil water characteristic allows the calculation of effective pore size distribution. Matric potential of soil water is related to equivalent spherical pore radius (r) by the relationship (Marshall and Holmes, 1988):

$$\psi_m = \frac{2\gamma}{\rho_w g r} \qquad \ldots \quad (2.7)$$

where γ is the surface tension of water, ρ_w is the density of water and g the acceleration of gravity. This approximates to:

$$\psi_m = \frac{1.5}{r} \qquad \ldots \quad (2.8)$$

where r and ψ_m have units of mm, and cm of water respectively. A description of laboratory methods for measuring the water characteristic curve is given by Klute (1986), whilst field methods were described by Bruce and Luxmoore (1986).

The Hagen-Poiseuille equation for laminar flow of a fluid through a capillary tube of radius, r, is given by:

$$Q = \Pi r^4 x \frac{\Delta p}{8\eta z} \qquad \ldots \quad (2.9)$$

where Q is the volume flow through a section of length z per unit time, η is the viscosity of the fluid, and Δp is the pressure drop over the distance z. Laminar flow occurs in most soil processes because of the narrowness of the soil pores. The Hagen-Poiseuille equation is used in many physical models predicting soil flow processes.

Soil pores are highly irregular in nature and hence are very difficult to describe. It is convenient when considering water flow through soil, to consider the overall average

of microscopic flow velocities over a large soil volume. The detailed flow pattern within the soil volume is ignored and it is treated as a uniform medium. The volume of water flowing through a unit cross-sectional area per unit time, (q), is given by Darcy's law:

$$q = - K \frac{dh}{dz} \qquad \ldots (2.10)$$

where K is hydraulic conductivity and dh/dz is the hydraulic gradient (hydraulic head difference per unit distance in the direction of flow). Hydraulic potential ($\psi_m + \psi_g$) and hydraulic head (h) are just different expressions, in different units, of the energy associated with pressure and elevation considered together.

In an unsaturated soil, water is subject to gradients in potential and therefore tends to flow from a zone of high water potential to a zone of low water potential. Vapour transfer is a secondary water transfer process which, in the absence of temperature gradients, is much slower than liquid flow when a soil is wet. However, in the surface zone of a soil where it becomes very dry and temperature gradients exist, vapour transfer can become the dominant water transport mechanism (Hillel, 1982).

In a saturated soil where all pores are water-filled and conducting, the continuity of the water films and hence the conductivity are at maximum. As water potential decreases, the large pores become air-filled and water flows in the small pores only, hence total conductivity decreases. As pores become air-filled the tortuosity increases, as water must flow around the air-filled pores. Thus, hydraulic conductivity decreases rapidly as a soil becomes unsaturated. A soil with a high proportion of large continuous pores will have a high conductivity at saturation, compared with a soil with a high proportion of micro-pores. However, in the unsaturated condition only small pores retain water and so the total conductivity of a soil with many small pores might exceed that of a soil with a high proportion of large pores (Figure 2.2). It is apparent that hydraulic conductivity is related to both soil water content and water potential. Total porosity, pore size distribution and tortuosity are all factors that influence hydraulic conductivity. Methods for the measurement of hydraulic conductivity were reviewed by Klute and Dirksen (1986), Amoozegar and Warwick (1986) and Green et al. (1986).

Figure 2.2 The dependence of hydraulic conductivity on matric potential in soils of different texture (after Hillel, 1982).

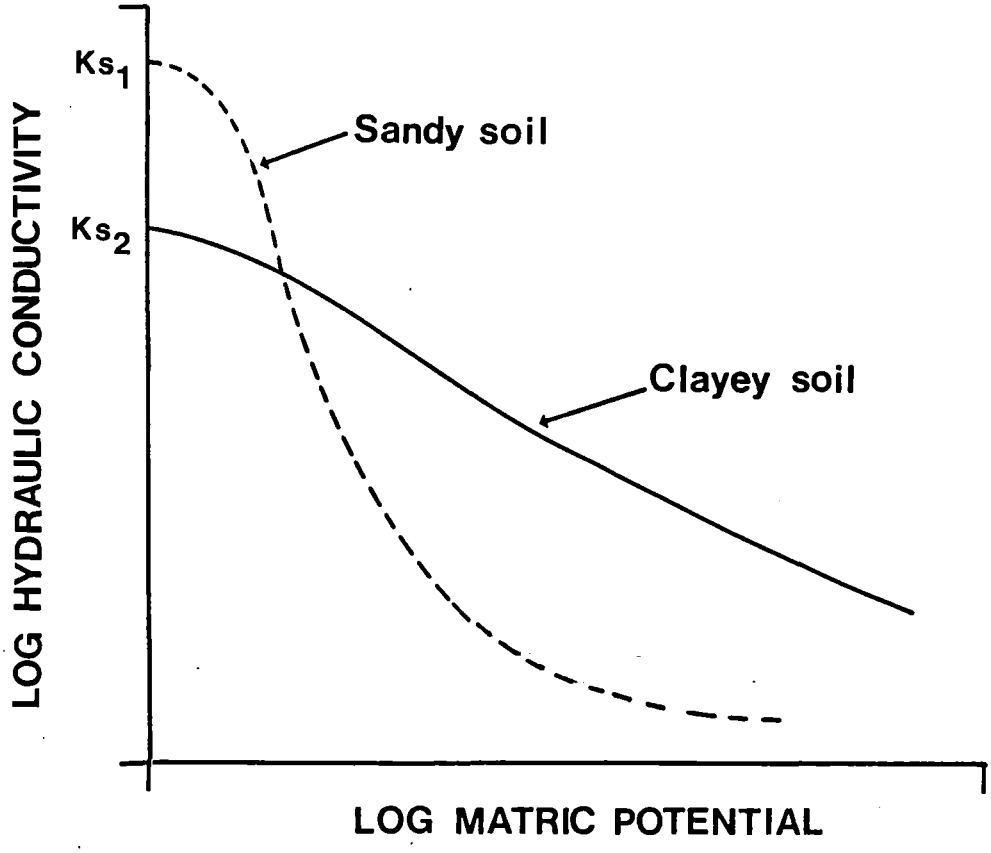

Darcy's law can be extended to unsaturated flow if conductivity is a function of matric potential:

$$q = - K(\psi_m) \frac{dh}{dz} \qquad \ldots (2.11)$$

In an unsaturated soil the matric potential is continually changing due to water movement and hence soil water content must also be changing. To describe the flow of water through a soil, when its water content is transient, the law of conservation of mass (continuity equation) must be combined with Darcy's law. In unsaturated soils in the field, flow of water is predominantly vertical with no significant horizontal component. Combining Darcy's law with the continuity equation for water flow in a vertical direction gives:

$$\frac{\partial}{\partial z}\left[K\ \frac{\partial \psi}{\partial z}\right] + \frac{\partial K}{\partial z} = \frac{\partial \theta}{\partial t} \qquad \ldots\ (2.12)$$

where θ is water content, t is time, and all other variables have been defined previously.

Unlike liquid water, which moves in the soil by the process of mass flow, vapour generally moves by the process of diffusion, in which different components of a mixed fluid move independently in response to vapour concentration differences from one place to another. In an unsaturated soil, water vapour is always present in the gaseous phase and diffusion occurs when vapour pressure gradients develop. It seems impossible to completely separate liquid from vapour movement, as overall flow can be a complex process of evaporation, vapour flow, condensation, liquid flow etc. (de Vries and Philip, 1986). The two phases apparently move interdependently and simultaneously due to water potential and vapour pressure gradients.

Temperature affects water movement in both vapour and liquid phases. Surface tension of water decreases with temperature, causing increased water potential. Hence, a temperature gradient in a soil of uniform water content will result in a gradient in potential, causing liquid water movement in the direction of decreasing temperature. A temperature gradient causes water vapour to move in the direction of decreasing temperature in response to a vapour pressure gradient. Vapour pressure of water is strongly temperature-dependent and large vapour gradients can occur.

Philip and de Vries (1957) developed a theory of non-isothermal water flow in the liquid and vapour phases that consolidated the previous knowledge by considering the temperature field on a micro-scale. De Vries (1958) extended the theory to include water and latent heat in the vapour phase, the heat of wetting, and the advection of sensible heat by water. The Philip and de Vries model uses volumetric water content as the dependent variable instead of pressure potential. The complexity and the number of soil and water equations and parameters in the Philip and de Vries model makes its applicability difficult in a practical sense. A general lack of adequate data, necessary to define the simultaneous heat and water transfer in porous media, has severely limited modelling of coupled non-isothermal systems and field testing of non-isothermal theories. For this reason the significance of thermally-induced flow, especially under field conditions, has been difficult to assess.

b) Methods to predict unsaturated hydraulic conductivity

Mathematical models of soil water movement frequently use unsaturated hydraulic conductivity (K) as a function of soil water matric potential (ψ_m). The determination of this relation by direct measurement is desirable but difficult because: (i) The $K(\psi_m)$ function is soil specific and its measurement is time-consuming; (ii) The soil variability is such that the amount of data required to represent the hydraulic properties accurately is enormous; (iii) The values of hydraulic conductivity of some soils can vary by several orders of magnitude within the water content range of interest and most measurement systems cannot effectively cover such a wide range (Alexander and Skaggs, 1986; Mualem, 1986). Furthermore, different methods of $K(\psi_m)$ determination yield different results and it is unclear which method best represents the hydraulic characteristics of the site (Dane, 1980). Methods have been developed to approximate $K(\psi_m)$ from the relationship between volumetric water content (θ_v) and ψ_m. These have been reviewed by Alexander and Skaggs (1986) and by Mualem (1986).

2.4.5.4 The estimation and measurement of evaporation

I) Meteorological methods of evaporation estimation

Numerous meteorological methods have been developed for estimating or measuring evapotranspiration (ET) or evaporation (E); they vary in accuracy and reliability. The basic principles of some commonly used methods are described here but more comprehensive descriptions of these and other methods have been given by Tanner (1967), Kanemasu et al. (1979) and Rosenberg et al. (1983).

a) Micrometeorological methods

i) Mass transport methods

A general formula was suggested by Dalton in about 1800 to predict free water evaporation (E_o) as a function of vapour pressure:

$$E_o = N(e_o - e_a) \qquad \ldots (2.13)$$

where N is an empirical constant involving some function of windiness, e_o is the vapour pressure at the surface, and e_a is the actual vapour pressure at some point above the surface. This method is not easily applied because of difficulty in determining e_o (Rosenberg et al., 1983). An analysis of errors in Dalton type equations was given by Hage (1975).

ii) Aerodynamic method

Thornthwaite and Holzman (1942) applied an aerodynamic approach to ET estimation. Gradients of specific humidity and the logarithmic wind profile were included. At their present stage of development, aerodynamic methods are not suitable for routine applied uses such as irrigation scheduling (Rosenberg et al., 1983). Further information on aerodynamic methods is given by Kanemasu et al. (1979).

iii) Resistance methods

The transport of sensible heat from surface to air (H) is at a rate directly proportional to the temperature gradient and inversely proportional to the aerial resistance to heat transfer (r_a):

$$H = \rho_a C_p \frac{T_a - T_s}{r_a} \qquad \ldots (2.14)$$

where ρ_a is the density of air, C_p is the specific heat of air and T_a and T_s are air and surface temperature respectively. Similarly, the transport of vapour is directly proportional to the gradient in vapour pressure from the evaporating surface to the air and inversely proportional to aerial resistance to the transport of water molecules. Resistance models estimating L_vE have been proposed by Monteith (1963) and by Brown and Rosenberg (1973).

b) Climatological methods

i) Air temperature based formulas

Thornthwaite (1948) proposed an empirical index for measuring monthly potential evapotranspiration which is successful on a long-term basis because both temperature and ET are similar functions of net radiation and are therefore correlated over long time periods. Other air temperature based formulas are those of Blaney and Criddle (1950), Hargreaves (1974) and Linacre (1977).

ii) Solar radiation formulas

ET is correlated with solar radiation (R_s) and potential ET (ET_p) is linearly and strongly dependent on solar radiation (Aslyng, 1974). The relationship of ET_p and R_s has been established empirically and can be described by simple linear regression. Regression models are simple to use but have only a limited range of applicability due to their empirical nature.

iii) Combination formulas

Methods which consider both the energy supply to, and the turbulent transport of water vapour away from an evaporating surface are known as combination models. In combination models L_vE is calculated as the residual in the energy balance equation. Sensible heat flux is estimated by means of an aerodynamic equation. One form of the combination equation is (Rosenberg et al., 1983):

$$L_vE = -\left[R_n + S + \rho_a C_p \frac{(T_a - T_s)}{r_a}\right] \quad \ldots (2.15)$$

where all terms have been previously defined. The method has been shown to provide reliable estimates of L_vE fluxes when surface temperature is measured directly by infra-red thermometry both under advective and non-advective conditions, as well as on both a short period and a daily basis (Verma et al., 1976; Blad and Rosenberg, 1976; and Heilman and Kanemasu, 1976). Any combination solution assumes that the turbulent transfer coefficients for water vapour and sensible heat are equal (Rosenberg et al., 1983).

When T_s cannot be measured directly, T_a-T_s can be eliminated by application of the Clausius-Clapyron equation. Kanemasu et al. (1979) give detailed descriptions of the transformations involved. It is from this application of the Clausius-Clapyron equation that the combination methods of Penman, van Bavel, and Slatyer and McIlroy are derived. These methods were described by Rosenberg et al. (1983).

van Bavel and Hillel method

Van Bavel and Hillel (1976) proposed a method for evaporative flux determination that required only the following common weather variables: global radiation, air temperature, air humidity and windspeed. The model (called CONSERVB) is a combination method in that the surface energy balance is combined with the simultaneous transport of heat and water vapour in the air above the surface, as well as the simultaneous transport of heat and liquid water in the soil below the surface. This approach is a further extension of the original combination or Penman formula, but is much more comprehensive and accounts for soil properties and changes therein as evaporation proceeds. Similarly it reflects changing surface properties and atmospheric stability (refer to Chapter 6). This model represents one example of a comprehensive simulation modelling approach for predicting evaporation (see Chapter 6 for others). Following satisfactory verification studies, such models might make possible the evaluation of the net affects of various specific processes or parameters on the overall soil water and thermal regimes. The development and verification of such models is seen as a research priority.

c) Water balance method

Evapotranspiration (ET) can be determined using a water balance approach. This hydrologic approach for ET estimation is widely used. Errors associated with the water balance approach invalidate it for estimating ET on a daily basis however (Rosenberg et al., 1983).

II) Direct measurement of evaporation with lysimeters

a) Lysimetry

Lysimetry involves the volumetric measurement of all incoming and outgoing water from a container which encloses an isolated soil mass with a bare or vegetated surface. This incoming and outgoing water flux can be represented as a water balance. Lysimetry is the only hydrological method which enables a complete knowledge of all the terms in the water balance equation. Thus, the method has importance both for gathering evaporation information and as an independent check on the suitability of micrometeorological methods and for calibrating empirical formulas used for estimating evapotranspiration.

b) Lysimeter design and operation

The validity of the lysimetric method of evaporation measurement is dependent on the evaporation from the isolated body of soil being the same as from a comparable non-isolated body (Boast, 1986). Hence in lysimetry, the conditions of the enclosed soil mass are critical to the outcome of the measurements. The soil conditions in the lysimeter container must be representative of surrounding field conditions. In studies comparing the hydraulic properties of disturbed and undisturbed soils (Shaykewich, 1970) sample disturbance has been shown to influence water retention, lower the limit of available water and reduce the unsaturated hydraulic conductivity of the soil.

Light, strong, poorly-conducting, non-metallic wall material has been recommended for construction. Weighing lysimeters have inner tanks (soil containers), outer tanks or retaining walls, and an air-filled space in between. The width and nature of the lysimeter annulus (containing walls plus retaining walls and the air-filled gap) affect the thermal exchanges between the lysimeter soil mass and the surrounding soil, as well as the interception and dissipation of solar energy. The width of the lysimeter annulus should be kept as small as possible.

Special care needs to be given to the conditions and size of the buffer area around the lysimeter. The lysimeter must be sited in surrounds identical to the area under study, and the surrounds must be managed in the same manner. Other factors

which can cause a lysimeter to become unrepresentative of its surroundings include imposition of a barrier to water and heat flow at the bottom of the lysimeter and cutting of roots by lysimeter walls (Boast, 1986). A common approach to these problems is to employ very large lysimeters. The design and operation of large lysimeters was reviewed by Aboukhaled et al. (1982).

c) Micro-lysimeters

An approach avoiding both the soil disturbance and the water and heat flow barrier problems uses lysimeters which can be pushed into undisturbed soil and used only as long as the evaporation rate from them is comparable (to a desired degree of accuracy) to that from the surrounding soil. The micro-lysimeter approach uses small cores and relies on a relatively large number of these to obtain a suitably sized sampling area. Micro-lysimeters ranging in length from 44 to 200 mm have been evaluated, however it has been recommended that they should be at least 76 mm long and 76 mm in diameter (Boast, 1986). The success of this method depends on accurate determination of whether the moisture profile in the micro-lysimeter is representative of the surrounding soil and hence whether the evaporation rate is representative. Edge effects might become a limitation of this method. Wall materials and air spaces between inner and outer walls therefore assume greater importance. However, given the small individual core area, it has been shown by Boast and Robertson (1982), Walker (1983), Shawcroft and Gardner (1983), Lascano and van Bavel (1986), and others that the micro-lysimeter technique is valid for many applications and can provide consistent, direct measurements of evaporation. The method makes possible evaporation measurement under some conditions where traditional lysimetric methods are impractical or impossible.

2.5 Conclusions

Surface soil structure management is an essential aspect of any wind erosion control program. Tillage-induced structural changes have wide implications for production-related parameters other than soil erosion. Thus, in the evaluation of tillage management strategies for wind erosion control, each of these production-related parameters must be considered. Only then can tillage management be analysed within

the framework of an arable farming system. An illustration of some of the inter-relations between tillage affected soil properties and soil processes is given in Figure 2.3. Further research is required to define an optimal soil physical condition in terms of both crop growth and soil conservation and then to develop our understanding of soil dynamics, with the objective of being able to prescribe the soil manipulation which will produce the desired soil condition.

To properly define such a soil condition, improved understanding of the relationships between soil structure, soil water relations, crop growth and development, and soil erosion are required. The relationship between soil structure and soil water relations is complex, involving soil porosity, soil thermal properties, micro-topography, the surface energy balance and the micro-climate above the soil surface. The relation between shortwave albedo, surface soil structure and surface soil water content is an important aspect, as is the net effect of tillage-induced changes in shortwave albedo on soil water relations. Soil water relations, as affected by tillage-induced changes in soil structure, are of importance both from the wind erosion and plant productivity viewpoints. The effects of multiple-pass tillage, and of soil conditions at the time of multiple-pass tillage, on soil physical and hydraulic properties and likely subsequent effects on the soil water relations, have not been well documented.

There is a need to identify the structural features most important in determining loss of water from a tilled soil. Due to the complex interactions involved, a numerical simulation modelling approach for predicting changes in soil water status seems appropriate. The development of simulation models for soil water relations is a worthwhile research objective with the evaluation of existing models being a priority.

Figure 2.3 Tillage effects on soil properties and processes

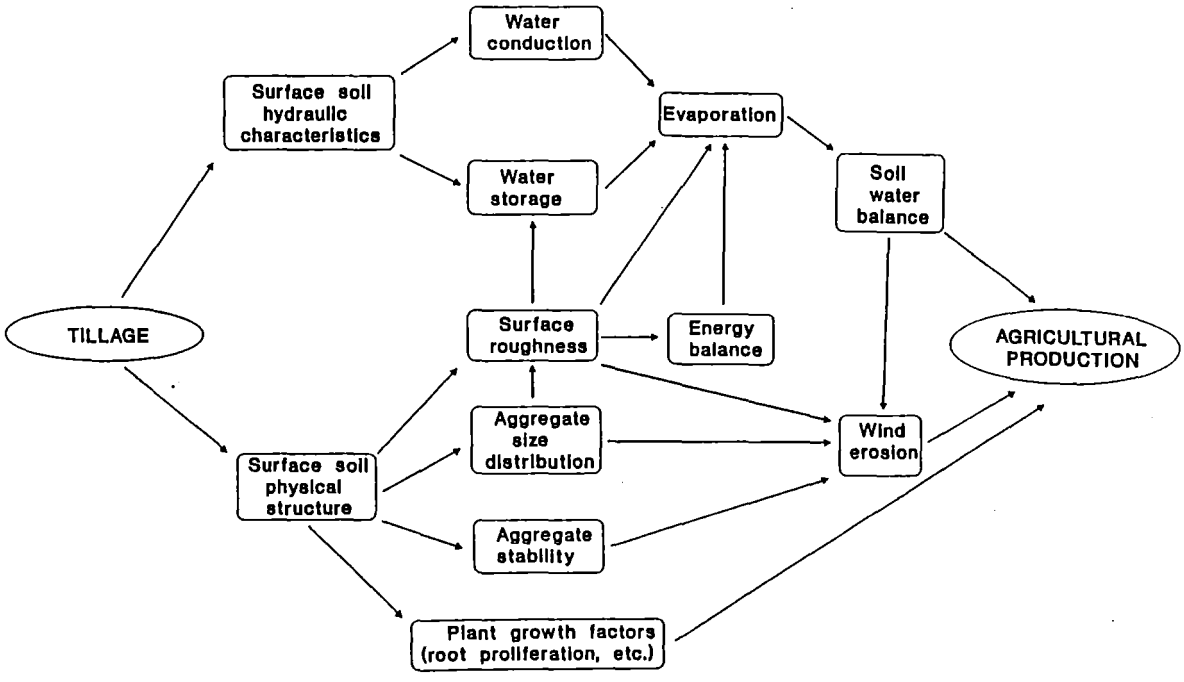

CHAPTER 3

Materials and Methods

3.1 Introduction

In this chapter descriptions are presented of the experimental site, experimental methods, measurement techniques and the instruments used. The first main section describes the investigation of tillage and water content effects on surface soil properties whilst the second describes the investigation of evaporation from a bare soil surface.

3.2 Tillage and water content effects on surface soil properties

3.2.1 Experimental site

The 1 ha experimental site was established near the centre of a 6.1 ha paddock located on the Research Farm, Lincoln University, Canterbury, New Zealand. During the previous seven years lucerne (Medicago sativa) had been grown in this paddock. Aerial photography was used to assist in the identification of a site with a minimum of surface soil variability. The site had a clear fetch to the north-east, the north-west and to the south-west. Near the eastern side there was a sealed roadway which was about 1 m above the height of the site. Approximately 100 m from the site in a southerly direction there was an irregular, thin shelter-belt about 3 m high. A house and barn approximately 160 m from the site, in a northerly direction, provided the most significant obstruction to the wind at what was otherwise a very exposed site.

The alluvial soil of the site is classified as Templeton silt-loam (Kear et al., 1967) (Udic ustochrept; USDA, 1983). The average coarse sand, fine sand, silt and clay contents of the experimental site (0-150 mm depth) were 29%, 20%, 30% and 21% respectively as determined by particle size analysis (Gradwell, 1972). The soil has developed on sand and fine sand underlain by greywacke gravel. A typical soil profile at this site is:

0-0.25 m	dark brown (10YR 3/3) silt-loam; friable to firm; moderately developed medium and fine nutty structure; diffuse boundary;
0.25-0.45 m	brown (10YR 5/5) sandy-clay-loam; firm; weakly developed medium and fine nutty structure;
0.45- m	firm weakly developed greywacke gravel and sand.

The lower plastic limit (lower Atterberg limit) determined for the surface 15 cm of soil using the method of Thomas (1973) was 30.4% (w/w, std. error = 0.39%, 30 samples). Soil organic matter determined by loss-on-ignition technique (Ball, 1964) was 6.2% (std. error = 0.06%, 30 samples). Dry bulk density and total porosity of the cultivation zone prior to tillage was 1.18 Mg m^{-3} (std. error = 0.007 Mg m^{-3}) and 53.5% (std. error = 0.32%) respectively.

3.2.2 Experimental procedure

The experiment was designed statistically as a split-plot, randomised, complete block with four replications. The main plots were three pre-tillage soil water contents (PTSW) (17.7, 23.2 and 31.5%, w/w). Each main plot was split into three 3.2 by 14 m sub-plots each of which had a different tillage treatment. The following tillage treatments were used:

(i) three heavy grubber passes ('minimum' tillage)

(ii) moldboard plough then three spring-tined harrow passes ('intermediate' tillage)

(iii) moldboard plough, three rotary cultivator passes followed by one spring-tined harrow pass ('excess' tillage)

A 'Kverneland' four-furrow reversible plough with 1.22 m long moldboards was used at a forward speed of 6.0 km h^{-1}.

The spring-tined harrows which were used ('Duncan 634 Rota-crumbler') had 29 light spring tines with 'duckfoot' type points 65 mm wide. The tine points were arranged in four rows with 400 mm tine spacings so that in one implement pass the tine centres move through the soil at 100 mm intervals. This implement has an angle crumbler and was operated at a forward speed of 7.2 km h^{-1}.

The heavy grubber had 13 heavy spring tines arranged in two rows with 440 mm tine spacings. Thus, tine centres move through the soil at 220 mm intervals during one implement pass. The chisel-type tine points were 62 mm wide. The implement was operated at a forward speed of 7.4 km h^{-1}.

A 'Howard Rotovator model AR' rotary cultivator was used with standard right-angle blade tines. The implement was operated with the rear shield lowered. Rotor speed was 193 r.p.m. and forward speed was 5.1 km h^{-1}.

The trial area was sprayed with a broad-spectrum herbicide ('Roundup', Monsanto, New Zealand; 36% glyphosate). Residual plant material was removed to ground level using a lawn mower prior to tillage. Soil water control was achieved primarily with a sprinkler irrigation system. Christiansen's coefficient for water application uniformity was 95% in still air (Christiansen, 1942). Water was applied at an average rate of 3.5 mm hr^{-1} through small, self-regulating sprinklers in calm conditions. Each main plot was sampled for soil water determination immediately prior to initial tillage. Gravimetric samples of approximately 300 cm^3 were taken from 12 randomly selected sites in each main plot at 0-150 mm depth. The samples were transported to the laboratory in sealed plastic pottles, weighed and then oven dried at 105^{o}C for 24 hours. They were then re-weighed and soil water content determined. Secondary tillage was completed within one hour of initial tillage. Replicates one to four were tilled on 28/9/87, 22/12/87, 3/3/88 and 22/4/88 respectively. Ploughing depth was kept constant at approximately 150 mm. No soil measurements were made in areas where tractor wheels travelled during tillage operations.

3.2.3 Experimental measurements

3.2.3.1 Aggregate size distribution and mechanical stability

Size distribution and mechanical stability of soil aggregates were determined using a modified rotary sieve (Lyles et al., 1970). The state and stability of the dry aggregates is a closer index of field structure in the wind erosion context than the state of water-stable aggregates determined by wet-sieving (Chepil, 1943). Neither sieving technique gives a complete representation of soil structure.

Surface soil samples weighing approximately 2.8 kg were obtained from the surface 40 mm of the soil using a flat-bottomed shovel. Three samples were taken from random positions within each sub-plot. The air-dried samples were sieved to determine aggregate size distribution before being re-sieved twice to determine aggregate stability. The aggregate size ranges determined were: <0.26, 0.26 to 0.84, <0.84, 0.84 to 1.47, <1.47, <4.85, <18.0 and >18.0 mm diameter. The proportion of aggregates less than 0.84 mm diameter after one sieving divided by the proportion of aggregates less than 0.84 mm diameter after three sievings was used as an index of the relative mechanical stability of the aggregates. Large pieces of crop residue were removed before sieving, disturbing the sample as little as possible.

3.2.3.2 Bulk density, particle density and total porosity

Dry bulk density was determined, using the method of Gradwell (1972), on four samples each of 2640 cm^3 taken randomly from each sub-plot (40 to 110 mm soil depth). Particle density was measured also using the method of Gradwell (1972). Total porosity (ϵ_T) was calculated from dry bulk density (ρ_b) and particle density (ρ_p) using Equation 2.6.

3.2.3.3 Soil surface roughness

Soil surface roughness was measured with a point gauge micro-relief meter which allowed measurement of surface elevations with a 1.0 mm resolution over a regular 0.5

by 0.5 m grid. The apparatus was levelled above the soil surface before readings were taken at 0.05 m spacings (hence 100 were made over the 0.25 m^2 area). Two of these measurement sets were completed on each sub-plot (i.e. 0.5 m^2 sample area). The soil surface roughness index calculation method is discussed in Section 4.4.

3.2.3.4 Near-saturation hydraulic conductivity

Near-saturation hydraulic conductivity was determined using a tension infiltrometer device (Clothier and White, 1981) as shown in Figure 3.1. The 65 mm internal diameter (i.d.) perspex tube has a 207 mm diameter base constructed from a membrane with 63 μm pores. The instrument is filled with water (1.8 l) by removing the rubber bung and immersing it in de-aerated water. Once the bung is replaced water can move through the porous membrane only if air enters through the hypodermic syringe. The syringe used had a bore radius of 0.235 mm (r) and was located 60 mm above the porous base (l). Matric potential, at the porous base (ψ_m), is calculated thus:

(ψ_m units = m)

$$\psi_m = l - \frac{2\gamma}{\rho_w g r} \qquad \ldots (3.1)$$

where γ is the surface tension of water, ρ_w is the density of water and g is the acceleration of gravity. Hence, using this apparatus, water was applied to the soil surface at a potential of -37 mm. Pores having a diameter less than 0.8 mm will not affect conduction of water from the tension infiltrometer. Field heterogeneity due to large channels and voids conducting water is, therefore, eliminated with this method. As recently tilled soils are the subject of the study this was seen as an important consideration.

Intact soil cores were taken by pushing circular plastic coring cylinders (150 mm deep, 200 mm i.d.) into the 0-150 mm soil depth while the soil was trimmed immediately ahead of the sharpened cutting edge. In this way the coring ring merely shaves the soil from a preformed oversize core and hence sample disturbance by compaction is minimised. The soil had been moistened then allowed to drain for 24 hours prior to sampling. A surface stabiliser solution (polyvinyl alcohol) was applied as a fine spray and allowed to dry prior to wetting of the sampling sites. Four cores were taken randomly in each sub-plot. The cores were saturated by placing them in a few

millimetres of de-aerated water until they became thoroughly wet by capillary uplift (i.e. when the upper surface of the core became thoroughly wetted). The de-aerated water level was then adjusted to within a few millimetres of the tops of the cores. After 24 hours the cores were removed from the water and placed on a steel-gauze-covered stand. Fine sand (air entry value approx. 30 cm water) was applied to the upper surface as a slurry to facilitate contact between the soil surface and the base of the tension infiltrometer. The infiltrometer was filled with de-aerated water of known temperature ensuring no trapped air bubbles. It was then placed on top of the core and rate of water outflow from the infiltrometer was monitored. When a steady state was reached, flow rate was determined.

Hydraulic conductivity (K) was then calculated (following Clothier and White, 1981):

$$K = J \times \frac{z}{(z + \psi_m)} \qquad \ldots (3.2)$$

where J is steady state flow rate (m s^{-1}), z is height of sample core (mm) and ψ_m is matric potential (mm). With z being 150 mm and ψ_m being -37 mm, flow rate (J) was multiplied by 1.327 to give K_1. By definition, K is the flow rate at unit potential gradient (i.e. gravitational flow). At the top of the soil core ψ_m is -37 mm while at the base, where free water is emerging ψ_m is 0. Thus, there exists a matric potential gradient which is opposite to the gravitational gradient. Equation 3.2 gives a correction for this gradient.

Hydraulic conductivity results were corrected to a water temperature of 20 ^{o}C using the following equation:

$$K_{20} = K_T \times \frac{\eta_T}{\eta_{20}} \qquad \ldots (3.3)$$

where K_T is the hydraulic conductivity at measured temperature T (m s^{-1}), η_T is the viscosity of water at temperature T, η_{20} is the viscosity of water at 20^{o}C and K_{20} is the corrected hydraulic conductivity.

Figure 3.1 Tension infiltrometer apparatus (after Clothier and White, 1981).

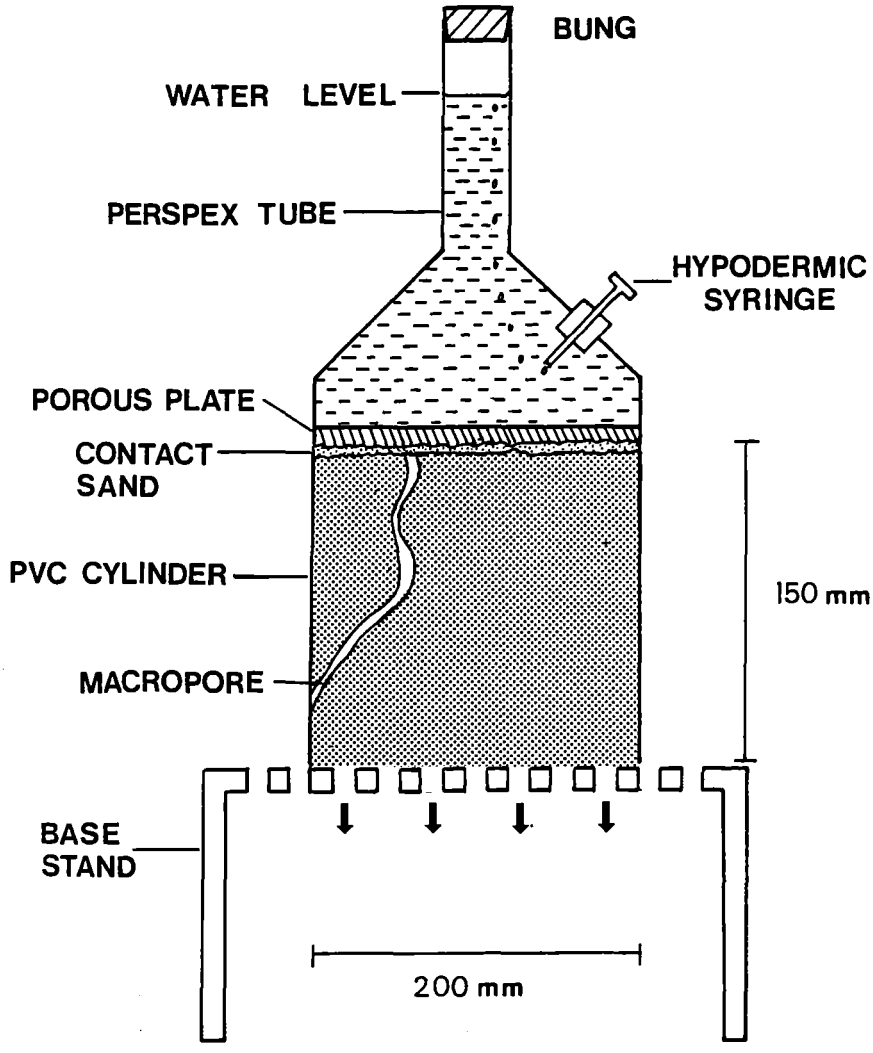

3.2.3.5 Pore size distribution

Pore size distribution was determined from the matric potential-volumetric water content relationship, often referred to as the water characteristic or water retention curve. Matric potential of soil water (ψ_m) is related to equivalent spherical pore radius (r) in Equation 2.8.

Soil macro-porosity is defined as the total volume of pores drained at -10.0 kPa matric potential (i.e. pores >30 μm equivalent spherical diameter (e.s.d.)). Macro-

porosity corresponds to the summation of soil aeration capacity and transmission porosity where transmission porosity is defined as the volume of pores that drain between -1.0 and -10.0 kPa matric potential (300-30 μm e.s.d.). The total volume of pores which drain between -10.0 and -1500 kPa matric potential (i.e. pores between 0.2 and 30 μm e.s.d.) are commonly regarded as the pores which, when water-filled, contain water which is readily available to plants. Residual porosity is defined as the volume of pores which drain at less than -1500 kPa matric potential, pores less than 0.2 μm e.s.d. (De Leenheer, 1977).

Tension tables were used to determine the gravimetric soil water content at matric potentials of -1.0, -3.0, -5.0 and -10.0 kPa. Volumetric soil water contents were calculated by multiplying the gravimetric values by measured bulk density. The tension tables were constructed from 420 by 360 by 40 mm perspex trays using silica flour ('Snowsil', ACI Resources Ltd., Victoria, Australia; mean particle size approx. 70 μm) as the porous bed.

Four intact soil cores were taken randomly in each sub-plot by pushing a sampling cylinder into moistened soil while trimming ahead of the sharpened cutting edge. Metal sampling cylinders 70 mm deep and 200 mm i.d. were used in those plots subjected to either the 'minimum' or 'intermediate' tillage treatment while a plastic cylinder 50 mm deep and 104 mm i.d. was used in the finer tilth 'excess' tillage plots. In each case the inside of the sampling cylinder was smeared with petroleum jelly to minimise edge effects. The lower surface of each core was trimmed flush and covered with a fine nylon cloth. The cores were treated with formaldehyde (4 %, w/w) to flush out earthworms and a fungicide ('Kocide', Shell Chemicals NZ Ltd.) before being saturated with de-aerated water and placed on the tension table. After equilibration the cores were weighed before being transferred to the next tension table. Gravimetric water contents were determined at matric potentials of -1.0 and -3.0 kPa on four samples per sub-plot while water contents at potentials of -5.0 and -10.0 kPa were determined for two samples per sub-plot where the larger samples were used and four samples per sub-plot where the smaller samples were used. At completion of the -10.0 kPa measurement a sub-sample was taken by carefully pushing a thin-walled bevelled aluminium ring (15 mm deep by 42 mm i.d.) into the centre of the tension table sample. After careful removal the sub-sample was trimmed and a fine gauze mesh secured over the bottom of each ring. Gravimetric water contents were then measured at

potentials of -33, -100, -300, -500 and -1500 kPa using pressure plate apparatus (Soil Moisture Equipment Corp., Santa Barbara, California, USA.). Water contents at -33 and -100 kPa were determined on three samples per sub-plot. One sample per sub-plot was used at -300, -500 and -1500 kPa, although -1500 kPa measurements were repeated from two replicates only. Volumetric water content-matric potential data was used to calculate pore size distributions following Ball and Hunter (1980).

3.2.3.6 Unsaturated hydraulic conductivity

One of the more commonly used methods to approximate $K(\psi)$ from the relationship between volumetric water content (θ_v) and ψ_m (e.g. Higuchi, 1984; Reid and Hutchison, 1986; Lascano and van Bavel, 1986) is that of Jackson (1972). The calculation procedure of Jackson (1972) was used in this study. The Jackson method for predicting $K(\psi_m)$ is based on a capillary tube model of water flow through soil pores. The model is based on the matric potential-pore radius relation (Equation 2.7) and on the Hagen-Poiseuille law (Equation 2.9) and the Darcy equation (Equation 2.11). The Jackson method is a further development of the Childs and Collis-George (1950) model and of the Marshall (1958) model. It is categorised as a 'series-parallel' type model (Brutsaert, 1967), one in which the soil is assumed to behave like a bunch of parallel tubes with constrictions due to tube connections, a porous body in which the distribution of pores of various sizes in space is entirely random.

Consider a column of such a porous body, with a unit cross-section, cut in two thereby exposing two surfaces each with a representative pore size distribution (after Childs, 1969). On one surface there is a particular pore group with average size ρ and range Δr and hence size range $\rho - \Delta r/2$ to $\rho + \Delta r/2$. On the other exposed surface a pore group has mean size σ and range Δr. The area of the exposure taken by a particular pore group is equal to the part of the porosity accounted for by that group which, in turn, equals the product of concentration of pore volume (i.e. pore volume per unit pore size range) about the chosen size, and the width of the range. The concentration of pore volume at the given pore size is a distribution function of the pore size. Hence the area of exposure of pores of mean size ρ is:

$$A_\rho = f(\rho)\ \Delta r \qquad \ldots\ (3.4)$$

while on the other surface the area of exposure of pores of mean size σ is:

$$A_{\sigma} = f(\sigma)\ \Delta x \qquad \ldots\ (3.5)$$

In the undisturbed column the two exposures are assumed to come together at random and so the area of the junction occupied by pore sequences characterized by mean pore sizes of ρ on the first side and σ on the second side is the product of A_{ρ} and A_{σ}, denoted $A_{\rho\rightarrow\sigma}$:

$$A_{\rho\rightarrow\sigma} = f(\rho)\Delta x\ f(\sigma)\Delta x \qquad \ldots\ (3.6)$$

The next step is to assess the contribution to total hydraulic conductivity made by the pore sequence described and to compute total conductivity by summing the contributions made by all of the possible sequences covering the whole range of pore sizes in the material. Two assumptions are necessary to do this. First, as pore size decreases, resistance to flow increases so rapidly (following the Hagen-Poiseuille law) that the resistance of the coarser pore in the sequence can be neglected (i.e. flow resistance is calculated on the basis of one pore size, the smaller of the sequence). Second, all contributions to conductivity, except those due to direct sequences, can be ignored (i.e. capillary assumed straight not tortuous). These two assumptions provide opposite errors and, to some degree, mutually compensate (Childs, 1969). If σ is smaller than ρ in the sequence, the number of sequences occupying the area $A_{\rho\rightarrow\sigma}$ is proportional to $A_{\rho\rightarrow\sigma}/\sigma^2$ and by Poiseuille the rate of flow through each, per unit ψ gradient is proportional to σ^4, so that the contribution ΔK to the total hydraulic conductivity is:

$$\Delta K = M\sigma^2\ f(\rho)\Delta x\ f(\sigma)\Delta x \qquad \ldots\ (3.7)$$

and total conductivity is:

$$K = M \sum_{\rho=0}^{\rho=R} \sum_{\sigma=0}^{\sigma=R} \sigma^2 f(\rho)\Delta x\ f(\sigma)\Delta x \qquad \ldots\ (3.8)$$

where M is an experimental constant, R is upper pore size limit (after Childs, 1969). For unsaturated soil, R is the largest pore size which remains full of water at the ψ_m

appropriate to the prevailing θ. The distribution function $f(r)$, is determined from the water characteristic. The soil water characteristic curve is considered analogous to the pore radii distribution function. Using the capillary law (Equation 2.7), capillary tube radius (r) is uniquely related to the matric potential (ψ_m) at which the pore is filled and drained. By definition, $f(r)\Delta r$ is the contribution of the filled pores of radius $r \rightarrow r+\Delta r$ to the water content, namely (Mualem, 1986):

$$\Delta\theta(r) = f(r)\Delta r \qquad \ldots (3.9)$$

and thus:

$$\theta(R) = \int_{R_{min}}^{R} f(r)\Delta r \qquad \ldots (3.10)$$

Using this model, K can be computed for any given θ using the measured soil water characteristic curve. Childs and Collis-George (1950) suggested (to transform the $\theta(\psi_m)$ to a $\theta(r)$ curve [$r \propto 1/\psi_m$]) dividing it into constant r intervals and carrying out the computation by Equation 3.8.

This tedious computational procedure was improved by Marshall (1958) who suggested using equal water content intervals. Using this approach, the conductivities are actually obtained by dividing the $\theta(\psi_m)$ relationship into n equal θ increments, obtaining the ψ_m at each increment and calculating the conductivity using the equation (Marshall, 1958):

$$K_i = \left[\frac{1800\ \gamma^2}{\rho_w g \eta}\right]\left[\frac{\theta^p}{n^2}\right]\sum_{j=i}^{m}\left[(2j+1-2i)\psi_i^{-2}\right] \qquad \ldots (3.11)$$

$$i=1,2,3\ldots m$$

where K_i = hydraulic conductivity (cm h^{-1}) at the i th increment, γ is the surface tension of water (g s^{-2}), ρ_w is the density of water (g cm^{-3}), g is the gravitational constant (cm s^{-2}), η is the viscosity of water (g cm^{-1} s^{-1}), θ is the water filled porosity at lowest tension class (cm^3 cm^{-3}), p the exponent of θ is a constant whose value depends on computational method, n is the total number of pore classes, j and i are summation indices, ψ_m is matric potential (cm) and m is the number of increments for which the

calculation is to be made. Jackson (1972) showed that because p=2 the pore interaction term (θ/n) is constant for any water content. Jackson re-wrote the Marshall equation thus:

$$K_i = A \sum_{j=i}^{m} \left[(2j+1-2i)\psi_j^{-2} \right] \qquad \ldots (3.12)$$

with $A = (1800\ \gamma^2/\rho_w g\eta)(\theta/n)^2$, where any θ and its corresponding n can be used. This calculation method was shown to require a matching factor to adequately represent experimental data. Using the ratio of measured to calculated saturated conductivity K_s/K_i as the matching factor Jackson wrote:

$$K_i = K_s \left[\frac{\theta_i}{\theta_1} \right]^p \frac{\sum_{j=i}^{m} \left[(2j+1-2i)\psi^{-2} \right]}{\sum_{j=1}^{m} \left[(2j-1)\psi_j^{-2} \right]} \qquad \ldots (3.13)$$

where $p = 1$. This is the equation that will be evaluated here for calculation of the $K(\psi_m)$ relationship. Discrete $\psi_m(\theta)$ data is required and the K predictions that result are only for the range of $\psi_m(\theta)$ data available.

The Jackson method is thus based on the assumption that the soil is isotropic with the pore space randomly distributed so that there are no continuous channels. These conditions do not hold in field soils and hence can lead to calculation errors. Using measured saturated hydraulic conductivity as a matching factor will not necessarily overcome the problem because cracks and channels not allowed for in the model might contribute greatly to the actual conductivity at saturation, but not when unsaturated (Marshall and Holmes, 1988).

However, in suitable soils, hydraulic conductivity functions calculated using this type of 'cut and random re-join' pore model have been reported as being close to those determined by physical measurements. This is providing that a matching factor is used and the matching is done at some degree of unsaturation when necessary (Kunze et al., 1968; Green and Corey, 1971; Jackson, 1972; Alexander and Skaggs, 1986; Rab et al.,

1987). The Jackson (1972) model was tested by Field et al. (1984) who reported it to be successful in predicting unsaturated conductivities within the scatter of in situ values when field measured water characteristic data was used and the mean in situ saturated hydraulic conductivity was used as a matching factor. The apparent necessity of a matching factor indicates that the method does not really predict hydraulic conductivity as a function of water content, but rather, the rate of decrease in conductivity as expressed by the slope of the K(θ) curve (Denning et al., 1974). In this study, near-saturated hydraulic conductivity was used for matching because of the large macro-pore volume expected in the tilled soil. The assumptions inherent in the Jackson model make a saturated hydraulic conductivity matching factor inappropriate in a tilled soil.

3.2.3.7 Shortwave albedo

Shortwave albedo was measured using inverted and upright Kipp and Zonen pyranometers positioned 0.5 m above the soil surface. A correction factor to compensate for the shadow cast by the instruments was calculated from view factor theory (Reifsnyder, 1967) as follows. Consider two parallel disks (i and j), one above the other, separated by distance z, with disk j being some distance (r_k) from normal to the centre of disk i. Disk i represents the pyranometer (radius r_i) while disk j represents its shadow (radius r_j, assumed to equal r_i) on the soil, distance z below. Distance r_k varies through the day with sun elevation as well as varying with seasonal changes. The view factor (F_{ij}) is calculated thus:

$$F_{ij} = 0.5 \left[1 - \frac{s - 2 R_i^2 R_k^2}{\sqrt{s^2 - 4 R_i^2 R_k^2}} \right] \quad \ldots (3.14)$$

where:

$$s = 1 + (1 - R_i^2) R_k^2 \quad \ldots (3.15)$$

$$R_i = \frac{r_i}{z} \quad \ldots (3.16)$$

$$R_k = \frac{z}{r_k} \quad \ldots (3.17)$$

Sun elevation and subsequently distance r_k, was determined and the view factor and appropriate multiplier calculated for each albedo reading.

The inverted solarimeter was shielded to prevent error from sensing solar radiation from the horizons, this restricted the viewing area to 5.56 m^2. A view factor adjustment was calculated to compensate for the restriction using the following method (Incropera and De Witt, 1985; p630). Consider two parallel coaxial disks (i and j) separated by distance z. Disk i represents the pyranometer (radius, r_i = 0.01 m) and disk j represents the area viewed by the shielded pyranometer (radius, r_j = 1.33 m). Distance z = 0.50 m. The view factor (F_{ij}) is calculated thus:

$$F_{ij} = 0.5 \left[S - \sqrt{S^2 - 4 \left[\frac{r_i}{r_j} \right]^2} \right] \quad \ldots (3.18)$$

$$S = 1 + \left[\frac{1 + R_j^2}{R_i^2} \right] \quad \ldots (3.19)$$

$$R_i = \frac{r_i}{z} \quad \ldots (3.20)$$

$$R_j = \frac{r_j}{z} \quad \ldots (3.21)$$

The resulting view factor was 0.877, hence pyranometer output was multiplied by 1.14.

The output from the pyranometers was recorded with an automatic data-logging system using a 10 second sampling interval and a one hour integration time (CR21x, Campbell Scientific Inc., Logan, UT.). The calibration of each instrument had previously been checked against a brand new Kipp and Zonen model CM11 pyranometer and was found to be accurate to within 2.5%. Reflectance was recorded as the ratio of reflected to incoming solar radiation.

Albedo was measured from trial replicate two only on the plots which were tilled at PTSW contents of 17.7 and 31.5% (w/w) (i.e. 6 sub-plots in total). Each of the tilled

sub-plots was irrigated individually using a low volume, high-uniformity spray irrigation system. Albedo and concurrent surface soil water measurements continued until the soil surface was visibly air-dry. Albedo measurements continued from 2/1/88 until 24/1/88.

3.2.3.8 Surface soil water content (concurrent with shortwave albedo)

Surface soil water content was measured gravimetrically on samples of approximately 170 cm^3. On each sampling occasion concurrent with albedo measurement (hourly) 6 replicates of soil water content samples were taken from the 0-20 mm soil depth.

3.2.3.9 Soil surface roughness (concurrent with shortwave albedo)

Soil surface roughness was measured with a point gauge micro-relief meter which was previously described (Section 3.2.3.3). Two measurement sets were completed on each sub-plot (i.e. 0.5 m^2 sample area) used for albedo determination.

3.2.3.10 Statistical analysis

Statistical analysis was performed with the aid of the software packages 'Genstat' and 'Minitab'. The Lincoln University VAX (Digital Equipment Corp.) computer system was used; it has a VMS operating system.

3.3 Evaporation from a bare soil surface

3.3.1 Experimental procedure

The single 25 by 25 m plot was cultivated with a moldboard plough, rotary cultivate, Cambridge roll and Dutch harrow sequence. Following instrument installation, approximately 45 mm of water was applied using a low volume sprinkler irrigation system featuring high uniformity of water application. The experimental measurements described in the next section then commenced. The experiment was in progress from 16/3/89 to 11/4/89. Prior to the experiment a broad spectrum herbicide ('Roundup', Monsanto, New Zealand: 36% Glyphosate) was applied to the plot with a knapsack sprayer to ensure the absence of transpiring plants.

3.3.2 Experimental measurements

3.3.2.1 Soil water evaporation

Daily soil water evaporation was measured using micro-lysimeters (refer to Section 2.4.5.4). The micro-lysimeter cores were 207 mm in diameter and 150 mm deep. They were obtained by carefully pushing a plastic coring ring (wall thickness 6 mm) into the soil while trimming the soil immediately ahead of the sharpened cutting edge. In this way the coring ring merely shaves soil from a preformed oversize core and hence sample disturbance by compaction is minimised. The lysimeters were carefully removed after excavating the surrounding soil. A rigid plastic base plate was affixed, using heated glue, to seal the lysimeter. Fine nylon fishing line was attached to allow later removal of the lysimeter from its site. The mass of the lysimeter was determined to an accuracy of 1.0 g (equivalent to 0.03 mm of water) with an electronic balance. Once weighed, each lysimeter was inserted in an 'undisturbed' permanent site in a randomly determined position within the plot. These sites were formed by carefully pushing a thin steel ring with a sharpened cutting edge into the soil, excavating the soil from within the ring, and placing a plastic sheet over the site floor to prevent any loose soil from sticking to the lysimeter. The excavation depth allowed the exposed surface of the lysimeter,

once inserted at the site, to be flush with the surrounding soil. The air space between the lysimeter and the steel ring was kept to a minimum. Micro-lysimeter samples were re-weighed at 24 hour intervals before being discarded when the upward water flow restriction affected evaporation. New cores were then taken from random positions within the plot.

The accurate determination of when the water profile within the lysimeter has become unrepresentative of that within the plot is necessary. This was achieved by using three additional lysimeters 250 mm deep (150 mm diameter) to compare with the 150 mm deep cores. Error due to water (or heat) flow restriction from the lysimeter base would be shown by inconsistent evaporation rates between lysimeters of different depth. As a further check, lysimeters were gravimetrically sampled before being discarded, thereby allowing a comparison of water profile within the lysimeter with that in the plot.

Evaporation measurements were made from 10 lysimeters of 150 mm depth as well as from the three of 250 mm depth. The measurements did not commence on all 13 lysimeters on the same day, they were staggered ensuring that not all sample changes occurred on the same day. This allows a data continuation over time and reduces the variation in evaporation data which occurs from the soil variability effects with each sample change. On average, the lysimeters were changed every three days.

3.3.2.2 Soil water content

Soil water content was measured gravimetrically at the following depths : 0-20, 20-40, 40-60, 60-100, 100-150 and 150-200 mm. Samples were placed in sealed plastic pottles for transport to the laboratory before being weighed, oven dried at 105 ^{o}C for 24 hours and re-weighed. Sampling was repeated at each of these depths at six random locations within the plot daily. Soil water content was measured gravimetrically at depths of 200-250, 250-300, 300-350 and 350-400 mm in six random locations on days following irrigation or rainfall. Volumetric soil water contents were calculating using measured values of bulk density. Soil water content determination using a neutron moisture meter was considered for the lower soil depth increments. However, the quantity of stones in the soil made satisfactory access tube installation impossible.

3.3.2.3 Soil temperature

Accurate measurement of soil surface temperature is difficult. Any sensor placed on the soil surface has a different heat conduction, heat capacity and moisture content from that of the soil on which it rests. It might also shield the soil from solar and atmospheric effects. In previously documented surface temperature measurement techniques either the temperature on the surface is measured where the instrument is exposed to the combined influences of radiation, air temperature and soil temperature, or else the sensor is buried to some depth (Marlatt, 1967). Alternatively, infra-red thermometers are used, with the advantage of not being affected by the heat conductivity and evaporation problems mentioned earlier. They also have the advantage of recording a spatially averaged surface soil temperature instead of a point measurement as is recorded by discrete electronic sensors.

Here fast-response electronic temperature sensors (AD590JH, Intersil) were preferred over an infra-red thermometer because of the ease of operation with an automatic data-logging system. This allowed continuous hourly measurements and hence observation of diurnal variation in surface soil temperature. An infra-red thermometer (Everest Instruments, model 110) was used to make spot checks on the surface soil temperature representation from the electronic sensors. Identical electronic sensors were used for measurements of soil temperature as a function of depth. Manufacturer's specifications show maximum non-linearity of these sensors to be $\pm 1.5^{o}C$ over a range from $-55^{o}C$ to $+150^{o}C$. In the operating range used here (typically $0\text{-}25^{o}C$) non-linearity is negligible. A two point calibration against a precision mercury thermometer enabled calibration to within $0.2^{o}C$. Each sensor was encapsulated in the tip of a 5 mm diameter brass tube (200 mm long) which held the lead wires.

Surface soil temperature was measured at four sites within the plot and soil temperature as a function of depth was measured at two sites at depths of 0.02, 0.05, 0.1 and 0.2 m. Surface soil temperature sensor installation method was similar to that described by Buchan (1982). A steel drill bit was inserted upwards at an angle of about 30^{o} to the horizontal into the face of a small pit until it emerged from the surface of the 'undisturbed' soil about 0.170 m from the pit edge. The sensor was then inserted into the preformed hole so that its tip lay flush with, and visible at, the soil surface. The sensor tips were covered with a thin film of glue and sprinkled with fine soil so that when

half embedded they resembled small surface crumbs. Since the 'surface' of structured soil is essentially a crumb array, this arrangement should measure local surface temperature as accurately as is possible by a contact method. Compared with methods where the sensor is simply placed on the surface of the soil this configuration should give improved thermal contact with the soil (Buchan, 1982).

The sub-surface temperature probes were installed horizontally from installation pits using a similar technique. In each case the pits were carefully filled to minimise soil disturbance. Checks at the completion of the experiment showed no drift in temperature sensor calibration.

3.3.2.4 Global radiation

Global radiation was measured using a Kipp and Zonen model CM11 pyranometer mounted on the eastward perimeter of the plot. Instrument sensitivity is cross-related to a number of parameters including resolution, stability, cosine response, azimuth response, temperature response, non-linearity and spectral sensitivity. The upper limiting values of the resulting sensitivity variations translate to an expected maximum error in hourly radiation totals of 3%.

3.3.2.5 Shortwave albedo

Reflected radiation was measured with an older model Kipp and Zonen pyranometer. The calibration of this instrument was checked against the new model CM11 pyranometer and was found to be accurate to within 2.5%. The inverted instrument was shielded to prevent error from sensing solar radiation from the horizons; this restricted the viewing area to 5.56 m^2. A view factor adjustment was incorporated into the data to compensate for this restriction (as described in Section 3.2.3.7). The pyranometer was mounted 0.5 m above the soil surface in the south-east quarter of the plot and a correction was incorporated into the data to compensate for the shadow cast (as described in Section 3.2.3.7). Shortwave albedo was recorded as the ratio of reflected to incoming solar radiation.

3.3.2.6 Net radiation

Net radiation was measured with a 'Solar Radiation Instruments' SRI4 net radiometer of Funk (1959) design. Calibration accuracy supplied by the manufacturer was 2.5%. The instrument was mounted 1.5 m above the soil surface in the south-east quarter of the plot.

3.3.2.7 Wind velocity

Wind velocity at a height of 2.0 m was recorded in the centre of the plot with a three-cup, pulse-counting anemometer (Synchrotac, Melbourne, Australia). This instrument was wind tunnel calibrated prior to use. Unfortunately, due to the robust construction of this instrument the calibration had an offset of 1.54 m s^{-1}. The anemometer readings are thought to be insensitive at wind velocities less than 3.0 m s^{-1}. The calibration indicates that at higher velocities accuracy is acceptable.

3.3.2.8 Wind velocity height profile

Wind velocity height profile was measured in the centre of the plot using 'Rimco' miniature three-cup anemometers (Selbys Scientific Limited) mounted at heights of 0.16, 0.25., 0.40. 0.63 and 1.00 m from the soil surface. The instruments had previously been wind tunnel calibrated. Measurement sets to determine z_0 height were obtained, in duplicate, when wind was blowing from each of the north-east, north-west and south-west directions (the prevailing winds at this site).

3.3.2.9 Relative humidity

Relative humidity was measured in the centre of the plot at a height of 2 m with a capacitive type electronic humidity transducer (model 15-840-01, Automation Engineering, Auckland, New Zealand). The instrument was calibrated with a psychrometer. Over a relative humidity range of 30-80%, the mean deviation of the electronic transducer from the psychrometer was 1.3%. This is better than the

manufacturer's specification of 3% accuracy between 50 and 80% relative humidity. An accuracy of 10% is specified in the 20 to 90% range.

3.3.2.10 Air temperature

Air temperature was measured concurrently with relative humidity also at 2 m and in the centre of the plot so as to allow vapour pressure deficit and dew point calculations. A fast response electronic temperature probe (AD590JH, Intersil) encapsulated in perspex tubing was used. Both the relative humidity transducer and the air temperature sensor were mounted in a ventilated screen ensuring no exposure to direct solar or reflected radiation.

Saturation vapour pressure (e_s, kPa) is given as a function of temperature (T, ^oC) as (Rosenberg et al., 1983):

$$e_s = 0.61078 \exp\left[\frac{17.269\ T}{T + 237.30}\right] \quad \ldots (3.22)$$

and actual vapour pressure (e_a, kPa) is related to relative humidity (RH, %) and e_s by:

$$e_a = \left[\frac{RH}{100}\right] e_s \quad \ldots (3.23)$$

at dew point temperature (T_d) $e_a = e_s$ therefore:

$$e_a = 0.61078 \exp\left[\frac{17.269\ T_d}{T_d + 237.3}\right] \quad \ldots (3.24)$$

Following re-arrangement:

$$T_d = \frac{-237.3 \ln\left[\frac{e_a}{0.61078}\right]}{\ln\left[\frac{e_a}{0.61078}\right] - 17.269} \quad \ldots (3.25)$$

Vapour pressure deficit is the difference between saturated vapour pressure (e_s) and actual vapour pressure (e_a).

3.3.2.11 Rainfall

Rainfall was measured in three locations around the perimeter of the experimental plot. A rain-o-matic electronic tipping bucket raingauge (Pronamic, Denmark) was monitored hourly by the automatic data-logging system. A laboratory calibration was made before use. Daily rainfall measurements were made with two 'Marquis' catch-can type rain gauges (Commonwealth Moulding Pty. Ltd., NSW, Australia).

3.3.2.12 Automatic data collection system

An automatic data-logger (Campbell Scientific Inc., model CR7) was used to record soil temperature, global radiation, reflected radiation, net radiation, wind velocity (2.0 m height only), relative humidity, air temperature and rainfall (tipping bucket only). For each of these variables sampling interval was 10 seconds and integration time one hour. Data was stored on cassette tape. The voltage measurement by analogue input channels has a specified accuracy of 0.02% of full scale range.

3.3.2.13 Near-saturation hydraulic conductivity

Near-saturation hydraulic conductivity was measured using a tension infiltrometer device (Figure 3.1). The core sampling and hydraulic conductivity measurement technique was as previously described (Section 3.2.3.4). Hydraulic conductivity was determined for eight intact soil samples (150 mm deep and 207 mm i.d.) from the 0-150 mm soil depth and for a further eight from the 300-450 mm depth ('B' horizon).

3.3.2.14 Pore size distribution

Pore size distribution was determined from the soil water characteristic relationship which was measured using tension tables and pressure plate apparatus as previously described (Section 3.2.3.5). Eight tension table samples (50 mm deep and 104 mm in diameter) were taken from each of the 0-50, 50-100 and 100-150 mm depths, while a further 12 samples were from the 300-350 mm depth ('B' horizon).

Gravimetric water content of these samples was determined at matric potentials of -1.0, -3.0, -5.0 and -10.0 kPa. Separate samples (15 mm deep and 42 mm I.d.) were used for $\theta(\psi_m)$ determination using pressure plate apparatus. Eight samples were taken at or near each of the following soil depths: 25, 75, and 125 mm, while a further 12 samples were taken from about 300 mm depth ('B' horizon). Gravimetric water content was determined for all of these samples at matric potentials of -33, -100 and -300 kPa while at matric potentials of -500 and -1500 kPa only half of the number of samples taken from each depth increment were used. Gravimetric water contents were converted to volumetric by multiplication by measured bulk density values.

3.3.2.15 Unsaturated hydraulic conductivity

The $K(\psi_m)$ function was estimated with the method of Jackson (1972) using near-saturation hydraulic conductivity and the $\theta(\psi_m)$ relation as inputs. The method was explained in detail in Section 3.2.3.6.

3.3.2.16 Bulk density, particle density and total porosity

Bulk density was determined using the method of Gradwell (1972) from nine samples of 2640 cm^3 taken at each of the following soil depth ranges: 0-50, 50-100, 100-150 mm. Bulk density of the soil 'B' horizon was determined from the 12 'B' horizon tension table samples. The particle density previously determined for this soil was used together with bulk density data to calculate total porosity using Equation 2.6.

3.3.2.17 Aggregate size distribution

Samples for aggregate size distribution determination using rotary sieving (refer Section 3.2.3.1) were taken from eight random locations within the plot at each of the following soil depths: 0-40, 40-80, 80-160 mm. Samples were obtained using a flat bottomed shovel.

3.3.2.18 Soil surface roughness

Eight soil surface roughness determinations were made within the plot with a point gauge micro-relief meter. Each sample had an area of 0.25 m^2 and consisted of 100 elevation measurements. The measurement technique was previously described in Section 3.2.3.3, and the roughness index calculation method is described in Section 4.4.

CHAPTER 4

The Effects of Multiple-pass Tillage on Surface Soil Physical Properties

4.1 Introduction

This chapter describes the way in which soil water content at time of tillage and type of tillage operation influence the surface physical conditions of a medium-textured, wind-erosion-susceptible soil.

4.2 Aggregate size distribution

The aggregate size distribution is an important aspect of soil structure which directly influences a wide range of soil properties and processes (e.g. soil air and water movement). The definition of an optimal aggregate size range for agronomic objectives was discussed in Section 2.3.2.6. The quantity of aggregates less than 0.84 mm diameter is an index of the susceptibility of a soil to wind erosion (Chepil, 1942,1943). The proportion of aggregates less than 0.26 mm can be an important feature of the surface soil because of crusting susceptibility as well as wind erosion susceptibility. A high proportion of these aggregates would probably be reflected in increased crust formation where sufficient rainfall occurs. A surface crust might be beneficial in reducing wind erosion susceptibility but undesirable in terms of seed germination, plant emergence, aeration and infiltration (refer Section 2.3.2).

Analysis of variance (ANOVA) showed that tillage operation had a highly significant effect on each measured aggregate size range ($P<0.01$). The 'excess' tillage treatment produced greater amounts of smaller aggregates compared to the other tillage treatments (Figure 4.1). The 'intermediate' and 'minimum' tillage treatments produced

similar quantities of aggregates in the less than 1.47 mm diameter size range although the 'minimum' tillage treatment created more larger clods.

Figure 4.1. Tillage effects on aggregate size distribution as determined by dry sieving (error bars represent ± 1 std. deviation).

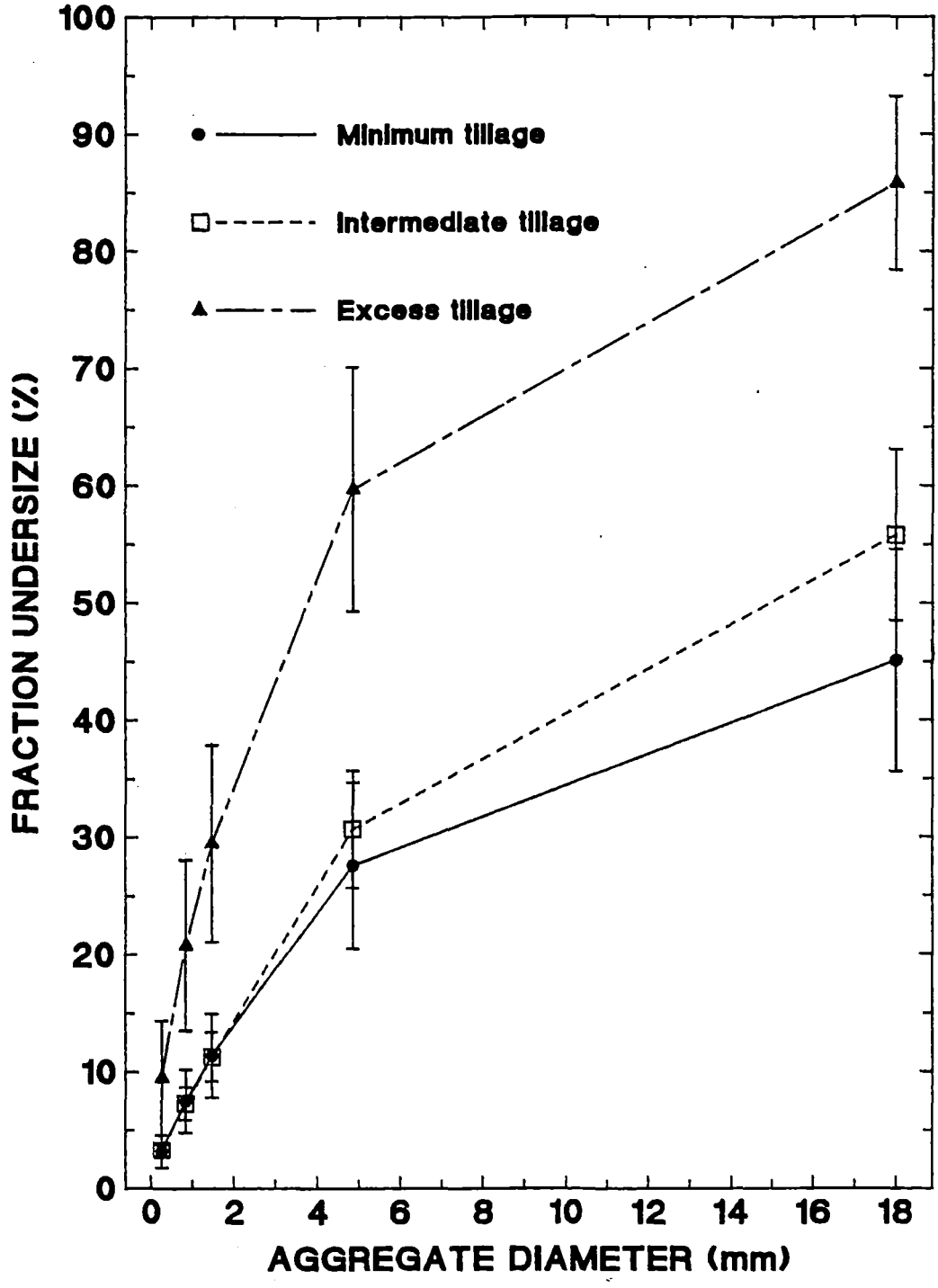

Figure 4.2. Effect of pre-tillage soil water content and tillage operations on the percentage of aggregates less than 0.84 mm in diameter (standard error of the mean = 1.77% ; means labelled with the same letter are not significantly different at the 5 % level as determined by Duncan's New Multiple Range Test).

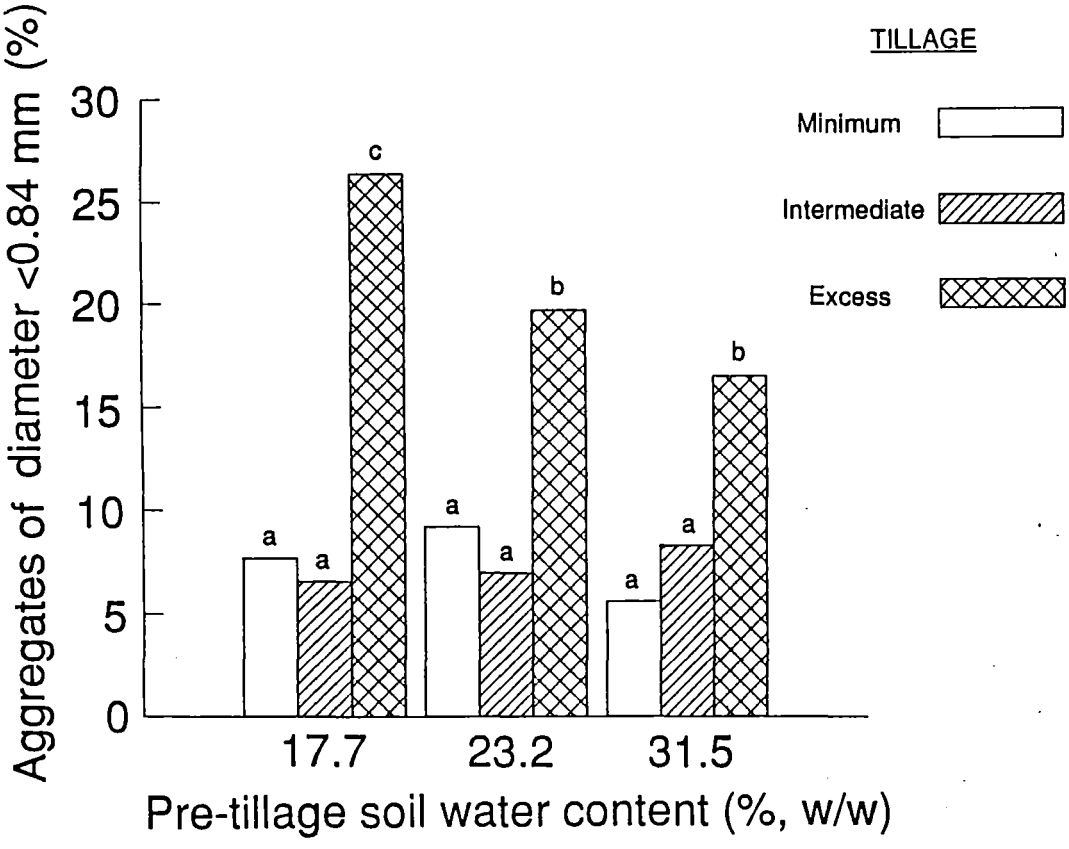

Analysis of variance has shown that the pre-tillage soil water content (PTSW) treatment (considered in isolation) had a non-significant effect on aggregates in the less than 0.84 mm size range. However, a significant interaction occurred between tillage treatment and PTSW (ANOVA, $p<0.05$). Significantly greater quantities of highly erodible aggregates in the less than 0.84 mm diameter size range were produced where a dry soil was subjected to 'excessive' tillage (Figure 4.2). Further analysis showed a PTSW effect (in isolation) on aggregates less than 0.26 mm diameter (ANOVA, $p<0.01$) as well as a PTSW/tillage interaction (ANOVA, $p<0.05$) (Figure 4.3). The proportion of aggregates of less than 0.26 mm diameter was largest following tillage at a PTSW of 17.7% (w/w) (0.58 of the Lower plastic limit (LPL)) and smallest at PTSW of 31.5% (w/w)

(Equivalent to the LPL). The PTSW effect was largest in the treatments which were subjected to 'excessive' tillage. Non-significant PTSW effects on aggregates between 0.26 and 0.84 mm diameter probably indicate that the PTSW/tillage treatment interaction evident on the less than 0.84 mm range is due primarily to the effect of PTSW on the less than 0.26 mm size range.

Figure 4.3. Effect of pre-tillage soil water content and tillage operations on the percentage of aggregates less than 0.26 mm in diameter (standard error of the mean = 1.04% ; means labelled with the same letter are not significantly different at the 5 % level as determined by Duncan's New Multiple Range Test).

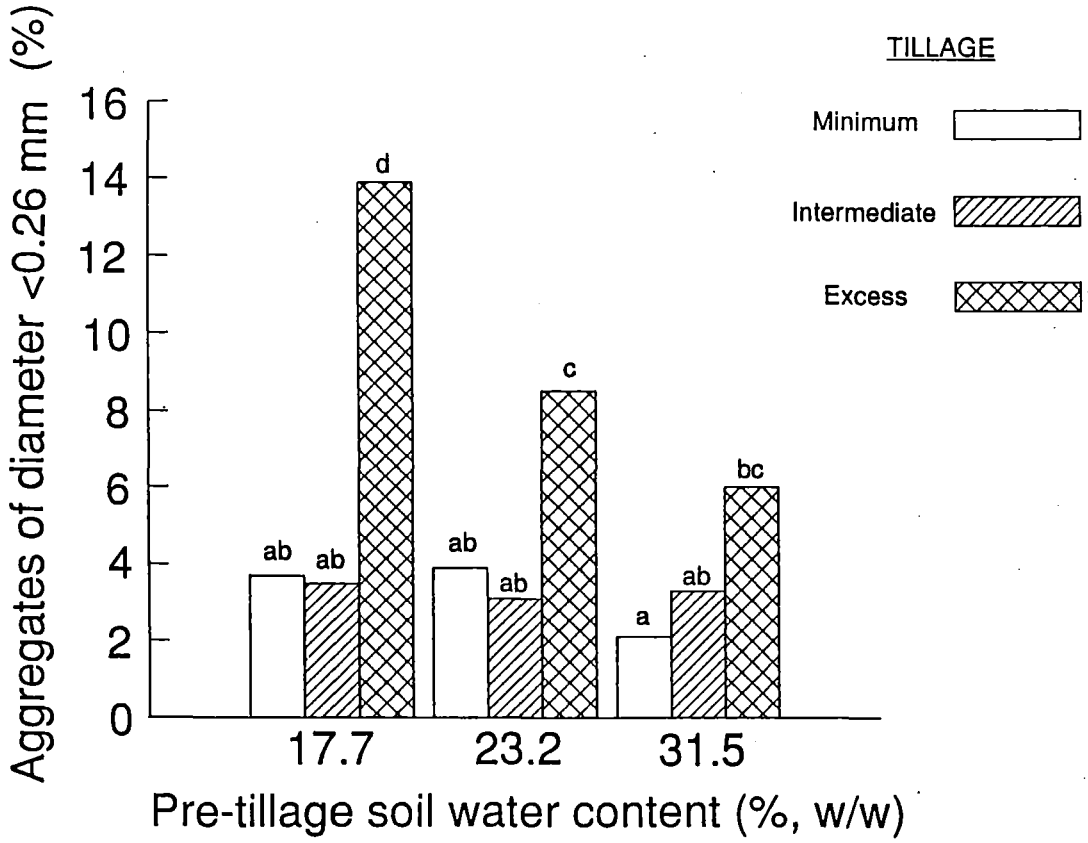

The decrease in proportion of aggregates less than 0.26 mm diameter in a soil subject to 'excess' tillage at the lower plastic limit, as compared with lower PTSW levels, could be the result of either: (i) aggregate reformation occurring following the mixing of

fine, moist, particles during tillage, or (ii) less aggregate breakdown from larger aggregate size classes into the less than 0.26 mm diameter range. Small soil aggregates and particles can demonstrate considerable cohesion. Inter-aggregate cohesion is at a maximum near the lower plastic limit (Spoor, 1982). The small aggregates and particles in an intensively-tilled soil would tend to stay separated when mixed during tillage when the soil is dry. In a wet soil however, they might tend to re-form into relatively unstable clods. This cohesion tendency would be greatest among small particles.

As the water content of soil increases up to the LPL, soil strength decreases (Taylor and Burnett, 1964; Taylor et al., 1966; Farrell et al., 1967). In a very dry soil the fragmentation process during tillage is achieved through brittle fracturing of clods tearing 'corners', by abrasive action between the clods themselves and the implement surfaces (Hadas and Wolf, 1983). The 'excess' tillage treatment, with rotary cultivation being included, appears to be causing a high degree of aggregate fragmentation on dry soil. This is due to the high energy input overcoming the high strength of the dry soil and to the abrasive action of the tillage process with this implement. It is likely that 'excess' tillage at a PTSW of 17.7% is resulting in a greater proportion of aggregates and particles less than 0.26 mm diameter as compared to the same tillage operations at PTSW 31.5%. In the dry soil inter-aggregate cohesion is low and so the aggregate reformation process is not occurring.

The PTSW effect occurs only on aggregates less than 0.26 mm diameter because the aggregate reformation process occurs only with small soil particles and because the abrasive type of breakdown during the 'excessive' tillage of dry soil results in a significant proportion of small particles. The significant PTSW effect with 'excess' tillage on aggregates and particles less than 0.26 mm diameter probably occurs because of aggregate reformation at PTSW of 31.5% and because of greater quantities of aggregates of less than 0.26 mm diameter being produced at PTSW 17.7%.

From a wind erosion susceptibility view-point, PTSW effects can be significant on medium-textured soils. The intensity of tillage operation, however, has a dominant effect on aggregate size distribution. The avoidance of excessive tillage on a medium-textured, wind-erosion-susceptible soil would reduce the likelihood of a PTSW effect on aggregate breakdown. Furthermore, the avoidance of low PTSW contents

would mean that the likelihood of producing large quantities of fine, wind-erodible material during secondary tillage is low, provided that the soil is not excessively tilled. A further reason for not tilling at low soil water contents is that there is a tendency for the proportion of large clods to decrease, and small aggregates to increase with increasing depth in the tilled layer. At low PTSW levels this is less pronounced (Ojeniyi and Dexter 1979b). Such an aggregate size distribution with soil depth is beneficial in reducing wind erosion susceptibility.

4.3 Aggregate stability

Large pores in the soil generally favour high infiltration rates and adequate aeration for plant growth (Section 2.3.2). Immediately after tillage most soils contain an abundance of these large pores. Their continued existence depends on the stability of the aggregates. Unstable aggregates at the soil surface can result in crust formation after rainfall. Surface crusting has been shown to be a generally undesirable surface structural feature (Section 2.3.2). Abrasion by impacts of particles transported along the soil surface by wind is an important phase of the wind erosion process on all soils. Non-erodible aggregates can gradually be broken down under impacts from saltating particles, thereby creating more erodible material (Chepil and Woodruff, 1963). Mechanical stability of soil aggregates gives a relative measure of the resistance of disintegration by abrasion experienced by the soil when it is eroded by wind. Abrasion varies inversely with mechanical stability (Chepil and Woodruff, 1963).

Tillage operation and PTSW content both had highly significant effects on the aggregate stability index (ANOVA, $p<0.01$). The high stability of aggregates left after 'excessive' tillage (Figure 4.4) is not surprising as the less stable clods produced from primary tillage will have been broken down into smaller, more stable aggregates with the subsequent tillage. Tensile strength of soil aggregates has been shown to be a function of aggregate size, the larger the aggregate the smaller the mean tensile strength (Braunack et al., 1979). This result of high aggregate stability after 'excessive' tillage pertains to the short-term dry aggregate stability of a freshly-tilled soil following just one sequence of tillage operations. Intensive tillage over a longer time period would be expected to cause a decline in soil organic matter content and a subsequent decrease in aggregate stability (refer Section 2.3.1.3).

Figure 4.4. Effect of pre-tillage soil water content and tillage operations on relative aggregate stability (standard error of the mean = 0.016 ; means labelled with the same letter are not significantly different at the 5 % level as determined by Duncan's New Multiple Range Test).

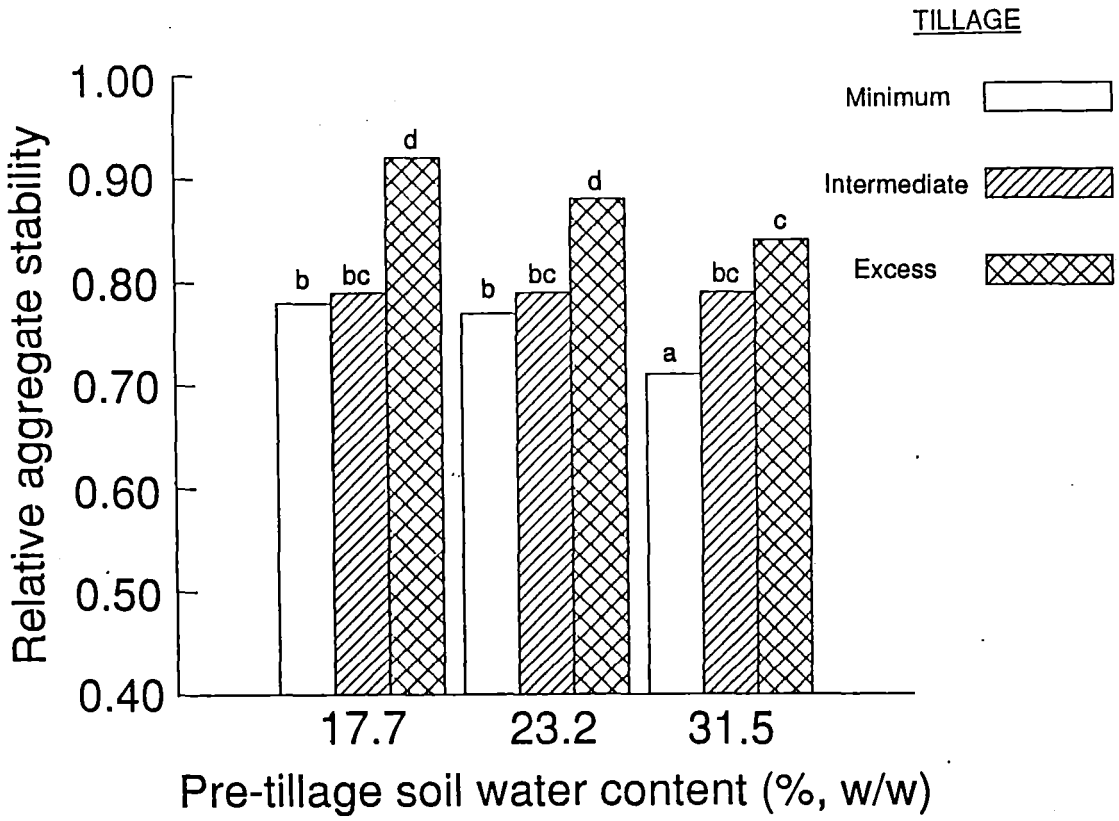

Clods produced during the tillage of soil with low and intermediate PTSW levels tend to be more resistant to mechanical breakdown than those produced during tillage at a water content near the LPL. The significantly lower stability of clods formed near the LPL during 'excessive' tillage (Figure 4.4) could be related to the aggregate formation process. Some of the clods formed under these conditions could have been re-formed from fine particles showing cohesion due to relatively high water content. The more stable structural units in the soil have been formed by physical forces such as wetting and drying, freezing and thawing, and the compressive and drying action of plant roots (Section 2.3.1.1). The clods reformed during tillage have not been subjected

to these physical aggregation mechanisms for any significant time period and are mainly held together by the cohesive force of the soil water. Subsequently, when in a dry state, they are relatively unstable. The low relative stability of the aggregates produced from tillage at soil water contents near the LPL is undesirable in terms of both surface crust formation and wind erosion susceptibility.

4.4 Soil surface roughness

4.4.1 Introduction

Random roughness is the surface configuration of the soil caused by the random oriented arrangement of soil aggregates and clods. Surface roughness is an important property of tillage systems. Infiltration (Burwell et al., 1968), evaporation (Allmaras et al., 1977), solar radiation reflection (Allmaras et al., 1977), and other phenomena such as turbulent air exchange with the atmosphere (Allmaras et al., 1977) are closely associated with the roughness of the soil surface. Burwell et al. (1968) have shown highly significant correlations of infiltration capacity prior to initiation of runoff with a roughness index. Falayi and Bouma (1975) also showed this correlation and reported the difference to be due to the nature of the sealed or crusted layer formed at the soil surface. Soils with a low random surface roughness can have dense surface crusts develop over the entire surface, while on more uneven surfaces crusts form mainly in surface depressions (Larson, 1962). Allmaras et al. (1977) have shown higher evaporation rates from rough surfaces; however, these soils also had increased porosity which might have influenced evaporation as much as the surface configuration. The roughness of the soil surface can have a considerable influence on the rate and amount of erosion.

Surface roughness of a tilled soil can consist of two components: 'oriented roughness' describing the furrows and ridges resulting from tillage implements and 'random roughness' describing the irregular peaks and depressions on both the ridges and furrows (Burwell et al., 1966). Oriented roughness must be removed mathematically from the data before random roughness can be calculated (Allmaras et al., 1966). The resulting random roughness value can be considered in terms of soil

strength and aggregate size relations (Allmaras et al., 1966) and allows comparisons to be made between implement effects on various soil types. Whether oriented roughness is removed from the data depends on the application of the resulting roughness index.

Previous workers have shown that slope correction is essential if any meaningful comparisons between treatments imposed on the soil are to be made (Currence and Lovely, 1970). Tillage tool marks and plot slope have obvious and significant effects on the roughness index (e.g. Currence and Lovely, 1970; this study Table 4.4). In this study oriented roughness was removed from the data and a slope correction was made to allow tillage comparisons on the basis of random roughness. The upper and lower 10% of height readings were retained in the data set in contrast to the widely adopted method of Allmaras et al. (1966) in which these measurements were discarded 'to reduce the effect of erratic height readings on the final result.' The correction procedure that was used followed Currence and Lovely, (1970):

$$h'_{ij} = h_{ij} - (\overline{h}_{.j} - \overline{h}_{..}) - (\overline{h}_{i.} - \overline{h}_{..}) - (\overline{h}_{..}) \quad \ldots (4.1)$$

where:

h'_{ij} = corrected height reading in the ith row and the jth column.
h_{ij} = original height reading in the ith row and jth column
$\overline{h}_{.j}$ = mean of readings in the jth column
$\overline{h}_{i.}$ = mean of readings in the ith row
$\overline{h}_{..}$ = overall mean

The random roughness considered here is distinguished from both micro-scale roughness, which is the arrangement of individual particles and small aggregates on a scale of millimetres or less, and macro-scale roughness which includes ridges, wheeltracks, field slope and other defined features. Random roughness is on a scale of a few centimetres and, for the purposes of this study does not consider micro- or macro-scale roughness components.

Several statistical measures have been used to characterise soil roughness (Zobeck and Onstad, 1987). Many of these measures represent the distribution of soil

surface elevations over a regular grid. Burwell et al. (1963) advocated a roughness index defined as the standard deviation of logarithms of soil elevation heights after oriented roughness had been removed from the data. It was considered that logarithms of the height elevations were more normally distributed than their arithmetic values. In the roughness index described by Allmaras et al. (1966) each height measurement was expressed as a natural logarithm. The effects of slope and oriented tillage tool marks were mathematically removed and the upper and lower 10% of measurements were eliminated. The index was then estimated as the standard error among adjusted logarithms of height. It was pointed out by Zobeck and Onstad (1987) that although Allmaras et al. (1966) and Burwell et al. (1963) are frequently cited as sources for roughness index calculation it is often difficult to determine whether all details of their procedures have been adhered to in other studies. In order for comparisons to be made between different studies of surface roughness it is important that full details of the methods used be reported.

4.4.2 Distributional form of the data set

To determine the most suitable index for describing the surface roughness measured in this study, the distributions of non-transformed and natural logarithm transformed data were tested for normality using the Kolmogorov statistic which was calculated using the SAS statistical computing package (SAS, 1985). In this procedure non-transformed and natural log transformed data were compared with normal distributions with the same mean and variance as the measured sample. The results of the test are presented in Table 4.1.

Natural log transformation of the data did not give a better approximation of a normal distribution. Of the 72 data sets, 45 were normally distributed, 5 were log-normally distributed and 22 were neither normally or log-normally distributed. Of the 27 data sets which were non-normal, 16 were from the 'minimum' tillage treatment, 6 from the 'intermediate' and 5 from the 'excess' tillage treatment. Each PTSW treatment had the same number (9) of non-normal data sets. Of the 16 data sets from the 'minimum' tillage treatments which were not good approximations of normal distributions 4 were log-normal, 3 were skewed, 3 probably platykurtic (showing low kurtosis, i.e. with a flattened peak on the probability density function), and the remaining 6 could not be

clearly differentiated. The relatively small data set of 100 elevations limits the normality testing procedure.

Table 4.1 Distributional form of surface roughness data before and after natural logarithmic transformation.

PROBABILITY OF DATA SET FITTING MODEL	NUMBER OF OCCURRENCES	
	MODEL	
	NORMAL	LOG NORMAL
> 0.99	19	14
0.95 - 0.99	13	13
0.90 - 0.95	10	4
0.85 - 0.90	3	12
< 0.85	27	29

This data set cannot be properly characterised by one distributional form, although the normal distribution provides the best approximation. However, the use of a standard deviation or standard error as an index of random surface roughness assumes normally distributed data. There is no clear physical reason why micro-relief data should fit one particular distributional form. Furthermore, the distributional form of this data set has been shown to be treatment-dependent. Treatment comparisons between 'minimum' tillage with either of 'intermediate' or 'excess' tillage using such an index are, therefore, probably invalid. If standard deviations or standard errors are to be used to index random surface roughness then the distributional form of the data must be thoroughly analysed and reported so that any treatment comparisons can be carefully made with full knowledge of the index calculation and its limitations.

4.4.3 Semi-variance method for surface roughness characterisation

Since the initiation of the work reported here a new semi-variance method for surface roughness characterisation has been reported (Linden and van Doren, 1986). This approach is based on the concept of a 'regionalised variable', one which varies from one place to another with apparent continuity but which is not easily represented with a workable function. Consider a series of points on a regular grid with some regionalised variable Z. If the regionalised variable is stationary (i.e. the statistical properties are unaffected by translations of the origin for time and location), we can compute the mean of these values and subtract it from each observation to transform the Z's to deviations around a mean of zero, deviations designated Z_i. We calculate the variance of Z (v_o) by:

$$v_o = \frac{\Sigma z_i^2}{n} \qquad \ldots (4.2)$$

where n is the number of observations. It is assumed that the value at a given point is related, in some manner, to the value at points some distance away. The influence of more distant points would be expected to be less than the influence of nearby points. Further, the degree of influence might vary with direction.

The relationship between equally spaced points, along a specific vector, can be expressed by a measure of covariance. Covariance can be determined only at regularly spaced sample points. Where the sample spacing is ΔX the covariance at the distances, $\Delta X.h$ (where h is an integer), is given by:

$$v_{\Delta h} = \frac{1}{n} \sum_{i=1}^{n} z_i \cdot z_{i+h} \qquad \ldots (4.3)$$

This states that covariances over distances $\Delta X.h$ along the vector are equal to the mean cross-product of values of Z at points Y_i with the values of Z at other points Y_{i+h}. These other points being a distance $\Delta X.h$ away. Here, n is the number of pairs of points a distance $\Delta X.h$ apart, in the vector direction.

The semi-variance ($\gamma_{\Delta h}$) is defined as the variance minus the covariance at distances Δh and equals one-half the difference (Z_i-Z_{i+h}), or:

$$\gamma_{\Delta h} = \frac{1}{2n} \sum_{i=1}^{n} \left[z_i - z_{i+h} \right]^2 \qquad \ldots (4.4)$$

Where n again represents the number of pairs of elevation points that occur in the data set at a lag interval. Semi-variance can be evaluated only at distances $\Delta X.h$ corresponding to multiples of the spacing between sample points in the vector direction. As the vector distance becomes infinitesimally small the variance and the covariance are defined by essentially the same points. Conversely as vector distance becomes larger, covariance will decrease because of progressively greater independence between points with increasing distance apart. Therefore semi-variance ranges from zero, when $\Delta X.h$ is zero, up to a value equal to the variance at some large value of h. This follows from the expansion of the squared term in Equation 4.4. These relationships are shown for different data sets when the semi-variance is plotted against $\Delta X.h$ to produce a variogram.

This method was applied to the parameterisation of surface soil roughness by Linden and van Doren (1986). Height elevations Z_i were measured on a regular grid. Spacings between the grid dimension (2 cm) and 50 cm were used for their semi-variance analysis (i.e. $\Delta X = 2$, h = 1 to 25, therefore $\Delta X.h$ was 2, 4, 6, ... 46, 48, 50.). Semi-variance was plotted against distance $\Delta X.h$ for observation of the pattern. Using 289 data sets Linden and van Doren reported that the semi-variance originated at zero (indicating no measurement or 'nugget' variance) and increased at a decreasing rate to the 'sill' or sample variance. The results showed a strong spatial dependence at close spacing but not at wider spacings.

Linden and van Doren (1986) suggested a modified spatial variability procedure termed the mean absolute-elevation-difference analysis. The mean absolute-elevation-difference (ΔZ_h) was defined as:

$$\Delta Z_h = \sum_{i=1}^{n} \left| \frac{z_i - z_{i+h}}{n} \right| \qquad \ldots (4.5)$$

When ΔZ_h was plotted against $\Delta X.h$ the elevation typically increased from zero at a decreasing rate approaching a plateau at 15-30 cm. An equation of the form:

$$\Delta Z_h = \frac{1}{b\left(\frac{1}{\Delta X.h}\right) + a} \quad \ldots (4.6)$$

was used to describe the curves of all 289 data sets considered by Linden and van Doren (1986). Where $1/\Delta X.h$ and $1/\Delta Z_h$ were used as regression variables, all had regression coefficients of $r^2>0.85$ and 80% had coefficients $r^2>0.98$. It was suggested that patterns of all data were sufficiently consistent to justify the generalisation of the shape function. Linden and van Doren (1986) defined two surface roughness parameters:

$$LD = \frac{1}{a} \quad \ldots (4.7)$$

$$LS = \frac{1}{b} \quad \ldots (4.8)$$

where a and b are regression coefficients from Equation 4.6 and $\Delta X.h$ was limited to 20cm. ΔZ approaches the value of LD as ΔX approaches infinity. $\Delta Z/\Delta X$ approaches infinity as ΔX approaches zero. LD is thus termed the limiting elevation difference as the spacing becomes large while LS is the limiting slope of the surface as the spacing becomes small. LS then can be considered as the change in elevation per unit change in horizontal distance between points. LD is an estimation of the central tendency of the difference in elevation between different points.

The method of Linden and van Doren (1986) has been applied to the data set collected in this study (following slope and tool mark correction). Transects 20 cm long were used. In each data set 40 transects were defined, 20 along rows of elevation measurements and 20 along columns. Grid spacing of the elevation measurements (ΔX) was 5 cm so mean absolute-elevation-differences were computed at distances ($\Delta X.h$) of 5, 10, 15 and 20 cm (h=1,2,3,4). ΔZ_h values were plotted against spacings and $1/\Delta Z$ and $1/\Delta X$ were used as regression variables. The computations were repeated on 36 data sets (i.e. 1440 transects in total). The r^2 values from the regressions were poor with 14 of the 36 being less than 0.60 (Table 4.2). Using 40 transects per data set, patterns were not sufficiently consistent to justify the

generalisation of the shape function (Equation 4.6). In many of the data sets there was no dependent relation between ΔZ_h and $\Delta X.h$ at grid spacings of 5 cm where 20 cm transects are considered. The goodness-of-fit was dependent on the roughness of the surface being considered, thereby precluding the use of the method, in this form, for comparing surfaces of different roughness. At 5cm spacings the rough 'minimum' tillage surface is better approximated by a distribution of the form of Equation 4.6 than is the 'intermediate' tillage surface while the smoother 'excess' tillage surface results in an even worse fit (Table 4.2). This result probably indicates that Linden and van Doren (1986) have actually suggested the use of a transect length of 20 cm based on the regression fit up to 20 cm in a 50 cm segment. In each 20 cm data segment the ΔZ_h at 20 cm is estimated from one pair of data only. This estimate represents one of only four points used for the regression. The imprecision of the estimation of this point could be contributing to the lack of fit from any one generalised relationship for this data set.

Table 4.2 Analysis of mean absolute-elevation-difference data fit to the generalised relationship suggested by Linden and van Doren (1986) where 20 cm transects were used and one sample consisted of 40 transects.

REGRESSION COEFFICIENT r^2	NUMBER OF OCCURRENCES			
	TOTAL	MINIMUM TILLAGE	INTERMED. TILLAGE	EXCESS TILLAGE
> 0.98	1	1	-	-
0.95-0.98	5	3	1	1
0.90-0.95	1	-	1	-
0.80-0.90	5	4	1	-
0.70-0.80	8	2	3	3
0.60-0.70	2	-	2	-
0.40-0.60	3	-	-	3
< 0.40	11	2	4	5

As a further investigation, ΔZ determinations were made using 50 cm transects. This should allow a better observation of the form of any pattern which might emerge. In addition, more data pairs contribute to the ΔZ_h value at small spacings on each transect. On each 50 cm transect then, the precision of the ΔZ_h estimates at $\Delta X.h$ of 5,

10, 15 and 20 cm increases substantially above that possible with 20 cm transects. The two slope and toolmark corrected elevation data sets which were measured on each experimental plot were combined to give 40 transects per plot for this analysis. Spatial dependence was observed, in most cases, at distances less than 20 cm. An equation of the form of Equation 4.6 was fitted to the data as suggested by Linden and van Doren (1986). The r^2 values indicating goodness-of-fit of the regression, together with the corresponding tillage treatments, are presented in Table 4.3. A relationship similar in form to that suggested by Linden and van Doren (1986) does occur in most of the data sets. In the six worst-fit cases, the spatial dependence occurred at a distance less than 20 cm. The goodness-of-fit was generally independent of tillage treatment. Following the work reported by Linden and van Doren (1986) the regressions could be expected to improve with a greater number of transects and a denser sampling pattern. It would appear that the consistency in form of the ΔZ_h - $\Delta X.h$ relation required for the success of the method does occur. In a plot of ΔZ_h versus $\Delta X.h$ there is greater precision in ΔZ_h values at small spacings due to the larger number of sample pairs considered. When fitting a regression line to the data a weighted regression giving greater influence to the values at small spacings would be appropriate.

4.4.4 A comparison of surface roughness indices

To characterise the random surface roughness of the tilled plots in this study an index based on the standard deviation of height measurements was used, together with the indices of Linden and van Doren (1986), in order to provide a comparison. The technique of Romkens and Wang (1986) could not be used in this study because of its high data requirement with 5 mm grid spacings and 1 m long transects. As logarithmic transformation of the elevation data did not normalise the distribution, the first index used here (denoted SR index) is simply the standard deviation of the non-transformed data after slope and toolmark correction using Equation 4.1. The upper and lower 10% of elevation measurements were retained. In each plot the SR index was calculated for each of the two data sets and the mean value used as the index for that plot. Results using this index are presented in Table 4.4.

Table 4.3 Analysis of mean absolute-elevation-difference data fit to the generalised relationship suggested by Linden and van Doren (1986) where 50 cm transects were used and one sample consisted of 40 transects. Regression at spacings 20 cm and less.

REGRESSION COEFFICIENT r^2	NUMBER OF OCCURRENCES			
	TOTAL	MINIMUM TILLAGE	INTERMED. TILLAGE	EXCESS TILLAGE
> 0.98	2	2	-	-
0.95-0.98	8	4	2	2
0.90-0.95	8	2	3	3
0.80-0.90	4	2	1	1
0.70-0.80	5	1	2	2
0.60-0.70	3	-	2	1
0.40-0.60	2	1	-	1
< 0.40	4	-	2	2

The LD and LS parameters were calculated on the slope and toolmark corrected data using the method previously described. On each plot 40 transects, each 50 cm long were defined, 20 along rows of measured elevation data and 20 along columns. The elevation measurements were made 5 cm apart on the grid (i.e. $\Delta X = 5$ cm). A relationship of the form of Equation 4.6 was fitted to the function of mean absolute-elevation-difference (ΔZ_h) with distance ($\Delta X.h$) over the part of the function where distance $\Delta X.h$ did not exceed 20 cm (i.e. h limited to 4, ΔX equals 5 cm). Results of the analyses are presented in Figures 4.5 and 4.6.

The LD index, being an estimation of central tendency of the difference in elevation between individual points, is similar to the SR index which is an estimate of central tendency of the difference in elevation points and the mean. The regression between the LD and SR indices for the 36 plots considered resulted in a coefficient (r^2) of 0.968 (Equation 4.9).

$$LD = -1.23 + 1.36SR \qquad \ldots (4.9)$$

where elevations are measured in millimetres. The goodness-of-fit indicates that LD is a roughness index as sensitive as the widely used SR type of index. It would also indicate that the LD index is not a large improvement on the SR index in this respect. The comparison of these indices is limited by the absence of an accurate, sensitive and generally accepted surface roughness index which can be used as a independent standard for evaluation.

Table 4.4 Treatment means for random roughness calculated using an index which is the standard deviation of elevation measurements (SR index).

TILLAGE	SLOPE & TOOLMARK CORRECTED			NON-CORRECTED DATA		
	PTSW			PTSW		
	17.7%	23.2%	31.5%	17.7%	23.2%	31.5%
MINIMUM	14.57bc	14.59bc	17.33c	22.31z	23.39z	23.59z
INTERMED.	13.36bc	12.05b	12.35b	15.95y	14.45y	14.31y
EXCESS	4.91a	6.58a	6.04a	6.85x	8.85x	8.39x

Any two treatments not labelled with the same letter are significantly different at the 5% level (as determined by Duncan's New Multiple Range Test, Steel and Torrie, 1981). No statistical comparison is made between random roughness indices calculated with slope and tool-mark corrected data and those calculated with non-corrected data.

Indices using standard deviations or standard errors of elevation data are not related directly to physical surface description (e.g. micro-relief versus distance) and they are not process-oriented parameters as are needed in the description of mass or

energy exchange systems (Linden and van Doren, 1986). They are are however, simple to use, able to characterise surface roughness and they are measurable parameters of tillage systems. A consistent form of the ΔZ_h-$\Delta X.h$ plot is required for valid LD and LS indices and this does occur even with the relatively small number of transects used in this study. With a greater number of samples the LD and LS indices will probably be more consistently correct than a distribution dependent statistic like the SR index. When using the LD and LS indices, the regression coefficients of the ΔZ_h-$\Delta X.h$ relation should be stated. The LD and LS indices are not dependent on distributional form of the field-measured elevation data, they are relatively simple to calculate and the data requirement is not excessive, especially with the availability of automated non-contact micro-relief meters. Together the LD and LS indices supply more information about the soil surface than indices of the SR type.

4.4.5 Tillage treatment effects on random roughness

The LD and LS indices are used to characterise soil surface roughness in this study. The results using the SR index are presented for a comparison and because of the large volume of random roughness information in the literature based on similar index types (Table 4.4). The tillage treatments used in this trial had a significant effect on random surface roughness (LD index) (ANOVA, $p<0.001$). The more intensive tillage reduces aggregate size and thus results in a smoother surface (Figure 4.5). Pre-tillage soil water (PTSW) did not significantly affect random soil roughness. Aggregate size distribution results showed that PTSW tended to affect the production of soil particles less than 0.26 mm diameter. The quantity of the large soil aggregates that tend to have a greater influence on random soil roughness were not affected by this treatment and the random soil roughness result reflects this.

The reduction in random soil roughness which occurs with 'excessive' tillage increases the susceptibility of the soil to wind erosion because a smooth surface is less effective in reducing surface wind velocity. A smooth surface does reduce wind turbulence, but the effect the decreasing turbulence has in reducing wind erosion usually does not compensate entirely for the increased surface velocity (Chepil and Milne, 1941). The considerable turbulence which would occur over a rough surface at higher wind speeds might be expected to enhance water vapour loss from the soil. The susceptibility of the 'excessively' tilled soil to crust formation would be greater than that

following less intensive tillage and the crust would be likely to affect a greater area of the soil surface.

Figure 4.5. Effect of pre-tillage soil water content and tillage operations on random soil roughness (LD index) (standard error of the mean = 2.47 ; random soil roughness LD index is calculated as described in the text ; means labelled with the same letter are not significantly different at the 5 % level as determined by Duncan's New Multiple Range Test).

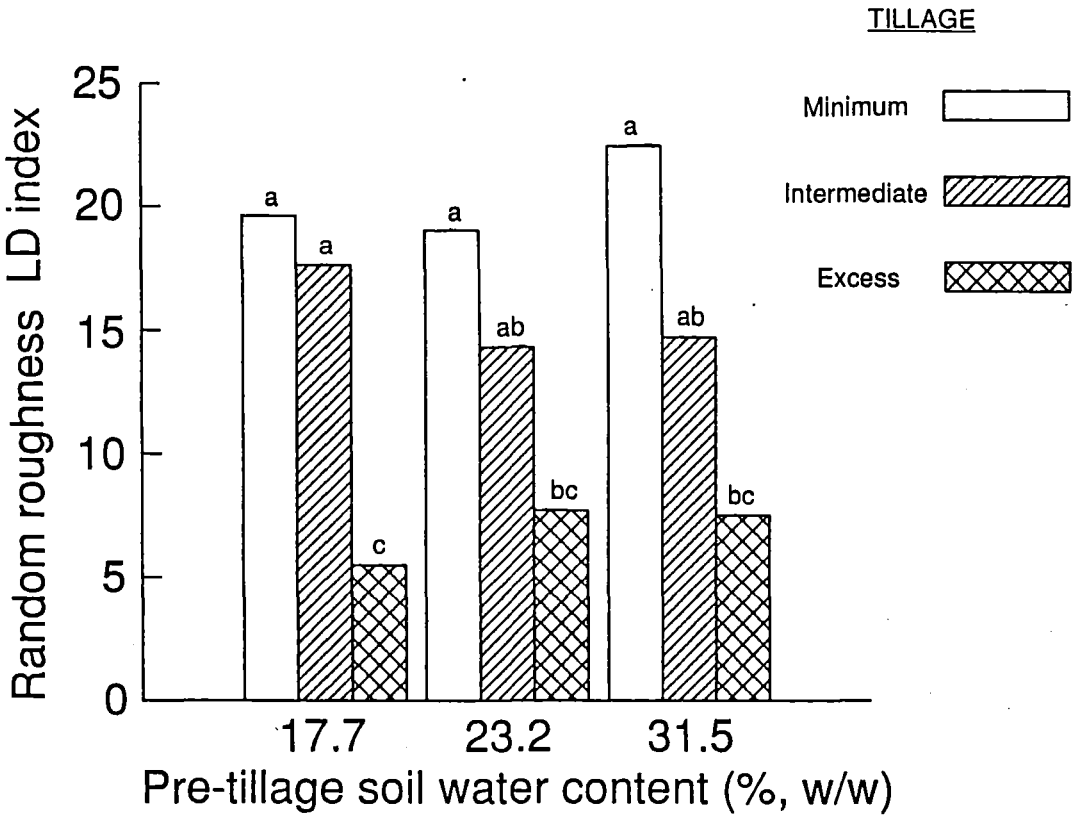

4.4.6 Soil surface area

Soil surface area will affect the exchange processes between the soil and the atmosphere. Increased surface area also has implications on the dissipation of energy from rainfall. The energy from rainfall is spread over a larger surface area on rough

surfaces so that the energy per unit surface area would be less than the energy on an equivalent horizontal area of a soil with a smoother surface. This could be a part of the reason for increased resistance to sealing or crusting on rougher surfaces. Surface area is, therefore, an important soil property.

Figure 4.6. Effect of pre-tillage soil water content and tillage operations on random soil roughness (LS index) (standard error of the mean = 0.287 ; random soil roughness LS index is calculated as described in the text ; means labelled with the same letter are not significantly different at the 5 % level as determined by Duncan's New Multiple Range Test).

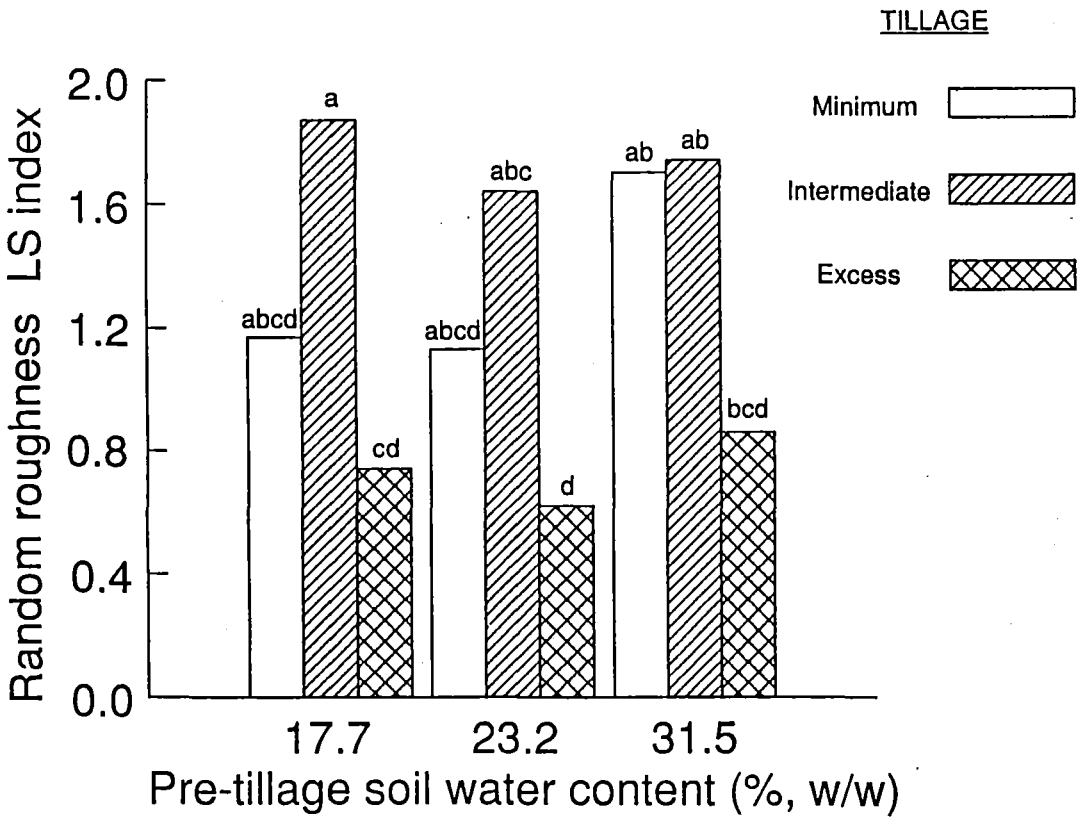

Using the LS index, soil surface area can be estimated using the equation (Linden and van Doren, 1986):

$$A_s = \sqrt{LS^2 + 1} \qquad \ldots (4.10)$$

where A_S is the area of the surface per unit horizontal area. LS was previously defined. An estimation of soil surface area with this method assumes straight line elevations between data points. This assumption becomes more valid as spacing decreases.

Figure 4.7. Effect of pre-tillage soil water content and tillage operations on soil surface area (surface area per unit horizontal area) (standard error of the mean =0.378 ; soil surface area is calculated as described in the text ; means labelled with the same letter are not significantly different at the 5 % level as determined by Duncan's New Multiple Range Test).

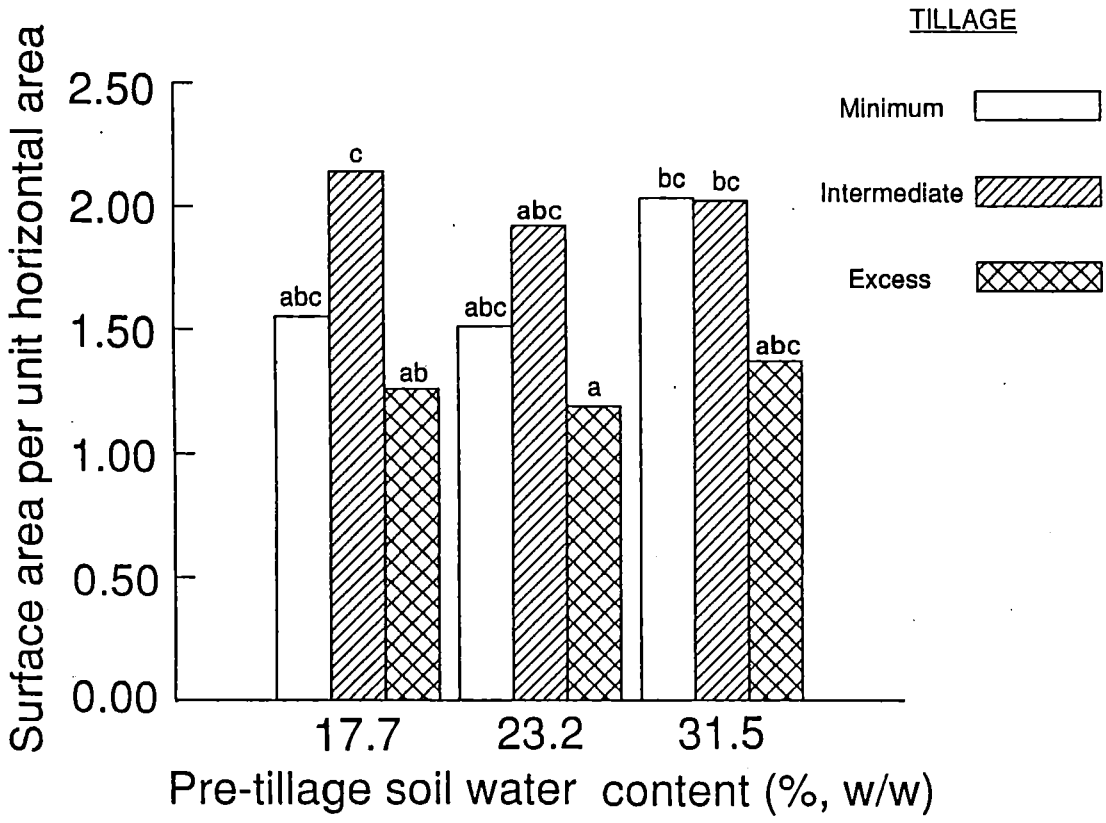

Tillage treatments had significant effects on soil surface area (ANOVA, $p<0.05$). 'Excess' tillage resulted in the lowest surface area while 'intermediate' tillage produced the highest values (Figure 4.7). PTSW treatments had no significant effect on soil surface area. Soil surface area is a function of both peak frequency and peak

magnitude. The occurrence of the highest soil surface area in the 'intermediate' tillage treatment, even though the LD index shows that there is greater variation in peak magnitude with 'minimum' tillage, indicates higher frequency of peaks per unit horizontal distance with 'intermediate' tillage. In the 'excess' tillage plots the peak magnitude appears sufficiently small to limit the surface area.

4.5 Dry bulk density

Bulk density is a soil physical property nearly always affected by tillage operations. Bulk density relates to soil porosity and mechanical impedance to plant growth (Section 2.3.2.4). The range in bulk density required for optimal plant growth cannot yet be defined for most soils (Cassel, 1982). Hence, although statistically significant differences in bulk density might occur due to tillage, the influence of this bulk density change on plant growth and yield is not well understood. At less than optimal bulk density poor water relations might exist; at higher bulk density poor aeration and high mechanical impedance could limit root extension.

Type of tillage operation had a highly significant effect on dry bulk density (ANOVA, $p<0.01$). Dry bulk density was lower for the 'minimum' tillage treatment than for either the 'intermediate' or 'excess' tillage treatment (Figure 4.8). Increased aggregate breakdown from more intensive tillage might have resulted in soil particles being broken from larger aggregates with these particles filling spaces that previously were air-filled. This is probably true for the 'excessively' tilled plots. However, the aggregate size distribution data suggests that in fact the 'intermediate' tillage treatment resulted in fewer small aggregates than the 'minimum' tillage treatment. It is likely that the greater number of tillage passes and the use of the spring-tined harrow (with its large number of small tines and rotary angle crumbler) on the 'intermediate' tillage intensity treatment resulted in greater compaction, and hence a higher dry bulk density. Field observation indicated that the 'minimum' tilled plots (which were not ploughed) had more organic material mixed in with the surface soil. The density of this organic material is much lower than that of soil and hence it is probable that this contributed, at least in part, to the low dry bulk density of the soil from these plots.

Figure 4.8. Effect of pre-tillage soil water content and tillage operations on dry bulk density (Mg m^{-3}) (standard error of the mean = 0.022 Mg m^{-3} ; means labelled with the same letter are not significantly different at the 5 % level as determined by Duncan's New Multiple Range Test).

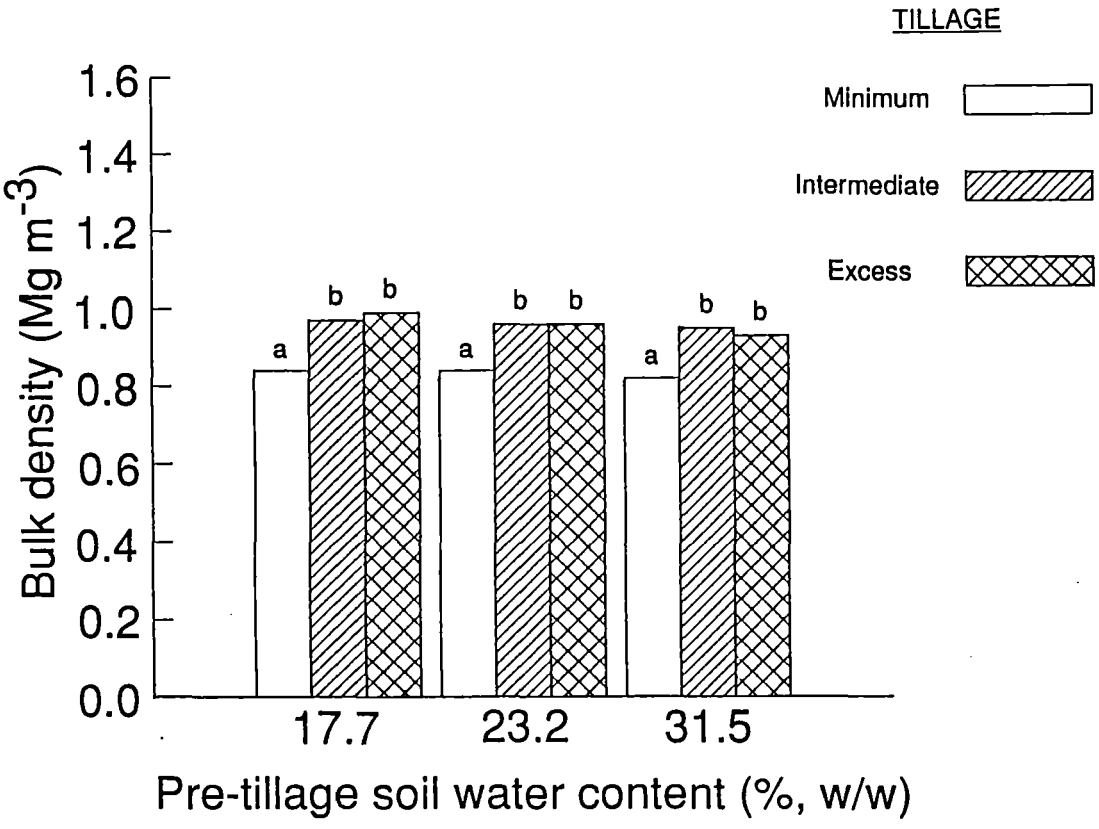

4.6 Conclusions

1. Multiple-pass tillage operations significantly affect soil aggregate size distribution, aggregate stability index, random surface roughness, soil surface area and dry bulk density.

2. Pre-tillage soil water content (PTSW) can have a significant effect on the quantity of highly wind-erodible aggregates less than 0.26 mm in diameter, however, the avoidance of excessive tillage removes the likelihood of a PTSW effect.

3. PTSW interacts with intensity of tillage operations in determining the aggregate size distribution resulting from tillage.

4. Clods formed during tillage near the lower plastic limit are significantly less stable than those formed during tillage at lower soil water contents.

5. On the basis of obtaining a consistent form of the relation between mean absolute-elevation-difference and sample spacing it is concluded that the LD and LS surface roughness indices, as proposed by Linden and van Doren (1986), appear to provide a consistent method for characterising the random roughness of a soil surface. The accuracy of the indices defined is not dependent on the measured elevation data fitting any particular distributional form.

6. The 'minimum' tillage treatment formed a soil structure in which dry bulk density was lower than with the other two tillage treatments.

CHAPTER 5

The Effects of Multiple-pass Tillage on Surface Soil hydraulic and Thermal Properties, and Shortwave Albedo

5.1 Introduction

The work described in this chapter is an investigation of how soil water content at time of tillage, and type of tillage operation, influence the surface hydraulic and thermal properties, and the shortwave albedo of a medium-textured, wind-erosion-susceptible soil. The chapter includes an assessment of the Jackson (1972) method for the calculation of unsaturated hydraulic conductivity.

5.2 Soil porosity

5.2.1 Introduction

The number and geometrical properties of the soil pores has been shown to directly influence the infiltration of water into the soil, evaporation, water storage capacity, soil water movement and soil aeration (Sections 2.3.2.1 and 2.3.2.2). These aspects are of importance in both soil-plant water relations and in soil conservation. Soil hydraulic properties allow quantitative analysis of water movement in the soil. Hence, they offer the possibility of assessing any change in the soil water regime which could occur from tillage-induced soil structural changes (Klute, 1982). In order to complete such an assessment, it is necessary to have a knowledge of the magnitude of the changes in these soil properties which occur following tillage operations.

5.2.2 Total porosity

The effects of pre-tillage soil water content (PTSW) and tillage operations on total porosity are shown in Figure 5.1. Analysis of variance (ANOVA) showed that whilst tillage treatment had a significant effect ($p<0.001$) on total porosity, PTSW content did not. Further analysis using Duncan's New Multiple Range Test (DNMRT; Steel and Torrie, 1981) showed that 'minimum' tillage operations resulted in significantly higher total porosity than both 'intermediate' and 'excess' tillage ($p<0.05$). There were no significant differences between the 'intermediate' and 'excess' tillage treatments.

Figure 5.1 Effect of pre-tillage soil water content and tillage operations on total porosity (Standard error of the mean = 0.86% ; means labelled with the same letter are not significantly different at the 5% level as determined using Duncan's New Multiple Range Test).

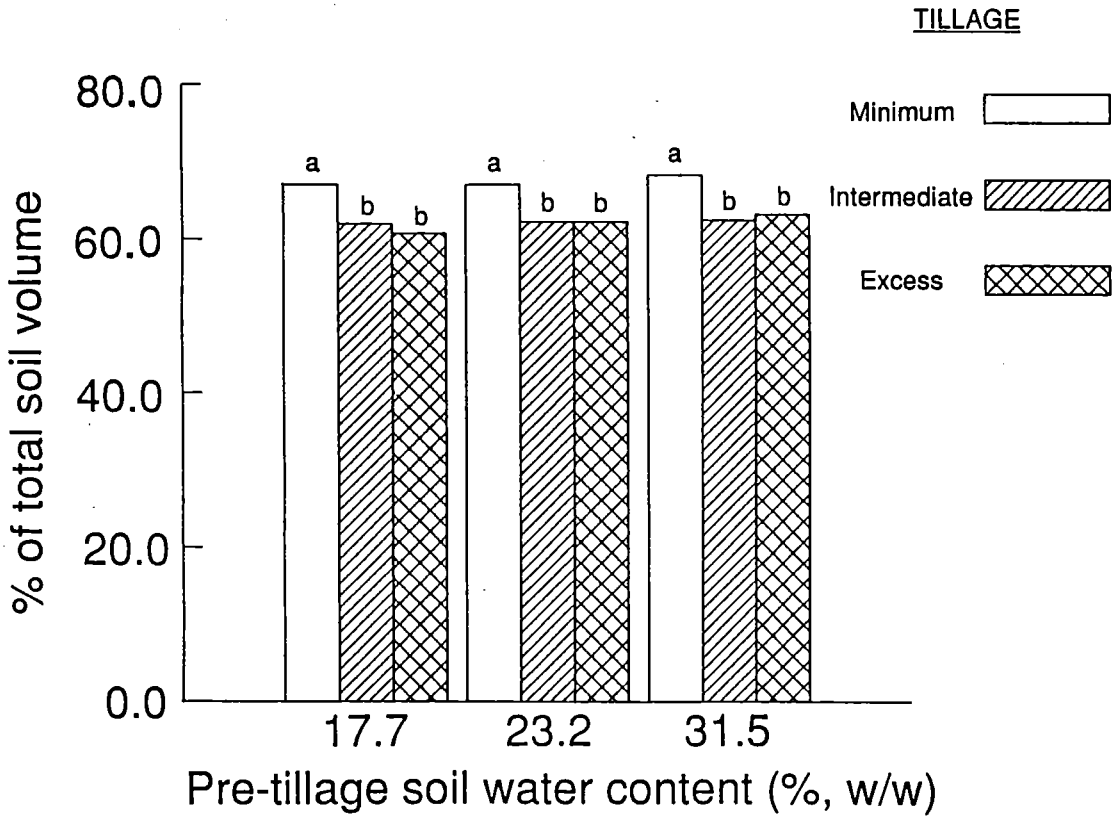

Figure 5.2 Effect of pre-tillage soil water content on the soil water characteristic.

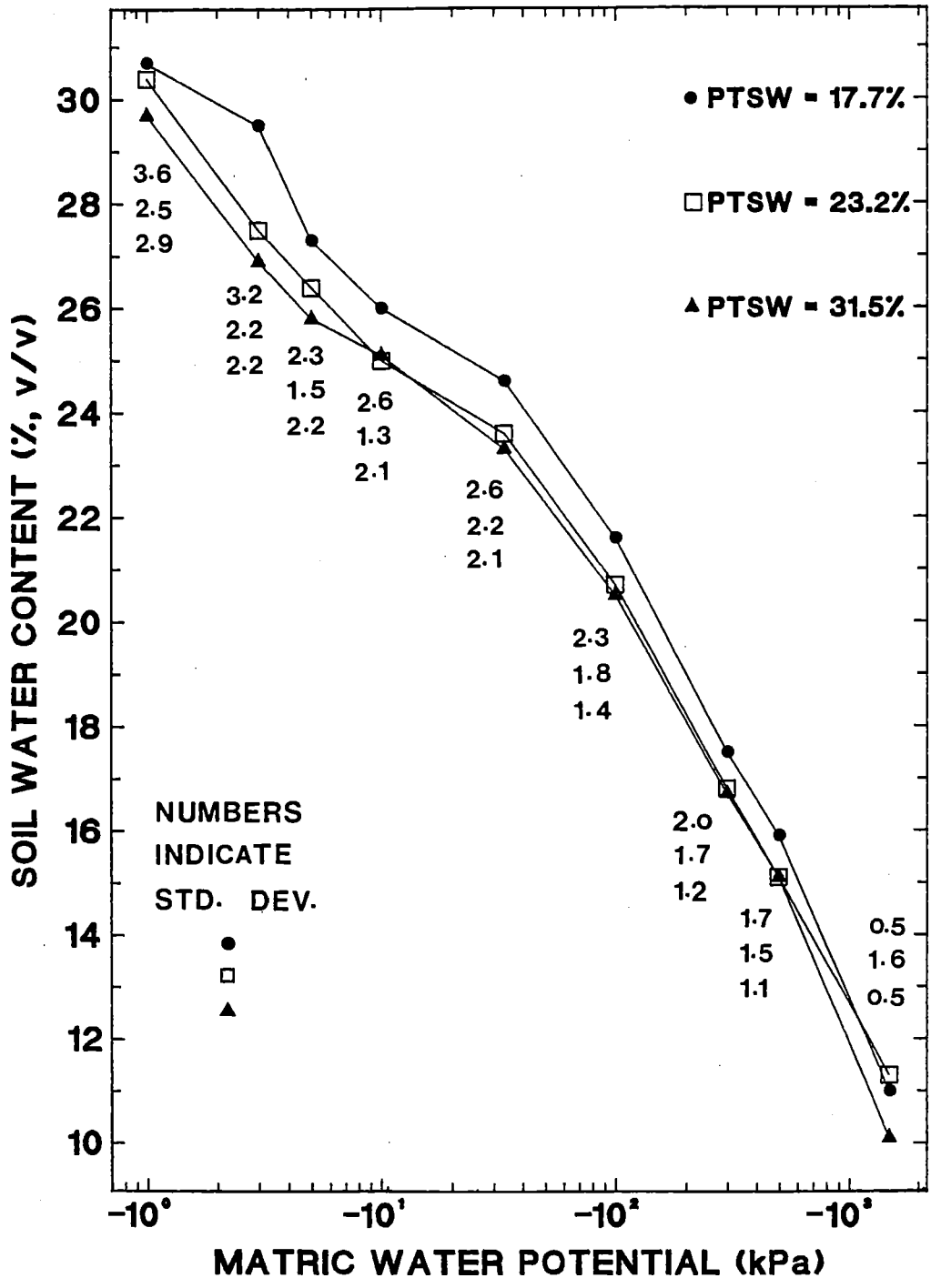

Figure 5.3 Effect of tillage operations on the soil water characteristic.

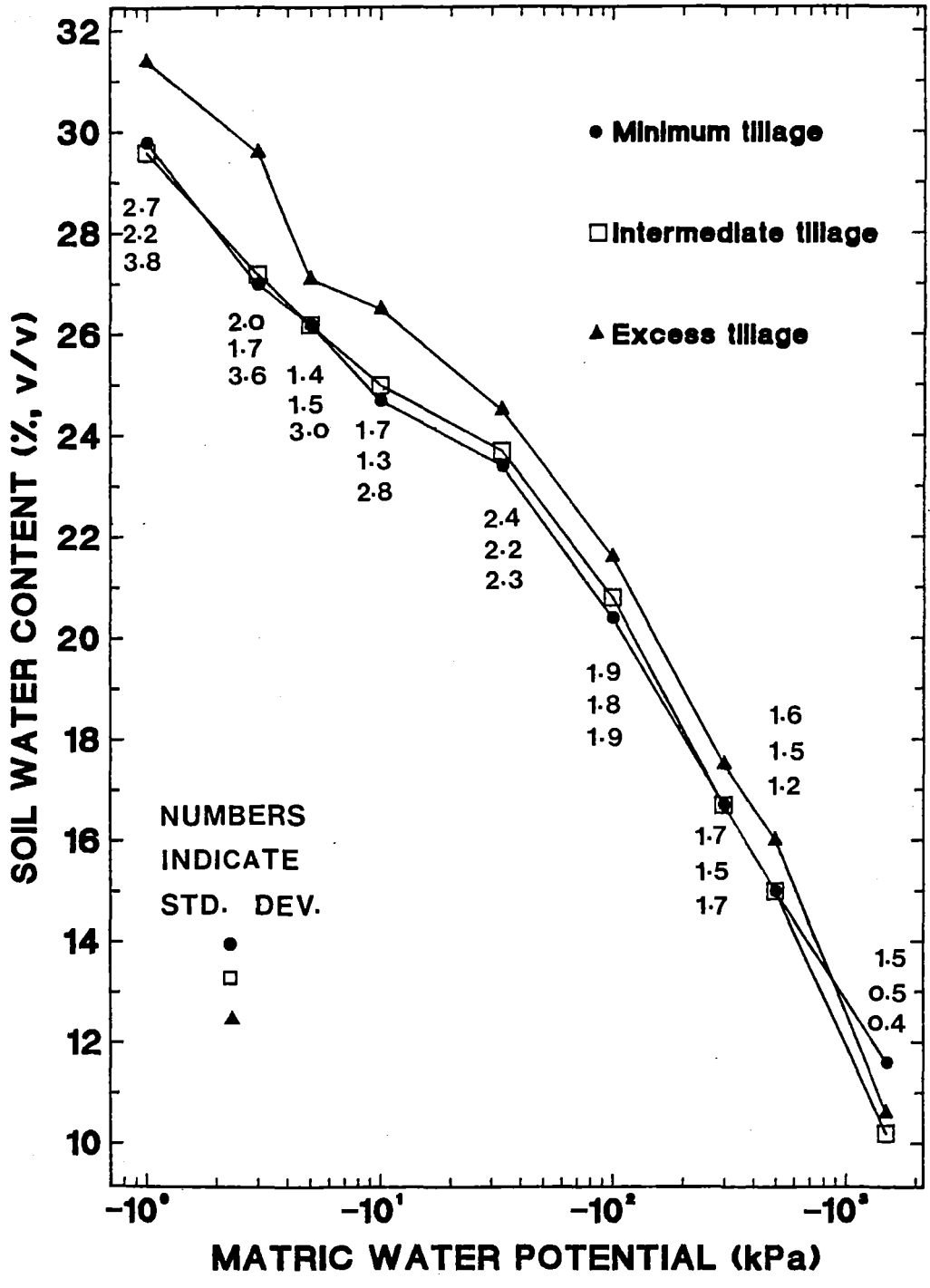

5.2.3 The soil water characteristic

The effects of PTSW and tillage operations on the soil water characteristic are shown in Figures 5.2 and 5.3. Analysis of variance of volumetric soil water content (θ_v) at each measured matric potential step in the relation showed that the PTSW treatments had a significant ($p<0.01$) effect on θ_v at -3.0 kPa but not at any of the other measured matric potentials. At each measured potential from -1.0 to -500.0 kPa PTSW treatments of 17.7% (w/w) resulted in the highest θ_v values. Further analysis showed θ_v at -3.0 kPa was significantly (DNMRT, $p<0.05$) higher for those plots with a PTSW content of 17.7% (w/w) as compared with those with a PTSW content of 31.5% (w/w). The middle PTSW treatment (23.2%, w/w) was not significantly different from either of the other two PTSW treatments at this potential. There were no significant differences between PTSW treatments at any of the other measured matric potentials.

The tillage treatment effects were significantly different at a matric potential of -3.0 kPa (ANOVA, $p<0.001$) as well as at -10.0, -100.0 and -300.0 kPa (ANOVA, $p<0.01$). At each measured matric potential (ψ_m) from -1.0 to -500.0 kPa the θ_v in the 'excess' tillage plots was higher than in those of either of the other two tillage treatments. At -3.0 kPa, θ_v was significantly higher (DNMRT, $p<0.05$) with 'excessive' tillage as compared to the other two tillage treatments. There were no significant differences (DNMRT, $p<0.05$) between tillage treatments at any of the other measured values of ψ_m. Observed variability in θ_v at a matric potential of -1.0 kPa was higher than that at any of the other measured potentials. This high variability makes isolating treatment effects difficult. At low matric potentials only very small pores are water-filled, this intra-aggregate porosity is primarily a function of soil texture. The treatments imposed in this study influence soil structure and inter-aggregate porosity. The apparent effect on water content at high matric potentials (-300.0 to -500.0 kPa) was unexpected and is unlikely to be a real treatment effect.

Where the nine individual treatments (three tillage operation treatments x three PTSW treatments) are considered separately, the 'excessive' tillage operations at 17.7% PTSW produced the highest θ_v at each measured ψ_m. This treatment resulted in a θ_v which, at -3.0 kPa, was significantly higher (DNMRT, $p<0.05$) than the other eight treatments. At -1.0, -3.0, -10.0, -100.0, -300.0 and -500.0 kPa 'excessive' tillage operations at 17.7% PTSW had a significantly higher (DNMRT, $p<0.05$) θ_v than

'minimum' tillage at 31.5% PTSW. At -33.0, -100.0, -300.0 and -500.0 kPa 'excessive' tillage at 17.7% PTSW resulted in significantly higher θ_V values than 'intermediate' tillage at 31.5% PTSW. There were no other significant differences between treatment combinations.

Figure 5.4 Effect of pre-tillage soil water content and tillage operations on macro-porosity (Standard error of the mean = 1.4% ; means labelled with the same letter are not significantly different at the 5% level as determined using Duncan's New Multiple Range Test).

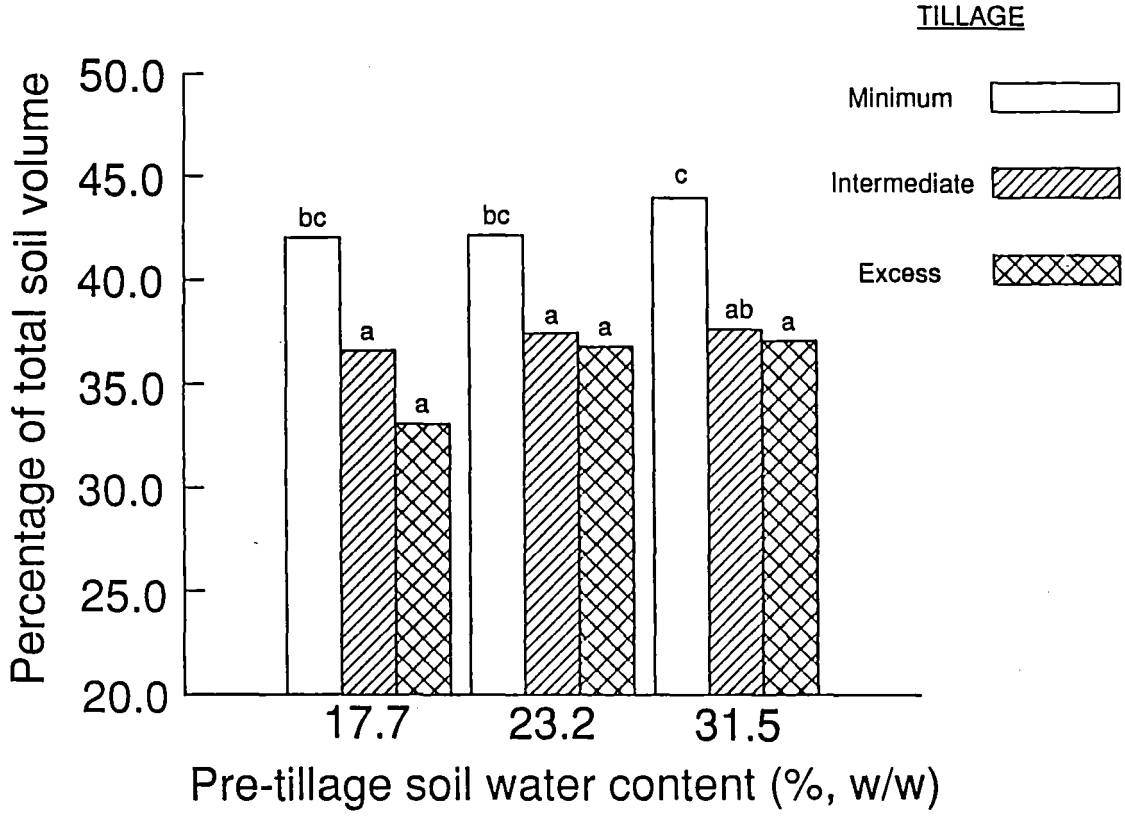

5.2.4 Functional pore size classes

Using the measured soil water characteristic functions described above, the effects of PTSW and tillage operations on the various functional pore size categories (Section 3.2.3.5) were determined. The equivalent spherical diameter of the soil pores which are grouped in the macro, aeration, transmission and available water functional pore size categories were previously defined as >30 μm, >300 μm, 300-30 μm, and 30-0.2 μm respectively (Section 3.2.3.5). Figures 5.4, 5.5, 5.6 and 5.7 show the effects of PTSW and tillage treatments on macro, aeration, transmission, and available water pore volumes. Analysis of variance showed PTSW did not significantly affect macro-porosity although tillage treatments had a significant effect ($p<0.001$). 'Excessive' tillage operations resulted in significantly lower macro-porosity (DNMRT, $p<0.05$) than 'minimum' tillage while neither were significantly different from 'intermediate' tillage (Figure 5.4).

Tillage treatments also had a highly significant effect on aeration porosity (ANOVA, $p<0.001$) (Figure 5.5). Aeration porosity was significantly higher for the 'minimum' tillage treatment (DNMRT, $p<0.05$) than for both the 'excess' and 'intermediate' tillage treatments, both of which had similar effects. Aeration porosity was not significantly affected by PTSW.

Analysis of variance between treatment groups indicated that transmission porosity was not affected significantly by either PTSW or tillage treatments. At PTSW 31.5% however, transmission porosity after 'excess' tillage was significantly higher than after 'minimum' tillage (DNMRT, $p<0.05$) (Figure 5.6). This indicates that the tillage treatments affect macro-porosity mainly by changes in the volume of pores in the >300 μm diameter (aeration pore) size range. Macro-pores are important for providing low impedance pathways for water and solute movement and root growth (Sections 2.3.2.1 and 2.3.2.4). Soil aeration is also dependent on macro-pores when soil is at or above field capacity (Section 2.3.2.2). Macro-pores are not so significant in terms of water storage in the surface soil because most of the time they are air-filled. Such pores do, however, play an important part in saturated and near-saturated water flow.

Figure 5.5 Effect of pre-tillage soil water content and tillage operations on aeration porosity (Standard error of the mean = 1.7% ; means labelled with the same letter are not significantly different at the 5% level as determined using Duncan's New Multiple Range Test).

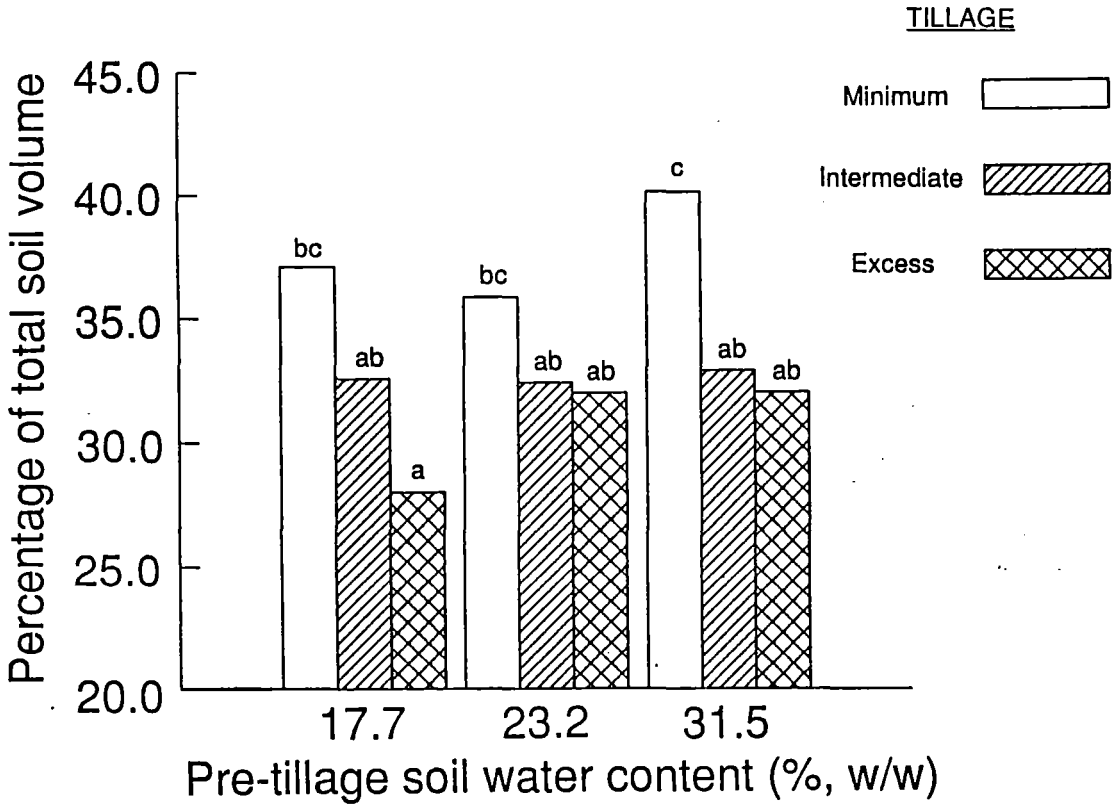

The volume of pores which correspond to the water in the surface soil matrix which is available to plants (available water holding capacity) was not affected by PTSW. Tillage treatments did have a significant effect (ANOVA, $p<0.01$) with available water holding capacity maximised when the soil was tilled 'excessively' (Figure 5.7), however the difference between 'excessive' and 'intermediate' tillage was not significant. No significant difference occurred in available water holding capacity between 'minimum' and 'intermediate' tillage. The available water holding capacity is of importance in terms of crop establishment and yield especially on shallow, drought-prone soils. The soil water content which corresponds to the lower boundary of the available water range (-1500.0 kPa matric potential) has been suggested as a critical boundary for soil movement by wind (Section 2.4.1). Chepil and Woodruff (1963) reported that the

natural wind is seldom able to overcome the cohesive force and move discrete soil grains when their water content is above that corresponding to a matric potential of -1500.0 kPa. The length of time that the surface soil water content stays above this critical level is influenced by the available water holding capacity and is of importance in the wind erosion context.

Figure 5.6 Effect of pre-tillage soil water content and tillage operations on transmission porosity (Standard error of the mean = 0.77% ; means labelled with the same letter are not significantly different at the 5% level as determined using Duncan's New Multiple Range Test).

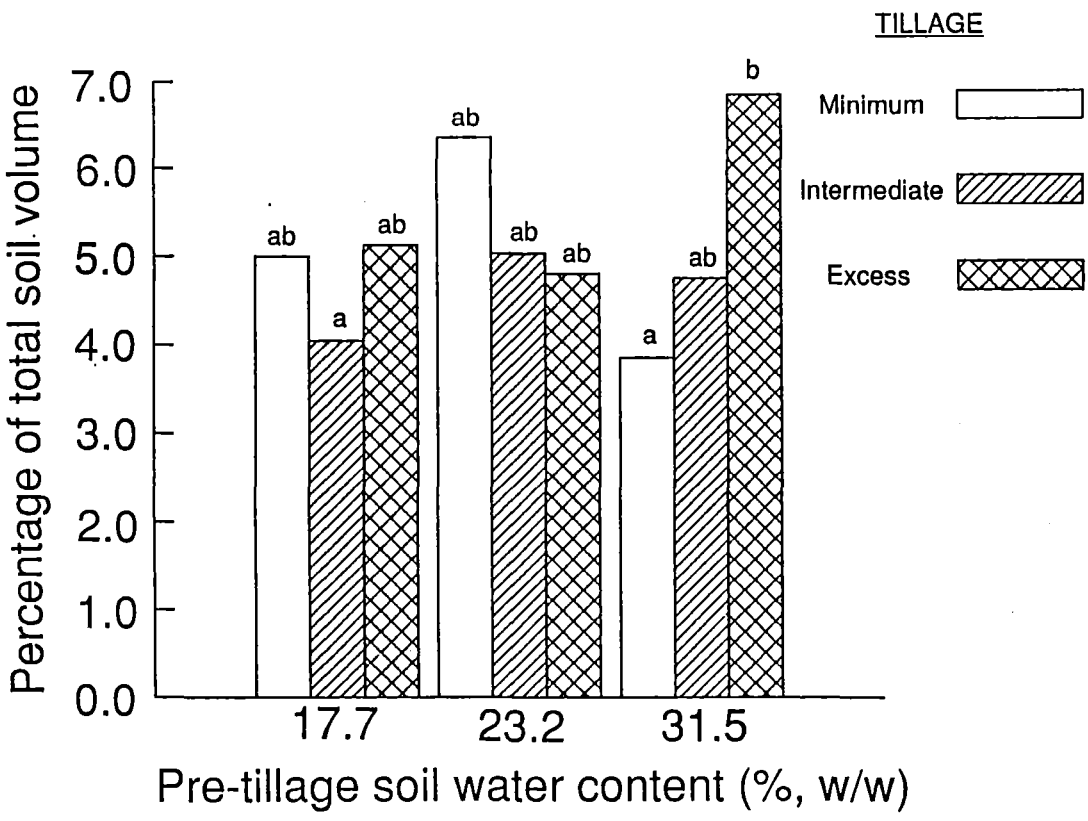

Figure 5.7 Effect of pre-tillage soil water content and tillage operations on available water holding capacity (Standard error of the mean = 0.89% ; means labelled with the same letter are not significantly different at the 5% level as determined using Duncan's New Multiple Range Test).

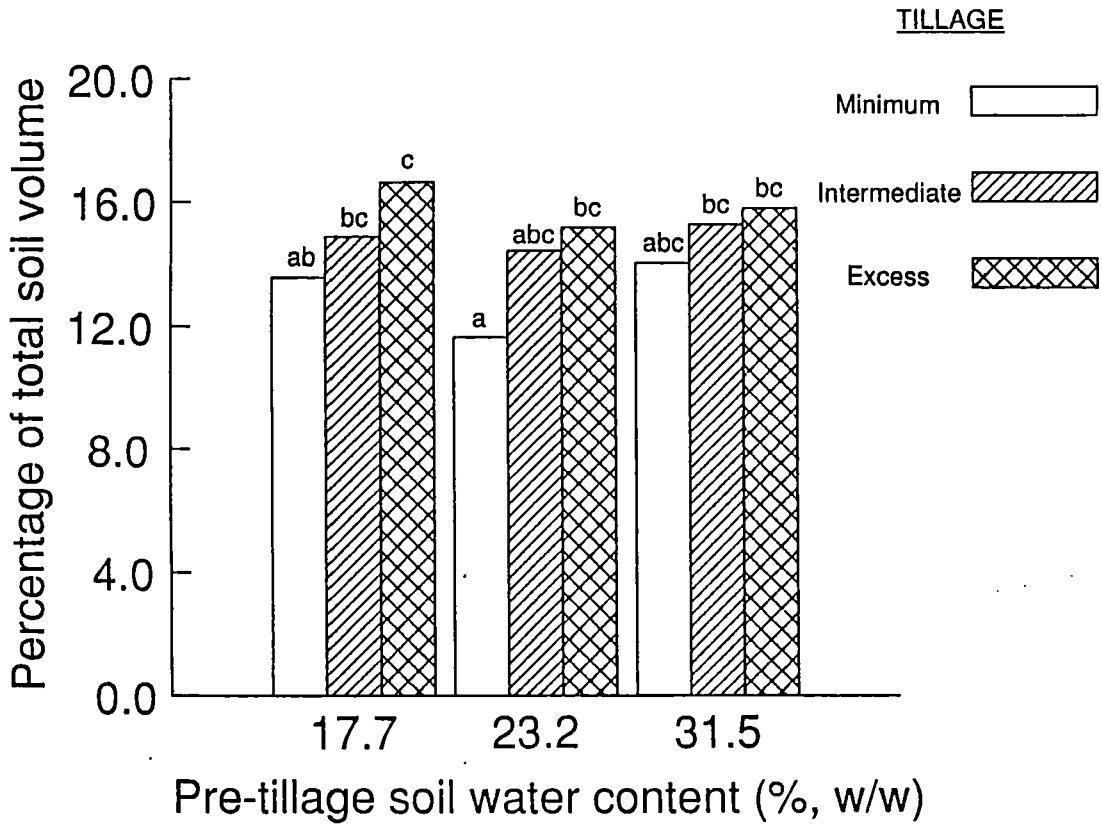

5.2.5 Further discussion

'Excessive' tillage has resulted in a very fine, pulverised soil with mainly small, granular aggregates that fit closely together. With 'minimum' tillage large aggregates, probably broken along natural planes of weakness, are mixed with a smaller proportion of small aggregates (Section 4.2). The large aggregates do not fit together as closely, resulting in a greater total porosity which occurs largely because of a greater volume of large aeration pores. The smaller effect of the PTSW treatments on aggregate size distribution compared to the tillage treatments is reflected in the pore size distribution.

The measurement of pore size distribution reported here was on a recently tilled soil which could be expected to settle over time as a result of rainfall and traffic from farming operations. This would probably cause a decrease in total porosity mainly through a reduction in volume of the less stable macro-pores (Klute, 1982). The wetting of soil samples during the measurement of the water characteristic will have caused the freshly-tilled soil to have settled to some extent. These porosity results will, therefore, not provide an exact reproduction of field conditions. This is unavoidable. This sample disturbance due to wetting was not a factor in the calculation of total porosity. The calculation of macro-porosity and aeration porosity utilises both total porosity data and water characteristic data.

5.3 Near-saturation hydraulic conductivity

Tillage operations had a significant effect on hydraulic conductivity measured at a matric potential of -0.37 kPa (ANOVA, $p<0.001$) while PTSW treatments had no significant effect. The mean conductivity after 'minimum' tillage was significantly higher (DNMRT, $p<0.05$) than that after 'excess' tillage whilst neither were significantly different from 'intermediate' tillage. The individual treatments resulting in the highest conductivity values were 'minimum' tillage at PTSW values of 17.7 and 23.2% (w/w) (Figure 5.8). These two treatments had significantly higher (DNMRT, $p<0.05$) conductivities than each of the 'excess' tillage treatments. There were no other significant differences between treatments.

These results confirm that tillage and PTSW treatments that result in a high macro-pore volume do result in high rates of near-saturation water flux. The high mean near-saturation hydraulic conductivity for the 'minimum' tillage treatment (4.13×10^{-5} m s^{-1}) reflects the high proportion of these large pores. The 'excess' tillage treatment resulted in lower macro-porosity and hence lower near-saturation conductivity. The Hagen-Poiseuille law (Equation 2.9) states that volume flow rate is proportional to the fourth power of the tube radius and hence it follows that large macro-pores need only comprise a small fraction of the pore volume to contribute substantially to total water flux. This has been confirmed with field measurements (Watson and Luxmoore, 1986).

Figure 5.8 Effect of pre-tillage soil water content and tillage operations on near-saturation hydraulic conductivity (Standard error of the mean = 1.01 cm hr^{-1} ; means labelled with the same letter are not significantly different at the 5% level as determined using Duncan's New Multiple Range Test).

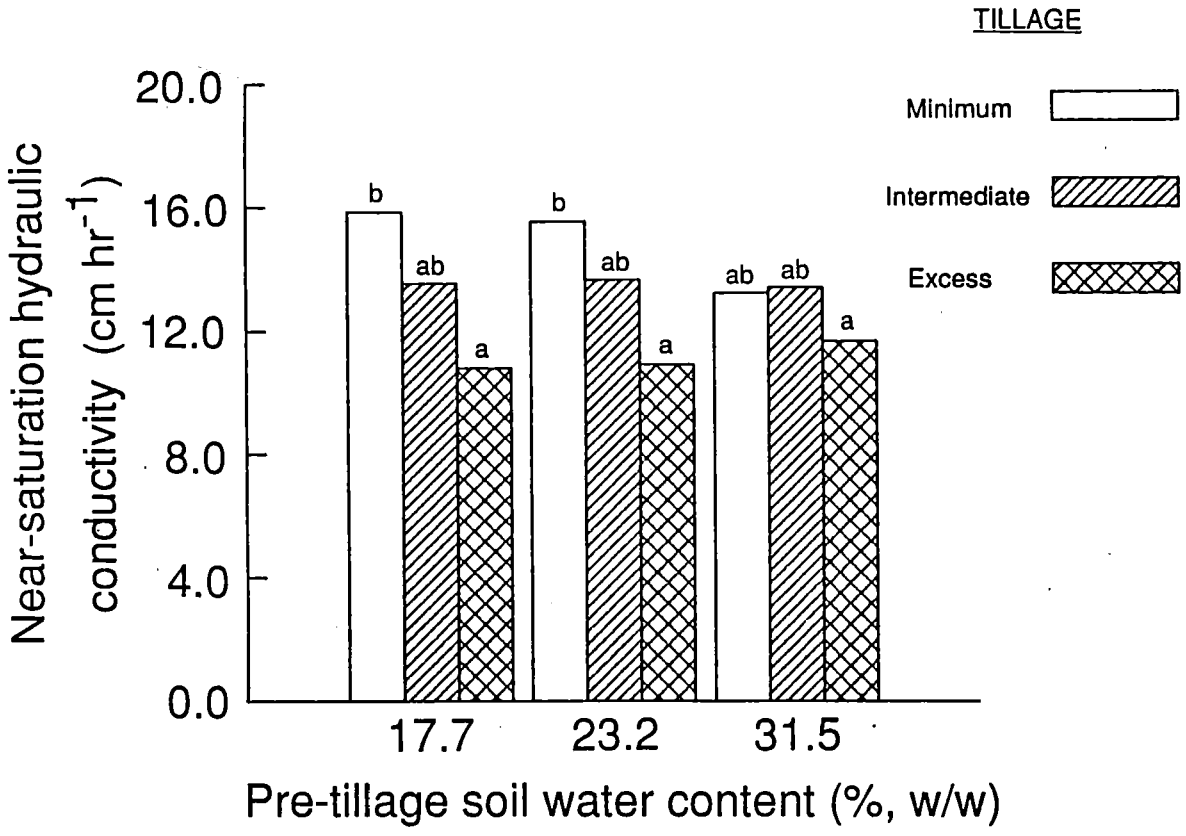

When a soil is saturated all pores are water-filled and conducting, hence for that soil conductivity and continuity of the water films are maximised. As the degree of saturation decreases (i.e. matric potential decreases) progressively smaller pores empty and become non-conducting. As more pores empty the tortuosity of the unbroken water films increase as the water must flow around the air-filled pores. Hence, in the tilled soil considered here, the large inter-aggregate pores which confer a high near-saturation conductivity become barriers to liquid flow when they become empty at relatively high matric potentials. For these reasons a steep drop in conductivity with decreasing matric potential would be expected.

5.4 Unsaturated hydraulic conductivity

5.4.1 Introduction

A layer of surface soil with a low hydraulic conductivity when unsaturated reduces the amount of water which can reach the surface to evaporate. The unsaturated hydraulic conductivity (K) of the surface soil is, therefore, of critical importance to the soil profile-controlled stage of evaporation and might also affect the constant-rate weather-controlled phase through effects on water re-distribution in the profile (refer Sections 2.3.2.1 and 2.4.5.1). Unsaturated hydraulic conductivity also affects the rate of water supply to plant roots and aspects of soil drainage. The difficulty of accurate characterisation of field hydraulic conductivity was discussed in Section 2.4.5.3 and the Jackson (1972) model for the calculation of unsaturated hydraulic conductivity was described in Section 3.2.3.6. An evaluation of the Jackson equation (Equation 3.13) by sensitivity analysis was considered desirable before its use in this study. The results of this analysis are described here.

5.4.2 Sensitivity analysis

The data which was used as input for the equation was mean near-saturation hydraulic conductivity at a matric potential of -0.37 kPa (3.75×10^{-5} m s^{-1} at θ_v = 34 %, v/v) and the mean water characteristic relation ($\theta_v(\psi_m)$) from the 'intermediate' tillage treatment from the field trial (Figure 5.3). Interpolation from Figure 5.3 was used to supply the ψ_m values which correspond, as required by the procedure, to the midpoints between θ_v values from 34% to 12% in increments of 1% (i.e. θ_v = 33.5, 32.5, 31.5, ... 11.5%, v/v). This data set will be referred to as initialisation (i).

Initialisation (ii) used the same measured near-saturation K matching factor and corresponding volumetric water content θ_v(mf). The same $\theta_v(\psi_m)$ relation was used at θ_v values of 31% and below. It differed in that θ_v values of 34, 33 and 32% were set to

ψ_m values of -0.35, -0.45 and -0.55 kPa respectively, 0.1 kPa higher than in the previous initialisation (refer Figure 5.9 and Table 5.1).

Figure 5.9 The water characteristic input functions for the sensitivity analysis of the Jackson (1972) model.

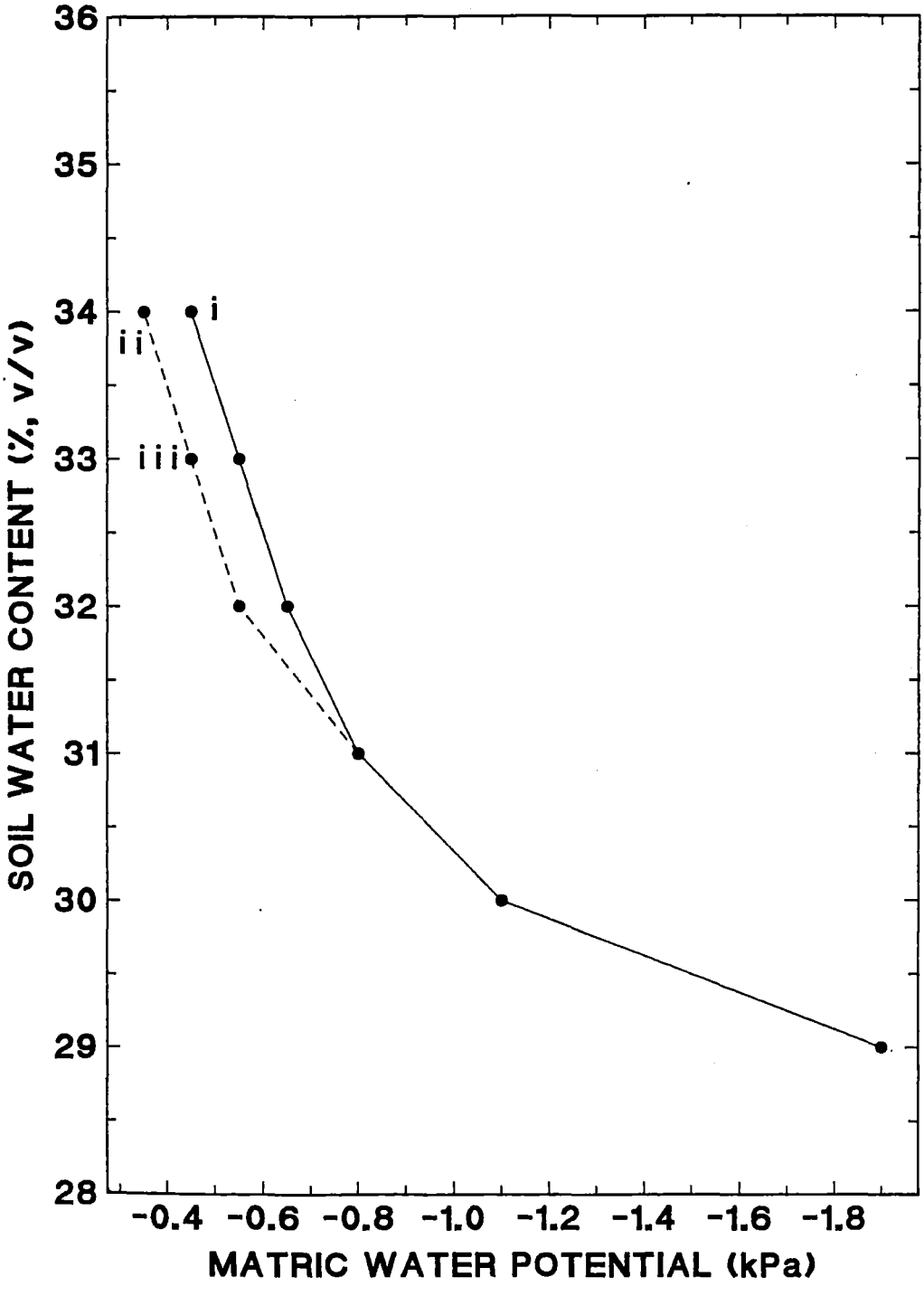

Table 5.1. Initialisation data and resulting hydraulic conductivity calculated using the Jackson (1972) model.

θ_v	INITIALISATION i		ii		iii	
%,v/v	ψ_m kPa	K m s^{-1}	ψ_m kPa	K m s^{-1}	ψ_m kPa	K m s^{-1}
34	-0.45	3.75×10^{-5}	-0.35	3.75×10^{-5}	-	-
33	-0.55	2.05×10^{-5}	-0.45	1.89×10^{-5}	-0.45	3.75×10^{-5}
32	-0.65	1.02×10^{-5}	-0.55	8.64×10^{-6}	-0.55	1.72×10^{-5}
31	-0.80	4.43×10^{-6}	-0.80	3.53×10^{-6}	-0.80	7.01×10^{-6}
30	-1.10	1.62×10^{-6}	-1.10	1.29×10^{-6}	-1.10	2.56×10^{-6}
29	-1.90	5.16×10^{-7}	-1.90	4.11×10^{-7}	-1.90	8.17×10^{-7}
28	-3.50	1.68×10^{-7}	*	1.33×10^{-7}	*	2.65×10^{-7}
27	-5.80	5.67×10^{-8}		4.51×10^{-8}		8.98×10^{-8}
26	-8.60	1.75×10^{-8}		1.39×10^{-8}		2.77×10^{-8}
25	-19.50	5.05×10^{-9}		4.02×10^{-9}		8.00×10^{-9}
24	-38.50	2.09×10^{-9}		1.67×10^{-9}		3.32×10^{-9}
23	-58.50	1.05×10^{-9}		8.32×10^{-10}		1.66×10^{-9}
22	-82.50	5.50×10^{-10}		4.38×10^{-10}		8.71×10^{-10}
21	-118.0	3.00×10^{-10}		2.38×10^{-10}		4.74×10^{-10}
20	-160.0	1.67×10^{-10}		1.33×10^{-10}		2.64×10^{-10}
19	-205.0	9.26×10^{-11}		7.37×10^{-11}		1.47×10^{-10}
18	-263.0	5.03×10^{-11}		4.01×10^{-11}		7.97×10^{-11}
17	-338.0	2.66×10^{-11}		2.11×10^{-11}		4.20×10^{-11}
16	-440.0	1.34×10^{-11}		1.07×10^{-11}		2.13×10^{-11}
15	-570.0	6.39×10^{-12}		5.09×10^{-12}		1.01×10^{-11}
14	-730.0	2.72×10^{-12}		2.16×10^{-12}		4.30×10^{-12}
13	-935.0	9.27×10^{-13}		7.38×10^{-13}		1.47×10^{-12}
12	-1200	1.84×10^{-13}		1.47×10^{-13}		2.91×10^{-13}

* remaining data in this column is the same as shown for initialisation (i) at the corresponding value of θ_v.

Volumetric soil water content is designated θ_v, matric potential ψ_m, and hydraulic conductivity K.

With initialisation (iii) the θ_v(mf) value was set to 33% (v/v) and the $\theta_v(\psi_m)$ function was modified so the θ_v values 33 and 32% are set to ψ_m values of -0.45 and -0.55 kPa respectively. The matching factor K remained unchanged from either of the previous initialisations as did the $\theta_v(\psi_m)$ relation at θ_v values of 31% and below (refer Figure 5.9 and Table 5.1). So, in this initialisation the known ψ_m value which corresponds to the measured K matching factor is kept consistent with that from initialisation (i). The $\theta_v(\psi_m)$ function remained unchanged from that in initialisation (ii). Consider Figure 5.9 to clarify the three input data sets. Point (i) lies on the water characteristic curve detailed for initialisation (i) at the position corresponding to where the matching factor conductivity was determined. Points (ii) and (iii) represent initialisations (ii) and (iii) respectively. As can be seen (ii) and (iii) both lie on an identical water characteristic curve but their matching factor K values were determined at different θ_v and different ψ_m values. (i) and (iii) have different $\theta_v(\psi_m)$ functions. The matching factor K values were determined at the same matric potential but these represent differing θ_v values. (i) and (ii) also have different $\theta_v(\psi_m)$ functions. The matching factor K values were determined at the same θ_v values but these represent differing ψ_m values.

The hydraulic conductivity at each corresponding θ_v and ψ_m step which resulted from using the three input data sets with the Jackson equation are shown in Table 5.1. The comparison of initialisations (i) and (ii) show that the equation is very sensitive to the $\theta_v(\psi_m)$ relation at high ψ_m values. Calculated unsaturated conductivity from (i) is approximately 25% higher than from (ii) over most of the $K(\psi_m)$ and $K(\theta_v)$ functions. The accuracy of this data when measured using conventional tension table methods might not be sufficient to ensure good results from the Jackson equation. At the very least, some intermediate data points would be required between 0 and -1.0 kPa matric potential. The sensitivity to this range of the soil water characteristic could be consistent with field behaviour as changes at high matric potential reflect changes in the quantity of large macro-pores. Large macro-pores have been shown to make substantial contributions to water transmission when a soil is near saturation (Watson and Luxmoore, 1986). The absence of a measured $K(\psi_m)$ function with which to compare the calculated values means that this sensitivity cannot be properly compared with the field soil water behaviour.

The unsaturated K values from the Jackson equation used with initialisation (iii) are markedly different from those from either initialisation (i) or (ii) (Table 5.1). Where results from initialisation (ii) and (iii) are compared, calculated K values over the full range of the $K(\psi_m)$ and $K(\theta_v)$ functions are approximately two times higher from initialisation (ii). The procedure is very sensitive to a change in θ_v corresponding to the matching factor K value (θ_v(mf)). When using the Jackson equation with an unsaturated matching factor, θ_v(mf) can be found by either direct soil water sampling, or else if the matric potential is known where K determination was made, the corresponding θ_v value can be read from a $\theta_v(\psi_m)$ function. Where the latter method is used (as in this study), this analysis shows that the conductivities calculated with the Jackson equation are much more sensitive to variability in the $\theta_v(\psi_m)$ function where it is used to define the θ_v(mf) value than where it is used as direct input into the equation. This is an inconsistency in the calculation procedure.

5.4.3 Application of the Jackson (1972) method

The Jackson equation is not suitable for determining changes in unsaturated hydraulic conductivity which might occur with tillage treatments on the same soil type. The very high sensitivity to the high ψ_m section of the $\theta_v(\psi_m)$ function and to the θ_v(mf) value would obscure any effects of tillage treatments on hydraulic conductivity.

Denning et al. (1974) found that agreement between calculated and measured hydraulic conductivity functions was not good on clayey pedal soil horizons in which a few relatively large pores determined conductivity in the wet range. In such media, the greatest fraction of total porosity is in the fine pores within the peds, and these contribute very little to the flow. Denning et al. (1974) recommended that calculation procedures not be used for determining the hydraulic conductivity of pedal soils (i.e. those with bi-modal pore size distributions). The same conclusion would seem to apply to the estimation of hydraulic conductivity of surface tilled soil in which a strongly bi-modal pore size distribution has been developed (bi-modal describes a pore size distribution with 2 peaks or maxima).

Reports from other workers (Jackson, 1972; Denning et al., 1974; Field et al., 1984) would suggest that the equation is useful for obtaining approximate unsaturated

conductivity values for particular soil types where a matching factor is used and the soils are apedal (such as a sand). The use of the Jackson equation should be restricted to this application.

5.5 Soil thermal properties

Soil temperature and its variation are critical factors in determining the rates and directions of soil physical processes and of energy and mass exchange with the atmosphere (e.g. evaporation and aeration). Soil temperature strongly influences biological processes such as seed germination, seedling emergence and growth, plant development and nutrient uptake as well as soil water and gas flow processes (Wierenga et al., 1982). Soil temperature varies in response to changes in energy exchange processes which take place primarily through the soil surface. The effects of these phenomena are propagated into the soil profile by a series of transport processes, the rates of which are affected by soil properties. Soil properties relevant to the thermal regime include volumetric heat capacity, thermal conductivity and thermal diffusivity as well as the internal sources and sinks of heat operating at any time (Hillel, 1982).

Thermal conductivity of the tilled soil layer was calculated using the de Vries (1963) dielectric analogue and measurements of total porosity and particle density. For the calculation the solid soil fraction was differentiated into three components: organic matter, quartz and other solid material. The quartz percentage assumed in the sand, silt and clay fractions of the soil were 50, 30 and 3% (w/w) respectively (P.J. Tonkin, pers. com., 1989). The thermal properties and densities of the individual solid soil constituents, water and air, and the shape factor for solid particles used in the calculations were taken from de Vries (1963).

Soil water content has a large effect on calculated thermal conductivity (Table 5.2). Thermal conductivities are porosity-dependent. Air is a poor thermal conductor ($0.025\ W\ m^{-1}\ K^{-1}$) and hence when the soil is oven-dry the highest thermal conductivities occur in the tillage treatments which resulted in the lowest total porosity (i.e. 'excess' tillage). When oven-dry an increase in total porosity between 60.75 and 68.25% resulted in a 20.2% decrease in thermal conductivity. The smaller differences in thermal conductivity between treatments in a saturated soil occur because water is a

better thermal conductor than air. The higher water contents at saturation in the high porosity treatments tend to offset the correspondingly lower contribution to the total thermal conductivity of the soil matrix which comes from the solid soil fraction. When saturated the same increase in total porosity resulted in an 11.4% increase in thermal conductivity.

Table 5.2 Tillage effects on soil volumetric heat capacity and thermal conductivity.

TREATMENT	TOTAL POROSITY %	VOL. HEAT CAPACITY kJ m^{-3} K^{-1}		THERMAL CONDUCTIVITY W m^{-1} K^{-1}	
		AIR-DRY	SAT.	AIR-DRY	SATURATED
PTSW 17.7%					
MINIMUM	67.0	690.0	3504	0.104	1.10
INTERMEDIATE	62.0	794.2	3398	0.120	1.19
EXCESS	60.75	810.9	3362	0.125	1.21
PTSW 23.2%					
MINIMUM	67.0	690.0	3504	0.104	1.10
INTERMEDIATE	62.25	785.5	3400	0.119	1.18
EXCESS	62.25	785.5	3400	0.119	1.18
PTSW 31.5%					
MINIMUM	68.25	662.6	3529	0.100	1.07
INTERMEDIATE	62.50	781.5	3406	0.119	1.18
EXCESS	63.25	766.8	3423	0.116	1.17

Increasing porosity resulted in a decrease in volumetric heat capacity of an oven-dry soil but an increase in volumetric heat capacity of a saturated soil (Table 5.2). This occurs because the volumetric heat capacity of soil water is greater than that of the solid soil fraction.

It is apparent that changes in porosity due to differing tillage operations can significantly affect soil thermal properties. Changes in soil water content also have large effects on soil thermal properties. The application of the de Vries (1963) thermal

conductivity model in this study might have been improved with laboratory measurements of the thermal conductivity of the soils, when saturated, to check the shape factor value for the solid particles (refer Section 2.4.4.2.) (De Vries and Philip, 1986). However, the results from the de Vries model are not very sensitive to the shape factor value (G.D. Buchan, pers. com., 1989).

5.6 Bare soil shortwave albedo

5.6.1 Introduction

Soil temperatures are determined by soil surface heat flux as well as by the soil thermal properties. Both the radiant energy absorbed by the soil surface and the partitioning of net radiation at the surface influence soil heat flux. Shortwave albedo is an important soil property which directly influences radiant energy absorption.

5.6.2 Zenith angle effects on shortwave albedo

In order to relate the reflection coefficient of shortwave solar radiation incident on a bare soil surface directly to soil water content, sun zenith angle effects must first be removed. The effect of zenith angle on shortwave albedo was measured on two widely differing soil tilths, both with air-dry surfaces (Figure 5.10). Measurements were made during clear sky conditions. In this study it was found that reflectance decreased with increasing zenith angle. Coulson and Reynolds (1971) also reported decreasing reflectance with increasing zenith angle on a disked Yolo loam soil with a rough surface condition. However, Coulson and Reynolds (1971) observed increasing reflectance with increasing zenith angle on a Sacramento clay soil. Idso et al. (1975) also observed increasing reflectance with increasing zenith angle on a smooth soil surface. They showed an increase in shortwave albedo of 0.02 between zenith angles of 20 and 50 degrees.

Figure 5.10 Effect of zenith angle on bare soil shortwave albedo of two soil surfaces with differing structure.

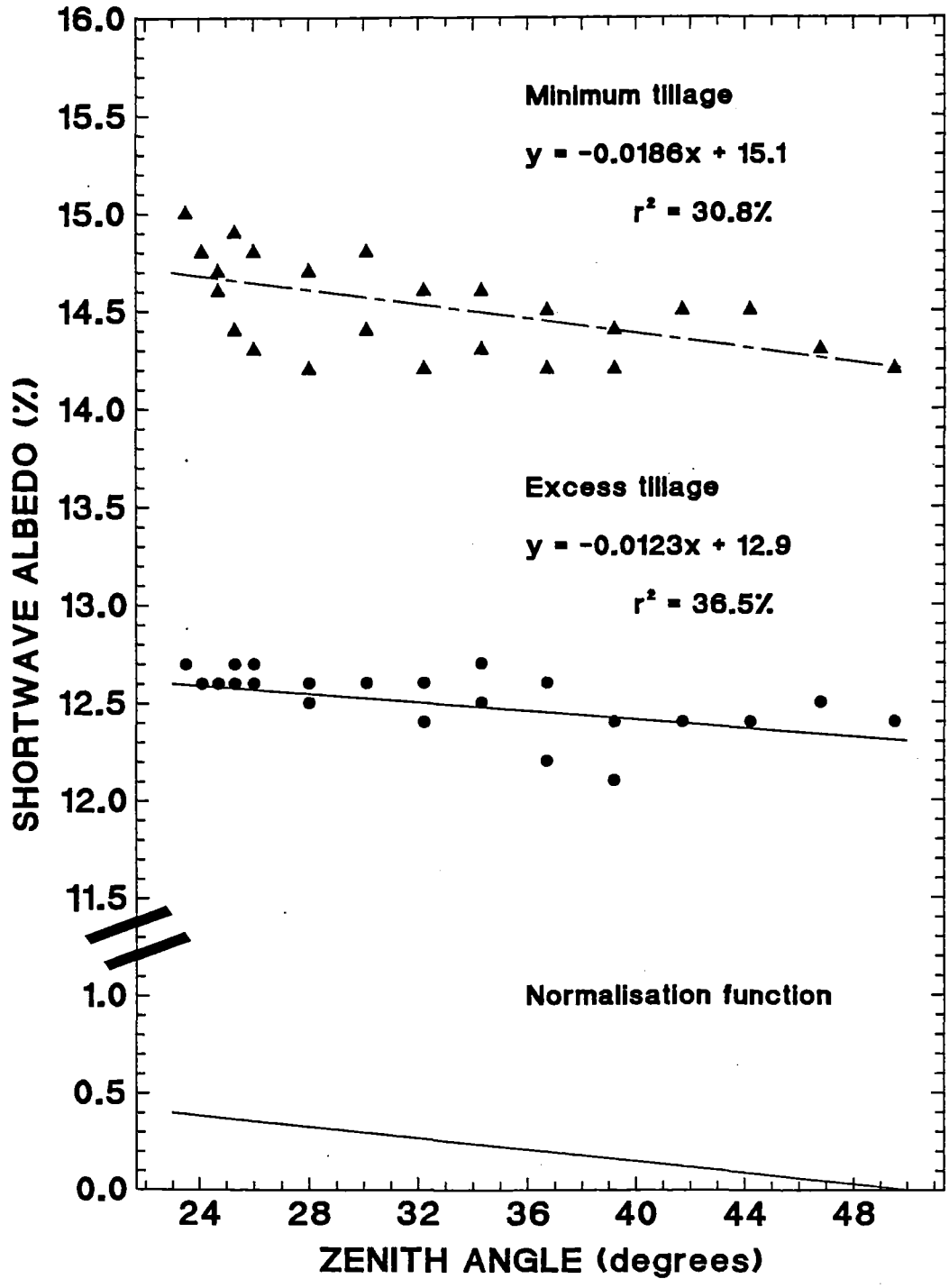

Figure 5.11 Effect of soil water content on the normalised bare soil shortwave albedo. All tillage treatments conducted at PTSW = 31.5%.

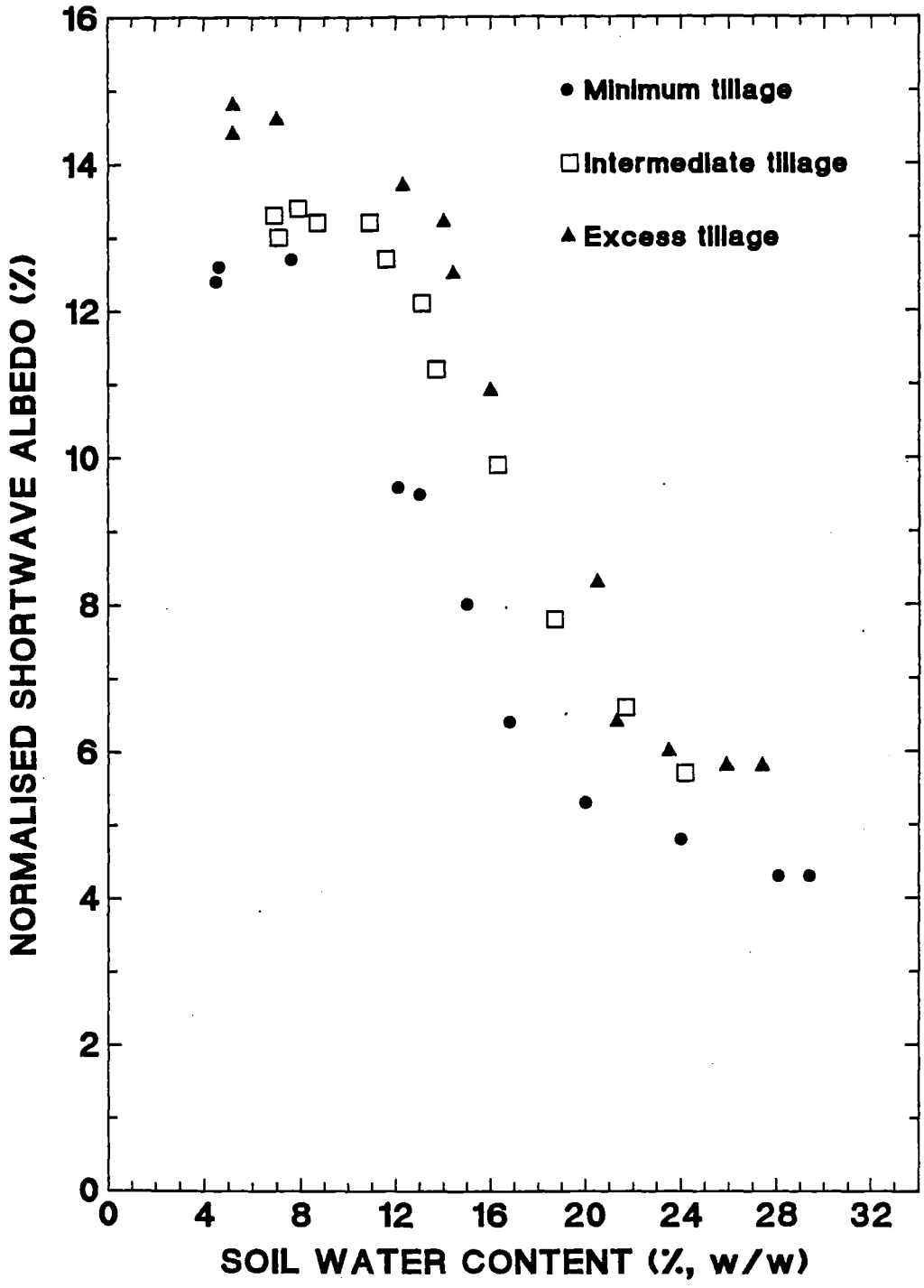

Figure 5.12 Effect of soil water content on the normalised bare soil shortwave albedo. All tillage treatments conducted at PTSW = 17.7%.

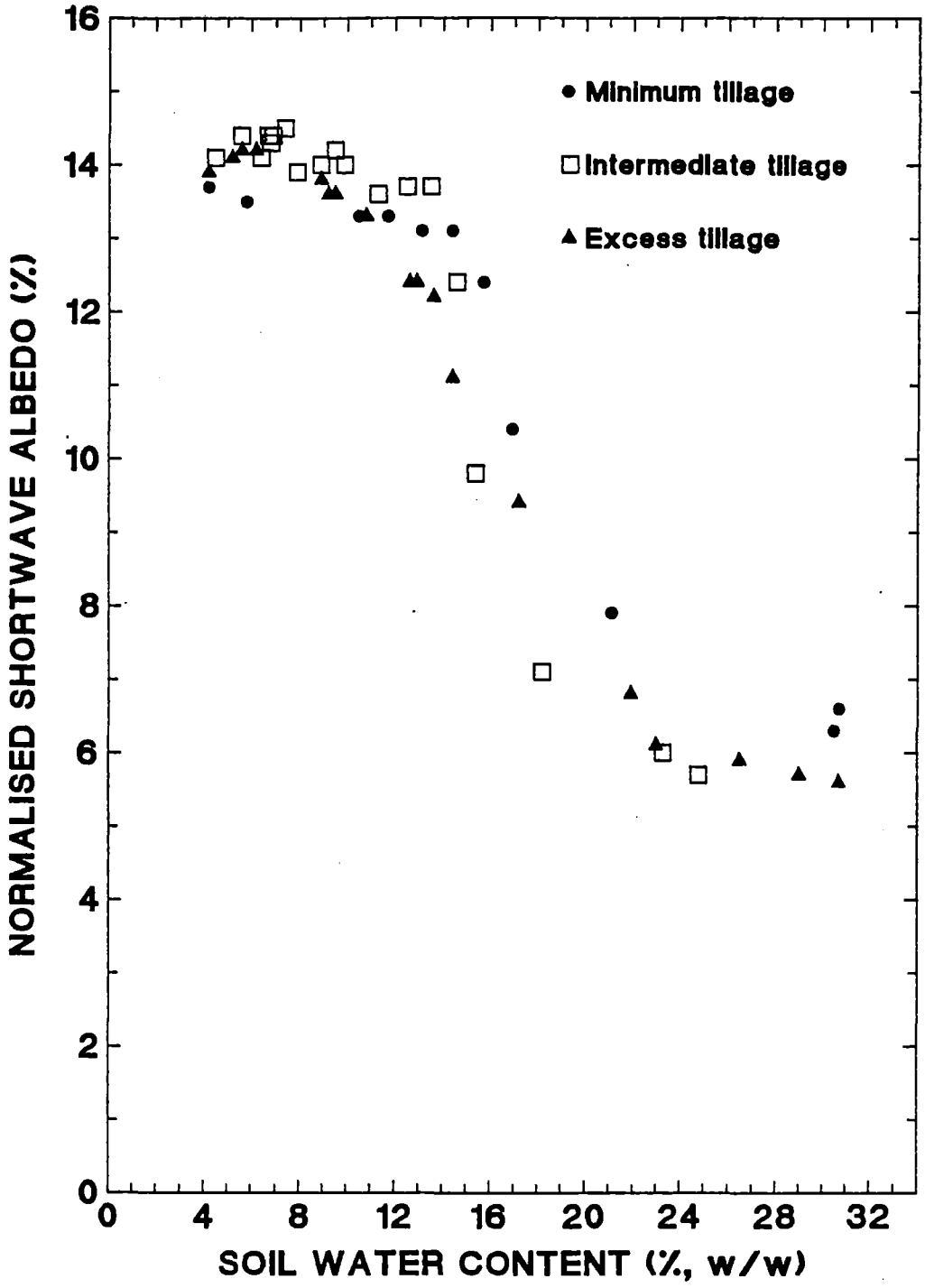

Coulson and Reynolds (1971) suggested that the change in reflectance with zenith angle was a net result from two opposing effects. The first is an optical light-trapping mechanism which is most effective where the incident radiation is exposed to, and trapped in, gaps between soil aggregates. This light-trapping (probably due to multiple internal reflection) would be maximised at small zenith angles where the incident radiation is more normal to the soil surface. The second effect is one of changing spectral composition of the incident radiation. Coulson and Reynolds (1971) showed that reflection from soils generally increases with increasing wavelength throughout the 0.320 to 0.795 μm region. This increase continues in the infra-red waveband until a maximum is reached between 1 and 2 μm (Monteith, 1973). Solar radiation contains a greater proportion of diffuse flux at high zenith angles (Monteith, 1973). A high diffusive flux would infer a high proportion of short wavelength radiation (Monteith, 1973) and hence reflection would be expected to be lower at high zenith angles.

The soil surfaces on which the effect of zenith angle has been evaluated in the present study and in that of Coulson and Reynolds (1971) (Yolo loam soil) appear to be rougher than those used in the studies of Idso et al. (1975) or on the Sacramento clay also used by Coulson and Reynolds (1971). Unfortunately neither Coulson and Reynolds (1971), or Idso et al. (1975), fully quantified the roughness of the surfaces with which they were working. It is probable that with the rougher soil surfaces, the effect of changing spectral composition of the incident radiation is dominating the effect of the light-trapping mechanism on reflectance at differing zenith angles. This has resulted in the observed decrease in reflectance with increasing zenith angle. On a rough soil surface irregular surfaces are presented to radiation incident even from high zenith angles, the light-trapping mechanism probably operates nearly as effectively at high and low zenith angles. With smoother soil, where a more uniform surface is evident, a greater zenith angle effect on light trapping could be expected. The zenith angle effect on reflection appears to be specific to a particular soil and surface condition.

The effects of zenith angle on reflectance was determined on dry soils only because the high evaporative demand during the experimental period made the maintenance of a wet surface during clear sky conditions difficult. Idso et al. (1975) showed that the zenith angle effect on reflectance was the same for the particular wet and dry soil surfaces that they considered. Any differences in zenith angle effect

between the wet and dry surfaces would probably be due to a reduced amount of internal reflection in the wet soil. On the smooth surface considered by Idso et al. (1975) the light-trapping mechanism was probably dominating the spectral composition mechanism in determining the effect of zenith angle on reflectance, and still the zenith angle effect was consistent for wet and dry surfaces. It follows that on the rougher surfaces considered in this study, where the light-trapping mechanism influence on the zenith angle effect is less dominant, there is unlikely to be a difference between wet and dry surfaces on zenith angle effect on reflection. The reflection coefficient data was normalised to a zenith angle of 23.5 degrees using a function the shape of which was derived as the mean of the two curves shown in Figure 5.10.

5.6.3 Soil water content and shortwave albedo

The effects of soil water content on normalised bare soil shortwave albedo are shown for soils with varying surface structure in Figures 5.11 and 5.12. When in dry condition the soil colour (Munsell standard colours) was greyish yellow brown (10 YR 2/3) and when wet, brown black (10YR 5/3). Measurements were made in clear sky conditions where possible. Where small amounts of cloud were present and reduced the total incoming radiation flux to below 600 W m^{-2} the reflectance measurements were discarded. This precaution was taken because the visible fraction (0.4 to 0.7 μm) of total solar radiation under a cloudy sky tends to be slightly greater than under a cloudless sky in otherwise similar conditions (Monteith, 1973). This could result in depressed reflection measurement. The reflectivity of a soil sample decreases as it gets wetter, probably because radiation is absorbed while being transmitted through water films before and after reflection from soil particles as well as being trapped in the water films by total internal reflection (Angstrom, 1927 as cited by Graser and van Bavel, 1982).

There are three characteristic regions of reflectance; the wet surface where reflectance is changing due to zenith angle effects, the drying surface with a rapidly changing surface colour and corresponding change in reflectance, and the dry soil where reflectance changes are again due to zenith angle. The characteristic shapes of the reflectance versus water content curves measured in this study concur with the observations of Idso et al. (1975) where the same depth of surface soil was sampled.

Idso et al. (1975) showed the relation between normalised reflection and volumetric water content of different surface layers between 0.2 and 10 cm deep and by extrapolation estimated the water content 'at the very surface.' They concluded that the decrease in reflectance with increasing water content was gradual and linear 'at the very surface' of the soil. In contrast, Graser and van Bavel (1982) observed abrupt changes in reflection over a small range of water content. They suggested that the linear decrease in reflectance with water content at the soil surface shown by Idso et al. (1975) might have been an artifact of their extrapolation process.

The field sampling technique used here is essentially similar to that of Idso et al. (1975) although no attempt has been made to estimate the water content of the very surface by extrapolation. Soil water content was determined at a depth of 0-20 mm. This sampling depth was necessitated by the rough nature of the soil surface. Reflectance is expected to be a function of the water content in the very surface of the soil. Water content changes drastically with depth, hence the use of a mean water content at this depth might dilute the reflectance-water content relation. These results then, are specific to the 0-20 mm soil depth and do not show the relation between short-wave albedo and the water content 'at the very surface' of the soil. The relation presented here is practically useful for field measurements although the depth of soil water content sampling means the actual albedo-surface soil water content mechanism is disguised. It is acknowledged that the data are not free of soil variability effects and that different parts of the soil surface viewed by the solarimeter would have reached different water contents and have correspondingly different reflectance values at different times. However, the size and number of the samples for soil water content and the random sampling procedure should mean that the results account for the observed spatial variability.

5.6.4 Surface soil structure and shortwave albedo

The mean wet and dry soil reflectance for the various treatments are shown in Table 5.3 together with the corresponding surface roughness (LD index) and the percentage of aggregates less than 18 mm diameter. The random roughness data presented included correction to remove the influence of plot slope and tool-marks. The effects of soil surface roughness on reflectance are generally small in comparison to the

soil water content effects. The surface roughness effect on reflectance is more closely related to the aggregate size distribution than to the random roughness index. The correlation of dry soil albedo with random roughness was -0.586 while the correlation with the percentage of aggregates less than 18 mm diameter was 0.808. On the soil surfaces considered here random roughness does not relate well to aggregate size distribution. The aggregate size distribution better relates to small scale roughness which, consistent with Angstrom's proposed mechanism, affects the reflectance. A few large clods on the soil surface which would have significant effects on random surface roughness index would not be expected to influence albedo to the same degree. The soil surfaces on which reflectance was measured represent an extreme range in a practical sense, although in terms of reflectance they are all 'rough' surfaces. In previous experimental work where large decreases in reflectance have occurred from roughening a surface (e.g. Idso et al., 1975) the comparison has been made with artificially smooth surfaces created by rolling or puddling.

5.6.5 Further discussion

The soil surfaces considered here have low reflectance values. This is probably due to the rough nature of the soil surfaces compared to those used for reflectance observations by other workers. The other main reason is the high organic matter content of this soil (6.2%, w/w). The organic material in the soil is one of the primary colouring constituents in the soil. Even a very small amount of organic matter can decrease the shortwave albedo of a soil. Oxidising the organic component of a loam which was 0.8% by weight increased its reflectivity by a factor of two over the whole spectrum (Bowers and Hanks, 1965).

The low reflectance observed here is unlikely to be due to any site-specific spectral differences. The ratio of diffuse to total radiation varies in response to aerosol presence as well as to zenith angle. The presence of an aerosol (dust, smoke etc.) can cause a loss of direct radiation with a compensating increase in diffuse radiation (Monteith, 1973). New Zealand has clear skies relatively free of pollution and if anything, a higher proportion of direct radiation would be expected here and hence a higher reflectance could be expected, other things being constant. Total shortwave

radiation receipt was very high in January 1988 when these measurements were made with irradiance values in excess of 1000 W m^{-2} being common.

Table 5.3 Effects of surface soil structure on shortwave albedo

TREATMENT	MEASURED DRY SOIL REFLECTION (%)	MEASURED WET SOIL REFLECTION (%)	SURFACE ROUGHNESS LD INDEX	AGGREGATES <18 mm DIAMETER (%)
MINIMUM TILLAGE PTSW31.5%	12.6	4.3	17.0	26.8
MINIMUM TILLAGE PTSW17.7%	13.6	6.3	21.4	58.9
INTERMED. TILLAGE PTSW31.5%	13.3	5.7	16.7	61.8
INTERMED. TILLAGE PTSW17.7%	14.4	5.7	14.7	61.8
EXCESS TILLAGE PTSW31.5%	14.6	5.8	10.2	78.0
EXCESS TILLAGE PTSW17.7%	14.2	5.6	5.8	93.4

Changes in soil water evaporation could result from changes in albedo which occur from tillage effects on surface soil roughness. Shortwave albedo will affect evaporation mainly in the initial constant-rate stage of evaporation (Section 2.4.5.1) which, in a tilled soil with a loose assemblage of clods, might last for only a few hours. Although short in duration, this stage of evaporation is one where soil water loss could be significant. The rate of evaporation during this stage determines the length of time that the soil near the surface stays moist enough to resist movement due to the force of

the wind. It would be beneficial to be able to determine the extent to which the soil water regime can be manipulated by managing the surface soil structure in order to change shortwave albedo.

5.7 Conclusions

1. Multiple-pass tillage operations significantly affect macro-porosity, aeration porosity and available water holding capacity. More intensive tillage results in decreased macro-porosity mainly because of a decrease in the volume of large aeration pores. Available water holding capacity was maximised with the 'excessive' tillage treatment. PTSW did not have significant effects on any of these parameters.

2. Tillage operations significantly affect near-saturation hydraulic conductivity while PTSW does not. More intensive tillage results in lower near-saturation hydraulic conductivity. Near-saturation hydraulic conductivity reflects macro-pore volume.

3. An analysis of the Jackson (1972) model for the calculation of unsaturated hydraulic conductivity has shown that the model is very sensitive to the water characteristic input at high matric potentials (i.e. near saturation). The model was also extremely sensitive to the volumetric water content at which the near-saturated hydraulic conductivity matching factor was determined. The extreme sensitivity of these inputs mean that this method is not suitable for reliably determining changes in hydraulic conductivity which might occur with tillage treatments on the same soil type.

4. Changes in total porosity of the tilled soil layer which result from the tillage treatments are reflected in large changes in thermal conductivity and volumetric heat capacity. Increasing total porosity within the range produced by the tillage treatments in this study resulted in increasing thermal conductivity with the increase being larger in oven-dry soil than in saturated soil. Increasing porosity resulted in decreased volumetric heat capacity of an oven-dry soil but increased volumetric heat capacity of a saturated soil.

5. Bare soil shortwave albedo variation with zenith angle appears soil specific. In this study reflectance decreased with increased zenith angle.

6. Water content of the surface soil has a large effect on bare soil shortwave albedo with a dry soil having a higher shortwave albedo than a wet soil. Soils with coarse surface soil structures generally had slightly decreased albedo although the differences in reflectance over the range of surface structures produced in this study were small and not always consistent.

7. Bare soil reflectance is more closely related to the small scale surface roughness derived from aggregate size distribution than to the larger scale random surface roughness index (LD index).

CHAPTER 6

Numerical Simulation of Soil Water Flux

6.1 Introduction

The dynamic and complex nature of the interacting processes in the soil-atmosphere system suggests that modelling might be an advantageous approach for studying tillage effects on soil water content. Simulation modelling has been developed for the purpose of providing a quantitative description of dynamic systems. The power of the simulation approach is that it can provide an essentially continuous monitoring of an entire system as it varies in response to any number of factors on the basis of cause and effect mechanisms (Hillel et al., 1976). Model development promotes identification of individual processes or components within the complex soil-atmosphere system. These components can then be studied individually or in conjunction with other components or processes. Sensitivity analysis in a model is sometimes the only way to study the effect of tillage-induced soil conditions on each of the processes relating to soil water and temperature (Cruse et al., 1982). Model development encourages organisation and incorporation of existing data into a unifying conceptual framework.

In this chapter the numerical simulation of soil water and heat flux is discussed. The importance of the validation process is considered before some recent soil water models are reviewed. The numerical simulation model CONSERVB (van Bavel and Hillel, 1976) is discussed in detail.

6.2 Model development - a validation problem

Simulation might aid the understanding of complex systems but results should only be accepted if they can be verified and their usefulness proven. 'Nowadays we have a plethora of theoretical models which as yet remain largely un-tested and hence un-proven. It has become altogether easier to formulate models than to validate them' (Belmans et al., 1979). The problem of how to validate a simulation model remains the most critical, difficult, and elusive of all problems associated with numerical simulation (Hillel, 1977).

A model might be considered scientifically valid if its assumptions conform to accepted scientific principles. However, internal scientific validity is not enough; a model must also be realistic. If a model is to portray a real system then it must incorporate the major processes which govern the system's behaviour. A model can be logically and scientifically valid within itself and yet fail to be realistic, because of the continual impact of factors disregarded in the analysis. The first thorough test of a model is the comparison of its behaviour with observations of the real system in an analogous situation. This behaviour includes, for instance, the general shape of the time-course of variables, the presence of discontinuities and the sensitivity of output to parameter values. The confidence with which simulation results can be used to guide the understanding and management of the real system is dependent upon how well the model has been validated.

When the results of a validated model are analysed, evaluated and summarised we can draw certain limited conclusions from our simulation experiments. These conclusions must be based on systematic testing of explicit hypotheses over a realistic range of values of input variables and parameters. The conclusions of a simulation model will always remain tentative and quantitatively uncertain due to the reliance on various assumptions made in the model (Hillel, 1977). As assumptions put bounds on a theory they structure a model and make it usable. It is important that assumptions made in computer simulation models be clearly stated and not hidden in the programming (Baker and Curry, 1976). The assumptions largely determine the purpose of a model and also the credibility ascribed to its predictions.

6.3 Soil-water simulation models - a review

Several numerical models linking the water and energy balances have recently been proposed. Such models account for soil properties and climatic conditions as they control evaporation. Most of the models deal with homogeneous soils, both in the horizontal and vertical planes. The models differ by the soil physical processes which are accounted for and by the manner in which the exchanges between the surface and the atmosphere are considered. It is apparent that few of the models that have been proposed have had thorough evaluations at the time scales for which the models have been designed to be used. Some recent models and their backgrounds are briefly described here.

Sophocleous (1979) proposed a model which attempted to modify and extend the Philip and de Vries (1957) equations (refer to Section 2.4.5.3) in order to make them applicable to non-homogeneous and saturated conditions. Pressure potential (ψ_p) was used as the dependent variable instead of volumetric water content (θ_v). However, the new liquid flux equation proposed has been shown to be incorrect (Milly, 1982). In a further attempt to generalise the Philip and de Vries theory by formulations with ψ_p rather than θ_v as a dependent variable, Milly (1982) proposed a model which accounted for the complications of hysteresis and soil heterogeneities. The effects of the heat of wetting on the transport processes were included.

Higuchi (1984) presented modified and extended forms of Philip and de Vries (1957) equations which also used ψ_p as the dependent variable. This model was used in an attempt to clarify the contribution of liquid and vapour fluxes to the total water flux, and the existence of thermally-induced water movement. It was concluded that isothermal liquid fluxes make a large contribution to total soil water flux, that isothermal vapour fluxes are negligible, and that thermal water fluxes are negligible at soil depths where temperature variations are quickly damped, but are larger near the soil surface where soil temperature gradients are higher.

The approach of Philip and de Vries (1957), as modified by Milly (1982), formed the basis for a model proposed by Passerat de Silans et al. (1989). Their model formulation coupled a lower atmosphere boundary layer model with the physically-based

formulation of water and heat transport. The surface boundary layer model accounted for thermal stratification of the lower part of the atmosphere, with inclusion of the viscous boundary sub-layer leading to different roughness lengths for water vapour, sensible heat and momentum transports. The model had to be calibrated due to the large number of parameters involved, the experimental uncertainties in the estimation of some of them (i.e. soil hydraulic properties) and the difficulty of determining some others (i.e. vapour flow coefficients). After calibration the model predictions were reasonable. Other recent soil water models are those of Sasamori (1970), Rosema (1975), Schieldge et al. (1982) and Camillo et al. (1983).

6.4 The CONSERVB model

6.4.1 General description

The numerical simulation model, CONSERVB, is used to calculate water content and temperature profiles of a bare soil given known initial conditions and a standard, time-dependent set of weather data. The model is derived from a simulation of rainfall infiltration (Hillel et al., 1975; Hillel and van Bavel, 1976) which was later modified to include the concurrent flow of water and heat in the soil (van Bavel and Hillel, 1976). The version of CONSERVB used here was documented by van Bavel and Lascano (1979). CONSERVB provides simultaneous solution of continuity equations for heat and water flow in the soil system. It generates an instantaneous evaporation rate from the ambient weather data and from the current values of soil water content and temperature. The evaporative flux is found from a combination of the surface energy balance and an aerodynamic model of the atmosphere above that surface. Geometrically, the model is of a one-dimensional vertical profile of a soil divided into horizontal compartments, not necessarily of the same thickness. The number of soil layers, their thickness, and hence the total profile depth is defined at model initialisation. The model is dynamic, the properties and processes of the soil-atmosphere system are repeatedly updated at frequent, fixed intervals.

6.4.2 Model inputs

At the beginning of any simulation period the model requires that the initial soil water and temperature profiles as a function of depth be specified. Matric potential (m) and hydraulic conductivity (m s^{-1}) are required as functions of volumetric water content (m^3 m^{-3}) for each soil horizon. The relationship between surface soil water content and shortwave albedo is a requirement as are saturated hydraulic conductivity (m s^{-1}), total porosity (m^3 m^{-3}) and the surface roughness coefficient, z_0 (m).

The time-dependent weather variables required as model input are: global radiation (either daily total, J m^{-2} , or hourly data); daily maximum and minimum air temperatures (^oC) with their corresponding relative humidities (or hourly temperature and dew point data) measured at a height of 2.0 m; average daily windspeed (m s^{-1}, or hourly data if available) measured at 2.0 m; and the amount and duration of rainfall.

6.4.3 Model solution sequence

The model regards the soil profile as a homogeneous soil column divided into a number of layers, each of defined thickness. At each time step, the model begins by finding, from the previous values of the water content and temperature of each soil layer, the corresponding hydraulic potentials, and the water and thermal conductivity values. Matric potential as a function of water content is found using the AFGEN subroutine which allows linear interpolation from the relation specified in the appropriate input table. Thermal conductivity is found by the method of de Vries (1963), where the relative proportions of soil, water and air in the soil layer are calculated, multiplied by their respective thermal conductivities and combined as a weighted sum to give the overall thermal conductivity of the layer. Next the inter-layer fluxes for water and heat are calculated, except the values at the surface layer which follow the energy balance equation. The flow of heat between layers is calculated using Fourier's law (Equation 2.3). The flow of water between layers is calculated using Darcy's law (Equation 2.11). The continuity equation then determines the changes in the volumetric heat and water contents of each soil layer over a short time interval, and hence their values a finite instant of time later.

Although this model deals with a semi-infinite vertical profile it compartmentalizes and simulates water and heat flows only in the uppermost soil layers, which must interact in some way with the underlying subsoil zone. For the purpose of simulation some lower boundary condition must be defined. In this case gravity drainage through the bottom boundary of the soil profile is permitted. This is done by specifying a downward flux equal to the hydraulic conductivity of the lower-most soil layer (i.e. unit hydraulic gradient). The value of this conductivity is dependent on the water content and is determined, in the long-run, by the net downward flow of water through the profile as a whole. The flow of heat at this bottom boundary is calculated by Fourier's law assuming that the temperature in the bottom layer stays constant.

The energy balance equation (Equation 2.1) is used to find the surface soil temperature and the evaporation rate from which the heat flux and water flux at the surface are calculated. To use the energy balance the model interpolates the meteorological inputs, calculates the surface albedo, the boundary layer resistance and the longwave sky irradiance. In using the energy balance the flux of sensible heat in the soil associated with liquid flux is ignored as negligible, as is any net evaporation below the surface and the associated water vapour flux in the soil. However, the latent heat flux caused by intermittent evaporation and condensation is taken into account. The net radiation component of the energy balance (R_n, W m^{-2}) is found as:

$$R_n = (1 - a)R_g + R_l - \epsilon \sigma (T_s + 273.15)^4 \quad \ldots (6.1)$$

where R_g is the global radiation (W m^{-2}), R_l the longwave sky irradiance (W m^{-2}), ϵ is the surface emissivity, σ is the Stephan-Boltzman constant (5.67×10^{-8} W m^{-2} K^{-4}) and T_s the surface temperature (^oC). Albedo (a) and emittance are not constant but are calculated by linear interpolation among the values in the appropriate input table and the volumetric water content of the surface soil layer.

Longwave sky irradiance is calculated from Brunt's formula, after Sellers (1965):

$$R_l = \sigma(T_a + 273.15)^4 \times \left[0.605 + 0.048 \sqrt{1370\ H_a}\right] \quad \ldots (6.2)$$

H_a is air humidity (kg m^{-3}), calculated from the dewpoint temperature using the equation of Murray (1967). Air temperature (T_a) is found from linear interpolation with time from a function which sets the inputs of minimum and maximum temperatures at times of 5.00 and 15.00 hours respectively. The constants 0.605 and 0.048 are empirically derived values. The equation is a statistical correlation of radiative fluxes with weather parameters at different sites and does not describe a direct functional relationship. It is most accurate under 'average' conditions (e.g. when the air is not unusually dry or humid). The equation is most appropriate for climatological studies of radiation balance and is less well suited for micro-meteorological analyses over a few hours (Monteith, 1973). In the Brunt formula reported by Sellers (1965), vapour pressure (mb) is used in place of the air humidity used above. The multiplier 1370 along with the substituted H_a has been included by the model authors as an approximation to the vapour pressure required in the original equation. This is only an approximation as the vapour pressure (e)-air humidity (H_a) relationship is temperature (T) dependent as shown (Monteith, 1973):

$$H_a = \frac{(217.0 \times e)}{T} \qquad \ldots (6.3)$$

Here the units used are H_a (g m^{-3}), e (mb) and T (K).

Calculation of the remaining terms in the energy balance equation is considered next. Sensible heat flux into the air (H, W m^{-2}) and the evaporation rate (E, kg m^{-2} s^{-1}) are calculated by defining, first, the corrected aerodynamic boundary layer resistance, r_c (s m^{-1}):

$$r_c = r_a \times St \qquad \ldots (6.4)$$

where r_a, the effective resistance to heat and vapour transfer in neutral conditions (i.e. the neutral value of r_c) is defined as:

$$r_a = \frac{\left[\ln\left[\frac{z}{z_o}\right]\right]^2}{k^2 \times u} \qquad \ldots (6.5)$$

Here z_0 is the surface roughness coefficient (m), z the height at which windspeed was measured (2.0 m), u is the windspeed (m s^{-1}) and k the von Karman constant (0.41).

Values of the average windspeed are set at noon and linear interpolation produces values at other times. This equation is valid only in neutral conditions when turbulent transfer is purely frictional and is not affected by thermal gradients.

The turbulent boundary layer of air above the soil surface exhibits mechanical turbulence due to frictional effects of the surface as well as thermal turbulence arising from buoyancy effects (i.e. vertical movement of parcels of air which are hotter or colder than their surroundings). In an unstable atmosphere air temperature decreases rapidly with height. Any parcel of air pushed upward by mechanical turbulence will continue to rise because it is warm, light and therefore buoyant compared to its surroundings. This buoyancy effect further enhances the turbulence of the air. When air temperature increases with height, buoyancy forces oppose any upward displacement and hence turbulence is suppressed. These are termed stable atmospheric conditions. The logarithmic wind profile implicit in (Equation 6.5) holds only in neutral atmospheric conditions; stable or unstable conditions modify the logarithmic wind profile. To account for this, a dimensionless stability correction, St, (Szeicz et al. (1973)) is introduced:

$$St = \frac{1}{(1 - 10Ri)} \qquad \ldots (6.6)$$

Ri is the Richardson number which describes the relative importance of mechanical and buoyancy forces. In neutral conditions Ri is zero (and hence St=1), while in stable conditions it is positive and in unstable conditions negative. Ri is defined as:

$$Ri = \frac{g \times (z - z_o) \times (T_a - T_s)}{(T_a + 273.15) \times u^2} \qquad \ldots (6.7)$$

where all terms have been defined previously. Note that if Ri should equal +0.1 or greater an unacceptable value for St would result. This would indicate extreme inversion at very low windspeed. To prevent this the value of Ri is limited to less than +0.08 (van Bavel and Hillel, 1976).

Now sensible heat flux (H) can be defined as:

$$H = \frac{(T_a - T_s) \times C}{r_c} \qquad \ldots (6.8)$$

and evaporation rate as:

$$E = \frac{(H_s - H_a)}{r_c} \qquad \ldots (6.9)$$

C, (J m^{-3}) is the volumetric heat capacity of air and H_s (kg m^{-3}) the absolute humidity of the air at the soil surface. H_s is dependent on surface temperature and on surface soil water content (van Bavel and Hillel, 1976):

$$H_s = H_o \exp\left[\frac{M\psi}{RT}\right]$$

$$= H_o \exp\left[\frac{\psi_p}{46.97 \times (T_s + 273.15)}\right] \qquad \ldots (6.10)$$

H_o is the saturation humidity at surface temperature T_s, while ψ_p (always negative in the model) is the pressure potential which corresponds to the water content of the surface layer of soil. R is the universal gas constant (8.314 kJ kg^{-1} K^{-1} mol^{-1}), T is absolute temperature (K), and M is the molecular weight of water. This approach assumes that the water content at the surface (z = 0) equals that of the surface layer and hence is approximate.

Latent heat of vaporization (L_v, J m^{-3}) as a function of soil surface temperature was given by Forsythe (1964) as:

$$L_v = 2.495 \times 10^9 - (2.247 \times 10^6 \times T_s) \qquad \ldots (6.11)$$

Up to this point each component of the energy balance, apart from soil heat flux (S), has been defined but determination of the surface soil temperature has not been considered. Note that T_s has featured in the explicit calculation of R_n, H, E, and L_v. In CONSERVB, T_s is calculated by an iterative procedure which uses air temperature as a first estimate of T_s. The energy balance at the soil surface is calculated with sensible heat flux, absolute humidity at the soil surface and evaporation rate being determined using the equations previously described. Using energy balance, soil heat flux is then determined as the difference between net radiation and the sum of the sensible and latent heat fluxes. This then allows the calculation of surface soil temperature using:

$$T_s = T_1 + \left[S \times \frac{z_1}{2\lambda_1} \right] \quad \ldots (6.12)$$

Here T_1 is the temperature at the centre of the surface layer of soil, λ_1 (W m^{-1} K^{-1}) is the thermal conductivity of that layer and z_1 its thickness. Using this T_s as the new estimate of 'final' soil surface temperature the iterative procedure is repeated with the components of the energy balance being recalculated resulting in yet another T_s value. When the latest T_s value obtained changes by less than 0.01 ^oC from the previous value the procedure terminates. Using the newly determined T_s value the soil heat flux, S (W m^{-2}), is recalculated as:

$$S = 2 \times (T_s - T_1) \times \frac{\lambda_1}{z_1} \quad \ldots (6.13)$$

Evaporation rate, sensible heat flux into the air and latent heat of vaporization are recalculated using the previously described methods before net radiation is also recalculated, this time by solution of the energy balance equation.

Finally, if needed, water flux at the soil surface is modified by the infiltration of water from rain or irrigation before the net flux of water and heat to each layer and the water and heat content values are updated. The complete procedure is then repeated for the next time step using the previous value of T_s as the initial estimate for the implicit calculation of the next T_s value.

6.4.4 Previous evaluations of CONSERVB

An experimental verification of the CONSERVB model was undertaken by Lascano and van Bavel (1983). The model was used to calculate water and temperature profiles of a bare soil over a 30-day period. The calculated values were compared with profiles measured on a silty-clay textured Norwood series soil in Texas. The model was adapted for hourly weather data input. Longwave sky irradiation was calculated with the equation of Idso (1981) (Equation 6.23) rather than the Brunt equation (Sellers, 1965) which was previously used with the model. The model evaluation period featured daily global irradiance totals averaging in excess of

21 MJ m^{-2}, daily maximum air temperatures averaging in excess of 36 ^{o}C, and a mean daily windspeed of 1.56 m s^{-1}.

Lascano and van Bavel (1983) concluded that the CONSERVB model showed good agreement between predicted and measured values in the conditions of the test. The model predicted the water content for different soil layers within one standard deviation of the measured average values. Predictions of soil profile temperatures were within one degree (celsius) of measured values. The soil surface temperatures were correctly predicted within the range 25.0-37.0 ^{o}C and under-estimated above 37.0 ^{o}C. The spatial variability estimations of the calculated values for water content showed that the variance of the calculated values was comparable to the measured variance of the data set.

A further test of the CONSERVB model was undertaken in 1986 (Lascano and van Bavel, 1986). The evaporation rates calculated by the CONSERVB model were compared with measured values. Measured and calculated soil water content and temperature values were also compared. The experimental soil was from the Olton series, it had a sandy-loam 'A' horizon and a 'B' horizon of clay texture. The experimental site was near Lubbock, Texas. The experimental period consisted of three drying cycles of 9, 8, and 20-days duration. Hourly weather data was used as model input. During the experimental periods average daily total global radiation was in excess of 25 MJ m^{-2}, average maximum daily air temperature was 31.3 ^{o}C and average daily windspeed was 1.32 m s^{-1}. Evaporation ranged from 8.24 to 0.66 mm d^{-1}.

Measured and simulated daily and cumulative evaporation showed good agreement over a range of soil water content and temperatures. Cumulative evaporation was predicted to within one standard deviation of the measured values and in 34 of the 37 cases daily rates were also within one standard deviation of the measured values. Water content and temperature values were predicted to within one standard deviation of the average measured values. Surface soil temperature, which is a sensitive indicator of evaporation rate, was calculated to within 1.0 ^{o}C and net radiation to within 40 W m^{-2}. The investigation highlighted model sensitivity to the value of thickness assigned to the first soil layer.

Lascano and van Bavel concluded, following their two investigations at sites of differing location and soil type, that CONSERVB was an accurate method to predict bare soil evaporation rates as well as soil-water and temperature profiles from known soil properties and measured weather data.

6.4.5 A pre-verification assessment of CONSERVB

The purpose of this section is to outline some of the assumptions and simplifications which have been made in the CONSERVB model.

6.4.5.1 Sub-surface evaporation

The CONSERVB model assumes that all evaporation takes place from the very surface of the soil. Net evaporation from below the surface and the associated vapour flux are ignored as negligible. In order to explore the consequences of these assumptions, aspects of the surface energy balance are discussed following Buchan (1989). Sub-surface evaporation has been shown to occur in a drying soil (de Vries and Philip, 1986) leading to a division of the soil heat flux into two components: thermal heat flux (S_t) driven by a temperature gradient, and isothermal heat flux (S_i) driven by a moisture gradient (i.e. the coupling of heat and vapour fluxes which accompanies sub-surface evaporation). Thus:

$$S_{total} = S_t + S_i \qquad \ldots (6.14)$$

(de Vries and Philip, 1986).

In a drying soil, during typical daytime conditions, thermal heat flux (S_t) is positive as heat flows into the soil. In addition, as sub-surface evaporation is occurring, a sub-surface heat sink exists. Thus a simultaneous isothermal heat flux (S_i) out of the soil is coupled with the vapour flux and hence a negative flux component exists. Total soil heat flux is less than thermal heat flux because of this negative isothermal heat flux component (during night-time conditions in a drying soil, the reversal of S_t could make both S_t and S_i aligned and negative). With sub-surface evaporation occurring total soil evaporation can be represented as:

$$E_{total} = E_o + E_{so} \quad \ldots (6.15)$$

where E_o is the surface evaporation (replaced by liquid flow from below) and E_{so} is sub-surface evaporation. E_{so} could be expected to be dominant where a soil has a dry surface. When applying the energy balance (Equation 2.1) if $E = E_{total}$, as is assumed in CONSERVB, then S must be reduced by $L_v E_{so}$ (sub-surface evaporation energy demand) for the energy balance to be maintained (S then = S_{total}). Thus, when using the energy balance to calculate total evaporation, S must be identified with S_{total} (Buchan, 1989). In CONSERVB, S is identified only with the thermal component S_t, the heat flux obtained by temperature gradient dependent methods. Sub-surface evaporation might account for several millimetres of water per day in the early stages of bare soil drying (Buchan, 1989). De Vries and Philip (1986) gave an example of 3 mm d^{-1}. A rate for E_{so} of 1 mm d^{-1} is equivalent to a latent heat sink of 29 W m^{-2} averaged over 24 hours. The neglect of isothermal soil heat flux might lead to an error in the energy balance in excess of 100 W m^{-2} (Buchan, 1989).

This is a potential problem with the CONSERVB model. While coupled-flow models which account for these processes have been formulated (Section 6.3) they themselves have serious draw-backs in that they have a very high level of complexity and would require local calibrations because some of the parameters used cannot be quantified (e.g. vapour flow coefficients). The behaviour of many of these models has not been compared with field data. In many cases the large, complex data input required for the use of these models is prohibitive.

6.4.5.2 Soil-atmosphere contact area effects.

The soil-atmosphere boundary contact area effect on the soil-limiting phase of evaporation is neglected in the CONSERVB model. It is also unable to account for the effects of surface roughness and soil heterogeneity on variations in infiltration caused by tillage, and on non-uniform drying caused by non-uniform radiation inputs. It was shown earlier (Section 4.4.6) that tillage affects the area of the soil surface directly in contact with the atmosphere. Linden (1982) speculated that when the limiting evaporation flux is just below the soil surface, increased soil-atmosphere contact area would increase the evaporation rate because of a horizontal water flux component. As evaporation

proceeds, the limiting flux would become vertical and thus would not be affected by soil-atmosphere contact area. The initial phase of evaporation is limited by atmospheric conditions and hence would also be unaffected by soil-atmosphere contact area. During the transition period between weather-controlled and soil vertical flux-limited evaporation rate, soil-atmosphere contact area might be expected to influence evaporation rate. Linden (1982) modelled the effect of soil-atmosphere contact area on evaporation by incorporation of horizontal as well as vertical water flow. The results showed only a small increase in net evaporation from increased soil-atmosphere contact area because the horizontal evaporation component reduced the subsequent vertical component. Based on this evidence, the exclusion of the soil-atmosphere contact area effects from the CONSERVB model is not seen as a serious limitation to its suitability for use in this study.

6.4.5.3 Surface soil layer thickness

The CONSERVB model assumes that the water content and absolute humidity in the surface soil layer equals that at the very surface of the soil. The thickness of the surface soil layer is arbitrarily defined at model initialisation. Model evaporation predictions have been shown to be sensitive to the surface layer thickness (Lascano and van Bavel, 1986). Increasing surface layer thickness increased simulated daily evaporation rates and hence the cumulative evaporation rate. Lascano and van Bavel reported that for practical purposes there were no significant differences between results obtained with values of 0.001, 0.002 and 0.005 m surface layer thickness. Using a value of 0.01 m caused cumulative evaporation to exceed measured values by as much as 20%. In using CONSERVB (and many other models numerically simulating evaporation), caution is needed in selecting an appropriate surface layer thickness. In their use of CONSERVB Lascano and van Bavel (1986) used a value of 0.005 m. This selection was a compromise between calculation accuracy and computer time usage. The use of a 0.005 m layer reduced computer time by 25% as compared to using a 0.001 m surface layer thickness. When using such small surface layers the model theory deviates from expected field behaviour. Surface roughness variation would be a large part of such a soil layer in a cultivated soil. The use of Darcy's and Fourier's laws for water and heat flow in the surface layer, where uniform transmission properties and simple mechanisms are assumed, might be unrealistic.

6.4.5.4 Aerodynamic resistance term calculation.

In the calculation of the aerodynamic resistance term (r_c), the problem of a singularity in the calculation of the stability correction (St) was referred to earlier (Section 6.4.3). Limiting the value of Ri to some value less than +0.1 does improve the fault. However, in very stable atmospheric conditions at low windspeed, when Ri could be greater than +0.1, this approach to correcting the problem would result in artificially reduced values of St and hence of r_c. The stability function (St) can be defined as a function of the Monin-Obukhov parameter as an alternative to the Richardson number. An aerodynamic model presented by Paulson (1970) was modified by Camillo and Gurney (1986) for use in modelling evaporation from bare soils. This model uses the Monin-Obukhov stability function in a formulation which avoids the problems apparent in the method used for calculating aerodynamic resistance in CONSERVB. In the Camillo and Gurney (1986) model aerodynamic resistance (r_c) was presented as:

$$r_c = \frac{\left[\ln \frac{z}{z_o} - P_1\right] \times \left[\ln \frac{z}{z_o} - P_2\right]}{k^2 \times u} \qquad \ldots (6.16)$$

where z is the height of windspeed measurements (m), z_0 is the roughness parameter (m), k is the von Karman constant, u is the windspeed (m s^{-1}), and P_1 and P_2 are stability corrections. The Monin-Obukhov length (MO) is defined as:

$$MO = \frac{T_a u^2}{g(T_a - T_s) \ln\left[\frac{z}{z_o}\right]} \qquad \ldots (6.17)$$

where T_a and T_s are temperature of the air and the surface respectively (K) and g is the gravitational acceleration. For a neutral atmosphere, defined for the model as being when $|T_a - T_s| \leq 0.1$ K, the stability corrections P_1 and P_2 are 0.

For an unstable atmosphere, ($T_a - T_s < -0.1$ K) the following equations are used:

$$X = \left[1 - 16 \frac{z}{MO}\right]^{0.25} \quad \ldots (6.18)$$

$$P_1 = 2 \ln\left[\frac{1 + X}{2}\right] + \ln\left[\frac{1 + X^2}{2}\right] - \left[2 \tan^{-1}(X)\right] + \frac{\Pi}{2} \quad \ldots (6.19)$$

$$P_2 = 2 \ln\left[\frac{1 + X^2}{2}\right] \quad \ldots (6.20)$$

where Π is the constant 3.142.

For a stable atmosphere ($T_a - T_s > 0.1$ K), the ratio of z to MO must be examined:

$$\text{If } \frac{z}{MO} \leq 1, \text{ then } P_1 = P_2 = \frac{-5 (z - z_o)}{MO} \quad \ldots (6.21)$$

or alternatively, if:

$$\text{If } \frac{z}{MO} > 1, \text{ then } P_1 = P_2 = -5 \ln\left[\frac{z}{z_o}\right] \quad \ldots (6.22)$$

When the results from the Camillo and Gurney (1986) model are compared with those from the aerodynamic model used in CONSERVB (Table 6.1) it is apparent that in unstable atmospheric conditions (when Ri and z/MO are negative), at a windspeed of 5.0 m s^{-1}, the two models give almost identical results for aerodynamic resistance. In neutral conditions, by definition, the stability variable must equal 1.0 and an unmodified logarithmic wind profile exists. In stable conditions, at a windspeed of 5.0 m s^{-1}, the models again give very similar results. However, in stable conditions at a low windspeed (0.5 m s^{-1}) some differences occur. In very unstable conditions r_c, as calculated from Camillo and Gurney (1986), is significantly larger than that calculated by the van Bavel and Hillel (1976) method. As atmospheric conditions tend toward neutral this divergence becomes less pronounced until, at neutrality, the results are identical. As conditions become stable at this windspeed Ri reaches the preset maximum of +0.08 and hence r_c reaches the maximum possible value of 2855.5 s m^{-1}. The Monin-Obukhov parameter continues to increase as atmospheric stability increases to a value of 1.0 at which time the maximum value for aerodynamic resistance using this model at 0.5 m s^{-1} windspeed is reached. This value is 20559.9 s m^{-1}. At the cost of

increased complexity the use of the Camillo and Gurney (1986) aerodynamic model appears to give consistent results, over a wider range of conditions, than does the formulation used by van Bavel and Hillel (1976). The Camillo and Gurney (1986) model has been used in CONSERVB for aerodynamic resistance calculation in this study.

Table 6.1 A comparison of methods for calculating aerodynamic resistance.

WINDSPEED AT 2.0 m HEIGHT $m\ s^{-1}$	SURFACE SOIL TEMPERATURE MINUS AIR TEMP (K)	AERODYNAMIC RESISTANCE*	
		VAN BAVEL AND HILLEL (1976) $s\ m^{-1}$	CAMILLO AND GURNEY (1986) $s\ m^{-1}$
5.0	1.8	54.49	54.32
	1.2	55.34	55.16
	0.6	56.21	56.08
	0.0	57.11	57.11
	-0.6	58.03	58.02
	-1.2	58.98	58.94
	-1.8	59.96	59.86
0.5	1.8	98.30	243.30
	1.2	135.98	278.02
	0.6	219.93	337.56
	0.0	571.11	571.11
	-0.6	2855	20559
	-1.2	2855	20559
	-1.8	2855	20559

* z_0 = 0.00232 m, Ri limited to less than +0.08 after van Bavel and Hillel (1976).

6.4.5.5 Longwave sky irradiance.

Various equations have been devised for estimating the effective emittance of a cloudless atmosphere. The formulations include those of Brunt (1932), Swinbank (1963), Idso and Jackson (1969) and Brutsaert (1975). Idso (1981) highlighted apparent

discrepancies between these equations and suggested a new equation which, when results were compared with experimental data, appeared to be an improvement over earlier formulations. The Idso formulation for the calculation of longwave sky irradiance is given as:

$$R_l = (\sigma \times T_a^4) \times \left[0.7 + 5.95\times10^{-5} \times \left[H_a \times \exp\left\{\frac{1500.}{T_a}\right\}\right]\right] \quad \ldots (6.23)$$

where R_l is longwave sky irradiance, σ is the Stephan-Boltzman constant, T_a is air temperature (K) and H_a is humidity of the air. This formulation is adopted in place of the previously used Brunt equation (Equation 6.2). Lascano and van Bavel (1983) also included this substitution in their version of CONSERVB.

6.4.5.6 Other aspects.

Total soil porosity is required as a model input to allow the calculation of volumetric heat capacity and thermal conductivity using the method of de Vries (1963). An average porosity value is used for the complete soil profile. In a tilled soil this is seen as inappropriate because of the widely differing bulk densities in the tilled and un-tilled soil zones. The model was modified so that soil thermal properties were calculated separately in the tilled and un-tilled soil zones.

Some other inaccuracies have been included in the CONSERVB model probably because they save computing time and might be regarded as unnecessary complications. These are:

(i) The implicit calculation of surface soil temperature by energy balance solution is a key part of the CONSERVB model. Two of the parameters involved in this solution sequence, r_c (stability corrected aerodynamic resistance) and L_v (latent heat of vaporization of water) are functions of temperature. Within the implicit loop for surface temperature calculation the values of r_c and L_v are not updated for temperature changes. This would decrease the accuracy of the energy balance solution but probably by an insignificant amount. The approximation of the air humidity variable in

the Brunt equation for the calculation of longwave sky irradiance was discussed in Section 6.4.3.

(ii) When the model is used with daily averages for meteorological input a daily distribution function for each input needs to be assumed. For global radiation a sine distribution is assumed during daylight hours. Where daily minimum and maximum air temperatures and their corresponding dew point temperatures are input, the minimum values are assigned at time 0500 hours and the maximum values at time 1500 hours. Linear interpolation is used to assign the values of these two parameters at other times. Where average daily windspeed is input, the mean value is assigned to time 1200 hours and linear interpolation between this mean value and the value assigned for the next day (at 1200 hours) is used to calculate windspeed at other times. It is apparent that each of the inputs fluctuate considerably during the day and these approximate, assumed distributions will not always give good estimates. The use of hourly input data, where available, should improve model predictions. The use of daily inputs reduces the data requirement and subsequently increases the likelihood of suitable data being readily available.

6.5 Conclusions

1. The CONSERVB model has been shown to be mechanistic and process-oriented. It predicts evaporation from a theoretical soil water and atmospheric flow system approach (as opposed to a statistical approach). As such, the model can be adapted for variations in soil condition which have resulted from tillage.

2. A model suitable for use in this study must be an adequate predictor of evaporation while incorporating tillage-affected variables. The CONSERVB model includes the following tillage-sensitive parameters: soil thermal properties (heat capacity and thermal conductivity), surface soil roughness as related to albedo and aerodynamic properties, and soil hydraulic characteristics including hydraulic conductivity and matric potential functions.

3. The CONSERVB model has been shown in previous evaluations to accurately predict soil temperature and water profiles, as well as evaporation rates, in

different conditions and on different soil types, without the need for any local calibrations.

4. The CONSERVB model is thus considered suitable for further, more extensive evaluation, with the object of using the verified model as an experimental tool in the investigation of tillage management effects on soil water evaporation and storage.

CHAPTER 7

Experimental Verification of the CONSERVB Model

7.1 Introduction

In this chapter an assessment is made of the ability of the numerical simulation model CONSERVB (van Bavel and Hillel, 1976) to accurately simulate evaporation rates, and water and temperature profiles in a bare soil.

7.2 Experimental method and model initialisation

7.2.1 Verification method

A study was undertaken to verify the CONSERVB model in New Zealand conditions by comparing predicted and measured evaporation, as well as water content and temperature profiles, to see if any disagreement would be within the range expected from natural experimental variability. CONSERVB was used to simulate water and temperature profiles over a 13 and an 11-day drying cycle (julian days 74 to 86 and 89 to 99, 1989). Approximately 40 mm of water was applied by irrigation to the initially dry soil surface at the beginning of the experiment and approximately 10 mm of rain fell between the two simulation periods. During the simulation 1.0 mm of rain fell on julian day 79 and 0.6 mm fell on julian day 82.

The model used for the simulations differed from that described in Section 6.4.3 in that it was adapted for hourly input weather data. The model was modified so that the soil thermal properties were calculated separately in the tilled and un-tilled soil zones (refer Section 6.4.5.6). The calculation of atmospheric resistance to vapour and heat transfer used the method of Camillo and Gurney (1986) as described in Section 6.4.5.4. Longwave sky irradiance was calculated using the method of Idso (1981) (Equation

6.23). The model was re-programmed from CSMP computer coding to FORTRAN for running on the Lincoln University VAX computer system. This necessitated the inclusion of extra subroutines as some calculations in the model are carried out with intrinsic functions in the CSMP language not available in FORTRAN. A complete listing of the CONSERVB model as used for the simulations described here is included in Appendix one.

7.2.2 Model initialisation

The methods of measurement of the constants, variables and functions considered in this section have been described previously (Chapter 3). For the simulations, the 0.40 m deep profile of the Templeton silt-loam soil was divided into 14 layers. The geometry of the soil profile is given in Table 7.1 together with the values of water content and temperature used for initialisation of the two simulation runs. The surface roughness coefficient (z_0) (Table 7.2) used for the simulations was the mean of values measured for each of the prevailing wind directions at the site.

Extrapolation to mean total porosity from the hydraulic conductivity-volumetric water content ($K(\theta_v)$) relation yielded an unrealistic value for 'A' horizon saturated hydraulic conductivity and so this value was estimated using the measured near-saturation hydraulic conductivity as a guide (Table 7.2). The saturated hydraulic input is used only in the calculation of infiltration rate in the CONSERVB model. In the simulations described here the maximum rate of the rainfall was well below the infiltration capacity of the soil and hence infiltration rate was determined by the rate of rainfall. Thus, the saturated hydraulic conductivity input was of little significance. Total porosity for each horizon is also presented in Table 7.2. The hydraulic conductivity-volumetric water content relations ($K(\theta_v)$) for the 'A' and 'B' horizons are presented in Figures 7.1 and 7.2 respectively. The water characteristic functions for the 'A' and 'B' horizons are shown in Figure 7.3. The generalised shortwave albedo-water content relation is shown in Figure 7.4. The meteorological inputs for the two drying cycles are summarised in Table 7.3. The hourly meteorological input data for both drying cycles is included in Appendix one.

Figure 7.1 Unsaturated hydraulic conductivity input function for the 'A' horizon.

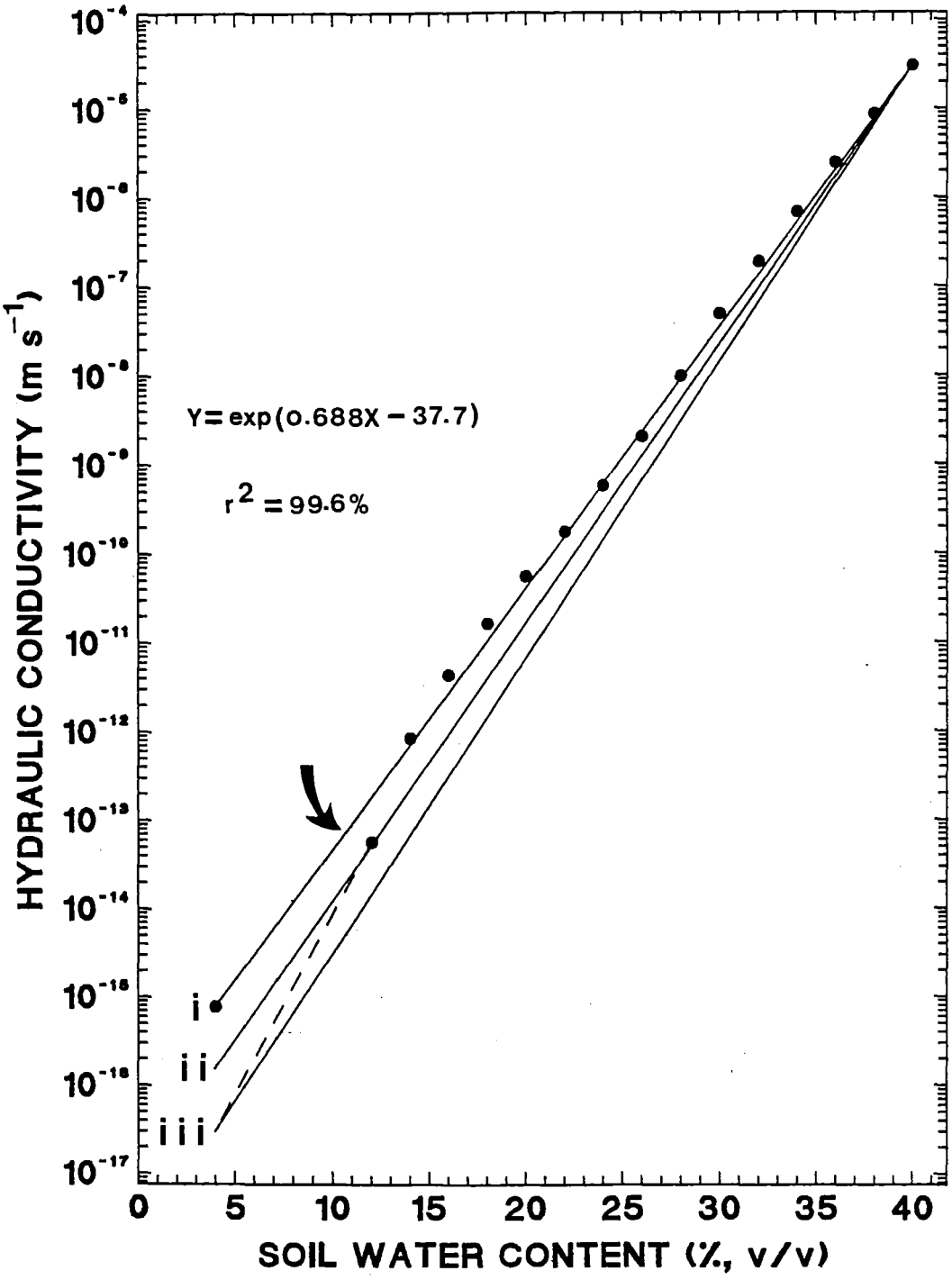

Figure 7.2 Unsaturated hydraulic conductivity input function for the 'B' horizon (arrow indicates extrapolated value).

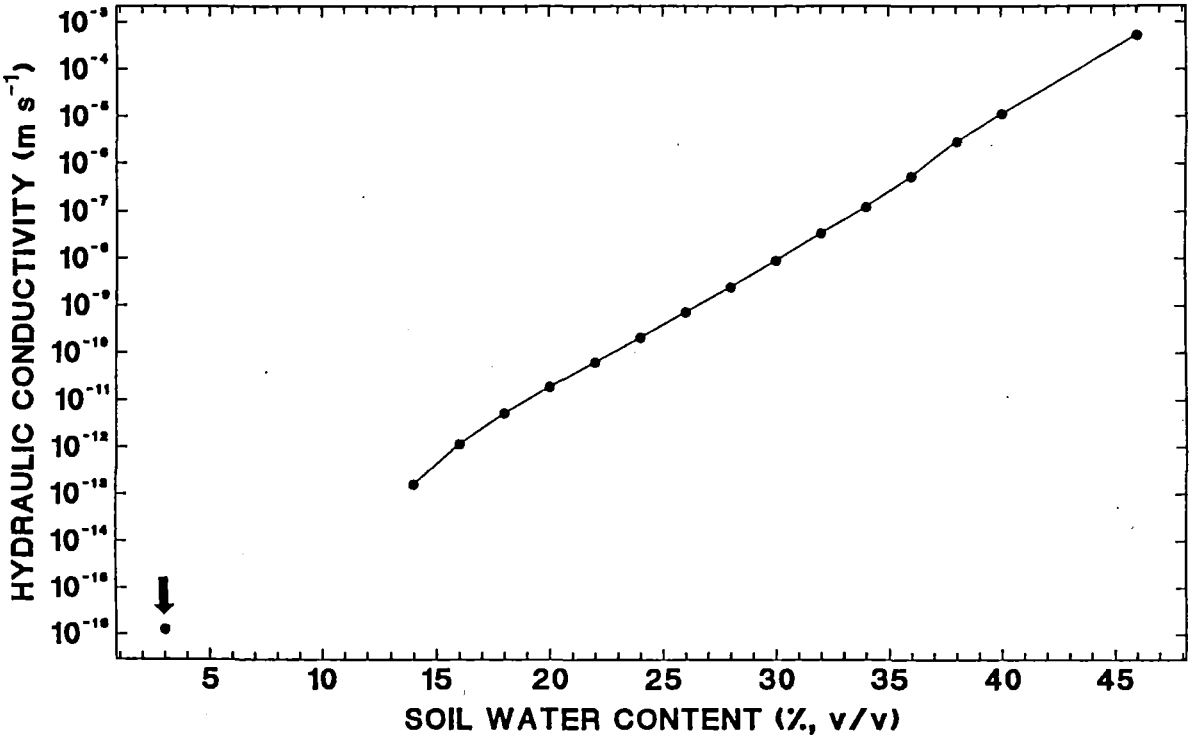

Figure 7.3 Water characteristic input functions for both 'A' and 'B' horizons (arrows indicate estimated values).

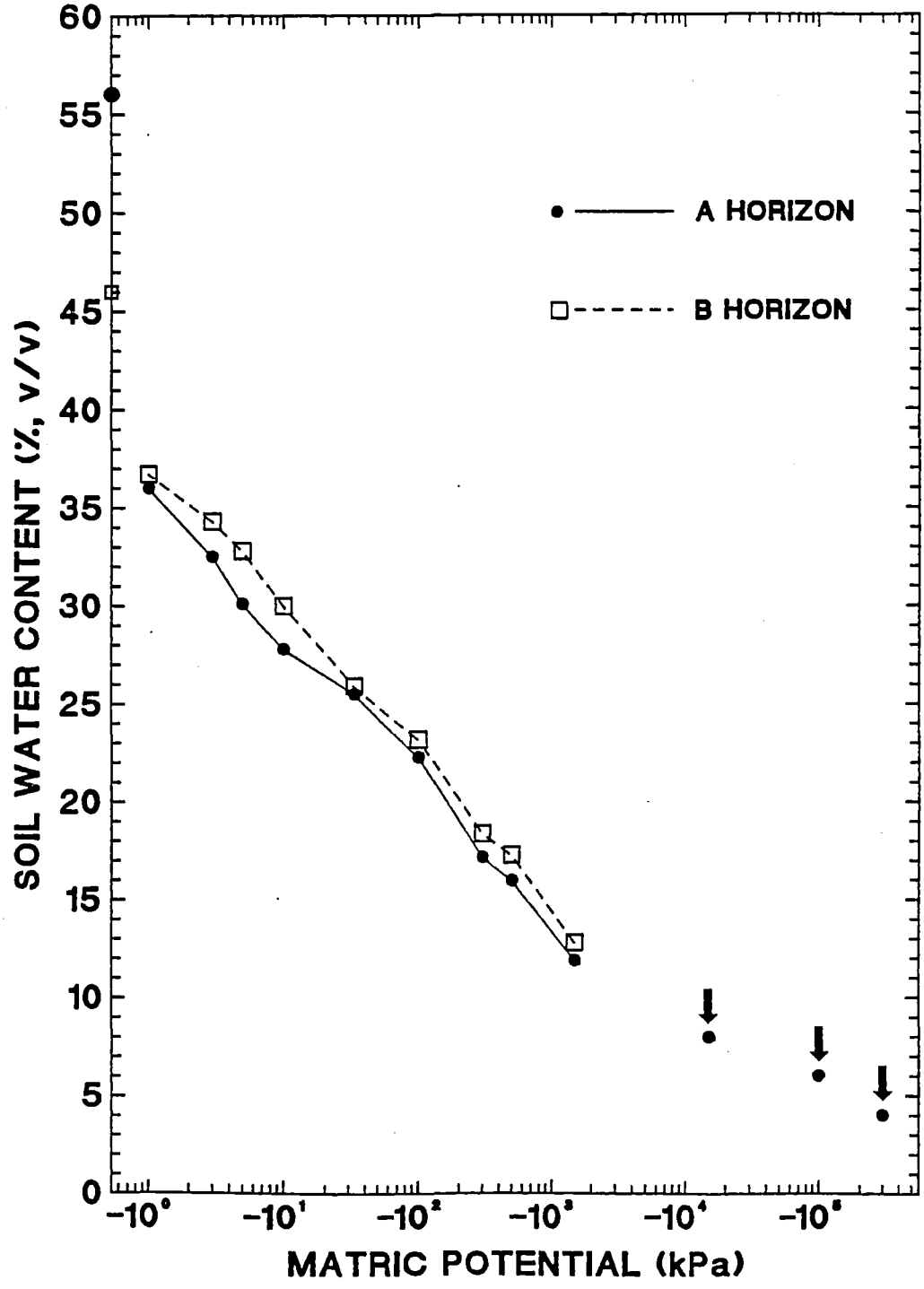

Table 7.1 Soil system geometry and initial values for the two simulations.

SOIL LAYER NUMBER	LAYER THICK-NESS m	INITIAL VALUES			
		JULIAN DAY 74#		JULIAN DAY 89#	
		WATER CONTENT m^3m^{-3}	TEMP ^oC	WATER CONTENT m^3m^{-3}	TEMP ^oC
1	0.01	0.205	22.0	0.230	7.1
2	0.01	0.205	20.6	0.230	7.5
3	0.01	0.261	19.9	0.227	7.9
4	0.01	0.261	19.4	0.227	8.5
5	0.02	0.276	18.6	0.232	9.4
6	0.02	0.282	18.1	0.225	10.0
7	0.02	0.282	17.6	0.225	10.7
8	0.02	0.277	17.3	0.212	11.3
9	0.03	0.277	17.1	0.212	12.0
10	0.05	0.279	16.8	0.210*	13.1
11	0.05	0.260	16.6	0.210*	13.8
12	0.05	0.245	16.6	0.210*	13.8
13	0.05	0.230	16.6	0.210*	13.8
14	0.05	0.230	16.6	0.210*	13.8

\# Initialisation on julian day 74 was at 1200 hours.
Initialisation on julian day 89 was at 0800 hours.

* Estimated values.

7.3 Results and discussion

7.3.1 A preliminary investigation

7.3.1.1 CONSERVB model calibration phase.

The CONSERVB model was initialised as at julian day 74 as previously described and run for the duration of the first drying cycle. The resulting cumulative evaporation predictions, together with measured values, are presented in Table 7.4. The predicted

cumulative evaporation was more than 4 mm above the measured value by julian day 86. It was apparent therefore, that the CONSERVB model was not accurately simulating the soil water and energy balances when used with the previously specified initialisation values and inputs. The model inputs were subsequently re-examined. For reasons that were discussed previously (Section 5.4), the hydraulic conductivity-water content relation was regarded as being only an approximation and, in the absence of experimental measurements, its accuracy could not be confirmed. For subsequent evaluation of the CONSERVB model the 'A' horizon $K(\theta_v)$ function was adjusted in such a way that model predictions for the first drying cycle matched the measured real-system behaviour as best they could.

Table 7.2 Parameters used in the initialisation of CONSERVB for the two simulations.

PARAMETER	VALUE
ROUGHNESS COEFFICIENT (z_0)	2.32 mm
MEAN TOTAL POROSITY - A horizon - B horizon	 0.56 m^3m^{-3} 0.46 m^3m^{-3}
SATURATED HYDRAULIC CONDUCTIVITY ('A' horizon)	$6.0x10^{-4}$ $m\,s^{-1}$
SOIL THERMAL CONDUCTIVITY (solid constituents only)	4.47 $Wm^{-1}K^{-1}$
VOLUMETRIC HEAT CAPACITY OF DRY SOIL	$1.02x10^6$ $Jm^{-3}{}^oC^{-1}$

The calibration of the CONSERVB model using the $K(\theta_v)$ function was achieved simply by a trial and error process. If, when using the 'modified' $K(\theta_v)$ function, the model predictions provided a good description of real-system behaviour for both drying cycles then the model could be considered to be giving a valid solution. The 'B' horizon $K(\theta_v)$ function was left unchanged from the original Jackson (1972) estimation. This

estimation could reasonably be expected to be more accurate in the 'B' horizon than the 'A' horizon because of the smaller macro-pore volume, and probable greater uniformity of pore geometry.

Figure 7.4 Generalised shortwave albedo-soil water content input function.

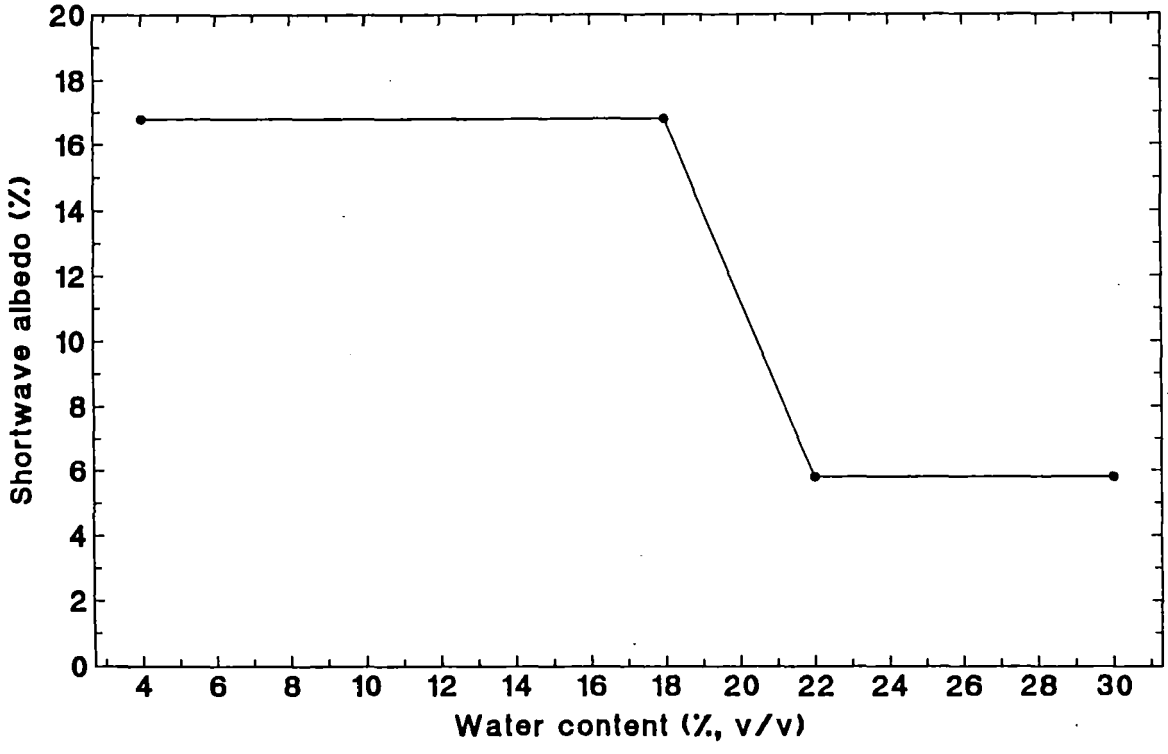

To evaluate the sensitivity of the CONSERVB model to changes in the $K(\theta_v)$ function a log-linear regression function was fitted to the data points previously calculated using the procedure of Jackson (1972). The regression function was:

$$K = \exp\ (0.688\ \theta_v - 37.7) \qquad \ldots\ (7.1)$$

$$r^2 = 99.6\%$$

where K is hydraulic conductivity (m s^{-1}) and θ_v is water content ($m^3\ m^{-3}$). The log-linear regression function (denoted 'i') and the data points estimated using the Jackson procedure are shown in Figure 7.1. The CONSERVB model was run for the

first drying cycle initialised with the data points (the model interpolates linearly between these) and with the regression function. The results (Table 7.4) show an increase in cumulative evaporation of 2.5 mm from using the linear regression function. The high r^2 value of the regression shows the regression function and the Jackson estimations to be very similar and hence the CONSERVB model appears very sensitive to the $K(\theta_V)$ input function.

A log-linear function between the measured hydraulic conductivity at 40% θ_V (3.00×10^{-5} m s^{-1}) and a value of 3.0×10^{-17} m s^{-1} at 4% θ_V was substituted into the CONSERVB model for evaluation (function iii, Figure 7.1). The results (Table 7.4) show a 10 mm decrease in cumulative evaporation during the first drying cycle as compared to the results using the $K(\theta_V)$ function estimated using the Jackson procedure. This result further emphasises the sensitivity of the CONSERVB model evaporation predictions to the $K(\theta_V)$ input function.

The log-linear $K(\theta)$ function shown as 'ii' in Figure 7.1 was identified as a function with which the CONSERVB model gave good estimates of evaporation (Table 7.4) (refer to Section 7.3.2). As with the other $K(\theta_V)$ functions considered, the measured hydraulic conductivity at 40% θ_V remained unchanged as a part of the function. A log-linear function might provide a better approximation of the actual $K(\theta_V)$ function at θ_V values greater than 12% than at lower values. To investigate this aspect further the CONSERVB model was again run for the first drying cycle this time with a $K(\theta_V)$ function identical to function 'ii' in Figure 7.1 at θ_V values of 12% and greater, but with a hydraulic conductivity value at 4% θ_V reduced to 3.0×10^{-17} (from 1.55×10^{-16} in the 'ii' function). This change had no effect on either the daily or cumulative evaporation predictions from CONSERVB. The log-linear 'ii' function in Figure 7.1 will be used as the 'A' horizon $K(\theta_V)$ function in the CONSERVB model for the subsequent model evaluation stages.

The extreme sensitivity of the CONSERVB model to the $K(\theta_V)$ input function in predicting evaporation is expected. During the field drying cycle the soil surface quickly becomes dry and thereafter the rate of evaporation is determined by the rate that water can be transported through the soil profile to the sites of evaporation. This rate of water transport is directly influenced by the soil hydraulic conductivity.

Table 7.3 Average daily meteorological input for the two simulation periods.

JULIAN DAY (1989)	DAILY TOTAL SOLAR RADIATION MJ m^{-2}	MEAN WIND-SPEED m s^{-1}	AIR TEMPERATURE °C			DEW POINT TEMP °C		
			MIN	MAX	AVER	MIN	MAX	AVER
RUN I								
74	20.0	6.05	12.9	25.9	17.6	4.5	12.3	8.1
75	20.5	7.98	10.3	24.3	17.1	-5.4	8.4	0.2
76	14.8	4.25	4.7	14.8	10.2	-3.5	3.0	-0.1
77	20.2	4.57	4.2	22.6	12.8	0.2	8.8	5.1
78	20.0	6.02	11.4	22.6	17.0	-0.8	9.2	4.9
79	6.7	6.31	10.5	17.4	12.9	-0.3	7.0	4.0
80	18.4	4.66	4.4	14.8	10.1	-0.9	2.4	0.8
81	13.4	3.43	3.9	17.7	11.1	0.8	8.9	5.7
82	12.0	5.30	10.5	19.6	14.7	7.6	12.0	9.9
83	18.3	6.42	10.7	27.5	18.6	7.8	12.9	11.5
84	16.7	5.15	9.5	23.6	14.8	3.4	9.6	7.7
85	18.3	4.65	8.7	21.6	13.7	3.3	9.6	7.2
86	18.3	4.10	3.7	22.9	12.6	1.5	10.7	6.3
RUN II								
89	17.3	4.59	7.6	23.2	13.3	4.4	9.5	7.0
90	14.1	3.75	10.4	18.0	13.0	6.7	10.3	8.6
91	16.7	4.73	8.5	21.4	13.3	6.0	12.3	8.7
92	16.7	3.48	4.8	17.0	11.1	2.7	10.1	7.0
93	15.6	3.44	5.7	17.7	11.7	3.1	10.0	7.3
94	16.5	2.85	7.7	19.8	13.2	4.3	11.0	7.8
95	16.5	4.09	3.3	19.8	11.1	0.8	10.9	6.8
96	13.9	3.48	9.8	18.6	12.9	8.0	9.8	8.7
97	15.9	6.43	10.1	20.6	14.6	7.9	12.7	10.2
98	6.5	3.78	7.7	15.9	12.4	6.0	12.0	9.7
99	13.0	3.75	7.1	15.0	11.4	0.2	6.8	4.4

Table 7.4 The effect of unsaturated hydraulic conductivity on simulated evaporation.

JULIAN DAY NUMBER	EVAPORATION RATE (mm d^{-1})					
	MEASURED		SIMULATED			
				$K(\theta_V)$ FUNCTION*		
	AVER.	STD DEV	JACKSON	i	ii	iii
74	6.3	0.7	7.0	7.0	6.7	5.8
75	3.5	0.8	4.7	5.8	3.0	1.7
76	1.3	0.3	1.9	2.0	1.2	0.9
77	1.0	0.4	1.9	1.9	1.3	0.7
78	1.5	0.6	2.3	2.6	1.8	1.4
79	1.0	0.2	1.0	1.1	0.8	0.5
80	1.1	0.2	0.9	1.0	0.6	0.5
81	0.1	0.2	0.7	0.7	0.5	0.3
82	1.4	0.1	1.6	1.7	1.5	1.3
83	0.7	0.2	0.9	0.9	0.6	0.5
84	1.3	0.3	0.7	0.9	0.6	0.4
85	0.2	0.1	0.6	0.9	0.4	0.4
86	0.6	0.1	0.6	0.8	0.5	0.4
TOTAL	20.0		24.8	27.3	19.5	14.8

* The hydraulic conductivity-volumetric water content ($K(\theta_V)$) functions referred to as JACKSON, i, ii and iii are described as follows:

JACKSON. Data points estimated using procedure of Jackson (1972) with the exception of K at 4% θ_V which was estimated from log-linear regression.

i. Log-linear regression line through the data points estimated from the Jackson (1972) procedure.

ii. Straight line (log-linear) between measured K value of 3.00×10^{-5} at 40% θ_V and K value of 1.55×10^{-16} at 4% θ_V.

iii. Straight line (log-linear) between measured K value of 3.00×10^{-5} at 40% θ_V and K value of 3.0×10^{-17} at 4% θ_V.

Refer to Figure 7.1 for graphical presentation of the $K(\theta_V)$ functions described here.

7.3.1.2 The effect of surface soil layer thickness on simulated evaporation

The effect of changing surface soil layer thickness on simulated evaporation was investigated following the previously reported sensitivity of the model to this parameter (Lascano and van Bavel, 1986) (refer Section 6.4.5.3). The results (Table 7.5) are consistent with those of Lascano and van Bavel (1986) in that they show greater cumulative evaporation with increased surface soil layer thickness. The greatest increases in evaporation occurred in the early weather-controlled and falling-rate stages. This behaviour follows the assumption that evaporation of the water within the surface layer occurs at a rate controlled by atmospheric demand, without any water movement required from the layer below. The rate of water movement within the soil restricts the amount of water moving into the surface layer from lower layers, but at initialisation the volume of water immediately available for evaporation depends on the initial water content of the surface layer and the size of the surface layer. Increased evaporation in the weather-controlled phase, from increased surface soil layer thickness, would not occur if the simulated initial evaporation phase was truly weather-controlled.

In this study a surface soil layer of 0.01 m gave the best results (Table 7.5). Thinner surface layers require that model iteration time interval be reduced, with a subsequently greater computer time requirement, in order to avoid regular oscillations in model output which sometimes occur. Thinner surface layers might also be less realistic because soil surface roughness variation would be equivalent to a large part of the surface soil layer. Attempts to run the model initialised for day 74 with a surface layer of 0.02 m failed. The 0.02 m layer appears to increase the difficulty that the model has in finding a stable solution when initialised at 1200 hours. This difficulty arises because at this time the soil energy balance is rapidly changing and a stable, iterative surface soil temperature solution is more difficult. Initialisation at another time when the soil energy balance is not changing so rapidly (e.g. midnight) partially alleviates the problem, but at that time, soil water contents for initialisation would have to be estimated.

Table 7.5 The effect of surface soil layer thickness on simulated evaporation.

JULIAN DAY NUMBER	EVAPORATION RATE (mm d^{-1})				
	MEASURED		SIMULATED		
	AVER.	STD DEV	THICKNESS OF SURFACE LAYER (m) 0.005	0.01	0.02
74	6.3	0.7	6.4	6.7	-
75	3.5	0.8	2.9	3.0	
76	1.3	0.3	1.4	1.2	
77	1.0	0.4	1.2	1.3	
78	1.5	0.6	1.8	1.8	
79	1.0	0.2	0.7	0.8	
80	1.1	0.2	0.7	0.6	
81	0.1	0.2	0.4	0.5	
82	1.4	0.1	1.4	1.5	
83	0.7	0.2	0.7	0.6	
84	1.3	0.3	0.6	0.6	
85	0.2	0.1	0.5	0.4	
86	0.6	0.1	0.6	0.5	
TOTAL	20.0		19.3	19.5	
89	3.5	0.2	3.5	4.0	4.5
90	0.9	0.3	1.3	1.2	1.8
91	1.1	0.2	0.9	0.8	0.8
92	0.8	0.1	0.7	0.7	0.6
93	0.6	0.1	0.5	0.6	0.5
94	0.7	0.2	0.6	0.5	0.6
95	0.5	0.2	0.3	0.3	0.4
96	0.5	0.1	0.5	0.4	0.4
97	0.4	0.1	0.2	0.3	0.2
98	0.1	0.1	0.3	0.3	0.3
99	0.7	0.1	0.5	0.4	0.4
TOTAL	9.8		9.3	9.5	10.5

* see text for explanation of missing values.

Figure 7.5 Measured and simulated daily evaporation (error bars indicate ± one standard deviation).

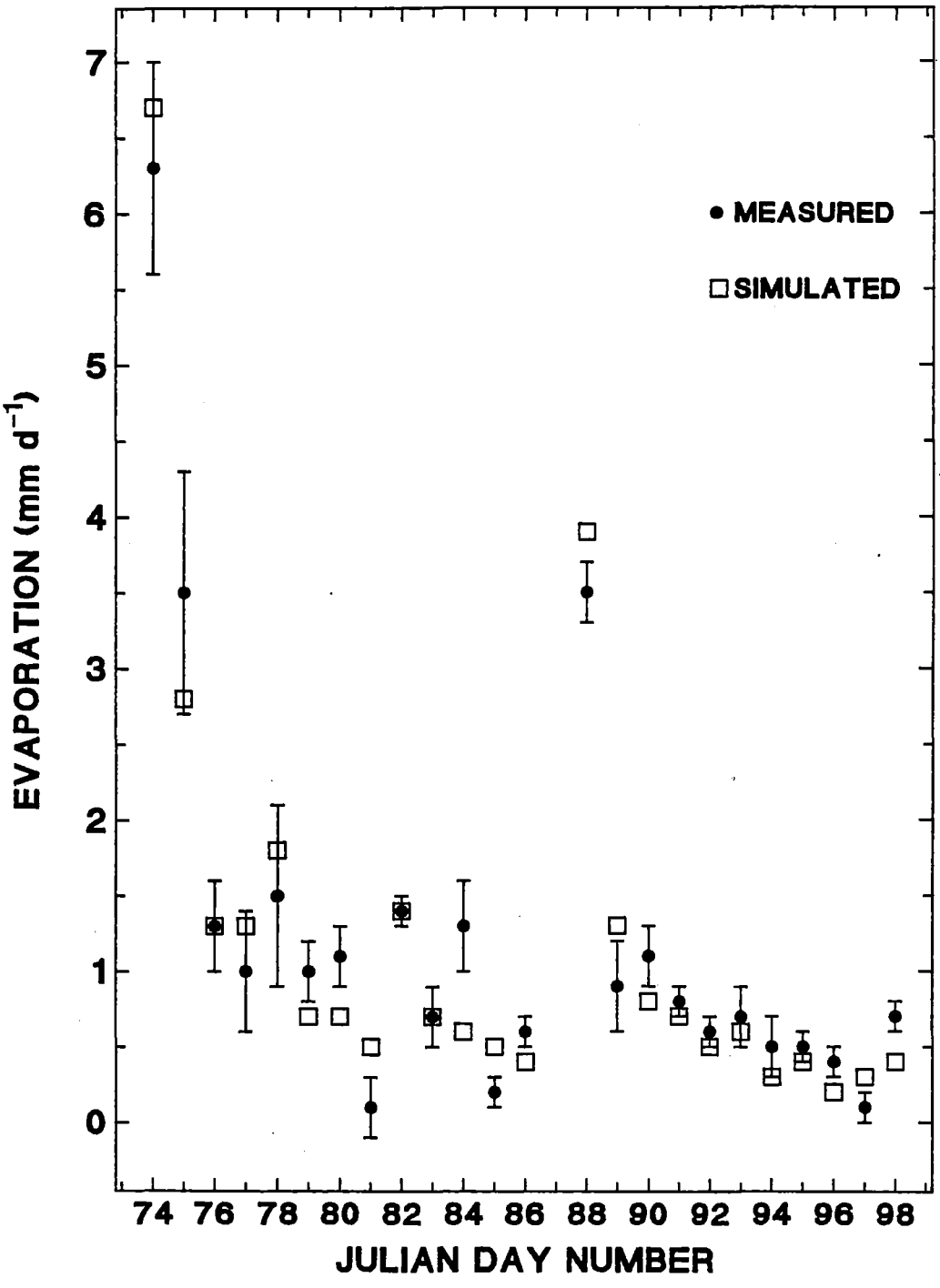

Figure 7.6 Measured and simulated cumulative evaporation.

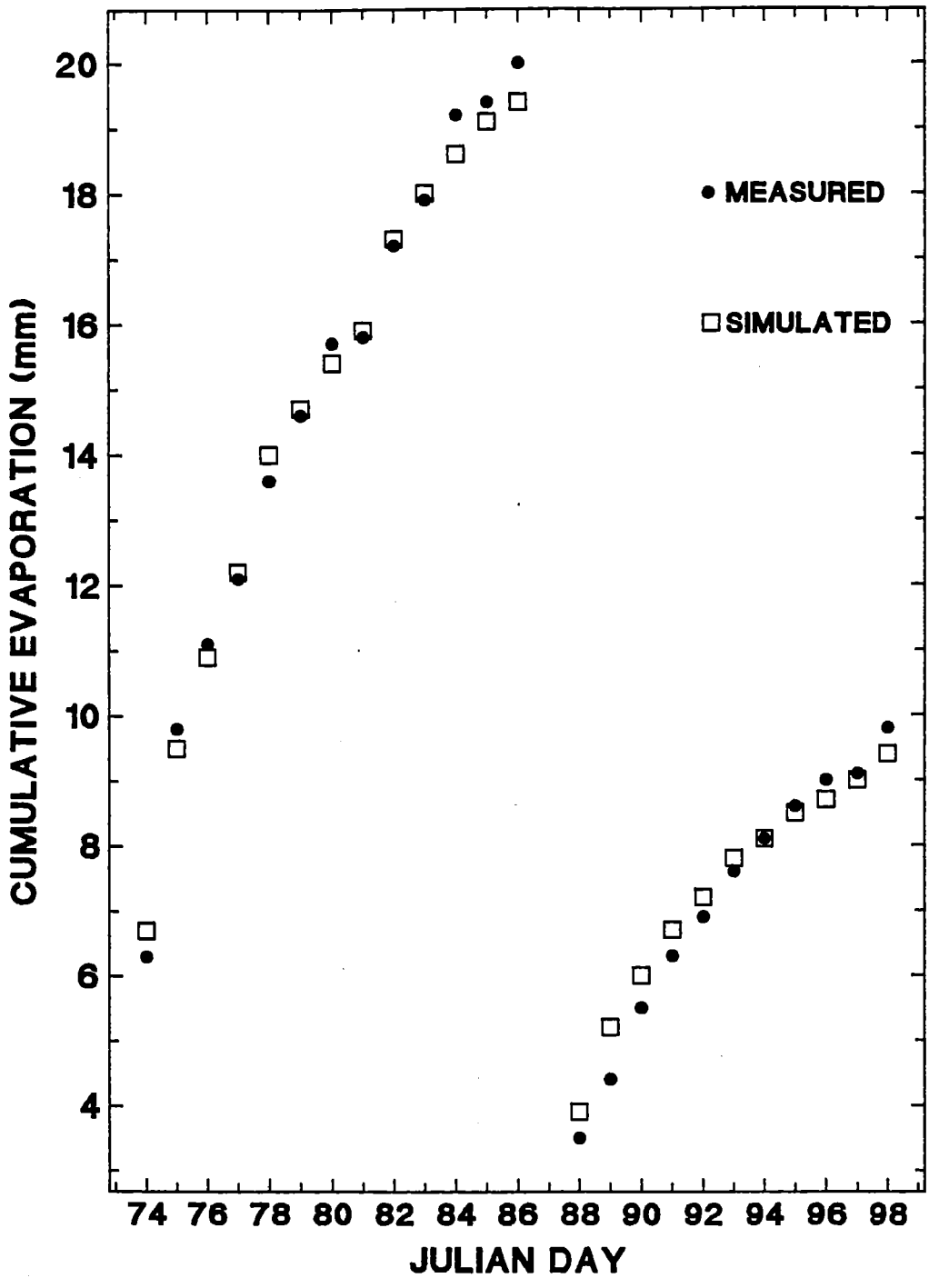

7.3.2 A comparison between measured and simulated evaporation

Measured and simulated daily evaporation for the two drying cycles is presented in Figure 7.5. Cumulative evaporation is plotted in Figure 7.6. In each drying cycle daily evaporation decreased rapidly as the soil surface dried. A maximum measured value of 6.3 mm d^{-1} occurred on julian day 74. The larger variation in each daily evaporation measurement for the first five days, as compared to the remainder of the experimental period, is probably due to non-uniformity of irrigation water application.

Simulated daily evaporation rates agreed well with the average measured values for both drying cycles (Figure 7.5). On day 84 simulated evaporation was 0.7 mm less than the measured value, this represented the largest discrepancy in evaporation during the experimental period. All simulated values, with the exceptions of days 80, 84, 89 and 99, were within two standard deviations of the measured daily evaporation. On most days the standard deviation of the measured values represented small amounts of evaporation in absolute terms. This is confirmed by the excellent comparison between measured and simulated cumulative evaporation. After completion of the first and second drying cycles simulated cumulative evaporation was 0.5 mm and 0.3 mm lower than the measured cumulative value.

7.3.3 An evaluation of the simulated soil surface energy balance.

A comparison of measured and simulated surface soil temperature gives a good indication of the accuracy of the simulated soil surface energy balance. Measured and simulated soil surface temperatures for both drying cycles were compared by regression analysis as shown in Table 7.6. All measured and simulated data (hourly measurements) for each complete drying cycle were included in the analysis. The simulated output represents the surface soil temperature exactly at the corresponding time, whereas the measured temperature corresponding to that time is an average over a one hour period extending from 30 minutes before to 30 minutes after the time. This comparison is a valid one because the model uses linear interpolation between the

hourly meteorological data inputs. It could therefore be expected that the simulated instantaneous result on the half-hour corresponds to a measured hourly average value.

Table 7.6 Regression analysis of measured and simulated surface soil temperature and net radiation for the two simulation periods.

VARIABLE*	REGRESSION	r^2 (%)	NUMBER OF OBSERVATIONS
NET RADIATION			
- 1st DRYING CYCLE	Y = 1.119X - 8.54	99.1	309
- 2nd DRYING CYCLE	Y = 1.166X - 12.0	98.9	265
SURFACE SOIL TEMPERATURE			
- 1st DRYING CYCLE	Y = 1.149X - 1.42	96.4	309
- 2nd DRYING CYCLE	Y = 1.174X - 2.19	96.1	265

* The Y variable in the regression equations is the simulated variable and the X variable is the measured variable. Surface soil temperature has units of ^{o}C, and net radiation has units of W m^{-2}.

During the first drying cycle, within a temperature range of 0 to 16 ^{o}C, simulated surface soil temperature was within 1.0 ^{o}C of the measured values. Between 16 and 22 ^{o}C, simulated surface soil temperature was within 2.0 ^{o}C of the measured values. At surface soil temperatures greater than 22 ^{o}C simulated values are in excess of 2.0 ^{o}C higher than measured values. During the second drying cycle, the discrepancy between measured and simulated surface soil temperature was less than 1.0 ^{o}C in the measured range of 7 to 18 ^{o}C, and between 1.0 and 2.0 ^{o}C in the measured ranges 2 to 7 and 18 to 24 ^{o}C. As in the first cycle, at high temperatures the simulated values exceed the measured values by more than 2.0 ^{o}C. The soil surface energy balance solution as simulated by CONSERVB thus appears satisfactory.

Figure 7.7a Simulated energy flux partitioning over a moist soil surface

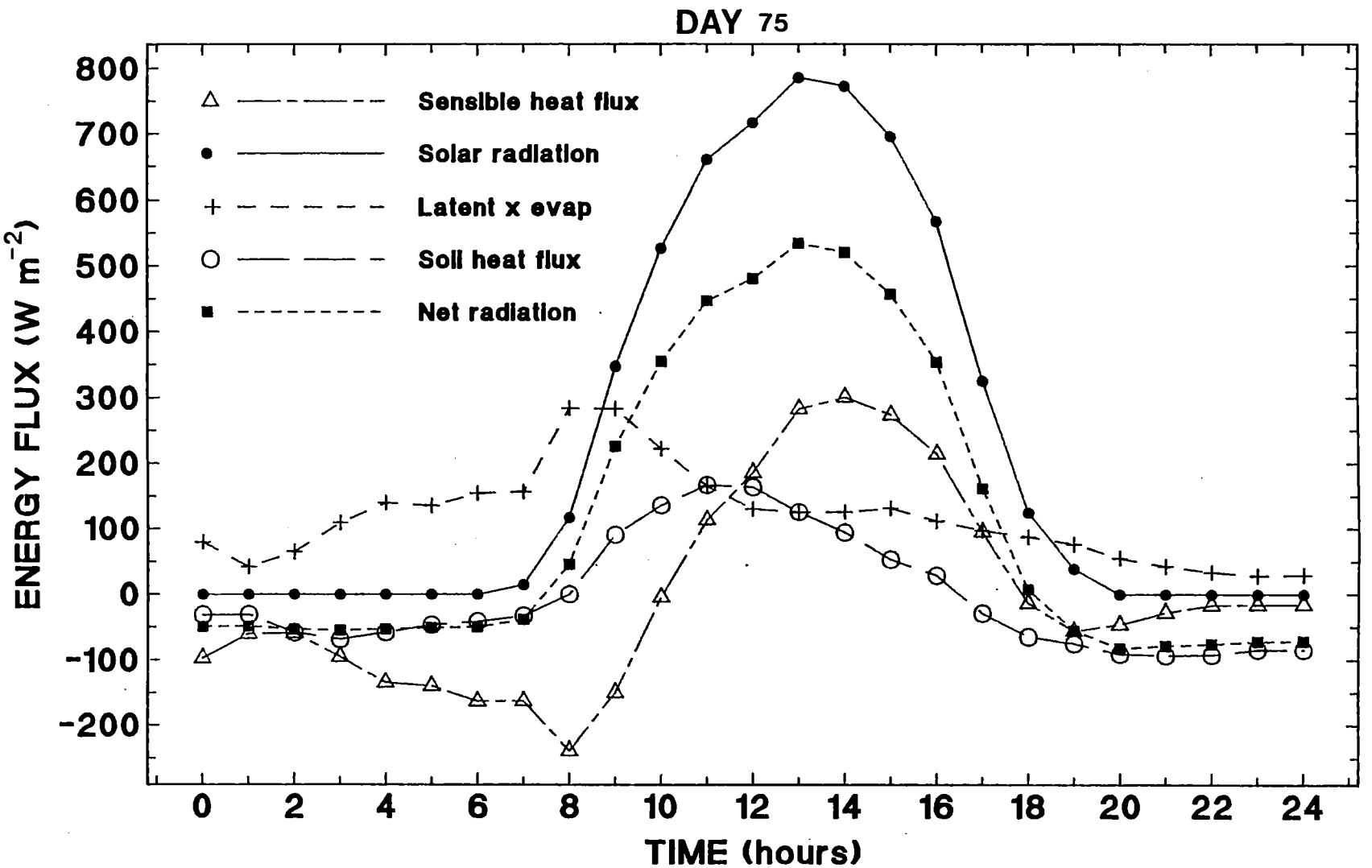

Figure 7.7b Simulated energy flux partitioning over a dry soil surface

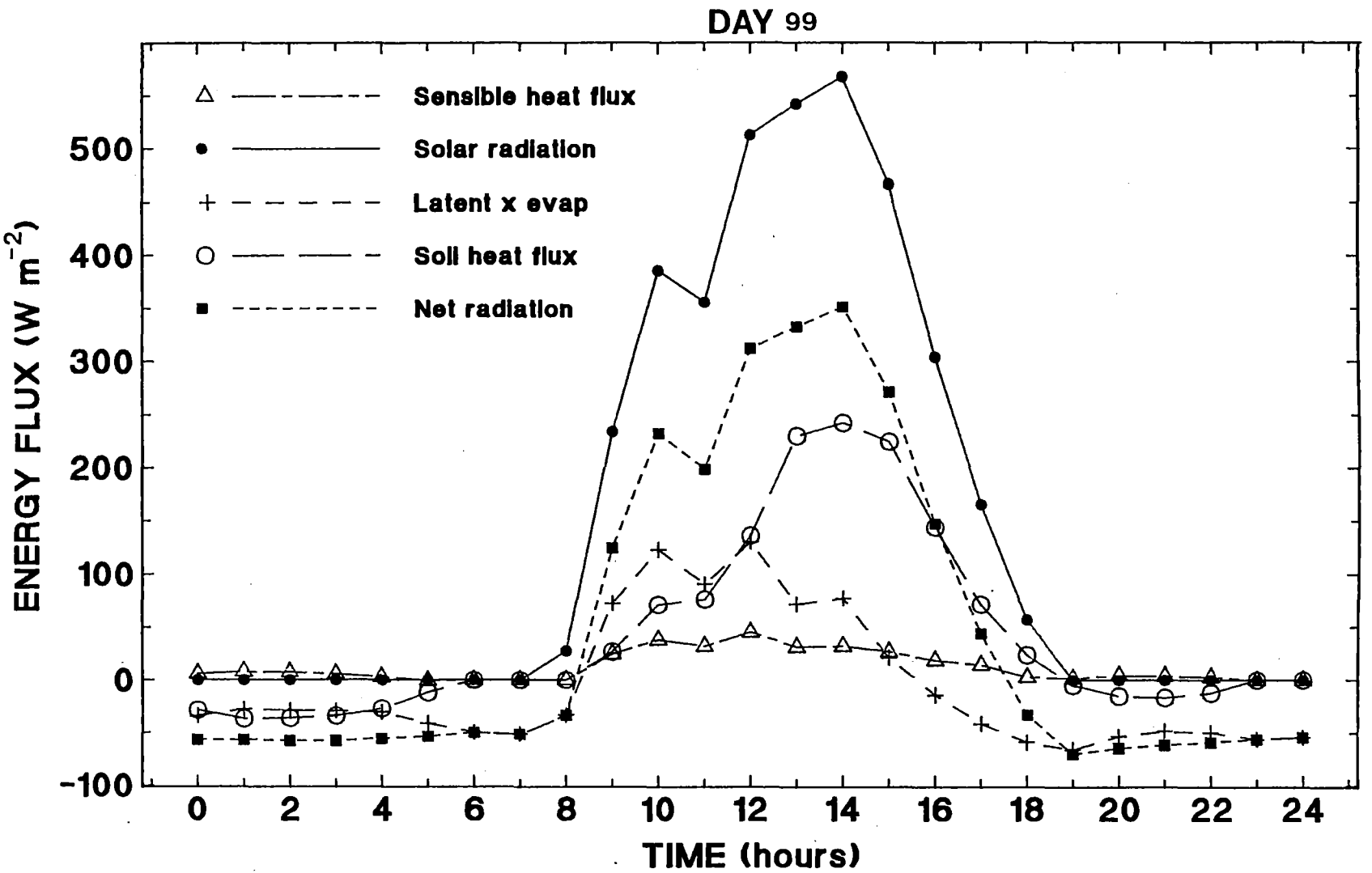

Figure 7.8a Time course of measured and simulated surface soil temperature.

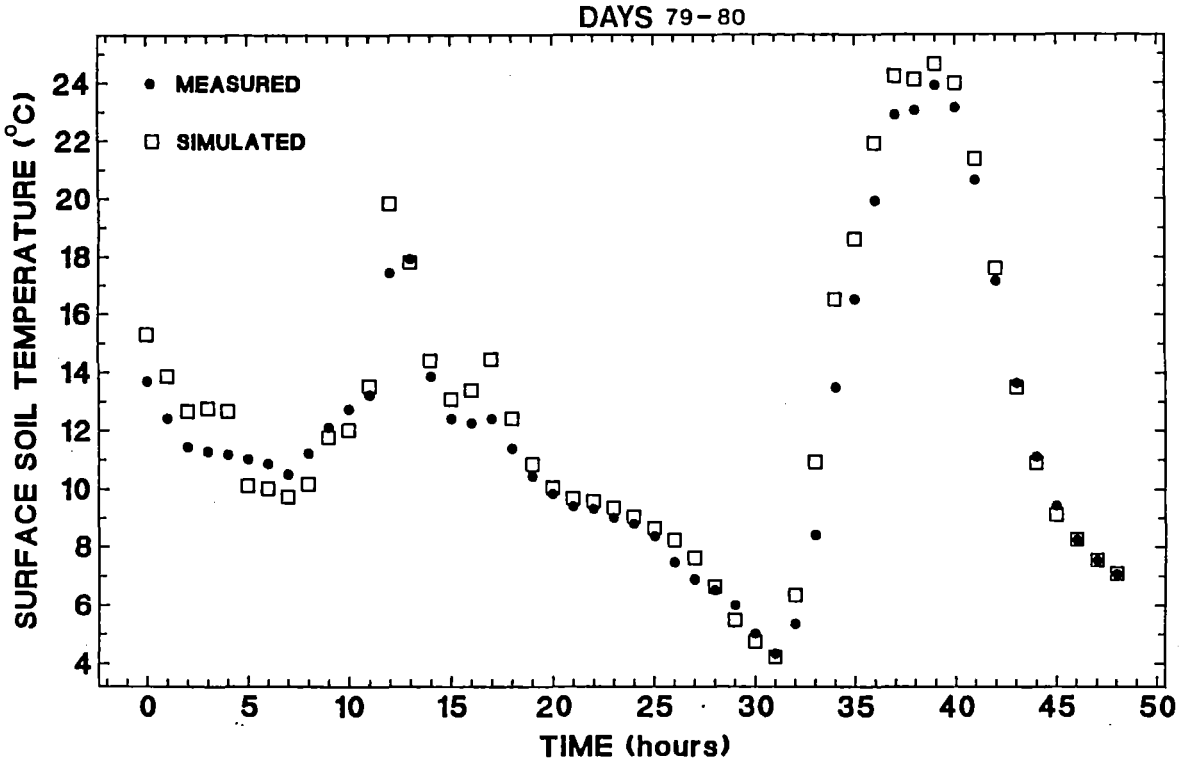

Figure 7.8b

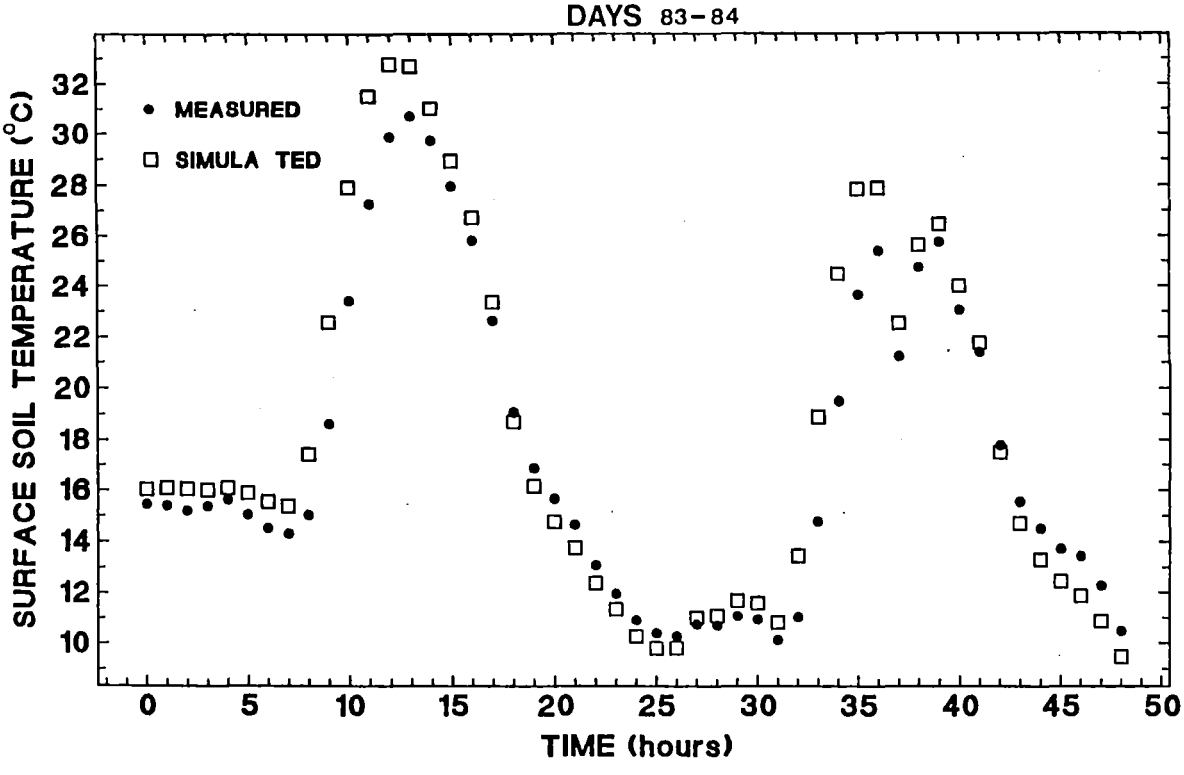

Figure 7.8c

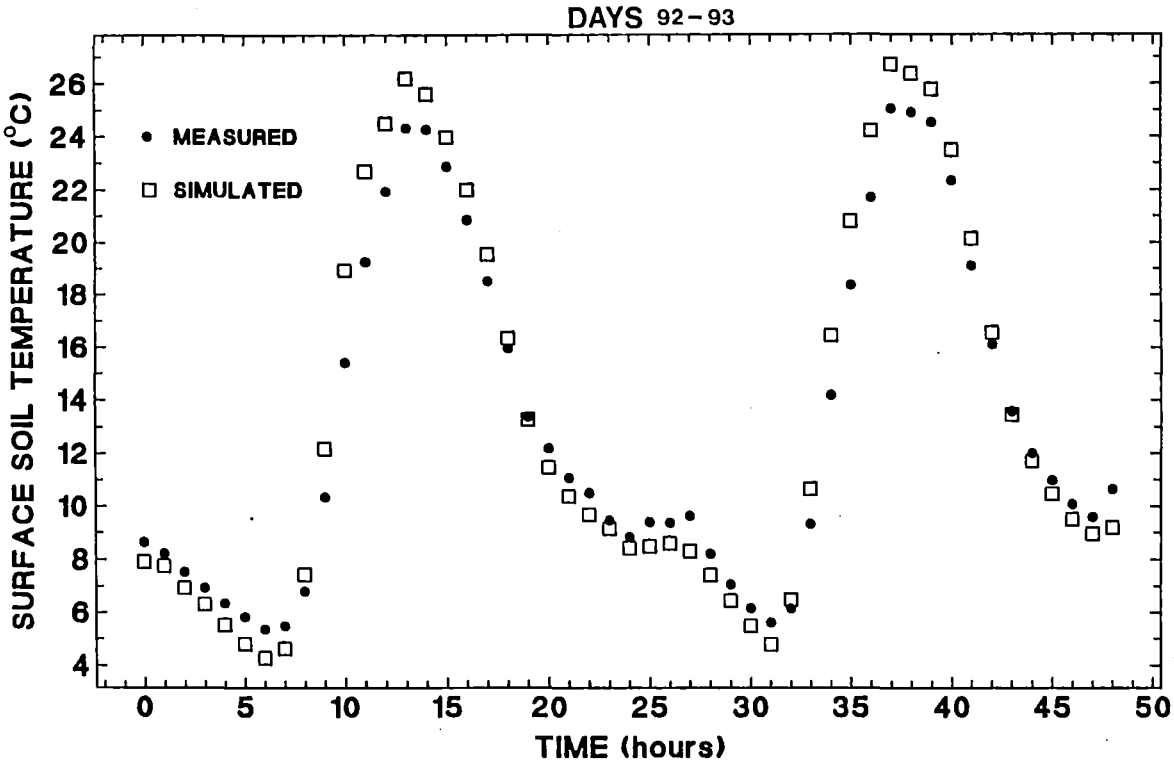

Figure 7.8d

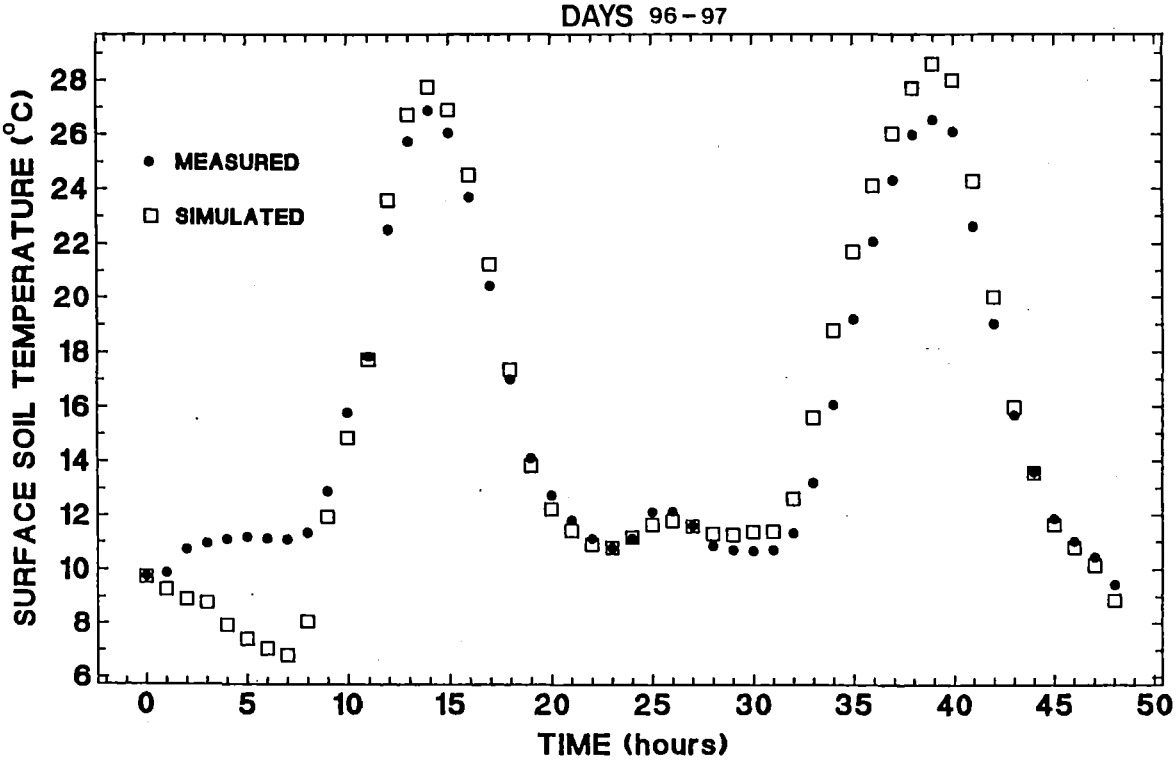

A comparison of measured and simulated net radiation (Table 7.6) supports this conclusion. Simulated values are instantaneous, while measured values are hourly averages. During the first drying cycle, where measured net radiation was in the range up to 400 W m^{-2}, the simulated net radiation was within 40 W m^{-2} of the measured value. For all measured values above 400 W m^{-2} the discrepancy was within 55 W m^{-2}. Daytime simulated net radiation tended to be higher than the measured values. A similar comparison occurs in the second drying cycle where simulated net radiation was within 40 W m^{-2} of the measured value in the measured range up to 300 W m^{-2} and was within 70 W m^{-2} in the 300 to 490 W m^{-2} range.

The simulated intra-diurnal variations of the energy balance components over a soil with a moist surface (julian day 75) and a soil with a very dry surface (julian day 99) are shown in Figures 7.7 (a) and (b). The availability of water generally determines the partitioning of energy among sensible, latent and soil heat fluxes (Rosenberg et al., 1983). When a soil is wet a greater proportion of the energy supplied as net radiation is consumed as latent heat while smaller quantities of energy are partitioned into soil and sensible heat flux. As the soil dries the consumption of net radiation as latent heat is reduced and a greater proportion is partitioned as sensible heat. This process has been observed by Fritschen and van Bavel (1962). The simulated energy partitioning appears consistent with field observation of the process. Figure 7.7 (a) shows a higher proportion of net radiation partitioned into latent flux while the soil is moist early in the day. As the soil surface dries the sensible heat flux increases. The very small latent heat component where the soil is very dry is illustrated by Figure 7.7 (b). Here most of the energy is partitioned into sensible and soil heat fluxes.

A comparison of the time-course of measured and simulated surface soil temperature gives further insight into model performance. Figures 7.8 (a), (b), (c), and (d) show the time-course of measured and simulated surface soil temperatures for some different days during both drying cycles. These results give a representative sample of the results obtained showing both intermediate and final stages of the two drying cycles. The simulated surface temperatures closely follow the measured values most of the time with the greatest discrepancies usually occurring during the period of soil warming during the morning and near the middle of the day where temperatures reach their maximum values. The simulated increase in surface soil temperature during the morning would appear to be occurring 20 to 30 minutes ahead of the measured

increase. The model appears to be most accurate during cooler conditions with evidence of a slight imbalance in warmer conditions.

7.3.4 A comparison of measured and simulated soil water and temperature profiles.

To give a comparison of measured and simulated soil water profiles a representative sample of the results obtained for each drying cycle are presented in Figure 7.9. The simulated soil water profile matches the measured profile very well at soil depths greater than 3 cm in most cases. At the very surface of the soil the simulated soil water contents tend to be lower than the measured values. In the top 2 cm of soil the difference between measured and simulated water content is generally within 4% v/v. When viewing these results, the difficulty of sampling to a precise depth in the surface layer of a tilled soil and the non-homogeneous nature of this soil should be considered.

Simulated soil temperature profiles are compared to the measured profiles in Figure 7.10. The results presented are representative of the intermediate and final stages of each drying cycle. They show that the simulated soil profiles become warmer than the measured ones near the middle of the day reflecting the high simulated soil surface temperatures. As the hottest part of the day passes and the soil profile cools, the discrepancy between simulated and measured values is reduced, with the simulated values becoming representative of the measured values. Near midday, simulated soil temperatures can become as much as 4 ^{o}C higher than the measured values. For most of the day however, simulated soil temperatures are within 2-3 ^{o}C of the measured values. The greatest discrepancies in soil temperature usually occur near the surface of the soil profile. The reasons for the apparent imbalance in soil surface temperature prediction in warm conditions are not evident.

Figure 7.9a Measured and simulated soil water profiles (error bars indicate ± one standard deviation). (0900 hrs)

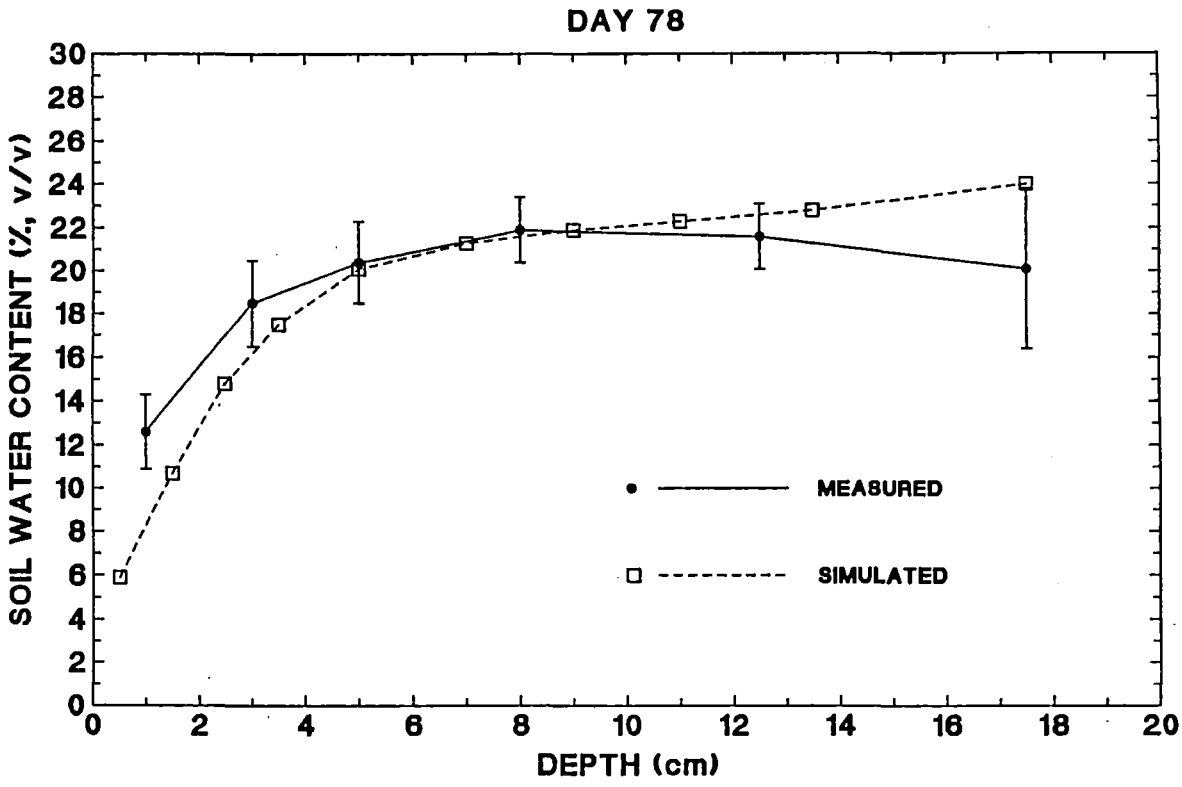

Figure 7.9b

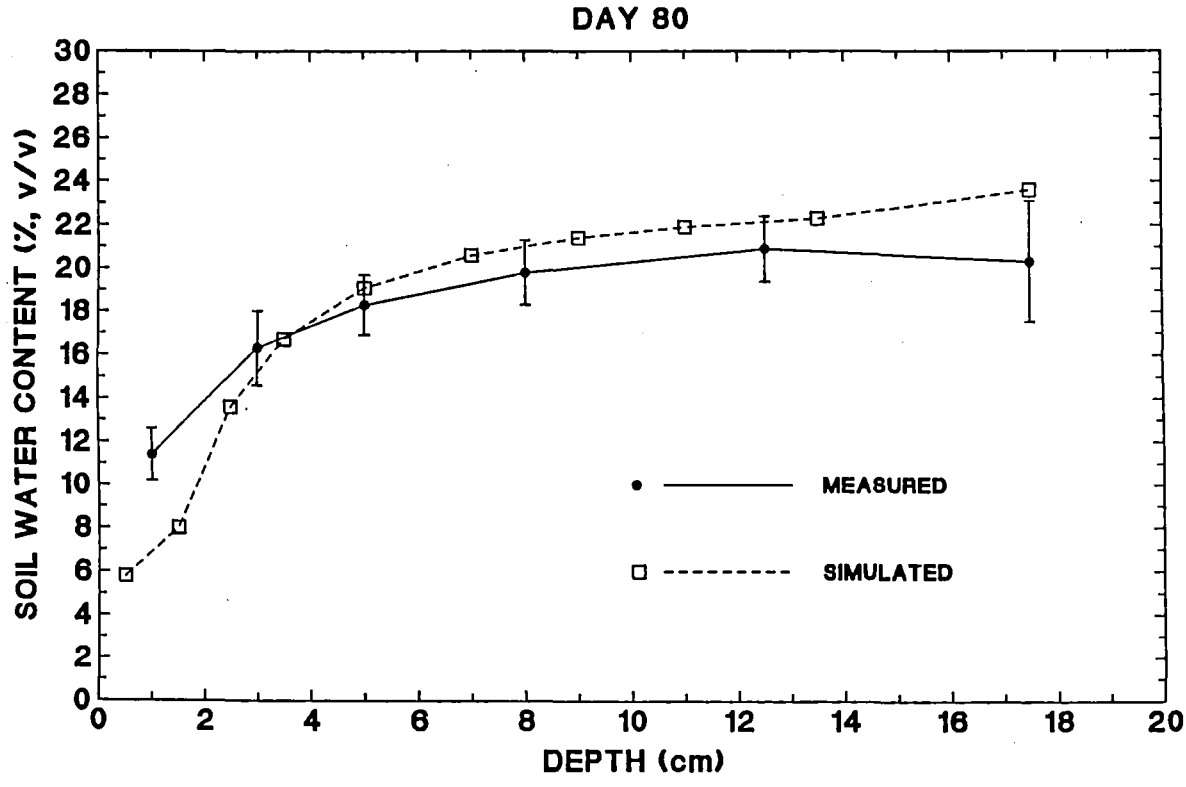

Figure 7.9c

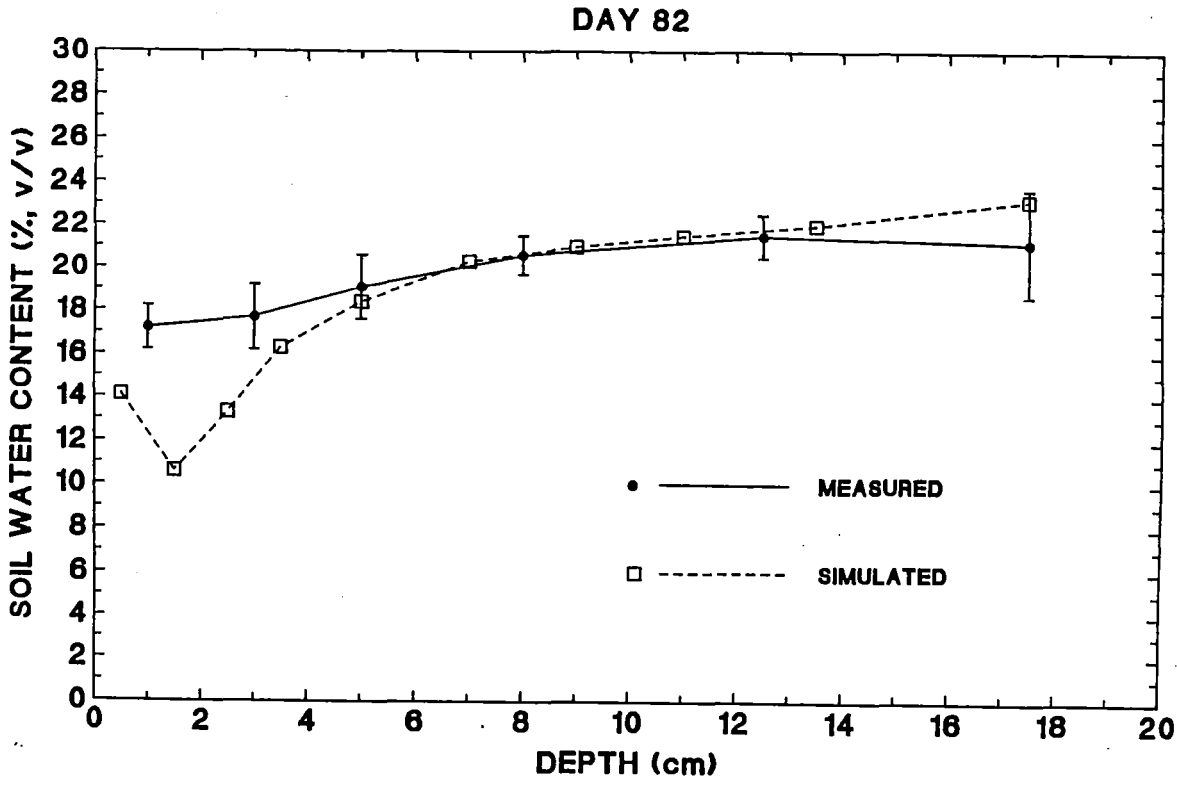

Figure 7.9d

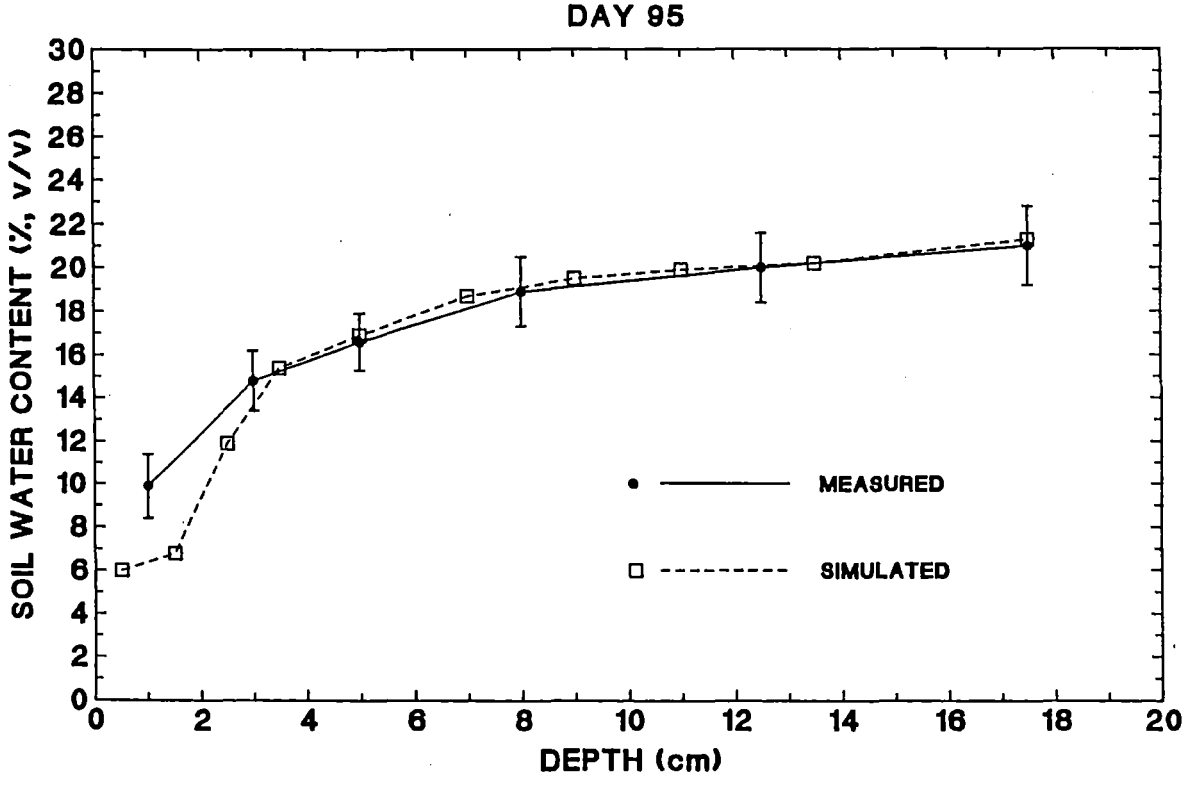

Figure 7.9e

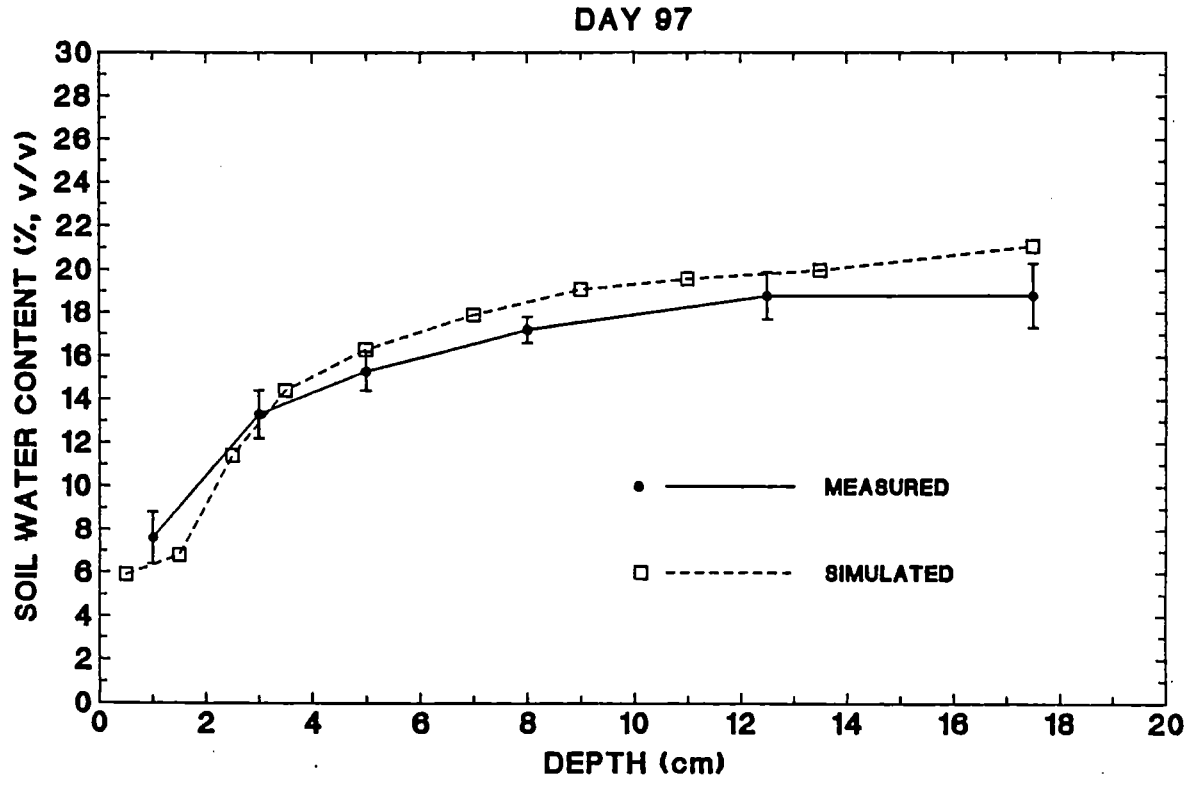

Figure 7.9f

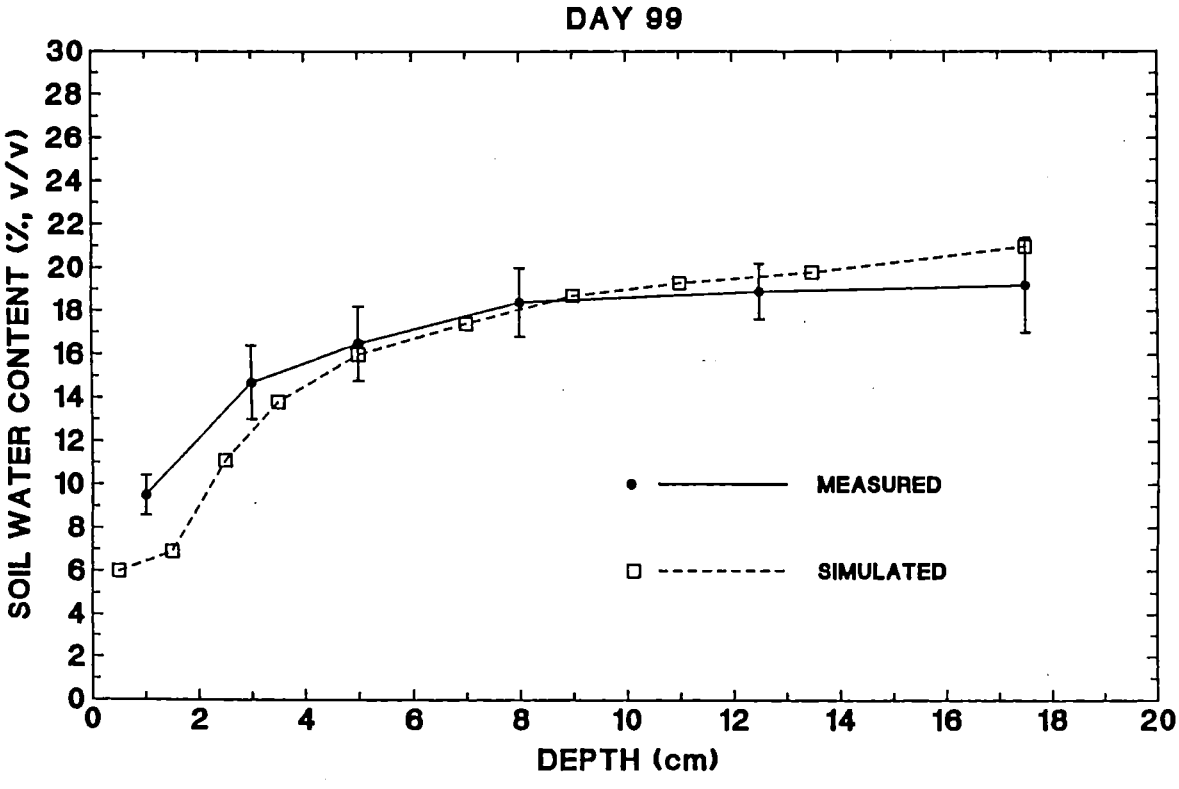

Figure 7.10a Measured and simulated soil temperature profiles (error bars indicate ± one standard deviation).

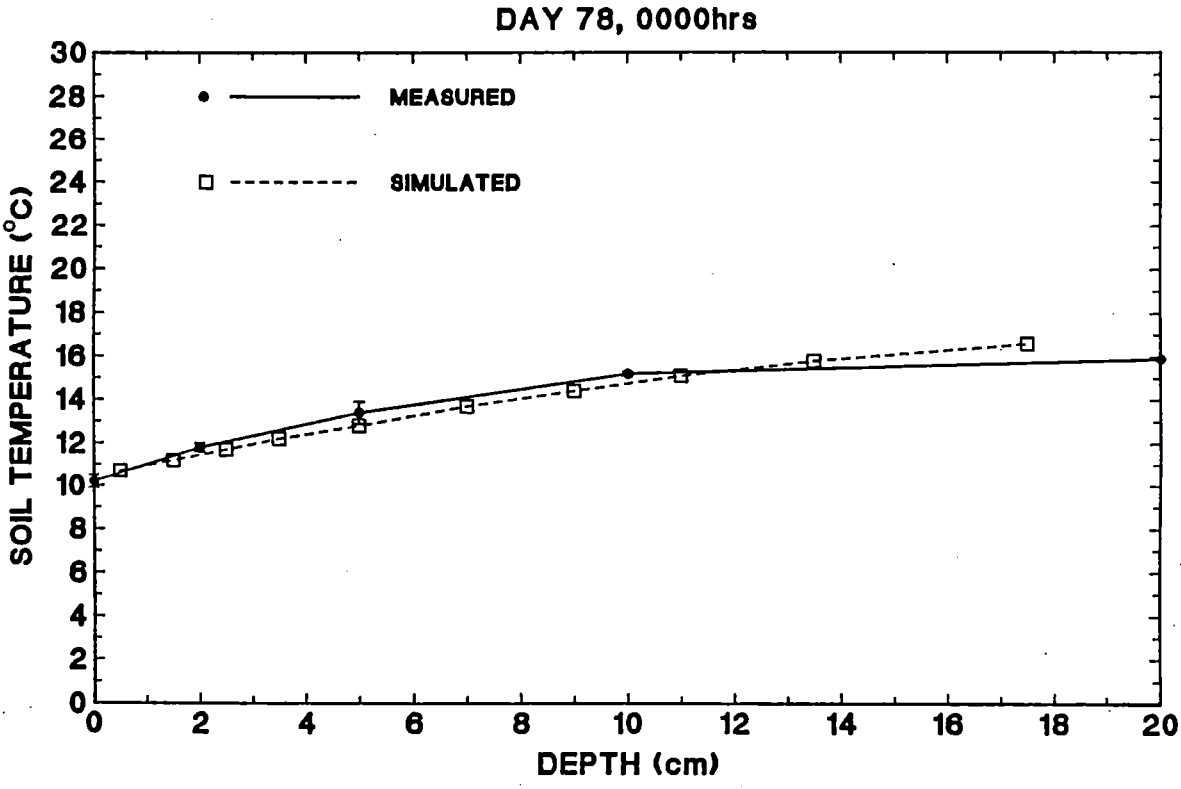

Figure 7.10b

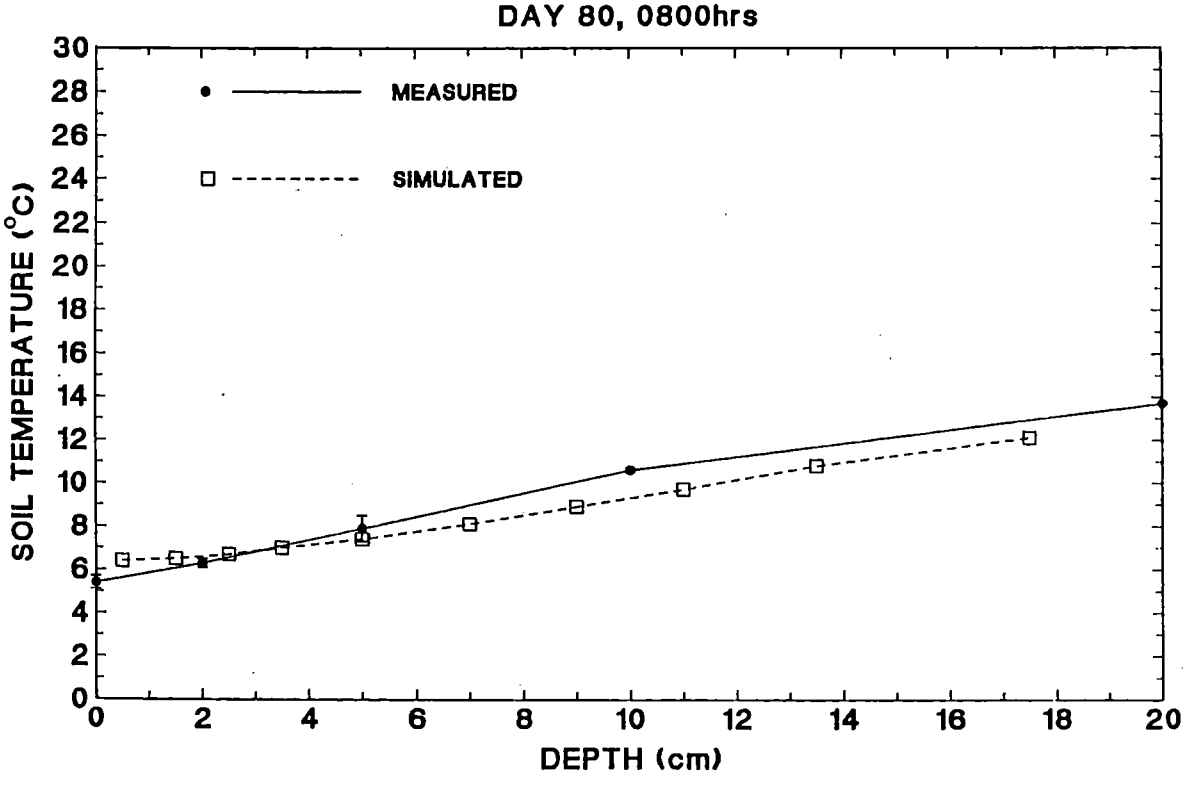

Figure 7.10c

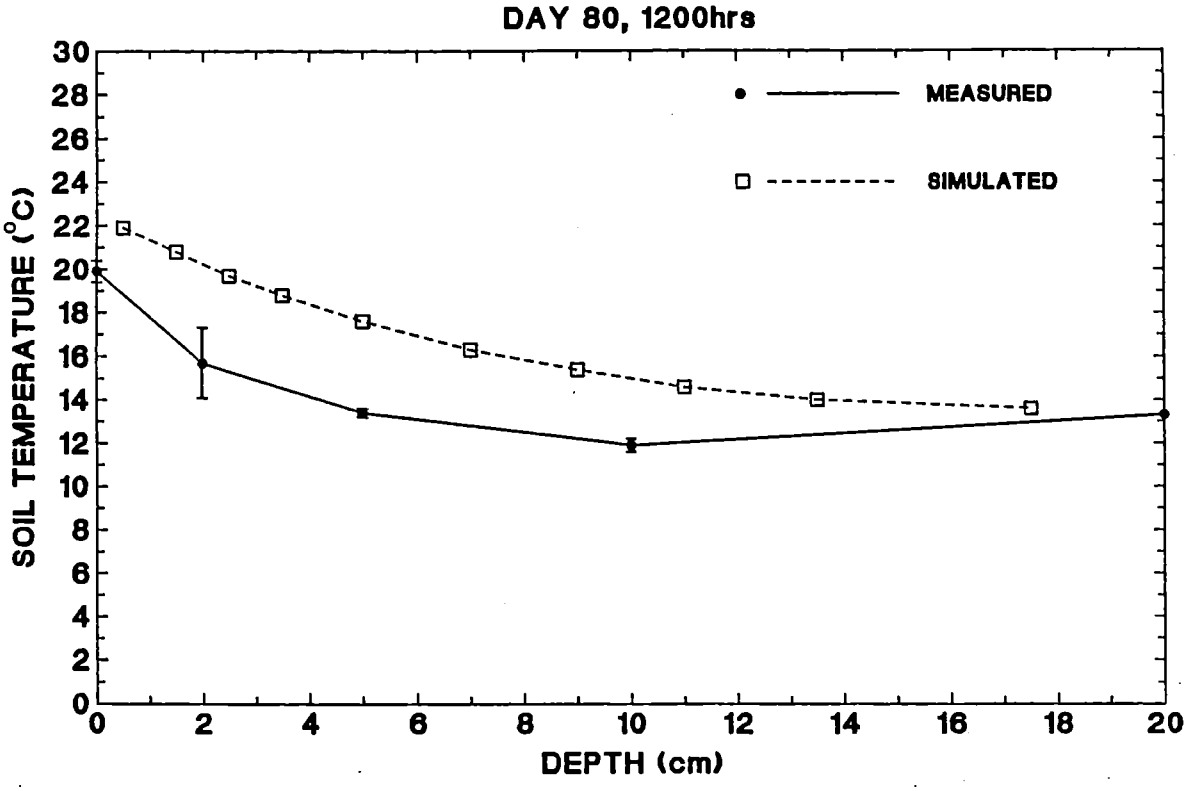

Figure 7.10d

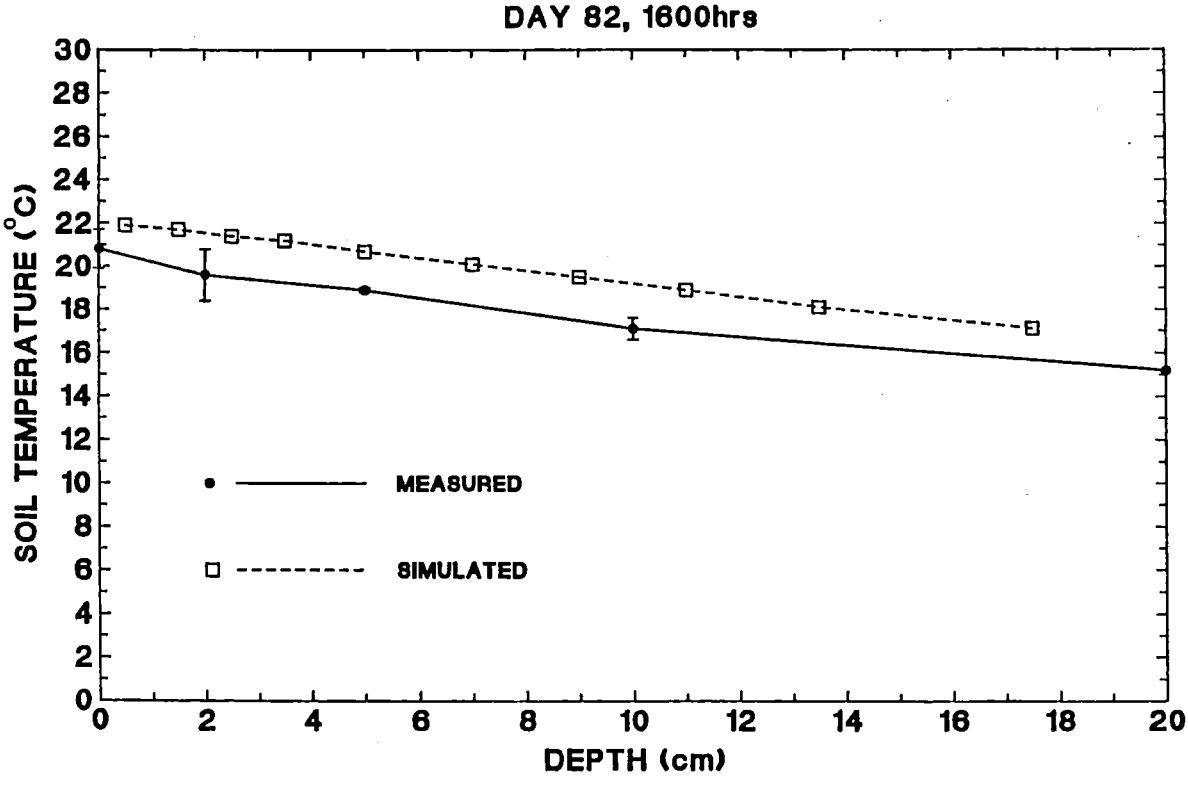

Figure 7.10e

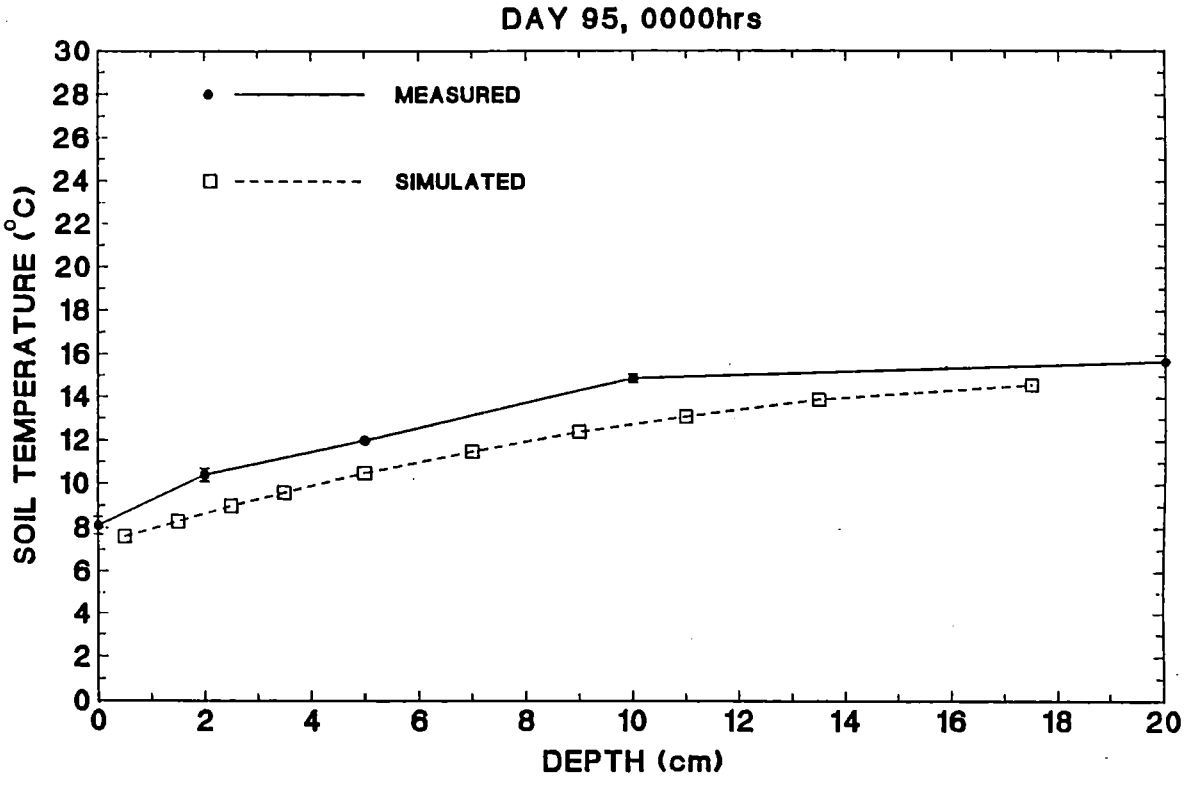

Figure 7.10f

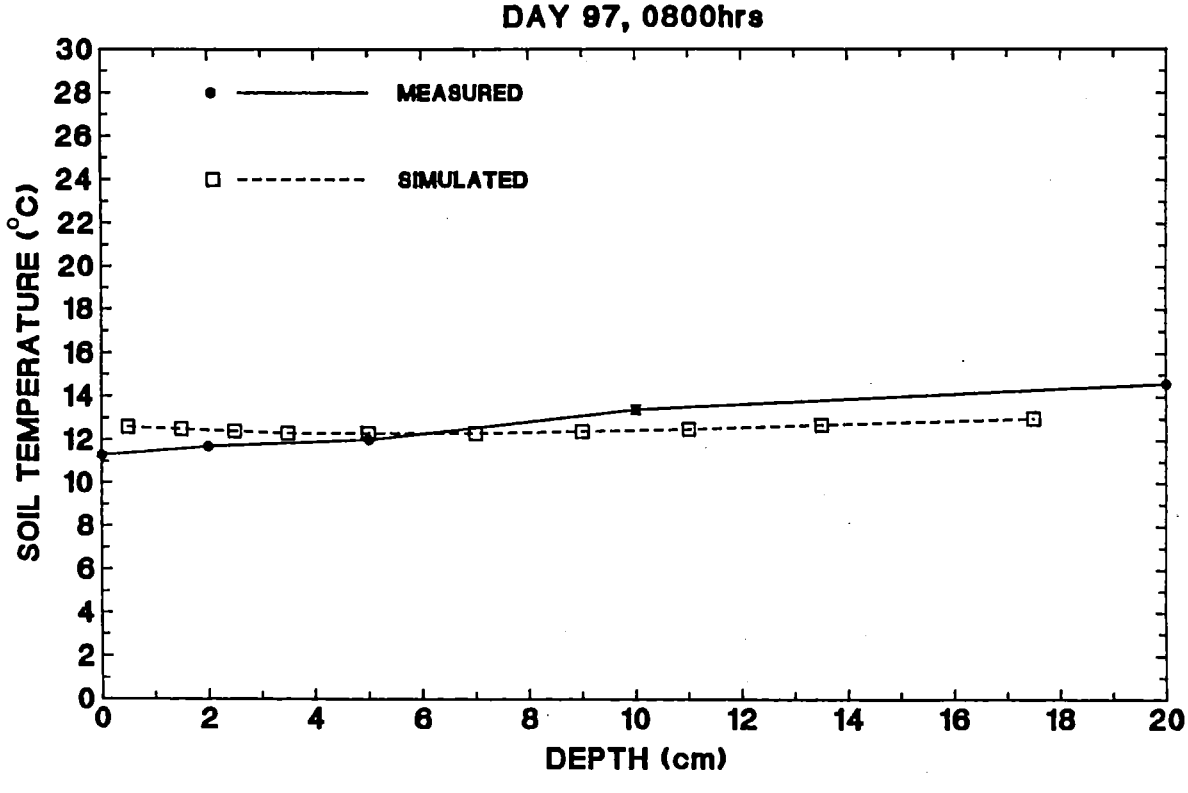

Figure 7.10g

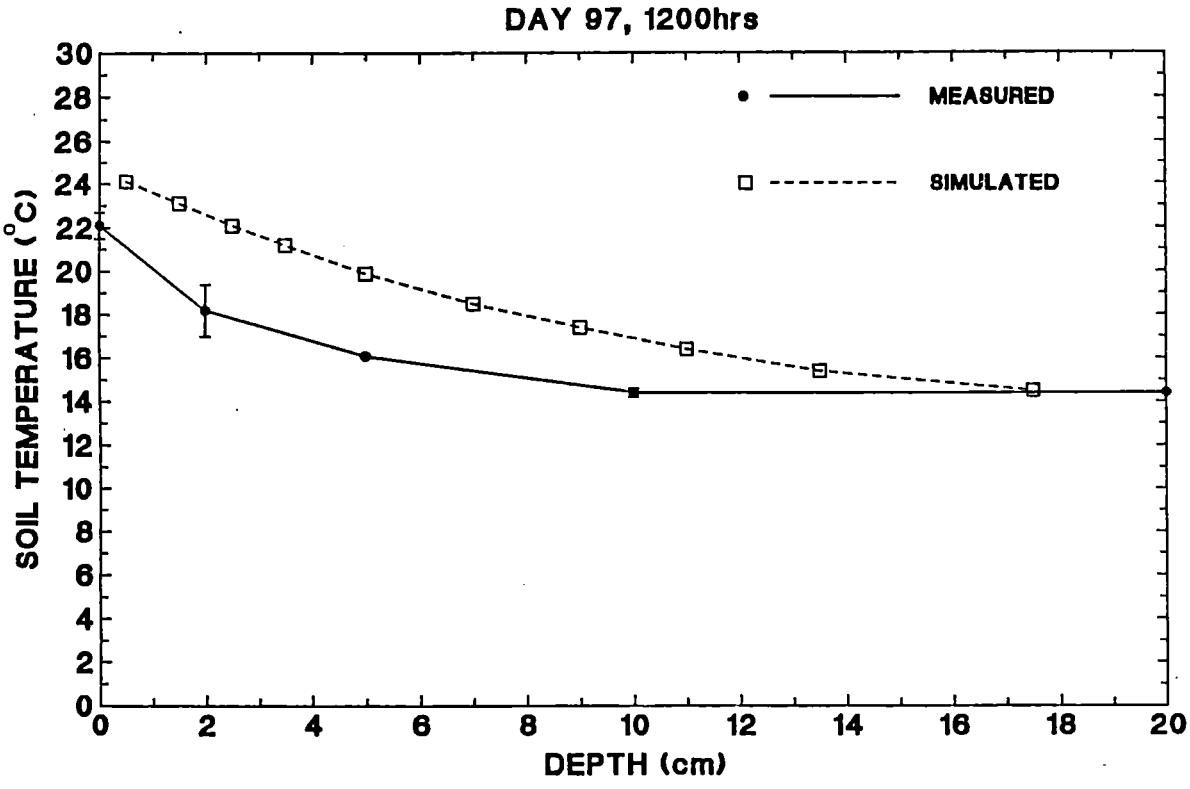

Figure 7.10h

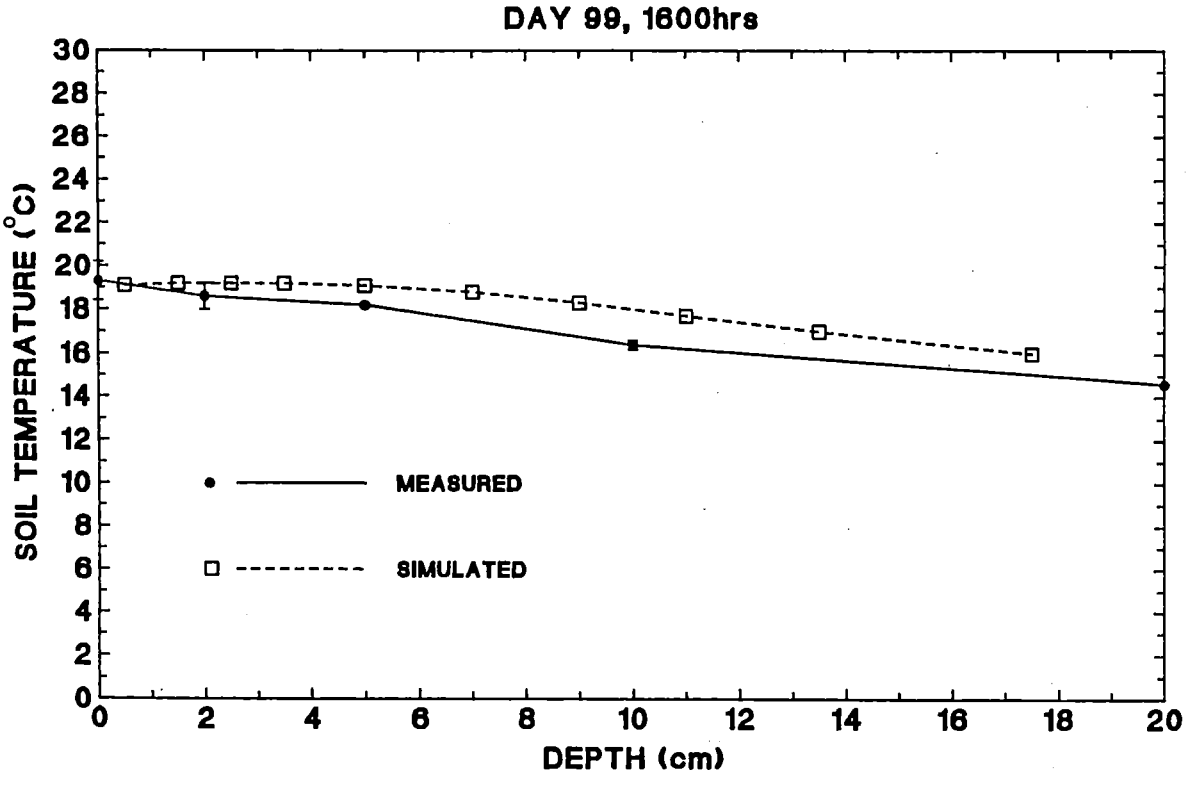

7.3.5 Sensitivity and error analysis

The results presented in Table 7.7 follow the investigation of the sensitivity of simulated surface soil temperature to errors in model input parameters. The results discussed are all for the second drying cycle. The estimation of soil thermal conductivity by the method of de Vries (1963) requires that the proportions of quartz, organic matter and clay minerals in the solid portion of the soil matrix be known. The altered value (Table 7.7) represents the calculated value when the proportion of quartz is increased by 10% while the proportion of organic matter stays constant (i.e. the proportion of clay is decreased to compensate). The altered value of soil volumetric heat capacity (Table 7.7) is an arbitrarily chosen 10% increase over the original value. Model sensitivity to changes in these soil thermal properties was low (Table 7.7). The results indicate that accurate measurements of the relative proportions of quartz, organic matter and clay minerals are not required for estimation of these soil thermal properties in the initialisation of the CONSERVB model.

Surface emissivity was not measured in the experimentation reported here, but an approximated function was used in CONSERVB. The low sensitivity of the model to a change corresponding to the estimated maximum error of this parameter would indicate that a generalised emissivity function is adequate in the CONSERVB model. The results indicate model sensitivity to an increase of 0.02 in the reflection coefficient. The reported variations in reflection coefficient for differing soils with differing surface conditions (e.g. Idso et al., 1975; Graser and van Bavel, 1982; Iqbal, 1983; Potter et al., 1987) would suggest that measurements of the relation of reflection coefficient with surface soil water content are necessary when initialising the CONSERVB model.

The CONSERVB model was sensitive to a change in surface roughness coefficient (z_0) which corresponded to the estimated maximum error of this parameter. An increase in z_0 from 2.32 to 3.32 mm resulted in a decrease in the mid-day divergence between modelled and observed mean surface soil temperature although cumulative evaporation was unaffected. When initialising the CONSERVB model accurate estimations of the surface roughness coefficient are essential.

Table 7.7 The sensitivity of the CONSERVB model to selected input parameters.

INPUT VARIABLE	VALUE OR FUNCTION		ΔT_s*
	ORIGINAL	ALTERED	(K)
SOIL THERMAL CONDUCTIVITY (solid phase) $W\ m^{-1}\ K^{-1}$	4.47	4.66	+0.01
DRY SOIL VOLUMETRIC HEAT CAPACITY $10^6\ J\ m^{-3}\ K^{-1}$	1.02	1.12	+0.01
EMISSIVITY	ϵ=0.90 + (0.18xθ_V)	ϵ=0.92 + (0.18xθ_V)	-0.06
REFLECTION COEFFICIENT#			
- dry soil	0.058	0.078	
- wet soil	0.168	0.188	-0.10
ROUGHNESS COEFFICIENT z_0, mm	2.32	3.32	-0.15

* ΔT_s is the change (altered-original) in mean surface soil temperature over the complete second drying cycle.

\# Although only 'dry' and 'wet' soil reflection coefficient values are presented, the altered reflection coefficient function is 0.02 higher than the original reflection coefficient function over the complete range of soil water contents (refer Figure 7.4).

7.4 The application of the CONSERVB model to a range of tillage-induced soil structural conditions.

7.4.1 Model initialisation

The CONSERVB model was initialised using the soil physical and hydraulic properties which were measured following imposition of the 'minimum', 'intermediate' and 'excess' tillage treatments (described in Section 3.2.2). In the earlier field trial, each tillage treatment was repeated at each of three pre-tillage soil water contents. These values have been averaged and hence the model initialisations represent the mean effect of each tillage intensity treatment.

There was one simulation for each of the three tillage treatments. The simulations were over the same period as the second drying cycle used to evaluate the performance of the CONSERVB model (i.e. Julian days 89 to 99). The average daily meteorological input for the simulation period was presented in Table 7.3. As with the earlier simulations, the 0.40 m deep profile of the Templeton silt-loam soil was divided into 14 layers. The soil system geometry and the initial values of soil water content and temperature used for the simulation period was identical to that used previously (Table 7.1). The version of CONSERVB used for this investigation was unchanged from the one evaluated in Section 7.3.

The initialisation values for total porosity (ϵ_t) and the surface roughness coefficient (z_0) are presented in Table 7.8. The saturated hydraulic conductivity input which is required for the CONSERVB model is used only in the calculation of infiltration. During the period of simulation there was no rainfall and hence the K_s input is not used and is of no significance.

The values used as initialisation of the surface roughness coefficient (z_0) for each tillage treatment were not directly measured but were estimated from the surface roughness index which was measured. The estimations were made based on the

relation between measured z_0 and measured surface roughness index from the plot used in the experiment to evaluate the CONSERVB model.

Table 7.8 Parameters used in the initialisation of CONSERVB for the simulation comparing tillage treatments.

PARAMETER	MINIMUM TILLAGE	INTERMEDIATE TILLAGE	EXCESS TILLAGE
ROUGHNESS COEFFICIENT z_0, mm	5.56	4.52	2.12
MEAN TOTAL POROSITY			
- A horizon	0.67	0.62	0.62
- B horizon $m^3\ m^{-3}$	0.46	0.46	0.46

The $K(\theta_V)$ function and the water characteristic ($\psi_m(\theta_V)$) for the soil 'B' horizon are assumed unchanged by the three tillage treatments. The functions used are the same as for earlier simulations and were presented in Figures 7.2 and 7.3. The 'A' horizon water characteristic for each of the three tillage treatments as used for model initialisation was presented in Figure 5.3. The 'A' horizon $K(\theta_V)$ function for each tillage treatment was estimated from the water characteristic using the method of Jackson (1972). Near-saturated hydraulic conductivity measurements were used as matching factors. The estimated $K(\theta_V)$ functions are presented in Figure 7.11.

7.4.2. Results and discussion

7.4.2.1 Simulation results

The results of the simulations indicate that cumulative evaporation from the fine, smooth seedbed produced from the 'excess' tillage treatment was lower than that from

either of the other treatments (Table 7.9). The soil from the 'intermediate' treatment had the highest water loss. The differences in cumulative evaporation between treatments at the end of the drying cycle were large, with 'intermediate' tillage resulting in 8.5 mm more evaporation than the 'excess' tillage.

Figure 7.11 Unsaturated hydraulic conductivity in the 'A' horizon following tillage operations.

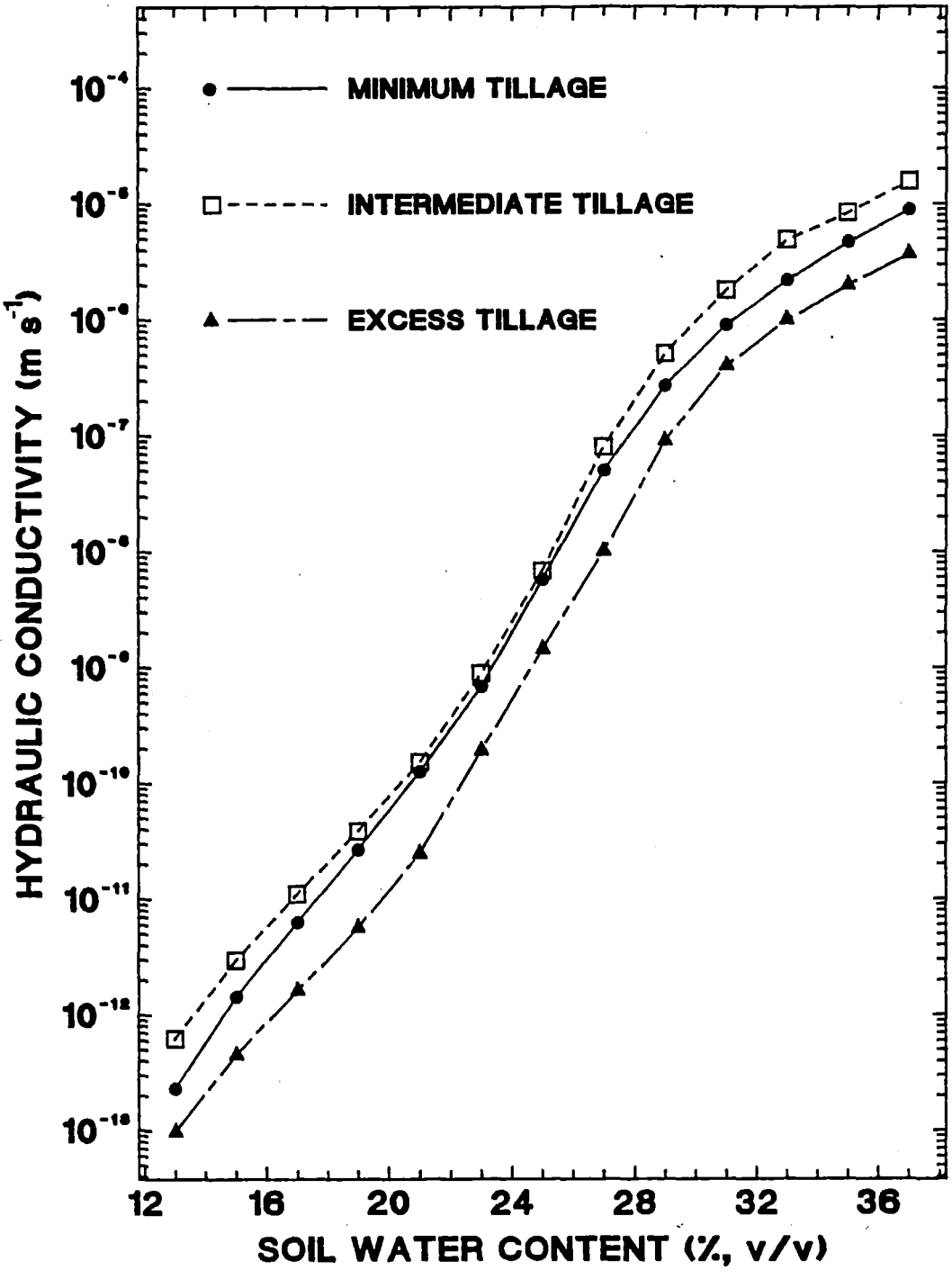

7.4.2.2 The unsaturated hydraulic conductivity input function

The hydraulic conductivity of the surface soil influences water movement to the sites of evaporation and is therefore, of importance, especially to the profile-limiting evaporation stage. In accordance, the CONSERVB model has been shown as being very sensitive to the unsaturated hydraulic conductivity input in the prediction of evaporation and soil water content (Section 7.3.1). Clearly, for any predictive assessment of evaporation, an accurate hydraulic conductivity input is a pre-requisite.

The hydraulic conductivity functions derived from the Jackson (1972) equation might not be accurate representations of the field situation. 'Minimum' tillage resulted in the largest volume of pores greater than 300 μm diameter (Section 5.2.4). Near-saturation hydraulic conductivity was highest in the 'minimum' tillage treatment as the large soil pores were water-filled and conducting large quantities of water. As the soil water content decreases (and matric potential decreases) with large pores draining first, followed by progressively smaller pores, hydraulic conductivity also decreases. The water characteristic results for the three tillage intensity treatments (Figure 5.3) indicate that the volume of pores in the 0.6 to 300 μm size range is larger for the 'excess' tillage treatment than for either 'intermediate' or 'minimum' tillage. When the soil has dried sufficiently for the pores larger than 300 μm diameter to have been emptied, the 'excess' tillage treatment is expected to have the largest volume of pores conducting water. Therefore, if pore continuity is equivalent with the three treatments, hydraulic conductivity could be expected to be highest in the 'excess' tillage treatment over the range in water content and matric potential which corresponds to the 0.6 to 300 μm pore size range.

The estimates from the Jackson method (Figure 7.11) indicate that the expected result does not occur. 'Excess' tillage resulted in the lowest, and 'intermediate' tillage in the highest, unsaturated hydraulic conductivity over a wide range of water content (and matric potential). This is a result of the strong influence of the matching factor hydraulic conductivity in the results from this calculation method. In the absence of hydraulic conductivity functions which have been confirmed as reliable (i.e. measured unsaturated hydraulic conductivity) the results reported from this simulation experiment are, at most,

speculative. This exercise illustrates how the simulation modelling approach could be applied in tillage research.

Table 7.9 The effect of surface soil structure on simulated evaporation.

JULIAN DAY	SIMULATED EVAPORATION mm d^{-1}		
	MINIMUM TILLAGE	INTERMEDIATE TILLAGE	EXCESS TILLAGE
89	4.8	5.0	3.9
90	2.1	2.6	1.4
91	1.4	2.1	1.0
92	1.1	1.7	0.7
93	0.8	1.3	0.5
94	1.0	1.4	0.7
95	0.6	1.1	0.4
96	0.8	1.1	0.5
97	0.4	0.8	0.3
98	0.4	0.6	0.3
99	0.8	1.0	0.5
TOTAL	14.2	18.7	10.2

7.5 Conclusions

1. The numerical simulation model CONSERVB has been shown to be extremely sensitive to the hydraulic conductivity-water content input function in the prediction of bare soil evaporation rates. In the absence of accurate field measurements of this input function a model calibration phase became necessary.

2. An experimental verification of the CONSERVB model has shown that for the conditions in which the model was tested it accurately predicted both the daily and cumulative bare soil evaporation.

3. A comparison of measured and simulated surface soil temperature and net radiation showed a generally satisfactory simulation of the energy balance. This

was supported by an analysis of the energy partitioning with wet and dry soil and by a comparison of the measured and simulated surface soil temperature as a function of time. Predicted soil surface temperature and net radiation tended to exceed the measured values during warm conditions.

4. Simulated soil water profiles were generally in good agreement with measured values. In the surface 30 mm of soil, simulated water contents tended to be lower than measured values although the discrepancy rarely exceeded 4% (v/v). Deeper in the soil profile measured and simulated water contents compared well.

5. The simulated soil temperature profiles were also generally in good agreement with measured values. Some discrepancy occurred in warm conditions, usually near the middle of the day, when simulated soil temperature exceeded measured values. As the atmosphere cooled, the simulated temperatures reduced and again compared well with measured values.

6. An analysis of the sensitivity of the CONSERVB model to some of the input parameters and functions indicated that reasonable estimates of soil thermal conductivity, soil heat capacity and emissivity were satisfactory for model initialisation. The analysis showed the model to be sensitive to the soil reflection coefficient-surface soil water content function and to the surface roughness coefficient.

CHAPTER 8

General Discussion and Conclusions

8.1 Introduction

In this chapter the results of the complete study are summarised and discussed together with recommendations for further research. The final section of the chapter lists the main conclusions of the study.

8.2 Result summary and general discussion

The literature review at the beginning of this study (Chapter 2) considered the use of tillage operations to produce a surface soil structural condition which satisfied the objectives of soil conservation, as well as of plant growth and yield. The soil water balance was identified as an important factor in both soil conservation and plant growth. The literature review highlighted the complex manner in which the soil physical and hydraulic properties inter-relate in the processes that control the soil water and energy balances (Figure 2.3).

A useful long-term objective was the identification of the soil properties which have the most significant effects on the soil water balance. Successful identification of these soil properties would contribute to a better definition of the soil condition required for agronomic objectives. Such a definition would be a product of the consideration of both soil conservation and plant yield related aspects and would involve some compromise between the two. Numerical simulation modelling is an approach which is able to incorporate the many tillage-affected soil factors in the processes determining the soil water and energy balances.

In order to better prescribe the soil manipulation appropriate for a given set of agronomic objectives, the soil properties affected by tillage, and the magnitude of these effects, needed to be clearly identified. Previous workers had identified soil water

content at time of tillage (PTSW) as having an important influence on the soil structure formed by tillage operations. However, little information on the effects of pre-tillage soil water content on multiple-pass tillage was available; this was a critical area in which further research was urgently required and was, therefore, a major motivation for this study.

8.2.1 The effects of multiple-pass tillage on soil physical properties

This study confirmed that the pre-tillage soil water content (PTSW) of a Templeton silt-loam soil affected the soil condition produced by multiple-pass tillage. An interaction between intensity of tillage operations and pre-tillage soil water content was identified. The PTSW effect on aggregate size distribution was greatest (Section 4.2) when tillage was most intensive. When the soil was intensively tilled in a dry condition, a high proportion of small, wind-erodible soil aggregates and particles was produced. Intensive tillage of the soil in a wet condition produced a smaller proportion of fine soil aggregates. On this soil, the avoidance of 'excessive' tillage reduces the likelihood of a significant PTSW effect occurring. The effect of the tillage intensity treatments on aggregate size distribution was greater than the effect of the PTSW treatment. The combination of PTSW and tillage intensity treatments produced a range in percentage of aggregates less than 0.84 mm diameter of 5.6 to 26.4% (Figure 4.2).

The expression of PTSW levels as proportions of the lower plastic limit (LPL) allows comparisons of results with those from other soil types. The work of Lyles and Woodruff (1962), Bhushan and Ghildyal (1972) and Ojeniyi and Dexter (1979a) (described in Section 2.3.3.3) considered primary tillage operations at differing PTSW levels. The results of each of these studies seemed consistent in that more smaller aggregates and fewer large clods were produced at intermediate PTSW levels (approximately 0.8 to 0.9 of the LPL). That result might appear inconsistent with the findings reported here because this study has shown that in general, more smaller aggregates were produced from tillage operations at 0.58 times the LPL than at 0.76 or 1.0 times the LPL. However, this study differs from earlier work in that a tillage treatment consisted of both primary and secondary tillage operations at each of three PTSW levels.

The 'minimum' tillage treatment in this study provides the closest comparison to the primary tillage operations reported by these other workers even though three implement passes were involved. The 'minimum' tillage treatment produced the largest proportion of aggregates in the less than 0.84 mm diameter range at the 23.3% (0.76 LPL) PTSW level (Figure 4.2). This effect was also apparent in each of the other measured aggregate size ranges. Results might have been more consistent with other workers had the tillage been less intensive. When interpreting results of PTSW level effects on surface soil structure, the interaction of tillage intensity and the PTSW effect on aggregate size distribution must be considered. That the effect of PTSW levels is greatest on aggregates less than 0.26 mm diameter emphasises the importance of this pre-tillage soil property in terms of soil conservation. The aggregate size range affected (<0.26 mm diameter) is very susceptible to erosion by wind, as well as to surface crusting and thus to erosion by water. While the importance of PTSW in producing a particular soil condition is widely recognised, the interaction of tillage intensity with PTSW is not. This study serves to identify this interaction and emphasise its importance.

The aggregates formed during tillage at a soil water content near to the lower plastic limit were shown to be less mechanically stable (when dry) than aggregates produced by tilling a drier soil (Section 4.3). This PTSW effect is not widely recognised but has important consequences for the susceptibility of the soil to erosion by wind and to surface crusting. Relative aggregate stability following the tillage and PTSW treatments ranged from 0.71 to 0.92. Repeated intensive tillage has been reported to result in reduced soil organic matter content and hence lower aggregate stability in the long-term (Section 2.3.1.3), an effect opposite to the short-term one reported here. The results indicate that in assessing the most appropriate PTSW content for the desired tillage objectives, aggregate stability must be considered as well as aggregate size distribution.

For any tillage system, the identification of the optimal soil water content is important to ensure that the tillage operations produce the desired result. The investigation of the interaction of tillage intensity with PTSW on soils of different textural type would be useful because the effects reported in this study might be specific to silt-loam soils. PTSW effects on surface soil structure following multiple-pass tillage might

be more significant on soils with higher clay contents. In this study measurements were made on freshly-tilled soil and hence the treatment effects reported here are short-term only. The surface structure of the freshly-tilled soil will change with time. Long-term effects of the treatments imposed in this study on the soil structure might differ from the short-term results detailed here.

In investigating the effects of tillage intensity and PTSW on surface soil roughness it became apparent that indices previously used to quantify surface roughness had limitations due to their dependence on the distributional form of the field-measured elevation data (Section 4.4.2). Methods using standard errors or standard deviations as a surface roughness index were dependent on the measured elevations (from a benchmark height to the soil surface) fitting an assumed normal distribution. Therefore, in deciding which index is most appropriate, field data sets must be tested for normality. The most appropriate method to use will depend on the distributional form of the data and its intended use. However, the geostatistical method of Linden and van Doren (1986) (described in Section 4.4.3) does not rely on elevation data fitting any assumed distribution. The method allows a quantification of surface roughness without the problems of distributional form.

In this study, the method of Linden and van Doren (1986) was compared with an index (SR) based on the standard deviation of elevation measurements. However, the field data was not always of a normal distribution and so the results from the SR index might not have provided an accurate standard by which to assess the geostatistical method. The LD index from the method of Linden and van Doren did give very similar results to the SR index indicating that the sensitivities of the two methods to random roughness were similar. The Linden and van Doren method gives more information than SR type indices, for example by providing estimates of soil surface area. The success of the geostatistical method is dependent upon the form of the regression of mean absolute-elevation-difference against sample spacing, as the roughness indices (LD and LS) are derived directly from the coefficients of this regression. The accuracy of the calculation of the indices is thus dependent on the regression giving a very good description of the measured function. Within the limitations of the number of samples measured in this study, it appeared that this regression form was consistent (Section 4.4.3). This, together with the theoretical basis of the technique, makes it appear

promising. Further evaluation of the geostatistical technique using a larger data set is warranted.

Intensive tillage reduces aggregate size and results in a smoother soil surface. Pre-tillage soil water content did not significantly affect random roughness (Section 4.4.5). 'Excess' tillage produced a surface area that was less than that from either of the other two tillage intensity treatments (Section 4.4.6). A rough soil surface might have both advantages and disadvantages in relation to agronomic objectives. It has been shown that a rough soil surface might have a higher rate of infiltration with lower runoff and decreased water erosion as compared to a smooth soil surface (Zobeck and Onstad, 1987). A surface crust is less likely to form on a rough soil surface than on a smooth one. A smoother soil surface is generally more susceptible to wind erosion. A rough soil surface is, therefore, desirable in the context of soil conservation. However at high wind speeds, a rough soil surface induces air turbulence which might enhance vapour transport away from the soil surface, resulting in a higher evaporative loss during the weather-controlled stage of evaporation. A greater number of large voids are likely to be associated with a rough soil surface, possibly resulting in increased water loss through evaporation (Ojeniyi and Dexter, 1984). A rough soil surface has been shown to exhibit low shortwave albedo. Decreases in shortwave albedo result in increased potential evaporation (Idso et al., 1975; van Bavel and Hillel, 1976) or, where soil water is not abundant, increased soil temperature. It would be helpful to be able to assess the significance of the various processes influenced by random roughness on the overall soil water regime.

8.2.2 The effects of multiple-pass tillage on soil hydraulic properties

The pre-tillage soil water content treatment had only small effects on the soil water characteristic (Section 5.2.3). The tillage intensity treatments had significant effects on some parts of the water characteristic function. The 'excess' tillage treatments, which produced the finest surface soil structure, resulted in the highest water content at each measured matric potential in the range from -1 to -500 kPa. The soil hydraulic characteristic is a function of the size and continuity of the soil pores and this system, in turn, is defined by the aggregate and particle size and their arrangement. However, the

measured PTSW effect on aggregate size distribution was not very apparent on the soil water characteristic. This might reflect the different soil zones which were sampled for aggregate size distribution and for the water characteristic.

The PTSW treatment had no significant effect on total porosity or on any of the soil porosity functional size ranges which were considered (Section 5.2). As intensity of tillage increased, soil macro-porosity tended to decrease, mainly through a decrease in the volume of pores in the aeration pore size class. Macro-porosity ranged from 33.1% to 44.0% (Figure 5.4). The available water holding capacity was maximised in the 'excess' tillage treatments and was progressively lower in the 'intermediate' and the 'minimum' tillage treatments. Available water holding capacity ranged from 11.6 to 16.6% (Figure 5.7).

The tillage intensity treatments had significant effects on near-saturated hydraulic conductivity with conductivity being highest after 'minimum' tillage (Section 5.3). Near-saturated conductivity generally reflected the soil macro-pore volume, as would be expected. A range in near-saturated hydraulic conductivity from 3.0×10^{-5} m s^{-1} to 4.4×10^{-5} m s^{-1} was observed. As a tilled soil settles and undergoes field wetting and drying cycles, macro-pore volume would be expected to decrease; consequently decreasing near-saturated conductivity.

The measurement of the water characteristic curve, and hence the derivation of the functional pore size classes, requires the soil samples to be saturated with water. Under these conditions some soil structural changes probably occurred. The results reported are thought, therefore, to be more representative of a soil which has undergone a field wetting cycle than of a freshly-tilled soil. The total porosity values differ in that they are calculated from the bulk density of the dry soil in which structural change would be less than from a wetting. The total porosity measurements then, probably are more representative of a freshly-tilled soil. The calculation of the soil macro-porosity and aeration porosity functional pore size classes utilises both water characteristic data and total porosity data and hence might not fully represent a freshly-tilled or a wetted soil.

The water characteristic was measured on a drying soil and hysteresis was ignored. The usage of the desorption curve is justified because in the field situation

soils are drying from an initially wet condition. Soils gain water much faster than they lose it, hence for most of the time the drying curve applies. In interpreting the results presented here it should also be appreciated that the pore size distribution calculated from the water characteristic is a generalisation, not a detailed description of pore space geometry. Such a detailed description is nearly impossible because no single dimension of a pore can be identified unambiguously as its size. Pore shape is extremely variable, even over short pore-lengths.

It must be emphasised that the tillage results presented in this study are specific to the type and condition of soil on which the experiments were carried out. The soil structural condition before tillage, the soil texture and the soil organic matter levels are all factors likely to influence the soil structure resulting from the tillage treatments imposed in this study. At the beginning of the tillage experiments the Templeton silt-loam soil was high in organic matter content and well-aggregated. In general agronomic terms, the soil structure was good.

Small changes in the soil hydraulic properties can have a large effect on the field soil water balance. Further research is required to determine the effect of particular soil hydraulic properties on soil water storage and loss by evaporation. For the soil used in this study there is now some indication of the likely magnitude of changes in the soil hydraulic properties with widely differing tillage practices. A useful future research objective would be to determine the effect of these changes on the overall soil water balance.

Hydraulic conductivity data in tilled soils are difficult to measure, over a wide range of water contents or matric potentials, and are not common in the literature. The measurement of unsaturated hydraulic conductivity would have strengthened this study. The evaluation of the Jackson (1972) method for calculating unsaturated hydraulic conductivity was by sensitivity analysis. This evaluation might be improved by comparison with measured conductivity data. Nevertheless, the analysis clearly showed the extreme sensitivity of the Jackson (1972) method to the 0 to -1.0 kPa matric potential section of the water characteristic input (Section 5.4.2). This analysis indicates that previously reported work relying on unsaturated hydraulic conductivity estimates using the Jackson (1972) method must be carefully interpreted. This represents a

significant finding as the Jackson method has been widely used, possibly without knowledge of the extreme sensitivity of the method to parts of the input data.

In using the Jackson method, it is suggested that the water characteristic input should have at least two data points between 0 and -1.0 kPa matric potential, especially where the soil being considered has a large volume of 'aeration pores'. In a freshly-tilled soil a large number of macro-pores and a bi-modal or uni-modal pore size distribution might exist. Calculation methods based on Darcy and Hagen-Poiseuille theory might be less appropriate with a tilled soil than with, for example, an un-tilled sandy textured soil. Hydraulic conductivity estimates calculated using the Jackson (1972) method were not reliable enough to allow the evaluation of the effect of tillage treatments on this important soil property. It is therefore recommended that in future tillage studies unsaturated hydraulic conductivity should be measured directly, rather than relying on estimates from the Jackson (1972) procedure.

8.2.3 The effects of multiple-pass tillage on soil thermal properties and shortwave albedo

Soil temperature is a function of the net amount of heat which enters or leaves the soil and of the thermal properties of the soil. Changes in soil porosity due to tillage treatments were shown to affect soil thermal properties (Section 5.5). The 'minimum' tillage treatments, which had the highest total porosity, generally showed the lowest soil thermal conductivity. Differences in thermal conductivity between soils with high and low total porosity were greatest when the soil was in its driest state. Increasing soil porosity resulted in a decrease in volumetric heat capacity in an oven-dry soil but an increase in volumetric heat capacity in a saturated soil.

Thermal properties of the topsoil dominate the temperatures of the entire profile (Wierenga et al., 1982). Surface soil with low thermal diffusivity should warm up faster near the surface with periods of rising temperature, whilst the remainder of the profile should remain cooler. The reverse would probably be true during periods of decreasing temperature, with soils of low thermal diffusivity in the upper profile remaining warmer in the sub-soil but cooling at the surface. A change in the thermal properties of the surface soil could, therefore, be expected to lead to modification of the

amplitude of the daily temperature wave (Wierenga et al., 1982). A brief increase or decrease in the amplitude might cause a significant physiological change in a crop as well as a change in the yield (Wierenga et al., 1982).

Shortwave albedo is another important property which influences the soil thermal regime and hence the soil water balance. Surface soil structure and surface soil water content had been identified previously as factors affecting shortwave albedo. In assessing the effect of surface soil structure and water content on shortwave albedo, the influence of sun angle on reflectance measurements must first be removed from the data. A comparison of the sun angle effect measured in this study, with measurements reported elsewhere, indicated that the effect is specific to a particular soil and its particular surface structural condition (Section 5.6.2). This study confirmed earlier reports of large surface soil water content effects on shortwave albedo (Section 5.6.3).

Surface soil structural condition also affected shortwave albedo but to a smaller extent than previous studies indicated. Large changes in surface roughness and in aggregate size distribution between the plots on which shortwave albedo was determined, translated into relatively small and sometimes inconsistent changes in shortwave albedo (Section 5.6.4). The overall magnitude of the shortwave albedo measured here was small, probably a result of high soil organic matter and rough surfaces. Measured dry-soil albedo ranged from 12.6% to 14.6%. Shortwave albedo was correlated more closely with the aggregate size distribution of the surface soil than with the surface roughness index. This might be because the aggregate size distribution represents surface roughness on a smaller scale, a scale which is more representative of that at which the reflection mechanism is working.

On tilled surfaces found in practical farming situations, changes in shortwave albedo due to changes in tillage operations are not expected to be large in absolute terms. However, if soil water relations were influenced to a large extent by shortwave albedo, small absolute changes might be of importance. It would be useful therefore, to be able to ascertain the likely sensitivity of the field soil water regime to changes in albedo due to tillage-induced soil structure. This study has produced an indication of the likely ranges in shortwave albedo following various tillage treatments, this important data is a pre-requisite for future studies of tillage-induced shortwave albedo effects on the soil water balance.

8.2.4 Evaluation and testing of the CONSERVB simulation model

The numerical simulation model CONSERVB (Van Bavel and Hillel, 1976) was considered suitable for use in this study because: (i) in earlier studies it had been shown to simulate soil water and temperature profiles of a bare soil accurately, (ii) it had realistic data requirements, (iii) it was mechanistic and process-oriented, (iv) it could account for the main tillage-sensitive variables, and (v) it could be adapted for variations in soil condition that result from tillage.

The CONSERVB model was described in detail with some of its assumptions and limitations being identified (Sections 6.4.3 and 6.4.5). The aerodynamic resistance calculation in CONSERVB was improved by including a more recent method based on the Monin-Obukhov length (Camillo and Gurney, 1986). The assumptions of no sub-surface evaporation and of un-coupled heat and vapour transport were seen as potential limitations to model performance. However, the greater complexity and data input requirements of models simulating sub-surface evaporation and coupled heat and vapour flow make them more difficult to apply. Such models are not as well suited to the study of tillage effects on soil water and temperature as the CONSERVB model. The significance of sub-surface evaporation and coupled heat and vapour flow in the soil-atmosphere system needs to be determined and is a worthwhile research objective. Such research would give a basis for the comparison of models using coupled heat and vapour flow and sub-surface evaporation with models which do not account for these processes.

A field trial was carried out to collect the necessary data to allow a comparison of measured values with simulated soil water and temperature profiles. Evaporation was measured using a micro-lysimeter technique (Section 3.3.2.1). Although labour intensive, this technique enabled convenient, low cost, high resolution evaporation measurement and is recommended for future studies of evaporation from tilled soils.

The performance of the CONSERVB model was assessed on the basis of comparison with the field-measured data. A calibration phase was used to select, by

trial and error, a hydraulic conductivity function with which the CONSERVB model accurately simulated the field-measured evaporation during one drying cycle. Using this hydraulic conductivity function, the model accurately simulated evaporation rates during a second drying cycle; after an 11 day simulation period cumulative simulated evaporation was 9.4 mm and measured cumulative evaporation was 9.8 mm (Section 7.3.2). Simulated soil water and temperature profiles were generally good, although soil water content in the surface soil layers was sometimes under-estimated. Simulated soil water content in the top 3 cm of soil was usually within 0.04 m^3 m^{-3} of the measured values. Soil surface temperatures were sometimes slightly over-estimated when air temperatures were high. However, the model was shown to give a generally satisfactory energy balance solution and the time course of predicted variables was in accordance with field measurements. The lack of field measured unsaturated hydraulic conductivity data limited the verification study.

Difficulties in both the measurement and the modelling of soil water were encountered due to the rough, cloddy, nature of the tilled soil surface. With such a surface structure, surface soil water content had a high degree of spatial variability. Representative sampling was difficult because of the water content differences between and within individual aggregates. Defining the soil surface when sampling within prescribed soil depth increments was sometimes difficult. The assumptions of homogeneous soil layers made in the CONSERVB model are not very compatible with the heterogeneity of the soil surface. This, together with the sampling difficulties, contributed to the discrepancies in measured and simulated soil water content in the top 30 mm of the soil. The complexities of soil water movement and storage in a surface soil with such a bi-modal or uni-modal pore size distribution is beyond the scope of this type of simulation modelling approach. Some of the assumptions necessary to enable such a modelling approach are not valid for such a soil structural condition. The degree of success of the model performance might therefore be due, in part, to compensating error and spatial averaging unless the impact of the invalid assumptions is small. Hence it is thought that results generated with numerical simulation models must be interpreted with care. Research advances in the future might depend, then, on the simultaneous improvement of measurement techniques, soil water theory and simulation modelling.

The CONSERVB model could be used in the future as a research tool to aid in predicting benefits and risks from tillage operations. The main priority is to identify the

tillage-sensitive soil properties which have the greatest influence on evaporative soil water loss. Different soil properties are expected to influence water loss by different amounts, depending on the stage in the evaporation process. These critical soil properties need to be identified, as do the stages in the evaporation process during which each soil property is of most importance. The use of simulation modelling allows the isolation and study of single variables affected by tillage. The most likely approach to the identification of these critical soil properties is through analysis of model sensitivity to the various tillage-related inputs. Field measurements must then be used to verify any projections based on model sensitivity.

The hydraulic conductivity of the surface soil is important in determining the rate at which water can reach the soil surface to evaporate. Thus, hydraulic conductivity is likely to greatly influence the overall soil water regime, especially through effects on the soil-limiting evaporation stage. The sensitivity of the evaporation predictions from the CONSERVB model to this soil property was shown to be high (Section 7.3.1), concurring with expected behaviour and also with the evaporation modelling studies of Linden (1982). Unsaturated hydraulic conductivity is therefore, likely to be a soil property of major importance in the soil water balance. It would be useful to be able to better predict the likely effect of different tillage operations on the surface soil hydraulic conductivity. The field verification of the simulation modelling predictions that evaporation is highly sensitive to surface soil hydraulic conductivity is another useful future research objective.

8.2.5 Soil temporal variability

Tillage-induced surface soil structure is not a static condition but changes with exposure to climatic conditions. It is emphasised that the results reported here are short-term in that they apply to freshly-tilled soil. Prior to this study there had been very little quantitative information about the effects of tillage on soil structure before the soil settles following rainfall. Immediately after tillage, while the soil is loose, the surface dries quickly and wind erosion susceptibility might be very high. Although the unstable period of the freshly-tilled soil might not last for a long time, the water relations during this period might be of major significance in the overall water regime.

Surface soil roughness decreases after exposure to wetting and raindrop action. When a freshly-tilled surface is exposed to direct raindrop impact roughness changes rapidly, with the rate of change decreasing with time (Allmaras et al., 1966; Burwell et al., 1968). Porosity has also been shown to decrease with exposure to rainfall, mainly through a decrease in the volume of large pores and voids (Allmaras et al., 1966). Surface sealing can also occur with exposure to rainfall. Tillage treatment effects on surface structure would, therefore, be expected to change over time. The tillage treatments in this study have been shown to significantly affect the volume of aeration pores. Since the volume of this size class of pore is expected to decrease significantly as the soil settles, differences in macro-porosity due to tillage treatments might become less pronounced over time. Long-term treatment effects could be much different from the short-term effects reported here. In the full evaluation of soil management practices both short and long-term effects need to be evaluated. There is a general need for better determination of the dynamic nature of surface soil properties.

In the adoption of a simulation modelling approach to aid in assessing the effect of tillage management on soil water relations, a description of changes in soil condition should be included. The CONSERVB model could allow for some of the surface soil parameters affected by climatic conditions over time to be updated at scheduled intervals. Examples would be the surface roughness coefficient (z_0), total porosity, the unsaturated hydraulic conductivity function and the water characteristic function. In order to be able to do this, however, the dynamic nature of each surface soil property needs to be determined. Such determinations need to include generalised relationships between surface soil structural parameters and rainfall amount, rainfall energy, or time.

8.2.6 Soil spatial variability

The surface soil properties measured in this study vary for reasons other than the imposition of tillage operations. Spatial variability occurs in the experimental plots both in the vertical and in the horizontal planes because of natural variation in soil texture, soil organic matter content and soil structure. Past management practice might have accentuated this natural variation. In this study soil samples were not collected from those areas over which tractor wheels had passed during secondary tillage operations. Horizontal spatial variation in the non-wheelmarked areas was thought to be adequately

accounted for by the size and number of soil samples which were taken from random locations.

Spatial variability in a vertical plane might have been a more significant factor in interpreting the results from this study. Systematic treatment-dependent spatial variation could have occurred with soil depth. The observation of aggregate size distribution changing with soil depth depending on tillage treatment, as reported by Ojeniyi and Dexter (1979b), indicates the likelihood of such variation occurring. Tillage could alter soil properties only at selected depths rather than throughout the soil profile, or to differing degrees at different positions in the soil profile. In order to account fully for these positional effects of tillage a sampling design that allows for rigorous statistical analysis is desirable. Positional effects can then be isolated.

The aggregate size distribution and aggregate stability results reported in this study pertain to the top 40 mm of the soil profile. This surface soil layer is of most importance in considering the susceptibility of soil to wind erosion and to surface crusting. It is also the soil layer most relevant in the investigation of the effects of surface soil structure on shortwave albedo. Samples for determination of bulk density and the water characteristic were taken from the centre of the tilled layer. The bulk density samples and water characteristic samples from the 'minimum' and 'intermediate' treatments were 70 mm in depth and hence represented the 40-110 mm section of the 150 mm tilled soil zone. No samples were taken at other depths in the tilled zone and so the spatial variability in the vertical plane in the tilled zone has not been fully characterised. However, the sampling of such a large proportion of the tilled layer (in the vertical plane) should ensure a result giving a representative mean value of the bulk density and water characteristic of the complete tilled layer. The 15 mm deep pressure plate sample can only give a representative result if the treatment effects in the centre of the tilled zone reflect the mean effects over the whole of the tilled zone. The samples for near-saturated hydraulic conductivity determination were 150 mm deep and hence did give a full representation of the tilled soil zone.

8.3 Conclusions

The main conclusions from this study are:

a) The effects of multiple-pass tillage on soil physical properties.

1. On the Templeton silt-loam soil studied, pre-tillage soil water content (PTSW) is an important factor influencing the aggregate size distribution and aggregate stability produced by multiple-pass tillage.

2. Pre-tillage soil water content interacts with tillage intensity in determining the soil condition produced by multiple-pass tillage.

3. When tilling a soil, the identification of the optimal soil water content for the chosen tillage system and agronomic objectives is important in order to ensure that the tillage operations produce the desired result.

4. The LD and LS surface roughness indices proposed by Linden and van Doren (1986) provide a means of characterising random roughness which does not depend on measured elevation data being of any one assumed distributional form.

b) The effects of multiple-pass tillage on soil hydraulic properties.

5. Multiple-pass tillage operations cause changes in the soil pore size distribution and near-saturation hydraulic conductivity of the freshly-tilled soil. More intensive tillage decreases the volume of aeration pores and increases the available water holding capacity. PTSW does not significantly affect these properties on this soil.

c) The estimation of unsaturated hydraulic conductivity.

6. The Jackson (1972) method for calculating unsaturated hydraulic conductivity is considered unsuitable for giving reliable estimates of hydraulic conductivity in a

tilled soil. The results from the Jackson equation are extremely sensitive to the water characteristic input in the matric potential range 0 to -1.0 kPa.

d) The effects of multiple-pass tillage on soil thermal properties and shortwave albedo.

7. Large changes in thermal conductivity and volumetric heat capacity can occur with differing tillage operations.

8. The zenith angle effect on bare soil shortwave albedo is soil-specific and hence must be determined in any studies investigating the effects of soil properties on albedo.

9. Only small differences in shortwave albedo occur due to changes in surface soil structure following different multiple-pass tillage operations, but large changes in albedo occur due to changes in surface soil water content.

e) Numerical simulation modelling.

10. The numerical simulation model CONSERVB incorporates the important tillage-affected variables affecting the soil water balance. The model is capable of accurately predicting evaporation rates providing that accurate values of soil unsaturated hydraulic conductivity can be obtained.

11. Simulated evaporation from the CONSERVB model is very sensitive to the unsaturated hydraulic conductivity input. Verification studies are required to assess the importance of the unsaturated hydraulic conductivity on the soil water balance thereby further testing the model's representation of the soil-water system.

12. Soil water profiles simulated with CONSERVB are generally in good agreement with measured values although in the surface 30 mm of soil, simulated values tend to be lower than measured values. This probably reflects invalid model assumptions about the uniformity of the surface soil layers.

REFERENCES

ABOUKHALED, A.; ALFARO, A., and SMITH, M. 1982. Lysimeters. Irrigation and Drainage Paper No. 39. Food and Agriculture Organisation of the United Nations, Rome.

ADEM, H.H.; TISDALL, J.M., and WILLOUGHBY, P. 1984. Tillage management changes size-distribution of aggregates and macro-structure of soils used for irrigated row crops. Soil and Tillage Research 4 : 461-476.

ADU, J.K., and OADES, J.M. 1978. Physical factors influencing decomposition of organic materials in soil aggregates. Soil Biology and Biochemistry 10 : 109-115.

ALEXANDER, L., and SKAGGS, R.W. 1986. Predicting unsaturated hydraulic conductivity from the soil water characteristic. Transactions of the American Society of Agricultural Engineers 29 : 176-184.

ALLMARAS, R.R., and DOWDY, R.H. 1985. Conservation tillage systems and their adoption in the United States. Soil and Tillage Research 5 : 197-222.

ALLMARAS, R.R.; NELSON, W.W., and HALLAUER, E.A. 1972. Fall vs Spring plowing and related soil heat balance in the Western corn belt. Agricultural Experiment Station, University of Minnesota, Technical Bulletin No. 283.

ALLMARAS, R.R.; UNGER, P.W., and WILKINS, D.E. 1985. Conservation tillage systems and soil productivity. In: Soil Erosion and Crop Productivity. R.F. Follett and B.A. Stewart (Editors). American Society of Agronomy, Madison, Wisconsin.

ALLMARAS, R.R.; BURWELL, R.E.; LARSON, W.E., and HOLT, R.F. 1966. Total porosity and random roughness of the inter-row zone as influenced by tillage. USDA., Agriculture Research Service Conservation Research Report No.7.

ALLMARAS, R.R.; HALLAUER, E.A.; NELSON, W.W., and EVANS, S.D. 1977. Surface energy balance and soil thermal property modifications by tillage-induced soil structure. Agricultural Experiment Station, University of Minnesota, Technical Bulletin No. 306.

AMOOZEGAR, A., and WARRICK, A.W. 1986. Hydraulic conductivity of saturated soils : Field methods. In: Methods of Soil Analysis, Part 1. A. Klute (Editor), Agronomy 9 : 735-770. American Society of Agronomy, Madison, Wisconsin.

ANGSTROM, A. 1925. The albedo of various surfaces of the ground. Geografiska Annaler 7 : 323-342.

ARCHER, J.R. 1975. Soil consistency. In: Soil Physical Conditions and Crop Production. Ministry of Agriculture, Fisheries and Food, HMSO, London, Technical Bulletin No.29, pp 289-297.

ASLYNG, H.C. 1974. Evapotranspiration and plant production directly related to global radiation. Nordic Hydrology 5 : 247-256.

BAKER, C.H., and CURRY, B.R. 1976. Structure of agricultural simulators : a philosophical view. Agricultural Systems 1 : 201.

BALL, B.C., and HUNTER, R. 1980. Improvements in the routine determination of pore size distribution from water release measurements on tension tables and pressure plates. The British Society for Research in Agricultural Engineering. Departmental note SIN/314, unpublished, December 1980.

BALL, D.F. 1964. Loss-on-ignition as an estimate of organic matter and organic carbon in non-calcareous soils. Journal of Soil Science 15 : 84-92.

BATEY, T. 1988. Soil Husbandry - A practical guide to the use and management of soils. Soil and Land Use Consultants Ltd, Aberdeen (Publishers). 157 pp.

BAUMGARDNER, M.F.; SILVA, L.F.; BIEHL, L.L., and STONER, E.R. 1985. Reflectance properties of soils. Advances in Agronomy 38 : 1-44.

BELMANS, C.; FEYEN, J., and HILLEL, D.I. 1979. An attempt at experimental validation of macroscopic scale models of soil moisture extraction by roots. Soil Science 127 : 174-186.

BENNETT, H.H. 1939. Soil Conservation. McGraw Hill, New York, pp. 933.

BHUSHAN, L.S., and GHILDYAL, B.P. 1972. Influence of radius of curvature of mouldboard on soil structure. Indian Journal of Agricultural Science 42 (1) : 1-5.

BOAST, C.W. 1986. Evaporation from bare soil measured with high spatial resolution. In: Methods of Soil Analysis, Part 1. A. Klute (Editor). Agronomy 9 : 889-900. American Society of Agronomy, Madison, Wisconsin.

BOAST, C.W., and ROBERTSON, T.M. 1982. A micro-lysimeter method for determining evaporation from bare soil : description and laboratory evaluation. Soil Science Society of America Journal 46 : 689-696.

BOND, J.J., and WILLIS, W.D. 1969. Soil water evaporation : surface residue and placement effects. Soil Science Society of America Proceedings 33 : 445-448.

BOONE, F.R. 1976. Notes on soil structure, homogeneity and rootability. Proceedings, 7th Conference International Soil and Tillage Research Organisation (ISTRO), Uppsala, Sweden. pp 4 : 1-6.

BOONE, F.R. 1988. Weather and other environmental factors influencing crop responses to tillage and traffic. Soil and Tillage Research 11 : 283 - 324.

BOONE, F.R.; VAN OUWERKERK, C.; KROESBERGEN, B.; POT, M., and BOERS, A. 1984. Soil Structure. In: Experiences with three tillage systems on a Marine loam soil. II. 1976-1979. F.R. Boone (Editor). Pudoc, Wageningen, Agricultural Research Report No. 925, pp 24-46.

BOWERS, S.A., and HANKS, R.J. 1965. Reflection of radiant energy from soils. Soil Science 100 : 130-132.

BLAD, B.L., and ROSENBERG, N.J. 1976. Evaluation of resistance and mass transport evapotranspiration models requiring canopy temperature data. Agronomy Journal 68 : 764-769.

BLANEY, H.F., and CRIDDLE, W.D. 1950. Determining water requirements in irrigated areas from climatological and irrigation data. USDA Soil Conservation Service Technical Paper No.96. 48 pp.

BRAUNACK, M.V.; HEWITT, J.S., and DEXTER, A.R. 1979. Brittle fracture of soil aggregates and compaction of aggregate beds. Journal of Soil Science 30 : 653-667.

BROWN, K.W., and ROSENBERG, N.J. 1973. A resistance model to predict evapotranspiration and its application to a sugar beet field. Agronomy Journal 65 : 341-347.

BRUCE, R.R., and LUXMOORE, R.J. 1986. Water retention : Field methods. In: Methods of Soil Analysis, Part 1. A. Klute (Editor). Agronomy 9 : 663-686. American Society of Agronomy, Madison, Wisconsin.

BRUNT, D. 1932. Notes on radiation in the atmosphere. Quarterly Journal of the Royal Meteorological Society 58 : 389-418.

BRUTSAERT, W. 1967. Some methods of calculating unsaturated permeability. Transactions of the American Society of Agricultural Engineers 10 : 400-404.

BRUTSAERT, W. 1975. On a derivable formula for long-wave radiation from clear skies. Water Resources Research 11 : 742-744.

BUCHAN, G.D. 1982. Predicting bare soil temperature. II. Experimental testing of multi-day models. Journal of Soil Science 33 : 199-209.

BUCHAN, G.D. 1989. Soil heat flux and soil surface energy balance : a clarification of concepts. Paper presented to the 4th Australasian Conference on Heat and Mass Transfer, Christchurch, New Zealand.

BUCHAN, G.D. 1989. Personal communication.

BURWELL, R.E.; ALLMARAS, R.R., and AMEMIYA, M. 1963. A field measurement of total porosity and surface micro-relief of soils. Soil Science Society of America Proceedings 27 : 697-700.

BURWELL, R.E.; ALLMARAS, R.R., and SLONEKER, L.L. 1966. Structural alteration of soil surfaces by tillage and rainfall. Journal of Soil and Water Conservation 21 : 61-63.

BURWELL, R.E.; SLONEKER, L.L. and NELSON, W.W. 1968. Tillage influences water intake. Journal of Soil and Water Conservation 23 : 185-187.

BUSINGER, J.A. 1975. Aerodynamics of vegetative surfaces : heat and mass transfer in the biosphere. Part 1 : Heat transfer in the environment. D.A. de Vries and N.H. Afgan (Editors). Scripto Book Co., Washington D.C. pp 139-165.

CAMILLO, P.J., and GURNEY, R.J. 1986. A resistance parameter for bare soil evaporation models. Soil Science 141 : 94-105.

CAMILLO, P.J.; GURNEY, R.J., and SCHMUGGE, T.J. 1983. A soil and atmospheric boundary layer model for evapotranspiration and soil moisture studies. Water Resources Research 19 : 371-380.

CANNELL, R.Q.; ELLIS, F.B.; CHRISTIAN, D.G.; GRAHAM, J.P., and DOUGLAS, J.T. 1980. The growth and yield of winter cereals after direct drilling, shallow cultivation and ploughing on non-calcareous clay soils, 1974-1978. Journal of Agricultural Science, Cambridge, 94 : 345-359.

CASSEL, D.K. 1982. Tillage effects on soil bulk density and mechanical impedance. In: Predicting Tillage Effects on Soil Physical Properties and Processes. P.W. Unger and D.M. Van Doren (Editors). Special Publication 44, American Society of Agronomy, Madison, Wisconsin. pp 133-150.

CASSEL, D.K., and NELSON, L.A. 1985. Spatial and temporal variability of soil physical properties of Norfolk loamy sand as affected by tillage. Soil and Tillage Research 5 : 5-17.

CHANEY, K., and SWIFT, R.S. 1984. The influence of organic matter on aggregate stability in some British soils. Journal of Soil Science 35 : 223-230.

CHANEY, K.; HODGSON, D.R., and BRAIM, M.A. 1985. The effects of direct drilling, shallow cultivation and ploughing on some physical properties in a long-term experiment on spring barley. Journal of Agricultural Science, Cambridge 104 : 125-133.

CHEPIL, W.S. 1942. Measurement of wind erosiveness of soils by dry sieving procedure. Scientific Agriculture 23 : 154-160.

CHEPIL, W.S. 1943. Relation of wind erosion to the water-stable and dry clod structure of soil. Soil Science 55 : 275-287.

CHEPIL, W.S. 1945. Dynamics of wind erosion. I. Nature of movement of soil by wind. Soil Science 60 : 305-320.

CHEPIL, W.S. 1952. Improved rotary sieve for measuring state and stability of dry soil structure. Soil Science Society of America Proceedings 16 : 113-117.

CHEPIL, W.S. 1957. Sedimentary characteristics of dust storms. I. Sorting of wind-eroded soil material. American Journal of Science 255 : 12-22.

CHEPIL, W.S. 1958. Soil conditions that influence wind erosion. USDA Technical Bulletin No. 1185.

CHEPIL, W.S. 1962. A compact rotary sieve and the importance of dry sieving in physical soil analysis. Soil Science Society of America Proceedings 26 : 4-6.

CHEPIL, W.S., and BISAL, F.A. 1943. A rotary sieve method for determining the size distribution of soil clods. Soil Science 56 : 95-100.

CHEPIL, W.S., and MILNE, R.A. 1941. Wind erosion of soil in relation to roughness of surface. Soil Science 52 : 417-431.

CHEPIL, W.S., and WOODRUFF, N.P. 1963. The physics of wind erosion and its control. Advances in Agronomy 15 : 211-302.

CHILDS, E.C. 1969. An introduction to the physical basis of soil water phenomena. Wiley (Interscience), New York, 493 pp.

CHILDS, E.C., and COLLIS-GEORGE, N. 1950. The permeability of porous materials. Proceedings of the Royal Society A201 : 392-405.

CHRISTIANSEN, J.E. 1942. Irrigation by sprinkling. Californian Agricultural Experimental Station Bulletin No.670. pp 94.

CLAFLIN, L.E.; STUTEVILLE, D.L., and ARMBRUST, D.V. 1973. Windblown soil in the epidemiology of bacterial leaf spot of alfalfa and common blight of beans. Phytopathology 63 : 1417.

CLOTHIER, B.E., and WHITE, I. 1981. Measurement of sorptivity and soil water diffusivity in the field. Soil Science Society of America Journal 45 : 241-245.

COOPER, A.W. 1971. Effects of tillage on soil compaction. In: Compaction of Agricultural Soils. Barnes, K.K.; Carleton, W.M.; Taylor, H.M.; Throckmorton, R.I., and Vanden Berg, G.E. (Editors). American Society of Agricultural Engineers, St Joseph, MI, pp 313-364.

COULSON, K.L., and REYNOLDS, D.W. 1971. The spectral reflectance of natural surfaces. Journal of Applied Meteorology 10 : 1285-1295.

CRUSE, R.M.; LINDEN, D.R.; RADKE, J.K.; LARSON, W.E., and LARNTZ, K. 1980. A model to predict tillage effects on soil temperature. Soil Science Society of America Journal 44 : 378-383.

CRUSE, R.M.; POTTER, K.N., and ALLMARAS, R.R. 1982. Modelling tillage effects on soil temperature. In : Predicting Tillage Effects on Soil Physical Properties and Processes. P.W. Unger and D.M. Van Doren (Editors). American Society of Agronomy Special Publication No.44, Madison, Wisconsin.

CURRENCE, H.D., and LOVELY, W.G. 1970. The analysis of soil surface roughness. Transactions of the American Society of Agricultural Engineers 13 : 710-714.

DANE, J.H. 1980. Comparison of field and laboratory determined hydraulic conductivity values. Soil Science Society of America Journal 44 : 228-231.

DANIEL, H.A., and LANGHAM, W.H. 1936. The effect of wind erosion and cultivation on the total nitrogen and organic matter content of soils in the Southern high plains. Journal of the American Society of Agronomy 28 : 587-596.

DAVIES, D.B., and CANNELL, R.Q. 1975. Review of experiments on reduced cultivation and direct drilling in the U.K., 1957-1974. Outlook on Agriculture 8 : 216-220.

DE LEENHEER, L. 1977. Soil fertility study in maximizing crop yield on mechanical farms in Belgium : general and agricultural conclusions of a 15 year study (1961-1975), p.133-144. Proceedings of the International Seminar on Soil Environment and Fertilizer Management in International Agriculture, Tokyo, Japan.

DENNING, J.L.; BOUMA, J.; FALAYI, O., and VAN ROOYEN, D.J. 1974. Calculation of hydraulic conductivities of horizons in some major soils in Wisconsin. Geoderma, 11 : 1-16.

DE VRIES, D.A. 1958. Simultaneous transfer of heat and moisture in porous media. Transactions, American Geophysical Union 39 : 909-916.

DE VRIES, D.A. 1963. Thermal properties of soils. In: Physics of Plant Environment (Chapter 7). W.R. van Wijk (Editor), North Holland Publishing Co., Amsterdam, 2nd edition, pp 210-235.

DE VRIES, D.A., and PHILIP, J.R. 1986. Soil heat flux, thermal conductivity, and the null-alignment method. Soil Science Society of America Journal 50 : 12-18.

DEXTER, A.R. 1976. Internal structure of a tilled soil. Journal of Soil Science 27 : 267-278.

DEXTER, A.R. 1988. Advances in characterization of soil structure. Soil and Tillage Research 11 : 199-238.

DEXTER, A.R., and HEWITT, J.S. 1978. The structure of beds of spherical particles. Journal of Soil Science 29 : 146-155.

DOLGOV, S.I., and VINOGRADOVA, G.B. 1973. Reflection coefficient of moist soils. Soviet Soil Science 5 : 735-737.

DOUGLAS, E.; McKYES, E.; TAYLOR, F.; NEGI, S., and RAGHAVAN, G.S.V. 1980. Unsaturated hydraulic conductivity of a tilled clay soil. Canadian Agricultural Engineering 22 : 153-161.

EDWARDS, W.M. 1982. Predicting tillage effects on infiltration. In : Predicting Tillage Effects on Soil Physical Properties and Processes. P.W. Unger and D.M. Van Doren (Editors). American Society of Agronomy Special Publication No.44, Madison, Wisconsin.

EHLERS, W. 1975. Observations on earthworm channels and infiltration on tilled and untilled loess soil. Soil Science 119 : 242-249.

EHLERS, W. 1976. Rapid determination of unsaturated hydraulic conductivity in tilled and untilled loess soil. Soil Science Society of America Journal 40 : 837-840.

EHLERS, W.; KHOSLA, B.K.; KOPKE, U.; STULPNAGEL, R.; BOHM, W., and BAEUMER, K. 1980. Tillage effects on root development, water uptake and growth of oats. Soil and Tillage Research, 1 : 19-34.

EYLES, G.O. 1983. The distribution and severity of present soil erosion in New Zealand. New Zealand Geographer 39 : 12-28.

FALAYI, O. and BOUMA, J. 1975. Relationships between the hydraulic conductance of surface crusts and soil management in a Typic Hapludalf. Soil Science Society of America Proceedings 39 : 957-963.

FAO. 1960. Soil erosion by wind and measures for its control on agricultural lands. Food and Agricultural Organisation, Rome, Agricultural Development Paper No. 71. pp. 78.

FARRELL, D.A.; GREACEN, E.L., and LARSON, W.E. 1967. The effect of water content on axial strain in a loam soil under tension and compression. Soil Science Society of America Proceedings 31 : 445-450.

FIELD, J.A.; PARKER, J.C., and POWELL, N.L. 1984. Comparison of field and laboratory measured and predicted hydraulic properties of a soil with macro-pores. Soil Science 138 : 385-396.

FOLLET, R.F., and STEWART, B.A. (Editors). 1985. Soil Erosion and Crop Productivity. American Society of Agronomy Inc., Crop Science Society of America Inc., Soil Science Society of America Inc., Publishers. Madison, Wisconsin, USA.

FORSYTHE, W.E. 1964. Smithsonian Physical Tables. Smithsonian Institution, Publication 4169. 827pp.

FRITSCHEN, L.J., and VAN BAVEL, C.H.M. 1962. Energy balance components of evaporating surfaces in arid lands. Journal of Geophysical Research 67 : 5179-5185.

FUNK, J.P. 1959. Improved polythene shielded net radiometer. Journal of Scientific Instruments 36 : 267-269.

GARDNER, H.R. 1974 Prediction of water loss from a fallow field soil based on soil water flow theory. Soil Science Society of America Proceedings 38 : 379-382.

GARDNER, W.H. 1986. Water Content. In: Methods of Soil Analysis, part 1. A. Klute (Editor). Agronomy 9 : 493-544. American Society of Agronomy, Madison, Wisconsin.

GILL, W.R. 1967. Soil-implement relations. In: Tillage for Greater Crop Production. American Society of Agricultural Engineers Publication PROC-168. pp.32-36, 43.

GRADWELL, M.W. 1972. Methods for physical analysis of soils. N.Z. Soil Bureau Scientific Report 10C, DSIR., New Zealand.

GRASER, E.A., and VAN BAVEL, C.H.M. 1982. The effect of soil moisture upon soil albedo. Agricultural Meteorology 27 : 17-26.

GREEN, R.E., and COREY, J.C. 1971. Calculation of hydraulic conductivity : a further evaluation of some predictive methods. Soil Science Society of America Proceedings 35 : 3-8.

GREEN, R.E.; AHUJA, L.R., and CHONG, S.K. 1986. Hydraulic conductivity, diffusivity, and sorptivity of unsaturated soils : Field methods. In: Methods of Soil Analysis, Part 1. A. Klute (Editor). Agronomy 9 : 771-798. American Society of Agronomy, Madison, Wisconsin.

GUPTA, S.C.; LARSON, W.E., and ALLMARAS, R.R. 1984. Predicting soil temperature and soil heat flux under different tillage-surface residue conditions. Soil Science Society of America Journal 48 : 223-232.

HADAS, A.; LARSON, W.E., and ALLMARAS, R.R. 1988. Advances in modelling machine-soil-plant interactions. Soil and Tillage Research 11 : 349-372.

HADAS, A., and RUSSO, D. 1974a. Water uptake by seeds as affected by water stress, capillary conductivity, and seed-soil water contact. I. Experimental study. Agronomy Journal 66 : 643-647.

HADAS, A., and RUSSO, D. 1974b. Water uptake by seeds as affected by water stress, capillary conductivity, and seed-soil water contact. II. Analysis of experimental data. Agronomy Journal 66 : 647-652.

HADAS, A., and WOLF, D. 1983. Energy efficiency in tilling dry clod-forming soils. Soil and Tillage Research 3 : 47-59.

HAGE, K.D. 1975. Averaging errors in monthly evaporation estimates. Water Resources Research 11 : 357-361.

HAGEN, L.J., and WOODRUFF, N.P. 1973. Air pollution from duststorms in the Great Plains. Atmospheric Environment 7 : 323-332.

HARGREAVES, G.H. 1974. Estimation of potential and crop evapotranspiration. Transactions of the American Society of Agricultural Engineers 17 : 701-704.

HEILMAN, J.L., and KANEMASU, E.T. 1976. An evaluation of a resistance form of the energy balance to estimate evapotranspiration. Agronomy Journal 68 : 607-612.

HIGUCHI, M. 1984. Numerical simulation of soil water flow during drying in a non-homogeneous soil. Journal of Hydrology 71 : 303-334.

HILLEL, D.I. 1977. Computer simulation of soil-water dynamics : a compendium of recent work. International Development and Research Centre, P.O. Box 8500, Ottawa, Canada.

HILLEL, D.I. 1982. Introduction to Soil Physics. Academic Press Inc. (London). pp.365.

HILLEL, D.I., and HADAS, A. 1972. Isothermal drying of structurally layered soil columns. Soil Science 113 : 30-35.

HILLEL, D.I., and VAN BAVEL, C.H.M. 1976. Simulation of profile water storage as related to soil hydraulic properties. Soil Science Society of America Journal 40 : 807-815.

HILLEL, D.I.; VAN BAVEL, C.H.M., and TALPAZ, H. 1975. Dynamic simulation of water storage in fallow soil as affected by mulch of hydrophobic aggregates. Soil Science Society of America Proceedings 39 : 826-833.

HILLEL, D.I.; TALPAZ, H., and VAN KEULEN, H. 1976. A macroscopic-scale model of water uptake by a non-uniform root system and of water and salt movement in the soil profile. Soil Science 121 : 242-255.

HOYLE, B.J.; YAMADA, H., and HOYLE, T.D. 1972. Aggresizing to eliminate objectionable soil clods. Californian Agriculture 26 : 3-5.

IDSO, S.B. 1981. A set of equations for full spectrum and 8 to 14 μm and 10.5 to 12.5 μm thermal radiation from cloudless skies. Water Resources Research 17 : 295-304.

IDSO, S.B., and JACKSON, R.D. 1969. Thermal radiation from the atmosphere. Journal of Geophysical Research 74 : 5397-5403.

IDSO, S.B.; REGINATO, R.J.; JACKSON, R.D.; KIMBALL, B.A., and NAKAYAMA, F.S. 1974. The three stages of drying a field soil. Soil Science Society of America Proceedings 38 : 831-837.

IDSO, S.B.; JACKSON, R.D.; REGINATO, R.J.; KIMBALL, B.A., and NAKAYAMA, F.S. 1975. The dependence of bare soil albedo on soil water content. Journal of Applied Meteorology 14 : 109-113.

INCROPERA, F.P., and DE WITT, D.P. 1985. Fundamentals of Heat and Mass Transfer (2nd Edition). John Wiley and Sons, New York.

IQBAL, M. 1983. An Introduction to Solar Radiation. Academic Press, Toronto. pp390.

JACKSON, R.D. 1972. On the calculation of hydraulic conductivity. Soil Science Society of America Proceedings 36 : 380-382.

JOHNSON, C.B.; MANNERING, J.V., and MOLDENHAUER, W.C. 1979. Influence of surface roughness and clod size and stability on soil and water losses. Soil Science Society of America, Journal 43 : 772-777.

JOLLY, R.W.; EDWARDS, W.M., and ERBACH, D.C. 1983. Economics of conservation tillage in Iowa. Journal of Soil and Water Conservation 38 : 291-294.

KANEMASU, E.T.; WESELY, M.L.; HICKS, B.B., and HEILMAN, J.L. 1979. Techniques for calculating energy and mass fluxes. In : Modification of the Aerial Environment of Crops B.J. Barfield and J.F. Gerber (Editors). American Society of Agricultural Engineers Monograph 2 : 156-182.

KEAR, D.S.; GIBBS, H.S., and MILLER, R.B. 1967. Soils of the downs and plains of Canterbury and North Otago, New Zealand. Soil Bureau Bulletin No.14. DSIR., Wellington, New Zealand.

KEMPER, W.D., and ROSENAU, R.C. 1986. Aggregate stability and size distribution. In : Methods of Soil Analysis, Part 1, A. Klute (Editor). Agronomy 9 : 425-442. American Society of Agronomy, Madison, Wisconsin.

KIMBALL, B.A., and JACKSON, R.D. 1979. Soil heat flux. In : Modification of the Aerial Environment of Crops. B.J. Barfield and J.F. Gerber (Editors). American Society of Agricultural Engineers monograph 2: 211-229.

KLUTE, A. 1982. Tillage effects on hydraulic properties of soil : a review. In : Predicting Tillage Effects on Soil Physical Properties and Processes. P.W. Unger and D.M. Van Doren (Editors). American Society of Agronomy Special Publication No.44, Madison, Wisconsin.

KLUTE, A. 1986. Water retention : Laboratory methods. In : Methods of Soil Analysis, Part 1. A. Klute (Editor). Agronomy 9 : 635-662. American Society of Agronomy, Madison, Wisconsin.

KLUTE, A., and DIRKSEN, C. 1986. Hydraulic conductivity and diffusivity : Laboratory methods. In : Methods of Soil Analysis, Part 1. A. Klute (Editor). Agronomy 9 : 687-734. American Society of Agronomy, Madison, Wisconsin.

KOUWENHOVEN, J.K. 1986. Effect of moldboard and chisel ploughing and their timing on seedbed quality. Soil and Tillage Research 7 : 205-219.

KUIPERS, H. 1961. Water content at pF2 as a characteristic in soil-cultivation research in The Netherlands. Netherlands Journal of Agricultural Science 9 : 27-35.

KUNZE, R.J.; VEHARA, G., and GRAHAM, K. 1968. Factors important in the calculation of hydraulic conductivity. Soil Science Society of America Proceedings 32 : 760-765.

LADEWIG, H., and GARIBAY, R. 1983. Reasons why Ohio farmers decide for or against conservation tillage. Journal of Soil and Water Conservation 38 : 487-488.

LARSON, W.E. 1962. Tillage requirements for corn. Journal of Soil and Water Conservation 17 : 3-7.

LASCANO, R.J., and VAN BAVEL, C.H.M. 1983. Experimental verification of a model to predict soil moisture and temperature profiles. Soil Science Society of America Journal 47 : 441-448.

LASCANO, R.J., and VAN BAVEL, C.H.M. 1986. Simulation and measurement of evaporation from a bare soil. Soil Science Society of America Journal 50 : 1127-1132.

LINACRE, E.T. 1977. A simple formula for estimating evapo-transpiration rates in various climates, using temperature data alone. Agricultural Meteorology 18 : 409-424.

LINDEN, D.R. 1979. A model of multiple reflection absorbance of solar radiation on tillage-induced rough soil surfaces. Agronomy Abstract, American Society of Agronomy, Madison, Wisconsin. p.207.

LINDEN, D.R. 1982. Predicting tillage effects on evaporation from the soil. In : P.W. Unger and D.M. Van Doren (Editors) Predicting Tillage Effects on Soil Physical Properties and Processes. American Society of Agronomy Special Publication No.44, Madison, Wisconsin.

LINDEN, D.R., and VAN DOREN Jr, D.M. 1986. Parameters for characterizing tillage-induced soil surface roughness. Soil Science Society of America Journal 50 : 1560-1565.

LYLES, L. 1975. Possible effects of wind erosion on soil productivity. Journal of Soil and Water Conservation 30 : 279-283.

LYLES, L., and WOODRUFF, N.P. 1962. How moisture and tillage affect soil cloddiness for wind erosion control. Agricultural Engineering 43 (3) : 150-153, 159,

LYLES, L., DICKERSON, J.D., and DISRUD, L.A. 1970. Modified rotary sieve for improved accuracy. Soil Science 109 : 207-210.

LYNCH, J.M., and BRAGG, E. 1985. Micro-organisms and soil aggregate stability. Advances in Soil Science 2 : 133-171.

McCLEAN, S.P. 1980. The role of the plough in today's agriculture. Journal of Science, Food and Agriculture 31 : 414-419.

McGUIGAN, F.J. 1989. Wind erosion on the Canterbury Plains - October 1988. Unpublished report. North Canterbury Catchment and Regional Water Board.

MAFF. 1982. Consistency limits. In : Techniques for Measuring Soil Physical Properties. Ministry of Agriculture, Fisheries and Food, HMSO., London, Reference Book 441, pp 72-74.

MARLATT, W.E. 1967. Remote and in situ measurements of land and water surfaces. Journal of Applied Meteorology 6 : 272-279.

MARSHALL, T.J. 1958. Relation between permeability and size distribution of pores. Journal of Soil Science 9 : 1-8.

MARSHALL, T.J., and HOLMES, J.W. 1988. Soil Physics. 2nd edition, Cambridge University Press, Cambridge. pp374.

MIEKLE, L.N.; DORAN, J.W., and RICHARDS, K.A. 1986. Physical environment near the surface of ploughed and no-tilled soils. Soil and Tillage Research 7 : 355-366.

MILLY, P.C.D. 1982. Moisture and heat transport in hysteretic, inhomogeneous porous media : a matric head-based formulation and a numerical model. Water Resources Research, 18 : 489-498.

MONTEITH, J.L. 1963. Gas exchange in plant communities. In : Environmental Control of Plant Growth. L.T. Evans (Editor). Academic Press, New York. pp. 95-112.

MONTEITH, J.L. 1973. Principles of Environmental Physics. Edward Arnold, London. 241 pp.

MORGAN, R.P.C. 1986. Soil Erosion and Conservation. Longman Scientific and Technical, England (publishers). 298 pp.

MUALEM, Y. 1986. Hydraulic conductivity of unsaturated soils : prediction and formulas. In : Methods of Soil Analysis, Part 1, A. Klute (Editor). Agronomy 9 : 799-824. American Society of Agronomy, Madison, Wisconsin.

MURRAY, F.W. 1967. On the computation of saturation vapour pressure. Journal of Applied Meteorology 6 : 203-204.

NAPIER, T.L.; THRAEN, C.S.; GORE, A., and GOE, W.R. 1984. Factors affecting adoption of conventional and conservation tillage practices in Ohio. Journal of Soil and Water Conservation 39 : 205-209.

OJENIYI, S.O., and DEXTER, A.R. 1979a. Soil factors affecting the macro-structures produced by tillage. Transactions of the American Society of Agricultural Engineers 22 : 339-343.

OJENIYI, S.O., and DEXTER, A.R. 1979b. Soil structural changes during multiple-pass tillage. Transactions of the American Society of Agricultural Engineers 22 : 1068-1072.

OJENIYI, S.O., and DEXTER, A.R. 1984. Effect of soil structure on soil water status. Soil and Tillage Research, 4 : 371-379.

OSCHWALD, W.R. 1973. Chisel plough and strip tillage systems. In : Conservation Tillage. Proceedings of a National Conference. pp. 194-202. Soil Conservation Society of America, Ankeny, Iowa.

PAINTER, D.J. 1976. What cost windblown soil? New Zealand Farmer 97 (23) : 47-48.

PASSERAT DE SILANS, A.; BRUCKLER, L.; THONY, J.L., and VAUCLIN, M. 1989. Numerical modelling of coupled heat and water flows during drying in a stratified bare soil - comparison with field observations. Journal of Hydrology 105 : 109-138.

PATTERSON, D.E. 1982. The performance of alternative cultivation systems. Agricultural Engineer 37 (1) : 8-11.

PAULSON, C.A. 1970. The mathematical representation of wind speed and temperature profiles in the unstable atmospheric surface layer. Journal of Applied Meteorology 9 : 851-861.

PHILIP, J.R., and DE VRIES, D.A. 1957. Moisture movement in porous materials under temperature gradients. Transactions, American Geophysical Union 38 : 222-232, 594.

POTTER, K.N.; HORTON, R., and CRUSE, R.M. 1987. Surface soil roughness effects on radiation reflectance and soil heat flux. Soil Science Society of America Journal 51 : 855-860.

RAB, A.R.; WILLATT, S.T., and OLSSON, K.A. 1987. Hydraulic properties of a duplex soil determined from in situ measurements. Australian Journal of Soil Research 25 : 1-7.

RATHORE, T.R.; GHILDYAL, B.P., and SACHAN, R.S. 1982. Germination and emergence of soybean under crusted soil conditions. II. Seed environment and varietal differences. Plant and Soil 65 : 73-77.

RAWITZ, E.; HOOGMOED, W.B., and MORIN, Y. 1985. The effect of tillage practices on crust properties, infiltration and crop response under semi-arid conditions. Proceedings International Symposium Soil Science Society, Assessment of Soil Surface Sealing and Crusting, Ghent, Belgium, pp. 278-285.

REICOSKY, D.C., and RITCHIE, J.T. 1976. Relative importance of soil resistance and plant resistance in root water absorption. Soil Science Society of America Journal 40 : 293-297.

REID, J.B., and HUTCHISON, B. 1986. Soil and plant resistances to water uptake by Vicia Faba L. Plant and Soil 92 : 431-441.

REIFSNYDER, W.E. 1967. Radiation geometry in the measurement and interpretation of radiation balance. Agricultural Meteorology 4 : 255-265.

RITCHIE, J.T. 1972. Model for predicting evaporation from a row crop with incomplete cover. Water Resources Research 8 : 1204-1213.

ROMKENS, M.J.M., and WANG, J.Y. 1986. Effect of tillage on surface roughness. Transactions of the American Society of Agricultural Engineers 29 : 429-433.

ROSEMA, A. 1975. Simulation of thermal behaviour of bare soils for remote sensing purposes. In : Heat and Mass Transfer in the Biosphere. D.A. de Vries and N.H. Afgan (Editors). Wiley, New York, N.Y., pp. 109-135.

ROSENBERG, N.J. 1969a. Seasonal patterns in evapotranspiration by irrigated alfalfa in the central Great Plains. Agronomy Journal 61 : 879-886.

ROSENBERG, N.J. 1969b. Advective contribution of energy utilised in evapotranspiration by alfalfa in the East central Great Plains. Agricultural Meteorology 6 : 179-184.

ROSENBERG, N.J. 1972. Frequency of potential evapotranspiration rates in the central Great Plains. Journal Irrigation Drainage Division, American Society of Civil Engineers 98 : 203-206.

ROSENBERG, N.J.; BLAD, B.L., and VERMA, S.B. 1983. Microclimate - the Biological Environment. (2nd Edition) John Wiley and Sons. pp.495.

RUSSELL, E.W. 1973. Soil Conditions and Plant Growth. 10th Edition. Longman, Green and Co., London. 849 pp.

SAS INSTITUTE INC. 1985. SAS User's Guide : Basics, Version 5. Cary, N.C., USA. SAS Institute Inc.

SASAMORI, T. 1970. A numerical study of atmospheric and soil boundary layers. Journal of Atmospheric Science, 27 : 1123-1137.

SCHAFER, R.L., and JOHNSON, C.E. 1982. Changing soil condition - the soil dynamics of tillage. In : P.W. Unger and D.M. Van Doren (Editors) Predicting Tillage Effects on Soil Physical Properties and Processes. American Society of Agronomy Special Publication No.44, Madison, Wisconsin.

SCHIELDGE, J.P.; KAHLE, A.B., and ALLEY, R.E. 1982. A numerical simulation of soil temperature and moisture variations for a bare field. Soil Science 133 : 197-207.

SCHMUGGE, T.J.; JACKSON, T.J., and McKIM, H.L. 1980. Survey of methods of soil moisture determination. Water Resources Research 16 : 961-979.

SELLERS, W.D. 1965. Physical Climatology. Chicago : University Chicago Press. pp272.

SHAWCROFT, R.W., and GARDNER, H.R. 1983. Direct evaporation from soil under a row crop canopy. Agricultural Meteorology 28 : 229-238.

SHAYKEWICH, C.F. 1970. Hydraulic properties of disturbed and undisturbed soils. Canadian Journal of Soil Science 50 : 431-437.

SHEARER, A.M. 1982. Report on wind erosion. Unpublished report. Waitaki Catchment Commission.

SKIDMORE, E.L. 1976. Soil and water management and conservation : wind erosion. In : Handbook of Soils and Climate in Agriculture, V.J. Kilmer (Editor). CRC. Press.

SKIDMORE, E.L., and HAGEN, L.J. 1970. Evaporation in sheltered areas as influenced by windbreak porosity. Agricultural Meteorology 7 : 363-374.

SOPHOCLEOUS, M. 1979. Analysis of water and heat flow in unsaturated-saturated porous media. Water Resources Research 15 : 1195-1206.

SPOOR, G. 1982. Tillage for improved drainage. In : Proceedings of the International Soil Tillage Research Organisation, ISTRO, Osijek, 1982. 1 : pp. 650-655.

STAFFORD, J.V. 1988 Remote, non-contact and in situ measurement of soil moisture content : a review. Journal of Agricultural Engineering Research 41 : 151-172.

STEEL, R.G.D., and TORRIE, J.H. (Editors). 1981. Principles and procedures of statistics - a biometrical approach. McGraw-Hill International Book Company, Tokyo, 633 pp.

STRINGER, D.J. 1986. Personal communication.

SWINBANK, W.C. 1963. Long-wave radiation from clear skies. Quarterly Journal of the Royal Meteorological Society 89 : 339-348.

SZEICZ, G.; VAN BAVEL, C.H.M., and TAKAMI, S. 1973. Stomatal factor in the water use and dry matter production by sorghum. Agricultural Meteorology 12 : 361-389.

TANNER, C.B. 1967. Measurement of evapotranspiration. In : Irrigation of Agricultural Lands. R.M. Hagen, M.R. Haise and T.W. Edminster (Editors). American Society of Agronomy, Madison, Wisconsin. pp.534-574.

TAYLOR, H.M., and KLEPPER, B. 1975. Water uptake by cotton root systems : an examination of assumptions in the single root model. Soil Science 120 : 57-67.

TAYLOR, H.M., and BURNETT, E. 1964. Influence of soil strength on the root growth habits of plants. Soil Science 98 : 174-180.

TAYLOR, H.M.; ROBERTSON, G.M., and PARKER, J.J. (Jr) 1966. Soil strength - root penetration relations for medium to coarse textured soil materials. Soil Science 102 : 18-22.

TAYLOR, M.S. 1974. The effect of aggregate size on seedling emergence and early growth. East African Agriculture and Forestry Journal 40 : 204-213.

THOMAS, R.F. 1973. Test methods for soil engineering. New Zealand Soil Bureau Scientific Report 10E, DSIR., Wellington, New Zealand.

THORNTHWAITE, C.W. 1948. An approach towards a rational classification of climate. Geographic Review 38 : 55-94.

THORNTHWAITE, C.W., and HOLZMAN, B. 1942. Measurement of evaporation from land and water surface. USDA. Technical Bulletin 817 : 1-75.

TISDALL, J.M., and ADEM, H.H. 1986. Effect of water content of soil at tillage on size-distribution of aggregates and infiltration. Australian Journal of Experimental Agriculture 26 : 193-195.

TISDALL, J.M., and OADES, J.M. 1982. Organic matter and water-stable aggregates in soils. Journal of Soil Science 33 : 141-163.

TONKIN, P.J. 1989. Personal communication.

TRAULSEN, H. 1982. The role of the mouldboard plough? Agricultural Engineer 37 (1) : 12-14.

UNGER, P.W., and McCALLA, T.M. 1980. Conservation tillage systems. Advances in Agronomy 33 : 1-58.

UNITED STATES DEPARTMENT OF AGRICULTURE. 1965. Soil and water conservation needs - a national inventory. Miscellaneous Publication No.971, USDA, Washington, D.C.

UNITED STATES DEPARTMENT OF AGRICULTURE. 1983. Keys to soil taxonomy. Soil Management Support Services. Technical Monograph No.6, USDA, Washington, D.C.

UTOMO, W.H., and DEXTER, A.R. 1981. Soil friability. Journal of Soil Science 32 : 203-213.

VAN BAVEL, C.H.M., and HILLEL, D. 1976. Calculating potential and actual evaporation from a bare soil surface by simulation of concurrent flow of water and heat. Agricultural Meteorology 17 : 453-476.

VAN BAVEL, C.H.M., and LASCANO, R.J. 1979. CONSERVB. A numerical method to compute soil water content and temperature profiles under a bare surface. Unpublished report. Texas A and M. University, College Station.

VERMA, S.B.; ROSENBERG, N.J.; BLAD, B.L., and BARADAS, M.W. 1976. Resistance energy balance method for predicting evapotranspiration : determination of boundary layer resistance and evaluation of error effects. Agronomy Journal 68 : 776-782.

WALKER, G.K. 1983. Measurement of evaporation from soil beneath crop canopies. Canadian Journal of Soil Science 63 : 137-141.

WATSON, K.W., and LUXMOORE, R.J. 1986. Estimating macroporosity in a forest watershed by use of a tension infiltrometer. Soil Science Society of America Journal 50 : 578-582.

WEBB, T.H., and PURVES, A.M. 1983. Influence of soil type on yield of Autumn sown wheat and oats in Canterbury in a dry year. New Zealand Journal of Experimental Agriculture 11 : 289-294.

WIERENGA, P.J.; NIELSEN, D.R.; HORTON, R., and KIES, B. 1982. Tillage effects on soil temperature and thermal conductivity. In : P.W. Unger and D.M. Van Doren (Editors) Predicting Tillage Effects on Soil Physical Properties and Processes. American Society of Agronomy Special Publication No.44, Madison, Wisconsin.

WILSON, S.J., and COOKE, R.U. 1980. Wind erosion. In : Soil Erosion. Kirby, M.J., and Morgan, R.P.C. (Editors). John Wiley and Sons Ltd.

WINGATE-HILL, R. 1978. An assessment of tillage requirements for cereal crop production and their relationship to the development of new tillage machinery. In : Modification of Soil Structure. W.W. Emerson, R.D. Bond and A.R. Dexter (Editors). John Wiley, New York, pp. 363-370.

WISCHMEIER, W.H. 1973. Conservation tillage to control water erosion. In : Conservation Tillage. Proceedings of a National Conference. pp.133-141. Soil Conservation Society of America, Ankeny, Iowa.

WOLF, D., and HADAS, A. 1987. Determining efficiencies of various moldboard ploughs in fragmenting and tilling air-dry soils. Soil and Tillage Research 10 : 181-190.

WOODRUFF, N.P., and CHEPIL, W.S. 1956. Implements for wind erosion control. Agricultural Engineering 37 : 751-754, 758.

WOODRUFF, N.P., and SIDDOWAY, F.H. 1965. A wind erosion equation. Soil Science Society of America Proceedings, 29 : 602.

WORLD METEOROLOGICAL ORGANISATION 1983. Meteorological aspects of certain processes affecting soil degradation - especially erosion. World Meteorological Organisation Technical Note No.178.

ZOBECK, T.M., and ONSTAD, C.A. 1987. Tillage and rainfall effects on random roughness : a review. Soil and Tillage Research 9 : 1-20.

APPENDIX ONE

This appendix contains a listing of the CONSERVB numerical simulation model as was used for the simulations described in Chapter 7. The listing is contained in the file 'WATER2.FOR' in the directory 'CONSERVB' on the DSDD floppy disk inside the back cover of this document. The disk is formatted at 360 kb using MS-DOS version 3.20. In the same directory are the files MET1.DAT, MET2.DAT, INPUT1.DAT and INPUT2.DAT. Hourly meteorological input data for the CONSERVB model for the first and second simulation periods (julian days 74 to 86 and 89 to 99, 1989) are contained in the files MET1.DAT and MET2.DAT. The data in these files, by column, from left to right are: julian day number, time (hours), global radiation (W m^{-2}), air temperature at 2 m height (^{o}C), dew point temperature at 2 m (^{o}C), and windspeed at 2 m height (m s^{-1}).

The files INPUT1.DAT and INPUT2.DAT contain daily meteorological input data for the two simulation periods. The data in these files, by column, from left to right are: julian day, day-length (hours), daily global radiation (MJ m^{-2}), maximum daily air temperature at 2 m height (^{o}C), minimum daily air temperature at 2 m (^{o}C), dew point temperature corresponding to maximum daily air temperature (^{o}C), dew point temperature corresponding to minimum daily air temperature (^{o}C), average daily windspeed (m s^{-1}), time of beginning of rainfall period (hours), time of ending of rainfall period (hours), and total rainfall (mm).

When running this version of the CONSERVB model hourly meteorological data input is required. However, the daily input files (INPUT1.DAT and INPUT2.DAT) are still used for rainfall data input only. The other meteorological data contained in these files is not used by this version of the CONSERVB model. Before running the CONSERVB model data output files called OUTPT2.DAT and ENBAL2.DAT should be created.